Characterizing the Effect of Alcohol and Wnt/β-catenin Interactions on Melanocyte Development: Insights from Zebrafish (*Danio rerio*)

by

Praneeth Silva

A Thesis submitted to the Faculty of Graduate Studies of
The University of Manitoba
In partial fulfillment of the requirements of the degree of

Master of Science

Department of Oral Biology
Faculty of Dentistry
University of Manitoba
Winnipeg, Manitoba, Canada

ABSTRACT

Melanocytes, which are derived from the multipotent neural crest, are found in the skin, eyes, and other diverse anatomical locations of the vertebrates. The main aspects of melanocyte lineage are genetically determined and are influenced by a variety of extrinsic and intrinsic factors. Fetal alcohol spectrum disorder (FASD) is described as birth defects associated with prenatal alcohol exposure (PAE). PAE is likely one of the leading causes of severe congenital malformations but the pathophysiology of FASD-associated body pigmentation disorders is needed to be further investigated. Zebrafish (*Danio rerio*) (ZF) is identified as a well-established model organism to study FASD and melanocyte biology with remarkably high similarity to humans. The Wnt signaling pathway is a conserved signal transduction pathway that is important in embryonic development and it regulates many aspects of melanocyte lineage. The current study was designed to investigate the effect of ethanol and Wnt activity on ZF melanocyte formation, patterning, and melanogenesis.

Stereo-microscopic examinations were used for screening melanocyte counts, phenotypic differences and distribution of melanocytes in zebrafish meanwhile microscopic software tools were used for analyzing the morphometric differences of melanocytes against ethanol and Wnt regulatory chemical exposures. The chemical effect on melanosome biogenesis and melanogenesis was detected using toluidine blue stained histological sections, transmission electron microscopic (TEM) observations and spectrophotometric methods respectively. Whole-mount in situ hybridization (WMISH) was used to identify the gene expressions in melanocyte precursor cells. Ethanol and W-C59 exposed samples showed low melanocyte densities, and defects in melanocyte phenotype and patterning whereas LiCl demonstrated stimulatory action in most aspects of melanocyte development. Increased activity was observed in melanogenesis, melanoblast development, *dct+* and *Wnt3a+* gene expressions in melanocyte precursor cells and melanosome biogenesis in the cells of the RPE layer of the LiCl-treated fish. In contrast EtOH and Wnt inhibitors down-regulated the above-mentioned factors. Combined chemical-treated fish of EtOH and Wnt modulators displayed significant adverse effects on melanocyte development.

Our data confirmed that Wnt signaling plays a crucial role in melanocyte development and a balanced Wnt signaling level is important for proper melanocyte development. Further, prenatal ethanol exposure adversely affects melanocyte differentiation, patterning and melanogenesis.

ACKNOWLEDGEMENT

Foremost, I would like to express my deepest gratitude to my supervisor, Dr. Devi Atukorallaya for the opportunity and continuous support during my Master's degree programme over the last two years. I express my sincere gratitude for her invaluable guidance, encouragement, academic stimulus and generous help throughout the research project. Her great patience, kind guidance and feedback throughout this project were very important to complete this project successfully.

A profound sense of gratitude offers to my committee members, Dr. Gilbert Kirouac and Dr. Jeffrey Marcus for their constant inspiration, encouragement and guidance from the inception to the completion of my research project. Their valuable comments, suggestions, plentiful academic experience, motivation and in-depth analysis of my project further helped me to develop my research project.

Further, my sincere gratitude extends to the head of the department Dr. James Gilchrist and the rest of the academic staff members in my Department.

I must be thankful to my wonderful lab mate Parnia Azimian Zavareh, for the given immense support during this research period and for being a dedicated and good lab mate for me. This study would not be fulfilled successfully within the exact time period without her lab assistance, friendship and this partnership throughout this journey.

Further, my special gratitude goes to Vivianne, Ankita and Nisha for the assistance in laboratory work and for helping me with handling the equipment. This journey won't be possible without you guys. Mahamudul, Arian, Leanne, Bukky and Yasmin, thanks for the cherished time spent together in the university, labs, and, academic and social settings which made this 2-year journey so memorable for me.

I am hugely indebted to my dear parents and brothers on behalf of their unconditional and permanent love, sacrifices for me and confidence in me, which have encouraged me to move ahead in my studies and academic career.

Finally, and most importantly, I am much grateful to the University of Manitoba, funding agencies and my supervisor for taking care of my financial aid.

DEDICATION

I dedicate my thesis work to my loving parents and my brothers for their valuable support, sacrifice and love throughout my academic journey.

Especially, this thesis is dedicated to my mom U.A. Ranjani for her energy, dauntless encouragement and all the sacrifices to raise me into the person I am today.

&

Special dedication goes to my mother land Sri Lanka and all the people who sacrificed their lives, energy and money for giving me the free education.

Finally, to the entire universal life forms and energies, for bringing me on the best path of my life journey.

TABLE OF CONTENT

LIST OF FIGURES

LIST OF TABLES

LIST OF ABBREVIATIONS

~ - Approximately

ADH - Alcohol dehydrogenase

BMP- Bone Morphogenetic Proteins

cAMP - Cyclic adenosine monophosphate

CMZ- Ciliary marginal zone

CNS - Central nervous system

CYP2E1- Cytochrome P450 enzymes

DCT- Dopachrome tautomerase

DepC - Diethyl pyrocarbonate

dpf - Days post fertilization

Dvl- Dishevelled

EDTA – Ethylenediamine tetraaceic acid

EtOH- Ethanol

FASD- Fetal alcohol spectrum disorder

FGF - Fibroblast Growth Factor

Fzd - Frizzled

GSK-3β - Glycogen synthase kinase-3β

H_2O_2 - Hydrogen peroxide

hpf - Hours post fertilization

hrs- Hours

HPS- Hermansky–Pudlak syndrom

Hyb - Hybridization solution

L-R - Left and right

LRP - Lipoprotein-receptor-related protein

MC1R- Melanocortin 1 Receptor

MITF- Microphthalmia Transcription Factor

MS222- Tricaine methanesulfonate

NC- Neural Crest

NCC- Neural Crest Cell

NCCs -Neural Crest Cells

OCA - Oculocutaneous albinism

PAE- Prenatal alcohol exposure

PAX3- Paired box gene 3

PBS - Phosphate-buffered Saline

PBST - Phosphate-buffered Saline with Tween-20

PFA - Paraformaldehyde

PORCN- Porcupine

RA- Retinoic Acid

ROI- Region of interest

ROS- Reactive oxygen species

RPE- Retinal pigmented epithelium

RPM- Revolutions per minute

SEM - Standard Error of Mean

SHH- Sonic hedgehog

SOX10 - SRY-Box Transcription Factor 10

SSC - Saline-sodium citrate

TBS - Tris-buffered Saline

TBST - Tris-buffered Saline with Tween-20

TE - Tris-EDTA

TEM- Transmission Electron Microscopy

TH- Thyroid hormone

TYR- Tyrosinase

TYRP- Tyrosinase Related Protein

TYRP-1- Tyrosinase Related Protein-1

TYRP-2- Tyrosinase related protein-2

UV- Ultraviolet

WMISH - Whole-Mount in situ Hybridization

WT - Wild Type

Wnt- Wingless-related integration site

WS- Waardenburg syndrome

α-MCH - Melanin-Concentrating Hormone

α-MSH - Melanocyte-Stimulating Hormone

CHAPTER 1: INTRODUCTION

Animal body coloration and color patterns are multiplex phenotypical traits resulting from the interaction of numerous elements that evolve for the functioning of various roles [1, 2]. Across the animal kingdom, a large number of species rely on the colors and color patterns of their skin for various activities such as defense against predators, sexual selection and protection from UV (Ultraviolet) radiation [3, 4].

Coloration also provides valuable information about sex, maturity or availability for reproduction, and it is significant for ectothermic animals, such as fish, amphibians and reptiles, in which some color anomalies may have an effect on animal fitness [5-7]. Chromatophores are the basic functional units of body coloration, which produce vertebrate body color, patterns and eventually provide distinct phenotype for organisms [8, 9]. Chromatophores development involves many number of genes which vary according to the species, with 128 genes in human phenotypes, 243 genes in mouse and 325 genes in zebrafish phenotypes [10]. These pigment cells are derived from the neural crest cells (NCCs). NCCs are multipotent cells that originate at the dorsal neuroectodermal ridge. These cells migrate to different body sites to produce numerous cells, tissues and structures including chromatophores [11, 12]. Chromatophores are motile, large and branched, made up of many membrane bound organelles termed "chromatosomes" which contain pigment granules [13]. In higher vertebrates such as mammals and birds there is only one chromatophores type, called melanocytes, producing the pigment melanin [14]. Melanocytes are found in variety of body tissues including brain, eye, heart, inner ear and skin [15, 16]. By contrast, basal vertebrates such as fish, amphibian and reptiles and some invertebrates develop several chromatophore types which produce different colors [17]. Unlike humans, in lower vertebrates, melanocytes appear to play socio-environmental functions in addition to their direct functions in protecting the skin from UV radiation.

The chromatophores are usually dendritic in shape but polygonal, round, and oval shapes have been observed in iridophores without undergoing dendritic processes as well. Variations in cellular shapes cause to produce different colors and shades within the pigment contained chromatophores [18, 19]. Currently, seven different kinds of chromatophores have been identified in fish: melanocytes, iridophores, erythro-iridophores, xanthophores, leucophores, cyanophores and erythrophores [8, 20-22]. In the vertebrate animal body, pigment cells are scattered over the epidermis and dermis creating certain patterns. Melanocytes give rise to black, orange, red and gray color pigmentations in higher vertebrates of the animal kingdom. These cells can be found in the epidermis and the structures derived from epidermal tissue such as epithelial cells, hairs and feathers [23]. Meanwhile, melanocytes in the cold- blooded

vertebrates like fish have melanocytes distributed in dermal and hypodermal tissues. The melanocytes are also found in the epidermis of the skin and altogether result in black coloration of fish [24].

Different contributions of main two types of melanin: eumelanin and pheomelanin, cause to develop variety of pigment patterns in the skin of higher vertebrates [25]. This mechanism is mainly regulated by the down-regulation of genes involved in pigment cell development and pigment synthesizing pathways [26].

Melanocyte development and melanogenesis have been studied in terms of finding the effects of drug exposure, studying molecular pathways [27] by using zebrafish as a teleost fish model, avian embryos, murine models and *Xenopus laevis* embryos [28-32] but lack of studies have been focused on to investigate the principal aspects of the melanocyte biology such as melanocyte development, migration, arrangement and melanin synthesis over the developmental stages or until the maturation.

1.1 Zebrafish (*Danio rerio*)

1.1.1 Zebrafish as a model organism

The zebrafish (*Danio rerio*), represents a small teleost fish species classified under the family Cyprinidae [33]. Among other vertebrate and teleost fish models, *Danio rerio* is a forefront model used in a variety of research disciplines such as to understand the pathological basis of disease mechanisms and in embryogenesis and organogenesis [34-36]. The main advantages of using zebrafish embryos in research efforts could be stated as a high degree of similarity of zebrafish and mammals relating to cellular physiology and molecular mechanisms in development [37], ease of breeding and low maintenance in the laboratory environment, high fecundity (producing hundreds of eggs (~300) after every successful breeding of healthy male-female) allowing for statistically significant sample sizes, rapid embryonic development [37] and, external fertilization and external development facilitate manipulating embryos in different laboratory conditions. Further, optically transparent embryonic, larval and early adult stages allow direct examination of live cells, tissues and organ development under microscopy [38, 39], facilitation of zebrafish embryos for easy accession of drugs and small molecules, and zebrafish 26,000 entire protein-coding genes have 71% homology to the human genome and 82 % genotypes are of it, associated with human disease as counterparts [40, 41].

1.1.2 Zebrafish as a model organism for studying the melanocyte development

Zebrafish provide unique opportunities to approach the mechanisms underlying melanocyte development and melanin synthesis. Especially, viable mutant models of zebrafish offer openings for comprehending melanocyte gene function [42]. Moreover, unlike other vertebrate models, larval and early adult stages of zebrafish are optically transparent, and melanocytes and their pigmentation are conveniently visible under the microscope. Also, melanocytes of *Danio rerio* are naturally labelled with melanin, and melanocytes are analogous to melanocytes in mammals [43]. The existence of numerous genetic mutations in neural crest derived pigment cells is the biggest advantage of using this model for the analysis of genetic mechanisms of pigment cell development and melanin formation [27]. Therefore, it's a huge benefit in science for studying melanocyte development and defects in skin cells by using zebrafish as an animal model while having the capability of tracking the pigment cells in live animals. Additionally, zebrafish embryonic and early larval pigment patterns are completely established at 2 dpf (days post fertilization) and 6 dpf ages consecutively [44, 45]. As a whole, zebrafish is a valuable and efficient tool for investigating the mutations and disorders in all aspects of melanocyte development in terms of melanocyte formation, migration, arrangement, stripe formation and melanogenesis [46].

1.2 Development of melanocytes from NCCs in zebrafish (*Danio rerio*)

A key embryonic cell population in the development of vertebrates are derived from the neural crest, which arises shortly after the gastrulation of embryogenesis at the ectodermal dorsal edge of the neural plate [47]. NCCs are generated and located from the junction between the neural and epidermal ectoderm and break into numerous cell types, such as glial cells of the peripheral nervous system, connective tissues, craniofacial structures, neurons and pigment cells [48].

Induction of NCCs involves 3 major cell signaling pathways including Wnt (Wingless-related integration site), FGF (Fibroblast Growth Factor) and BMP (Bone Morphogenetic Proteins) [49, 50]. They all must be precisely orchestrated with variable spatio-temporal relationships. According to the, [49] states the necessity of intermediate levels of BMP and high levels of Wnt and FGF for proper induction of NCCs. However, much research has found that the essentiality of retinoic acid (RA), Sonic hedgehog (SHH) and Delta/Notch signaling pathways for the development of NCCs [51]. Thereafter, pre-migratory NCCs subject to an epithelial-to-mesenchymal transition (EMT), as a help to trigger onset of migration [52]. After the

specification, the NCC population is subdivided into at least 3 axial (overlapping) sub populations such as cranial, vagal/cardiac and trunk, and migrate extensively along distinct pathways as continuous waves to differentiate into a variety of derivatives [53]. In zebrafish migration of NCCs commences at around 15 hpf, initiating from cranial NC (neural crest) and progressing along the anterior–posterior length of the developing embryo in a caudal direction. NC which are located at cranial and caudal (including trunk) axial levels are important for melanocyte development [54].

1.2.1 Development of melanoblasts and migration

The melanocyte is the first pigment cell type which arises during embryogenesis in zebrafish [44]. In zebrafish, the development of melanocytes during the embryonic stage occurs directly from NCCs [55] as well as embryonic melanoblast cells, also termed as embryonic melanocyte stem cells (MSCs) (1^{st} wave of melanocytes) [56]. By contrast, early larval melanocytes are formed by the embryonic melanocyte progenitor cells derived from the NCCs (2^{nd} wave of melanocytes) as well as remaining embryonic melanocytes [57]**.** Melanocytes which formed in the early larval stage contribute to the establishment of mid-larval and juvenile pigment patterns [57]. Embryonic melanocyte progenitor cells remain until the mid-larval developmental stage of the zebrafish and contribute to the formation of adult melanocyte stripe patterns directly from the stem cells rather than migrating NCCs [58]. Additionally, some embryonic and early larval melanocytes persist until the mid-larval and adult stages [59].

Pigment cell precursors migrate from the neural crest along the dorso-lateral and ventro-medial pathways in a wave-like manner in order to generate embryonic and postembryonic melanocyte strip formation (Fig. 1.1) [56]. At approximately 30 hpf, melanocytes initiate to appear in the zebrafish embryo once cells are melanized posterior to the otic vesicle [60]. Overall, mechanisms of neural crest specification into the melanoblast cells and differentiation in to the melanocytes are conserved in mammals, chicks and zebrafish [43].

Figure 1. 1 Model of NCCs and melanocytes migratory pathways in zebrafish.

(1) The pigment cells of the melanocytic lineage migrate through the dorsolateral pathway between the ectoderm and somite. (2) Melanocyte cells migrate through the ventromedial pathway between the neural tube and somites (3) The trunk NCCs migrate through the ventromedial pathway and some of them give rise to dorsal root ganglia of the peripheral nervous system**.**

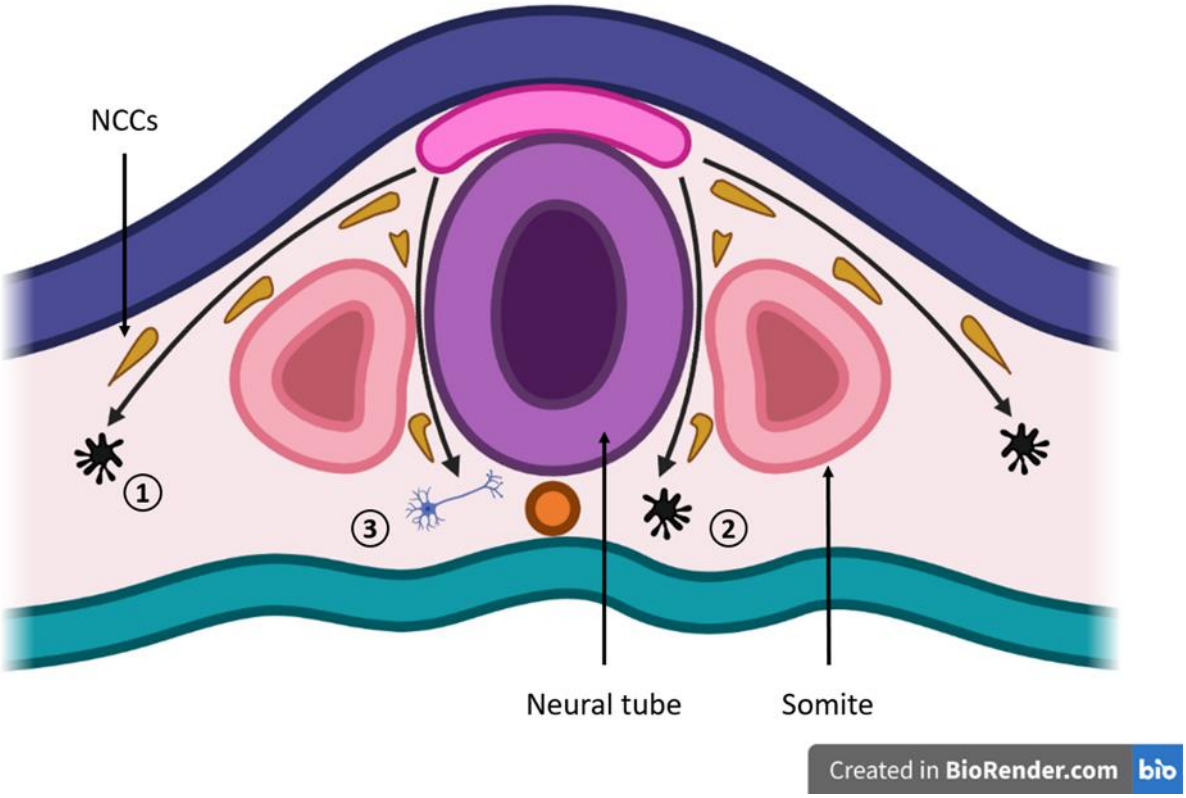

1.2.2 Intrinsic and extrinsic regulation of melanocyte development

Melanocyte specification and differentiation in zebrafish are controlled by many mechanisms which can be classified mainly as intrinsic and extrinsic factors [11, 61]. Processes involved in the transcriptional regulation of genes and silencing of some gene differentiation, taking place within the melanocyte or melanoblasts are some of the most intrinsic mechanisms in melanocyte development [62, 63]. Key intrinsic factors that regulate skin pigmentation are endocrine factors [estrogen, Melanocyte-Stimulating Hormone (α-MSH), Adrenocorticotropic hormone (ACTH), melanin-concentrating hormone (α-MCH) and endorphin), neural factors and inflammation-related factors, enzymes and transcription factors [64]. Extrinsic mechanisms involved in communication between the melanoblast and its extracellular environment include contact-dependent cellular interactions among melanocytes and adjacent cells as well as non-melanocyte lineages and signal interactions between melanoblasts and their surrounded extracellular matrices [8, 65], ultraviolet radiation and chemical drugs [66, 67].

Microphthalmia Transcription Factor (*MITF*) is the master regulator of the melanocyte lineage including melanocyte development and melanogenesis [68]. Thus, all the internal cellular signals converge on to this nodal point in order to activation of the downstream genes [69]. Loss-of-function researches have demonstrated the importance *MITF* gene function in melanocyte morphogenesis and melanogenesis [70]. The function of *MITF* gene is conserved across animal species. However, studies on dogs, hamsters, rats and quail suggest that any mutation in *MITF* causes a range of pigmentation defects including hyper pigmentation, hypo pigmentation and defects in melanocyte migration. These results indicate the necessity of *MITF* to specify cells as melanocytes [71-73]. Neural crest transcription factors of SRY-Box Transcription Factor 10 (*SOX10*) and paired box gene 3 (*PAX3*), paired box gene 7 (*Pax7*) are essential for melanocyte development and loss of these genes causes defects of pigment cells [74, 75]. *SOX10* is a determinant transcription factor for *MITFa* expression in zebrafish [76]. Moreover, Wnt signaling is recognized to be fundamental and crucial to regulate melanocyte development from neural crest via regulation of β-catenin activity [77].

The differentiated state of melanocytes is relatively similar among different organisms in the animal kingdom that bares melanocytes. Differentiated melanocytes are typically marked by three characteristics: (1) existing of black colored pigment or melanin accumulation, (2) melanin trafficking inside of the vesicles/organelles called as melanosomes and (3) dendritic morphology (mostly in mammals). The synthesis and accumulation of melanin pigment

involve several melanogenic enzymes originating from the tyrosinase related protein (*TYRP*) family, including tyrosinase related protein-1 (*TYRP-1*) , dopachrome tautomerase (Dct: also known as tyrosinase related protein-2, *TYRP-2*) and the rate-limiting enzyme, tyrosinase (*TYR*) [78, 79]. These enzymes are critical for catalyzing reactions, the ultimate production of melanin and for interactions among enzymes in order to regulate each other's interdependent activities [80]. These genes have been discovered to be expressed in presumptive melanoblasts [81, 82].

Cytoskeleton-dependent trafficking of differentiated melanocytes occurs inside melanosomes and is a very important process in vertebrates [83]. In mammals, the dispersion of melanosomes to the boundary margin of the cell is conducted by kinesin motors and it's essential for transferring melanosomes to the surrounding adjacent keratinocytes. Transportation and correct positioning of these melanosomes at the periphery of the melanosomes depends on complex molecular interactions between ras-related protein Rab-27A (Rab27A), melanophilin and myosinVa proteins majorly while the involvement of intracellular cellular organelle's interactions as well. These molecular interactions aid in the binding of melanosomes to the actin cytoskeleton. However, disruption of any of these components results in lighter body color [83].

In zebrafish, melanosome trafficking: aggregating and dispersion is mainly regulated in response to hormones and contrast changes of melanosome movements have been examined via the exposure of fish to the cyclic adenosine monophosphate (cAMP) signaling pathway stimulants or inhibitors [84]. Especially, in fish, birds and mammals, the Melanocortin 1 Receptor (MC1R) gene plays a vital role in regulating pigmentation [85] as the one and only receptor family expressed in melanocytes of mammals, by contrast, zebrafish contains three types of MCH-receptors which are homologous to the human [86, 87]. MC1R protein belongs to the receptor family of melanocortin. It's a seven-membrane G-protein–coupled receptor which responds to the melanocyte–stimulating hormone (α -MSH), when expressed on the surface of melanocytes activates the adenylyl cyclase and cyclic-AMP signaling. whereas melanin-concentrating hormone (MCH) is another peptide hormone that makes the changes in pigment granules distribution by reducing the cAMP signaling [84, 88, 89].

Thyroid hormone (TH) has been detected to regulate adult pigment patterns of zebrafish in addition to its main roles of metabolism and growth [90]. Studies have revealed that genetic activating mutation in thyroid stimulating hormone receptor (TSHR) directs to defects in melanocyte development in number (decreased) and pattern, and increase in xanthophores

meanwhile any genetic aberration of the TH synthesis and functional mutations of this receptor have shown to decrease the xanthophore count and an increase in melanocytes. Notably, this evidence suggests that TH plays an active role in repressing homeostatic melanocyte numbers [91].

Melanocyte's dendritic shape and morphology are important to its function. Especially, in humans, it is critical to transfer DNA-protecting melanosomes to adjoining epidermal skin cells or surrounding keratinocytes (tanning response). Here, melanocytes form cell projections to take on a highly dendritic appearance in order to interact with neighboring keratinocytes [92].

Melanocyte morphology of aquatic vertebrates like zebrafish is similar to that of human cells and other mammals, depending on their location even though they usually don't have a tanning response. Zebrafish epidermal melanocytes are round and smaller whereas dermal cells are dendritic in shape at immature state [93, 94]. Melanocytes in zebrafish are known to be matured at 2 dpf, and appear in a flattened morphology due to the accumulation of melanin in high levels. However, the characteristic morphology of melanocytes gets altered in response to environmental cues [14]. Melanocytes modulate its differentiated stage in response to UV exposure, hormonal changes and inhibitors and activators of melanogenic key signaling pathways and other types of stress [95].

1.2.3 Dct protein expression and importance

Dct enzyme attends the melanin pigment synthesis pathway [96, 97] and is relatively considered an early melanoblast marker in zebrafish [81]. It generally expresses in neural crest-derived melanoblasts and melanocytes as well as in non-neural crest-derived melanin generating cells of the retinal pigmented epithelium (RPE) [98, 99]. Unlike in mammals, *dct* expression could be examined 8 and 5 hrs prior to the melanin formation in the RPE and melanocytes, respectively and *dct* expression lasts in zebrafish wild-type melanocytes until around 5 dpf [100, 101].

1.2.4 Arranging the embryonic, larval and adult pigment patterns

The embryonic, larval, and adult pigment patterns in zebrafish are quite different from each other. After the melanoblast migration, the first melanocyte pattern is largely completed at 2 dpf embryonic stage (Fig. 1.2 A) [27] and over the next 12 days addition and loss of melanocytes occur minimally during the period of larval development [102, 103]. Then the

melanocyte pattern rearranges to the larval pigment pattern while fish are transforming to the larval stage. However, the early larval pigment pattern is established and completed around 6 dpf and at this stage typically melanocytes have arranged into a definite phenotypic pattern consisting of 4 longitudinal stripes: dorsal, lateral, ventral, and yolk sac stripe (Fig. 1.2 B) [45, 104]. All four stripes are laying parallel to the anteroposterior axis along the horizontal myoseptum. Dorsal stripe extends as a double row of melanocytes from the head to the tip of the tail above the brain and spinal cord along the dorsal apex of the myotomes. Melanocyte stripe patterns as a double row of melanocytes from between the eyes, over the dorsal yolk sac, and extends to the end of the tail termed as the ventral stripe. Melanocyte stripes which are organized as single rows of melanocytes at the middle level of the horizontal myoseptum in the trunk region make lateral stripes. The yolk sac band has a diamond shape configuration that accommodates at the bottom of the fish larvae, over the ventral surface of the yolk sac extending posteriorly as far as the yolk sac stump [102, 105].

The metamorphosis period of zebrafish, encompasses coordinated developmental changes consisting: changes in the body systems such as the peripheral nervous system, gut and kidneys, formation of scales, development of the adult paired and unpaired fins, and increased stratification of the skin [106] and contrast changes in melanocyte pigment patterns [107, 108]. According to the available literature and different hypothesis, the juvenile and adult melanocyte patterns develop mainly from the early larval 4 stripes melanocyte pattern of the 6 dpf larvae and additional melanoblast cells which differentiate into the melanocytes [102, 103, 109, 110]. During the metamorphosis, zebrafish life stage transforms from the embryonic phenotype to the larval phenotype around the 4 dpf and later again into the juvenile and adult forms. This process is majorly triggered by hormonal cues, especially TH [106].

The larval pigment pattern persists for around 2 weeks at which time a metamorphosis begins (larval-juvenile transition) and is gradually replaced by the adult melanocyte pattern between 2 to 4 weeks which is the time period in which the juvenile-to-adult metamorphosis occurs [46]. Stripe melanocytes appear around 14 dpf and distribute evenly on the flank region of the fish (with the arrival of 3rd wave of melanocytes). Over the next 14 days of the fish development these melanocytes combine together to form the first body stripes [46]. Following the fourth wave of adult metamorphic melanocytes, changes in pigment pattern happen dramatically such as stripes formation in the caudal and anal fins and the appearance of scale-associated melanocytes on the dorsum of the animal at 3 weeks with a marked increase in the number of melanocyte number [46]. After the establishment of the adult melanocyte pattern within the

first month of the life period, existing stripes are maintained, and new stripes are gradually added dorsally and ventrally as the animal grows. The melanocyte pattern of adult stage *D. rerio* consists of 4–6 stripes including regular two dark primary melanocyte stripes and additional secondary melanocyte stripes dorsally and ventrally to the horizontal myoseptum which do not resemble the earlier larval stripes [59, 104]. However, the mechanisms of larval and adult stripes development remain largely unknown in *D. rerio*. There is a huge research gap in the studies related to the effect of exogenous environmental chemicals and Wnt cell signaling regulators on the melanocyte pattern formation of vertebrates (zebrafish).

Proper melanocyte arrangement in the left and right (L-R) axis of the fish body is important for making a perfect pigment pattern formation in the animal body. One of the typical characteristics for defining vertebrates is the L-R symmetry of external structures and L-R asymmetry of visceral organs such as the heart, liver and pancreas [111, 112]. L-R asymmetry could be examined during embryonic development and is very crucial later in organ packaging, connectivity, and functioning at the matured adult stage. Bilateral symmetry or asymmetry of the body organs and its structures are governed by several factors: activity of Left Right Organizers (LROs) [113] and their cellular structures in the early embryonic development, signaling pathways, differences in membrane voltage potentials, patterns of gene expression, maternal factors and environmental factors [114, 115]. Many vertebrate model organisms have been used to investigate the mechanisms of L-R patterning events such as invertebrates: snails [114] and vertebrates of *Xenopus* [112], cavefish, surface fish [116], zebrafish [117] and mouse [118]. All of those studies are related to research on the patterning of organs and vasculature which are hidden beneath the skin. However, no study has been conducted on L-R patterning of melanocytes focusing on fish, whereas only one study has been carried out yet using *Xenopus laevis* embryos representing vertebrates [119].

Figure 1.2 Development of melanocyte pigment cell pattern in zebrafish (*Danio rerio*).

(A) Embryonic melanocyte pattern, where the first melanocyte strip phenotype could be observed at 2 dpf (B) Early larval melanocyte cell arrangement is complete at 6 dpf, and is mainly built up of melanocytes, arranged into four stripes: dorsal stripe (DS), lateral stripe (LS), ventral stripe (VS), and the yolk sac stripe (YSS). (Scale bar:100 µm)

1.3 Importance of RPE in research of melanocyte morphogenesis

In any organism visual system is very delicate and sensitive compared to the other body systems in vertebrates [120]. Inasmuch, eyes are used as a model organ to investigate how exogenous chemicals and other extrinsic factors affect organ development [121]. Presently, the optical system of zebrafish has become useful in modeling vertebrate diseases because of their rapid eye development, conserved structural and functional similarities with other vertebrate eyes: [122] including morphogenesis, molecular mechanisms, transcription factors involved in eye development and retinal histology, [123, 124] and, eyes are relatively large and easily accessible [125]. The development of zebrafish optic vesicles emerges first at around 10 hpf and starting at around 24 hpf, initiation of melanin synthesis in the RPE becomes apparent [126]. By 48 hpf, morphogenesis of the eye is largely complete in zebrafish but proceeds to further neurogenesis of some structures and is fully functional at around 5-6 dpf [127, 128]. Eye formation is complete at 6 dpf developmentally meanwhile melanocyte formation begins first from the RPE, followed by appearing on dorsolateral skin. This RPE is a single layer made up of cuboidal epithelial cells that lies posterior to the photoreceptors in the retina [129], between the outer nuclear layer of the retina and the choroid [127]. It's recognized as the most sensitive layer of the retina performing vital functions including the transport of nutrients and ions to photoreceptors and removing waste products, maintaining the photoreceptors and involving to regenerate photo-pigment [130]. However, apart from the above-mentioned roles, RPE is known to play a protective vital function in absorbing the excess light from the photoreceptors and the entire retina as a safeguard from light-generated oxygen-reactive species by composing with densely packed melanin-contained melanosomes [131, 132]. Any interruption in this key function could drive to deterioration of the retina, destruct the photoreceptors and eventually lead to blindness. Albinism and age-related macular degeneration have been detected in patients due to the changes in RPE pigmentation with aging [133]. Therefore, these aspects provide an opportunity for using RPE of patients who are having defects in vision, to screen and diagnose eye conditions, identify the ocular defects and evaluate treatment response [134]. To study the melanin defects in RPE, melanosome density and melanin content could be investigated using eye imaging techniques at the clinical and pre-clinical levels in patients as well as using animal models for research and enhancing patient care [135]. However, there is no comprehensive study has been carried out so far on the effect of fetal alcohol spectrum disorder (FASD) and Wnt regulatory chemicals on melanocyte

development in RPE. In this study, we are attempting to investigate how early embryonic exposure to alcohol and Wnt regulatory chemicals affect zebrafish RPE formation.

Figure 1.3 Panel illustrating the lateral position of the eye and lens protruding from the optic cup in the embryonic stage of zebrafish at 2 dpf.

Stereo-microscopic image of the eye of live zebrafish at 2 dpf embryonic stage (A). Outermost layer of the zebrafish eye is covered with black colored RPE cell layer. Toluidine blue stained transversal histological section (thickness – 300 nm) of the optic cup (B) at 2 dpf embryonic zebrafish, which illustrates the internal neural layers of embryonic eye. The histological micrograph further shows the location of ciliary marginal zone (CMZ) at the tip of the neural retina close to the lens (B).

Abbreviations: L- Lens; NR- Neural retina and RPE- Retinal pigmented epithelium. Scale bars: (A) 50 µm and (B) 1000 nm.

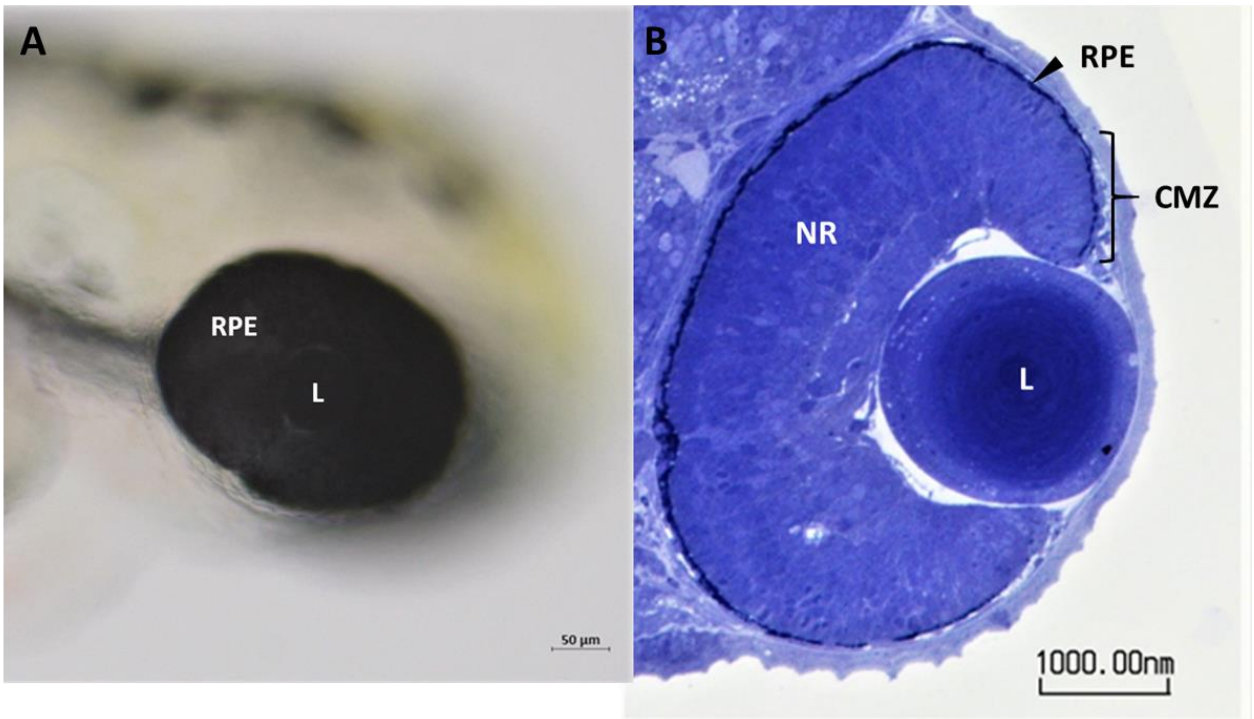

1.4 Melanocyte development in human and pathogenesis of defects

The life cycle of melanocyte development in humans can be categorized into several steps: specification of NCCs into melanoblasts, migration and proliferation of melanoblasts, differentiation of melanoblasts into melanocytes, maturation of melanocytes, transport of mature melanosomes to keratinocytes and cell death [136]. NCCs which reside at cranial and trunk regions have been found to rise into melanocytes in human skin. Mature melanocytes are oval or fusiform in shape and smaller than keratinocytes. It could be recognized by the characteristic dendritic shape and the presence of the same melanogenic specific proteins as mentioned in zebrafish [137]. Approximately human skin consists of 1,200 melanocytes per mm^2 of melanocyte density independently of the human race [138]. In humans, melanocytes exist in the basal layer (the stratum basale) of the skin's epidermis, stria vascularis of the inner ear, bones, heart, hair, the middle layer of the eye, cochlea, adrenal gland and pigment-bearing neurons of meninges [139, 140]. Melanocytes are found to be closely associated with keratinocytes in the ratio of 1: 10 in the epidermal layer and form the epidermal melanin units [141]. The relationship between the differentiated dendritic melanocytes and the keratinocytes supports the transferring of melanin-contained melanosome granules into the keratinocytes and accumulating above the keratinocyte nucleus. This process is important for the skin cells' photoprotection and for determining the skin color [142]. However, the exact mechanisms of determining the ratio of keratinocytes and melanocytes and transferring melanosomes to keratinocytes have not been investigated yet.

Human melanocyte development is mainly under the control of keratinocytes assisting with paracrine growth factors, cell adhesion molecules [143, 144], hormones [145], signaling pathways and dermal fibroblasts secreted factors [146, 147]. Pheomelanin and eumelanin are the two major types of melanin produced in the melanosomes and the pigmentation type is decided by the availability of substrates and the function of melanogenic enzymes on melanin synthesis [78]. Skin tone of different ethnic groups and hair color are basically determined based on the eumelanin content of the skin respective to the ratio between eumelanin: other melanin and eumelanin: pheomelanin in turn [148, 149]. Eumelanin has an increased ability to neutralize the reactive oxygen species (ROS) and found to be more effective in terms of photoprotection than the reddish pheomelanin [150]. Melanosome development has been classified into four stages in humans: Stage I (premelanosomes): melanosomes consisting of either round or small vesicles with an amorphous matrix premelanosomes, stage II: elongated

shape, organized, structured fibrillar matrix, stage III: melanosomes are elliptical or ellipsoidal initiating the melanin production and depositing melanin on protein fibrils, becomes brown color and the last stage IV: whole melanosome fills with melanin and color ranges from dark brown to black [151, 152].

The embryonic origin of human skin melanocytes is similar as mentioned in the zebrafish melanocyte development and other vertebrates. Melanocytes occupying the head region originated from the cranial NCC population meanwhile trunk NCC are responsible for the melanocyte formation in the remaining parts of the human body [153]. Both trunk NCC populations which are migrating along the nerves in dorso-lateral and ventro-medial pathways contribute to generating the melanocytes as occurring in the zebrafish [154]. It has been found that NCCs which are migrating along the ventro-medial path is maintained as precursor cells that are capable of differentiating into melanocytes later [136]. Melanoblast migration takes place between the 6 and 8 weeks of human embryonic development [155]. Altogether, melanocytes in the human skin originate directly from NCCs along the dorsolateral migratory pathway or arise from ventrally migrating multipotent progenitor cells of melanoblasts which multiply, disperse and reach their final destinations in the epidermis and hair follicles for differentiating into melanocytes [63]. Thus, it has been hypothesized that epidermal melanocytes are molecularly different from dermal melanocytes due to the double origination [156]. Around 12-13 weeks the majority are localized in the epidermis [157]. In humans, it is still unknown whether all the melanocytes and differentiated melanoblasts reach the epidermis. Dermal melanocytes have been observed only during fetal development of humans, but no evidence has been detected after birth. The bulge region of the hair located at the bottom of the hair follicle acts as a storage space of pluripotential and undifferentiated cells which are capable of developing into keratinocyte progenitors as well as melanoblasts for the hair as well as for the epidermis [158].

Molecular markers which are involved in melanocyte development in the early stages of human development are similar in zebrafish [159, 160] as well as Wnt/Frizzled (Fzd) protein/β-catenin-signaling pathway and *MITF* expressions are found to be essential and the main governing factors for melanoblast differentiation, proliferation, melanocyte development and survival. In addition to that, different genetic and epigenetic factors derived from keratinocytes, melanocytes, fibroblasts and pituitary gland, as well as environmental factors influence human melanocyte development during the embryonic period [161] The exact mechanism for human melanoblast migration is still mysterious and to be discovered [162].

1.4.1 Etiology of human pigment disorders

The melanin synthesis process occurring in melanosome granules of melanocytes plays a crucial role in mammals including humans in protecting the skin from the destructive effects of ultraviolet (UV) radiation. Numerous genetic and environmental factors affect each and every aspect of regulating melanocyte development: specification, proliferation, differentiation and migration. Any error of these factors that are involved in regulating melanocyte development results malformation in melanocyte counts and melanin formation, eventually cause for arising skin disorders showing abnormal skin pigmentation in excessive or deficient amounts of melanin [163]. Human pigmentation anomalies could be categorized based on the genotype, congenital or acquired presentation, defects in melanin synthesis in the skin including hyper melanosis and hypo melanosis, effects on melanocyte number (hypoplasia or hyperplasia) and effects on melanocyte function [164]. Melanin defects in color, quantity, and pattern are display through the most visible markers of human body organs, such as skin, hair, and eyes. However, etiology of all of these human pigmentation disorders, is interrelated with melanocyte genetics and appears as clinical phenotypes. Abnormal melanin formation produces symptoms of skin wrinkling and laxity, which directs for aging skin [165]. Human skin color and tanning response mainly depend on the amount of melanin production and cellular distribution of melanin [166]. Congenital pigment abnormalities of hypopigmentation are caused by a result of losing melanocytes during embryonic or fetal development in human. This condition is termed as melanocyte hypoplasia, characterized by a localized reduction in melanocytes. Piebaldism is one of the best examples of this and is associated with loss of function or deletion mutations in the transcription factor SNAI2 or in the tyrosine kinase receptor KIT. Phenotypically it expresses as skin and hair with a lack of melanin, most frequently appearing on the head and ventral trunk regions [167, 168].

Mutations of *PAX3*, *SOX10*, Endothelin Receptor Type B (*EDNRB*), Endothelin-3 (*EDN3*) and *MITF* melanogenic pathway genes that encode for proteins on melanocyte development, cause Waardenburg syndrome (WS) exhibits ocular hypopigmentation linked with congenital hearing loss and cutaneous hypopigmentation. This syndrome has been identified to range into four principal types, WS1–WS4 on the clinical and genetic basis. Mutation in *SOX10* causes Yemenite deaf-blind hypopigmentation syndrome (YDBS), displayed by deafness with regional hypopigmentation and hyperpigmentation [169, 170]. Albinism is caused by cell migration disorder of the neurocytes. Hypopigmentation is also resulted from altered

melanocyte function. Melanin synthesis and distribution are controlled by different genes including *TYRP-1*, *TYRP-2*, and *MITF*. Any downregulation of these genes/protein transcription factors directs to abnormalities in melanin pigmentation consisting of reduced melanin content and altered distribution of cytoplasmic melanin pigment granules but not any change in the melanocyte counts. These mutations cause disorders which are possible to inherit recessively to the next generation [171]. Oculocutaneous albinisms (OCAs) is one of the dominant hypopigmentation disorders caused by abnormal melanin production which results sequence of consequences in the melanin-producing organs such as severe reduction to complete absence of all skin, hair, and eye pigmentation with reduced visual acuity. Seven subtypes of OCA1-OCA7 have been distinguished based on the molecular etiology and all inherit in an autosomal recessive manner [172]. It has been estimated that 40 % of global prevalence for OCA1 [173] and all of these conditions are originated through the rise of mutations in different genes, especially *TYRP* encoding genes. Dominant types are OCA1 (*TYR*) and OCA3 (*TYRP1*) [174]. Hermansky–Pudlak syndrom (HPS) is an oculocutaneous hypopigmentation disorder caused by the association of mutated seven human *HPS* genes: *HPS1-HPS7* which are involved in regulating the lysosome-related organelle movements. These genetic mutations of autosomal recessive disorder result in abnormal melanosome formation, movement, or defects in melanosome transferring to keratinocytes. Clinical symptoms have been associated with hypopigmentation and impaired visual acuity [175, 176]. Congenital hyperpigmentation anomalies display increased amounts of melanin within the melanocytes or surrounding keratinocytes without increasing melanocyte counts. This condition is also known as melanotic hyperpigmentation. Familial progressive hyperpigmentation (FPH2), is distinguished by increased production of melanin pigmentation. *KITLG* gene encodes for the protein singling molecule which regulates melanin production through the receptor KIT. Mutations in *KITLG* gene are associated with both Familial progressive hyperpigmentation and hypopigmentation [177]. Additionally, dysregulation of RAS-MAPK signaling hyperpigmentation (Legius syndrome, NF1, LEOPARD syndrome, and Noonan syndrome), mutations of *KRAS*, *BRAF*, *MAP2K1* or *MAP2K2* genes are associated with human hyperpigmentation disorders [178, 179].

1.4.2 Mechanisms of pigment abnormalities of human

Oxidative stress caused by the accumulation of cellular ROS is found to be one of the most effective mechanisms in generating skin pigmentation disorders [180]. Oxidative stress develops when increasing the antioxidant capacity of oxygen-based free radical families within the cell as hydrogen peroxide (H_2O_2). ROS could be produced mainly by exposure to extracellular stimuli such as UV irradiation [181] and as by-products of intra-cellular metabolism including mitochondrial respiration [182]. In contrast, skin pigmentation is affected by oxidative stress leading to mitochondrial DNA mutations and mitochondrial dysfunction [183]. Nucleic acids (DNA) and proteins contain in the skin, are very sensitive to oxidative stress. Therefore, these ROS could damage the cellular macromolecules and ameliorate the pigmentation defects [184]. Studies have disclosed that ROS damage the melanocyte *TYRP* and can cause defects in skin pigmentation [185]. According to the clinical findings, it was proved that many congenital skin diseases associated with abnormal skin pigmentation are linked with mutations in DNA affecting mitochondrial function which are governed by different molecular mechanisms [186]. Skin hypopigmentation is caused by increased levels of ROS and antioxidant enzyme deficiency. Moreover, ROS accumulation directs to generating autoantigens, which is a main factor that governs the CD8+ T cell-mediated destruction of melanocytes. The downregulation of DNA repair mechanisms including the repair of nucleotide excision and double-strand breaks as well as the accumulation of DNA damages are considered to drive the skin pigmentation defects [187]. Most of these defects are associated with mutations of encoding proteins that participate in many aspects of DNA metabolism [188] including DNA replication and cellular responses to DNA damage, nucleotide excision repair, interstrand crosslink repair, telomere maintenance and DNA polymerase [189]. Telomeres are located at the end of chromosomes and protect the linear chromosome ends. Short telomeres have been found to be associated with pigmentation defects in humans [190]. Skin hyper melanosis is accompanied with mutations in the telomere maintenance machinery and genetic mutations in the telomere where the encoding for the proteins involved in telomere DNA repair [191]. These mutations lead to the loss of telomeres and defects in telomere sequences and maintenance. Especially the mutations of dyskerin pseudouridine synthase 1 (*DKC1*) and lamin A (*LMNA*) genes result in abnormal protein production while manifesting abnormal skin pigmentation [192]. The cutaneous neuroendocrine system also causes hyperpigmentation and hypopigmentation such as

aberrations of serum levels of melatonin and sex hormones: particularly testosterone and estrogen levels [193].

1.5 Effect of environmental factors on melanocyte development of humans

A handful of studies have been conducted to find out the environmental interaction in embryonic melanocyte development, but environmental factors play a major role in the arising the defects in melanocyte development via the alteration of gene expression. Most the clinical studies have revealed the acquired abnormal skin pigmentation effected by environmental factors rather than an environmental influence on the arising of congenital defects of melanocyte development [194, 195]. Multiple environmental factors can contribute to change the skin pigmentation including UV exposure, certain cosmetics, nonsteroidal anti-inflammatory drugs, certain antibiotics (sulfonamides and tetracyclines), pain relievers, diuretics and some psychoactive medications, estrogen-containing oral contraceptives and antiepileptic agents (mainly hydantoins) [196, 197]. Further, an extensive intake of drugs containing heavy metals consisting of silver, bismuth, arsenic and gold. Some drugs can cause to stimulate the melanogenesis pathway which makes hyperpigmentation of the skin [198]. Some external drugs promote the secretion of estrogen, progesterone, and MSH hormones and which make elevated deposition of melanin in the epidermis and dermis, and increase the surface area of melanocytes without any count change. Melanocyte number and melanin synthesis are enhanced in tanning response against UV radiation [199].

1.5.1 Effect of ethanol on melanocyte development

Ethanol is an organic compound that acts as an environmental teratogen in the human body depending on several factors such as duration, frequency, amount of exposure and method of ethanol exposure [200-202]. Ethanol is one of the commercial names for alcohol and is being used as the most popular psychoactive drug worldwide so far. Ethanol is recognised as the most prominent aetiological factor for alcohol-induced birth defects. Maternal exposure to ethanol during the pregnancy period is a serious health problem because it has negative effects on the developing embryo. Today, alcohol-induced birth defects are collectively termed FASD [203] and are described as birth defects associated with prenatal alcohol exposure (PAE), which includes general growth retardation and abnormalities of craniofacial structures, heart and kidney body organs and central nervous system (CNS). These malformations can lead to

lifelong disabilities of the affected animal. Maternal alcohol consumption and the fetal pathological outcome depend on several factors: maternal drinking patterns, maternal body metabolism, maternal age, health, genetic make-up, nutritional status and timing of alcohol consumption during the pregnancy period [200, 204]. Ethanol can affect three main stages of animal development: 1) gametogenesis, 2) preimplantation and 3) gastrulation of embryogenesis, and it can lead to epigenetic modifications for the manifestations of FASD [205]. Ethanol exposure effects on epigenetic mechanisms: DNA methylation, posttranslational histone modification and noncoding RNA disruptions [206]. Ethanol involves in the up-regulation or down-regulation of microRNA (miRNA) in the brain which leads to impairment of cell cycle induction and stem cell maturation, changes that could result in abnormal CNS development [207]. Ethanol competitively affects the RA pathway and causes varying degrees of developmental malformations in the craniofacial region of the vertebrates. Moreover, the SHH signal transduction pathway is also affected by ethanol and leads to characteristic midline phenotypes of cyclopia, neural tube defects and neural crest specific–cell death [208]. Embryonic alcohol exposure interferes with the insulin signalling pathway, which leads to neurodevelopmental abnormalities such as impaired viability due to altered neurodevelopmental signalling pathways, [209] and reduced Wnt signalling . Alcohol exposure inhibits some enzymes that are produced in the Golgi apparatus, a phenomenon that leads to cytoplasmic retention of neural cell adhesion molecules, impairs cellular interactions and causes cellular migration-related errors [210]. These changes result in defective neuron–glia interactions, synaptogenesis, neuronal migration, growth and morphogenesis [211]. The above-mentioned cellular defects are initiated with the formation of reactive free radicals such as the superoxide anion radical ($\cdot O_2$), H_2O_2 and the hydroxyl radical ($\cdot OH$) within the cell during alcohol metabolism. During neurogenesis, these highly reactive agents can lead to cascade reactions that inhibit cell differentiation, disturb cell–cell interactions and impair cellular metabolism. These changes could then lead to uncontrolled apoptosis [212, 213].

According to the clinical findings, PAE has been found to result in impaired vision. However, ophthalmological examinations have addressed that it is caused by alcohol-induced ocular abnormalities such as retinal dysplasia, optic nerve hypoplasia, microphthalmia, coloboma of the iris and choroid, and tortuosity of the retinal vessel etc. However, no evidence has been declared yet on the association of teratogen effect on retinal layer development and its' visual acuity [214, 215]. In contrast, few studies have been focused on investigating the effects of embryonic ethanol exposure on retinal development using zebrafish as a model organism.

Those studies have highlighted several findings, such as anatomical changes within the retinal cell layer as well as toxic effects of ethanol on photoreceptors, and predicted that these defects can directly damage visual function [216, 217]. Additionally, it has been found that alcohol exposure results in increased retinal cell death and abnormal proliferation but no effect on retinal cell differentiation induction [218]. This same study could have revealed that effective nutrient supplements like retinoids- RA and folate- Folic Acid (FA) are able to rescue the defects of the retinal cell layer. However, no study has exactly focused on the effect of alcohol or any other teratogen on the development of pigment in the RPE layer, especially from the perspective of FASD.

1.6 Mode of action of ethanol teratogenicity between mother and fetus

The chemical and physical properties of ethanol facilitate rapid diffusion from mother to fetus across the placenta and dispersion throughout the body water resulting in the presence of ethanol in fetal circulation. Maternal ethanol exposure results in the rising of maternal blood alcohol concentrations (BACs), followed by ethanol that can be present in the fetus within 1 min and reaches the maternal fetal circulation levels within 1h [219]. However, the gradient of increasing the blood ethanol concentration in the fetus is comparatively slower than the increase in maternal blood ethanol concentration but ultimately reaches to an equilibrium within the range from 0.005 to 0.210 g dl^{-1} at the delivery time. The ethanol entered into the body fluids in different concentrations is metabolized by enzymes in oxidative and non-oxidative pathways at the placenta, fetus, and neonate as the same as in the mother. Around 90 –95 % of the ethanol metabolism occurs in the liver by the involvement of the enzyme alcohol dehydrogenase (ADH) which converts ethanol into acetaldehyde [220] while Cytochrome P450 enzymes (CYP2E1) catalyze the remaining ethanol in a microsomal system [220]. However, studies have found that the human placenta doesn't play a significant role in the oxidative metabolism of ethanol because of placental ADH isozyme is considered to have low affinity and a reduced oxidation capacity for ethanol [221].

Ethanol which is contained in the fetal circulation is mainly metabolized by the ADH enzyme which can be detected around 2 months of gestation in the fetus [222]. The enzyme which has the highest oxidation capability for ethanol is CYP2E1, which begins to express in the fetal liver at 19 to 24 weeks of gestation [223]. The P450 enzymes contained in the fetal liver microsomes also aid in oxidizing ethanol mixed in the circulation [224]. Ethanol accumulation

and toxicity start increasing with the start of fetal swallowing by the 11th week of gestation while osmotic differences direct the absorption of amniotic fluid into the fetal circulation via the amnion [225]. These mechanisms of fetal swallowing of ethanol along the amniotic fluid and reabsorbing back into the circulatory system across the intramembranous pathway create prolonged exposure of the fetus to ethanol. Renal and pulmonary excretions are the two major mechanisms that the fetus removes the ethanol from the body since it has reduced capability of ethanol oxidation [226].

1.7 Wnt signaling pathway

Wnt signaling pathways play crucial roles in each and every aspect of the embryonic development of vertebrates including cell-fate specification, proliferation and differentiation, cell polarity and morphogenesis [227, 228]. The Wnt family, which includes 19 members in mammals and mice, is essential for embryonic development and tissue homeostasis [229] whereas the zebrafish genome consists of 25 Wnt genes due to the teleost-specific whole-genome duplication [230]. Wnt signaling begins once Wnt ligands corporate and bound with different cellular receptors and coreceptors which are located in the cell membrane of the responding cell including seven-transmembrane receptor Fzd, lipoprotein-receptor-related protein (LRP5/6), PTK7, RYK and proteoglycans. It leads to receptor activation and directs the transduction of the cellular signal towards the cell membrane and the nucleus [231]. Wnt proteins are secreted with the aid of Porcupine (PORCN) protein after the process of acylation [232]. Here, secreted ligands bind to the Fzd and LRP 5/6, activating the intracellular protein Dishevelled (Dvl). Then it attaches to the C-terminus of Fzd while recruiting Axin protein from the β-catenin destruction complex in the cytoplasm, thereby promoting the initial phosphorylation of LRP6 [233, 234]. Further phosphorylation of LRP6 by casein kinase 1 (CK1α) and glycogen synthase kinase-3β (GSK-3β), forms a cluster that consists of LRP6, Dvl, and Axin [231]. Phosphorylated LRP5/6 leads to inhibition of the β-catenin destruction complex, which is composed of a collection of proteins: Axin, GSK-3β, and adenomatous polyposis coli (APC). In the absence of Wnt signaling, β-catenin undergoes the ubiquitination process [235]. This mechanism is used to regulate the β-catenin level in the cytoplasm via phosphorylation of β-catenin by forming the APC-Axin-GSK-3β-catenin complex. Later, the phosphorylated β -catenin would be removed through the ubiquitin-proteasome system [236]. Inhibition of the β-catenin destruction complex leads to stabilization and accumulation of β-

catenin in the cytoplasm and is translocated to the nucleus where it generates the transcription of the Wnt target genes via binding to T-cell factor/lymphoid enhancer-binding factor (TCF/LEF) like transcription factors, Creb-binding protein or/and p300 protein [227, 237].

Since the Wnt signaling pathway acts an important role in regulating the main aspects of cell development, abnormal Wnt signaling is detrimental and obstructs the proper development and function of body organs and systems in any organism [238]. Therefore, Wnt signaling inhibitors and activators are administered as scientific tools for regulating the over-expression and reduced-expression of Wnt signaling in turn, to regulate the protein-protein interactions and disease progression [239]. Specific sites of Wnt signaling inhibition include the Fzd protein, the Dvl protein, the β-catenin destruction complex, nuclear β-catenin, and the enzymes PORCN and Tankyrase (TNKS) [240-243].

LiCl (Lithium Chloride) is one of the most prominent Wnt signaling activators that work on inhibiting the GSK-3β enzyme, which normally interrupts the formation of the β-catenin destruction complex, permitting translocation of β-catenin into the nucleus to participate in gene transcription and expression [244]. Wnt-C59 is a strong PORCN inhibitor. This protein includes for the membrane-bound O-acyltransferase (MBOAT) family. However, the inhibition of the Wnt signaling pathway is caused by the obstruction of the palmitoylation mechanism of the Wnt protein, conducted by the PORCN enzyme [245].

Figure 1.4 Schematic representation of the canonical Wnt signal transduction pathway.

(Left) The destruction complex of Axin, APC, GSK-3β, CK1α and β-catenin is formed when the Wnt ligands are not present in the cytosol and β-catenin is phosphorylated by CK1α and GSK-3β. (Right) In the presence of Wnt ligands, signaling pathway is stimulated by recruiting Dvl and Axin proteins to the cell membrane and binding to the receptors (Fzd) and co-receptors (LRP5/6) consecutively. This process allows for stabilization of β-cat in the cytosol and translocate into the nucleus for signal transduction.

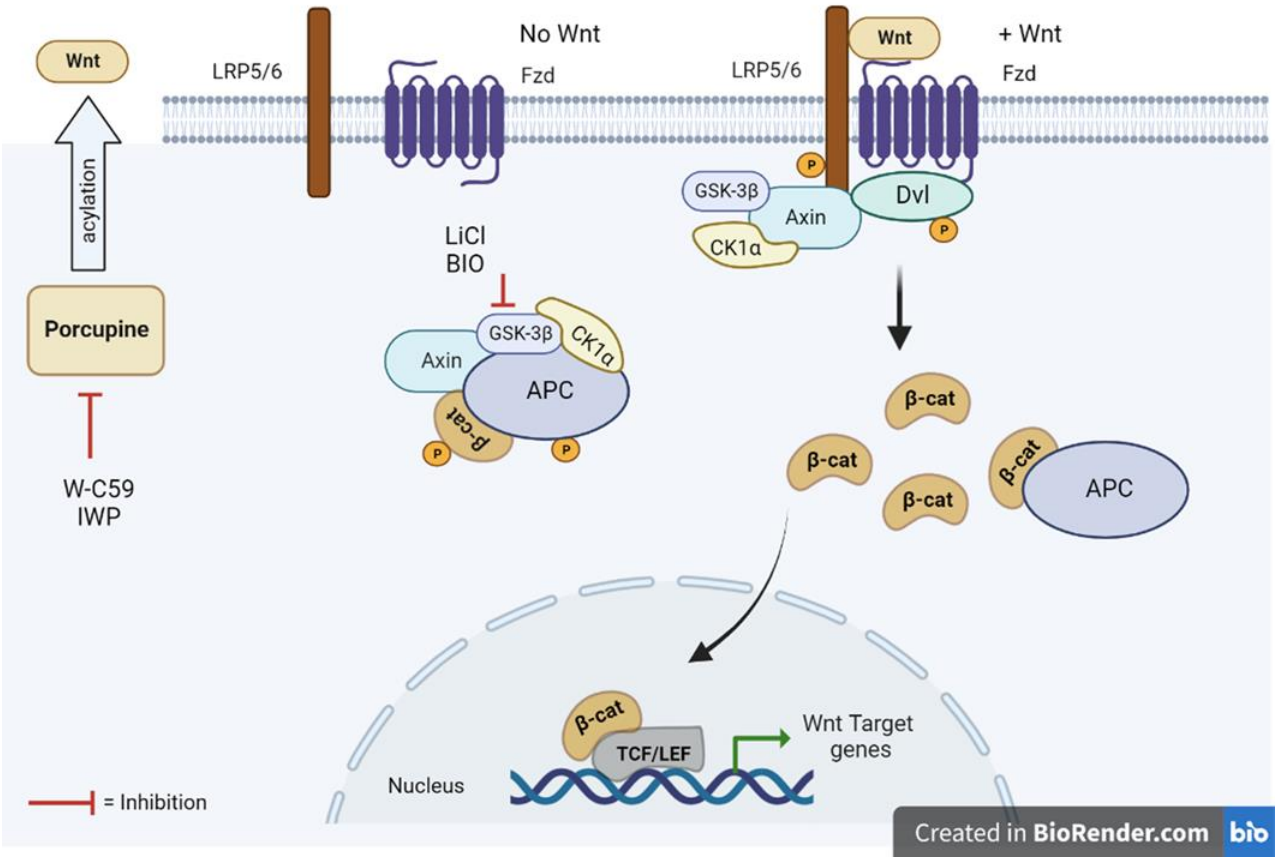

1.7.1 Wnt pathway on Melanocyte development

Wnt signaling plays a critical role in neural crest induction, NCCs specification, NCCs differentiation and melanocyte development. Especially, *Wnt3a* play a critical role in stimulating the generation of NCCs into melanocyte cells and without this protein NCCs are unable to differentiate into melanocytes [77, 246]. *Wnt3a* signals cause to increase in the melanocyte numbers by promoting melanoblasts to melanocytes, while *Wnt3a* and β-catenin are crucial for raising the differentiation of NCCs into melanocytes [31, 247]. Moreover, *Wnt3a* maintain and regulate the *MITF* activity of melanoblasts, in order to promote melanoblast differentiation into melanocytes [31]. The binding of Wnt ligand proteins to cellular membrane receptors directs to enhance the stability of β-catenin residing in the cytoplasm. It makes the translocation of cytoplasmic β-catenin into the nucleus and regulates the transcription of *MITF* through the interactions with *LEF/TCF* transcription factors [248]. Studies on melanocyte development revealed that β-catenin and *LEF1* cooperatively regulate the expression from the *MITF*-M promoter via the binding sites of *LEF1* [249]. Increased expression of β-catenin can lead to stimulating the melanoma condition, due to the effect of *MITF* expression [250]. *PAX3*, *CREB*, *LEF1*, Onecut-2, SOX10 and *MITF* protein itself bind to the *MITF*-M promoter and regulate *MITF* transcription [248].

Dickkopf 1 (DKK1) is known as an inhibitor of the WNT pathway. Melanocyte development and its' entire functions are inhibited by DKK1 through the downregulation of the expressions of β-catenin, GSK-3β, *MITF* and proteinase-activated receptor-2 (PAR-2) [251]. DKK1 protein mainly antagonizes LRP5/6 via binding and eventually inhibits the entire transduction of Wnt cell signaling [252]. The importance of this regulation has been shown in modulating the pigmentation process via dermo-epidermal intercompartment communication.

CHAPTER 2: OBJECTIVES, RATIONALE AND HYPOTHESIS

Objective

Animal body coloration and color pattern formation are determinant factors of animal survival. Chromatophore stem cell formation, differentiation, migration, and arrangement are crucial processes of coat color formation in animals. Despite the other chromatophores in animals, melanocyte development is very important for all vertebrates as it's the main chromatophore type as well as the only pigment cell type found in mammals. Hence, any defect in the mechanisms of the melanocyte development pathway results color and color pattern anomalies. Environmental factors and signaling pathways could have a potential effect on melanocyte development in both skin and the melanin-contained body organs. The effect of maternal ethanol exposure is one such occurrence, which has not yet been investigated that may influence melanocyte development. Therefore, my first objective was focused on understanding melanocyte development and patterning: density, phenotypic characteristics, migration and arrangement of melanocytes using the zebrafish as a model organism. Next, the impact of early embryonic ethanol exposure and Wnt regulatory chemicals on melanocyte development and patterning was investigated. My second objective was aimed to investigate the effect of the above-mentioned environmental factors on melanin pigment development. In this objective, it was mainly focused on examining the melanogenesis in the eyes as one of the melanin-contained body organs in zebrafish, to determine the expression of the melanogenic markers of *dct* and *Wnt3a,* and overall melanin synthesis of the fish upon the exposure of ethanol and Wnt signaling pathway modulators at the embryonic stage.

Objective 1: To understand the melanocyte development: density, phenotype, migration and arrangement of melanocytes of zebrafish.

2.1 Rationale for objective 1

The study of melanocyte pigment development has great value in cell biology and biochemistry. Furthermore, which provides a therapeutic approach to disclose the number of human diseases resulted by defects of melanocyte development. The formation of melanocytes from the neural crest requires a common set of cellular processes. The cells must migrate appropriately in order to their distribution is correctly patterned. Various intrinsic and extrinsic factors control the differentiation and proliferation of pigment stem cells during and after the migration, as well as those factors regulate and maintain melanocyte survival until and after

the maturation. Melanocyte development is a complex process and is tightly regulated by several genetic and epigenetic factors. Alcohol is known as the most abused drug among other various environmental factors and it has been identified to regulate melanocyte development. Meanwhile, the Wnt signaling pathway plays a crucial role in each and every aspect of the melanocyte development process. In order to addressing the first objective of my project, several aspects of melanocyte development were analyzed against ethanol, Wnt activators and inhibitors. Phenotypic-based screening along with the zebrafish developmental stages was conducted under stereo-microscopic observations as well as utilizing the microscopic software tools for examining the defects in melanocyte development of the fish body. Melanocyte density, morphology (size and shape) and distribution (migration and arrangement) were determined at definite key developmental stages and distinct regions of the zebrafish body.

2.2 Hypothesis for objective 1

We hypothesize that early embryonic exposure of zebrafish, to ethanol and Wnt signaling regulatory chemicals (activators and inhibitors) has an effect on melanocyte development: density, phenotype, migration and arrangement of melanocytes of zebrafish.

2.3 Sub-objectives of objective 1

1. To analyze the melanocyte density in zebrafish upon differential chemical exposure.
2 To examine the morphology and morphometric differences of melanocytes upon differential chemical exposure.
3 To analyze the migration and arrangement differences of melanocytes upon differential chemical exposure.

Objective 2: To decipher the effect of ethanol and Wnt signaling interactions on melanogenesis: Insight from zebrafish (*Danio rerio*)

2.4 Rationale for objective 2

Melanin is the primary pigment of humans generated by the melanogenesis pathway. Which is responsible for arising the color and development of many body organs including the eyes. Further, melanin pigment is acting as an excellent photo-protectant in vertebrates. However,

defects of this pathway result many disorders with hypopigmentation, hyperpigmentation and unpigmented melanocytes. Especially, PAE has been found to generate defects in vision with ocular abnormalities in infants. Melanocyte development and melanin production are initiated and regulated by the number of signaling systems and transcription factors. Among them, the *Wnt3a* gene has been found to be implicated in several aspects of melanocyte physiology, from developmental lineage differentiation to subsequent maintenance of melanocytes. Moreover, the expression of *dct* gene is essential to the development and survival of melanocytes by synthesizing enzymes in the melanogenic pathway.

However, no studies have been focused on investigating the effect of ethanol and the Wnt signaling pathway on melanin synthesis using the zebrafish as a model system. To investigate the second objective of this study, several techniques were used such as stereo-microscopic software tools, spectrophotometric absorbance measurement, toluidine blue-staining, cryosectioning, transmission electron microscopic (TEM) imaging, and whole mount insitu hybridization (WMISH).

2.5 Hypothesis for objective 2

We hypothesize that early embryonic exposure to ethanol and Wnt signaling regulatory chemicals (activators and inhibitors) affect the development of melanocyte precursor cells and melanogenesis in zebrafish.

2.6 Sub – objectives objective 2

1. To analyze the melanin intensity in zebrafish upon differential chemical exposure.
2. To investigate the melanin pigment development in RPE layer in zebrafish upon differential chemical exposure.
3. To determine the melanin formation in zebrafish upon differential chemical exposure.
4. To investigate the gene expressions of *dct* and *wnt3a* melanoblast markers upon differential chemical exposure.

CHAPTER 3: MATERIALS AND METHODS

3.1 Fish Husbandry (*Danio rerio*)

3.1.1 Zebrafish Rearing and Breeding

3.1.1 (a) System Maintenance

Wild-type zebrafish (WT-AB) were maintained in the Tecniplast rack system at the Bannatyne campus, University of Manitoba and the zebrafish breeding colony was originally purchased from The Hospital for Sick Children (SickKids), University of Toronto. Water physico-chemical parameters of nitrate (NO3-) <50 mg/L, nitrite (NO2-) <0.1 mg/L, hardness 50-100 mg/L, alkalinity 50-150 mg/L, conductivity 300 -1,500 µS, pH 6.8-7.5 and the water temperature 26-28.5 ˚C were maintained according to the standard conditions. The lighting conditions of the laboratory were 14:10 hr (light: dark). Water in the system circulates through the UV filters of the rack system and the system water of each separate tank (1.1, 3.5 and 8 L) is further cleaned through multiple life stage baffles (300, 500 and 800 µm).

3.1.1 (b) Feeding

Zebrafish were fed with dry food (food size from 100 microns for larvae to 300/400 microns for adult fish) or live food (brine shrimps). Commercially prepared zebrafish food was fed based on their development stage. The following feeding protocol was followed for larval-rearing. Larval fish between 5 dpf to 14 dpf (below one month old) were fed with Rotifers (*Brachionus calyciflorus*) and Gamma 75 (Gemma micro 75 ZF, SKRETTING). Aged between the 14dpf - 1month larvae were fed with *Artemia fransicana* (brine shrimps), Rotifera, and Gamma 75 (Gemma micro 75 ZF, SKRETTING). Fish (1-3 months old) were fed with Gamma 150 food (Gemma micro 150 ZF, SKRETTING), flakes and live *Artemia fransicana*.. Adult breeders were fed with Gamma 300 food, flakes and live *Artemia fransicana* (brine shrimps). Adult fish (~3 months of age) were started to prime two weeks before breeding. Feeding frequency was also increased by an additional feeding in the afternoon with brine shrimp.

3.1.1 (c) Breeding

For the purpose of spawning, double pair mating (as the ratio of two males to two females) was employed in one breeding tank and the sex of the fish was identified based on the external appearance. Sexually active breeding individuals were selected which included from the 3 months to less than 3 years' post-fertilization age interval. Zebrafish males are smaller and slenderer than females. Good female breeders were selected by the characteristic round, distended and larger belly of fishes who seem to be carrying more eggs. The breeding was set

up in the evening. All male and female fishes were placed in breeding tanks (either regular rectangular breeding tank or sloping breeding tank) separated by a tank divider. The removable insert was added between the fish and the floor of the tank, to prevent the predatory behavior of the parents. The water level of each breeding tank was set up to around a quarter of its entire volume, filled with the system water. The water temperature of the breeding tank was steadily maintained up to 28.5 ˚C in an inside water bath with a heater overnight. The following morning, dividers were removed in order to stimulate the fish for mating. At the same time, breeding tanks were slightly slanted (only for regular rectangular tanks) to make a shallow water area for breeders. This is important for getting the characteristic beach breeding where the female fish prefer egg laying. After two and half an hour of removing the dividers, the bottom of the tanks was checked for eggs. Male and female breeders in the existing mating tanks were removed and transferred back to their original tanks. All the laid eggs were put into a sieve and cleaned with embryo medium prepared with 0.1 % methylene blue and system water. Dead unfertilized eggs were removed by using a plastic pipette and fertilized eggs were transferred to another clean petri dish containing embryo medium. Bleaching of zebrafish embryos was carried out in order to reduce the transfer of potential surface pathogens to the fish facility (Appendix 1). Then, eggs were washed three times by sieving using the methylene blue contained media. Thereafter, eggs were examined under a microscope to determine their age and the damaged eggs were removed. The eggs were again transferred into a clean Petri dish (25 eggs per dish) containing embryo media and raised in an incubator at 28.5˚C for five days. At the 5 dpf, they were transferred into the larval-rearing nursery tanks of the rack system. The fish specimens used for this experiment come under the animal care protocol numbers 17-041 (AC11315) and 18- 021 (AC 11360).

3.2 Treatments (Ethanol, Wnt signaling pathway agonist and antagonist)

The samples were subjected to three main different chemical treatments at 10 hpf. Namely, ethanol, Wnt pathway agonist and antagonist. Here, LiCl and W-C59 were used as the Wnt pathway agonist and antagonist respectively. In addition to three main chemical treatments: (a) 1% EtOH (Ethanol) (Cat. No. AC615090000; Fisher Chemicals) (b) 2 mM LiCl (Cat. No. 866405-64-3; TCI America) and (c) 10 nM W-C59 (Cat. No. 500496; Sigma-Aldrich), two other combined chemical solutions were prepared using 1% EtOH combining with Wnt pathway activator and antagonist as five chemical treatments altogether, respectively (d)

combined treatment of 1% EtOH and 2 mM LiCl and (e) combined treatment of 1% EtOH and 10 nM W-C59.

Approximately 20 embryos, were placed in each treatment petri dish containing each of the above solutions. Embryos were stored in the incubator at 28.5 ℃ and kept in the dark, in order to exclude the effect of different external lightning conditions on the initial development of melanocytes of embryos. Treatments were terminated after 12 hours (hrs) of the treated time, (at the age of 22 hpf). Embryos were washed three times with embryo medium containing 0.1 % methylene blue to remove any residual chemical solutions. Then the embryos were transferred into new petri dishes with new embryo medium and separated into two batches. Then they were grown separately and the following experiments were performed.

To address the objectives of the project, several aspects will be determined in zebrafish (WT)-AB strain embryos by fixing embryonic and larval fish at different life stages following different techniques. Fishes were euthanized using 0.1 % Tricaine methanesulfonate (MS222) (Cat. No. 118000500; Fisher Chemicals) solution which was made with system water. The samples were fixed first in 4% Paraformaldehyde (PFA) in phosphate-buffered saline solution (Cat. No. J19943; Fisher Chemicals) overnight and replaced with Phosphate-buffered Saline (PBS) on next day (Cat. No. 22050105, Fisher Chemicals).

Table 3. 1 Key life stages of fish life cycle that were used for fixing to fulfil each criteria of this study.

Criteria	**Fixing age**
Melanocyte density	4 dpf to 10 dpf
Melanocyte morphometry	2 dpf and 6 dpf
Melanocyte migration (embryonic stage)	2 dpf
Melanocyte arrangement (early larval stage)	6 dpf
Melanin formation in RPE of eye	2 dpf and 6 dpf
Melanin content	2 dpf
Melanin intensity	4 dpf to 10 dpf
WMISH	2 dpf

3.3 Analyzing the melanocyte density

Development and density of melanocytes were analyzed at different larval ages of fish which were exposed to different chemical treatments ranging from 4 dpf to 10 dpf. PFA fixing could affect the xanthophores and iridophores' pigmentation but does not affect melanin [253]. Larvae were mounted in 0.2 % agar in embryo medium without a coverslip. Region of interest (ROI) was imaged in fixed fish by the bright field with Zeiss discovery V8 stereomicroscope. This ROI encompassed the dorsal view of the head from midway up the eyes (excluding the eyes themselves) to the base of the head measuring pigmentation from the dorsal pigment stripe only (Fig. 3. 1). Cells within an area more or equal to 50 % (≥50 %) lying in the corresponding regions were included. Melanocytes within the area of 91656.991 μm^2 of the ROI were applied for counting melanocyte number on the dorsal stripe melanocytes of the rostral portion were counted manually, from a dorsal view, and the wild-type control samples (untreated) were compared with the number of dorsal melanocytes of the chemical treated samples. The samples were examined (N = 10) and counts were made under the stereomicroscope under different magnifications and images were captured (enlarged using a stereomicroscope attached to a Nikon DSFi2 camera). The above measurements were calculated using the ZEN 2011 software (blue edition, Zeiss, Germany 2011). Figures were mainly generated by utilizing this software. The number of melanocytes was plotted against the life stage in the exact surface area for each analysis as mentioned earlier.

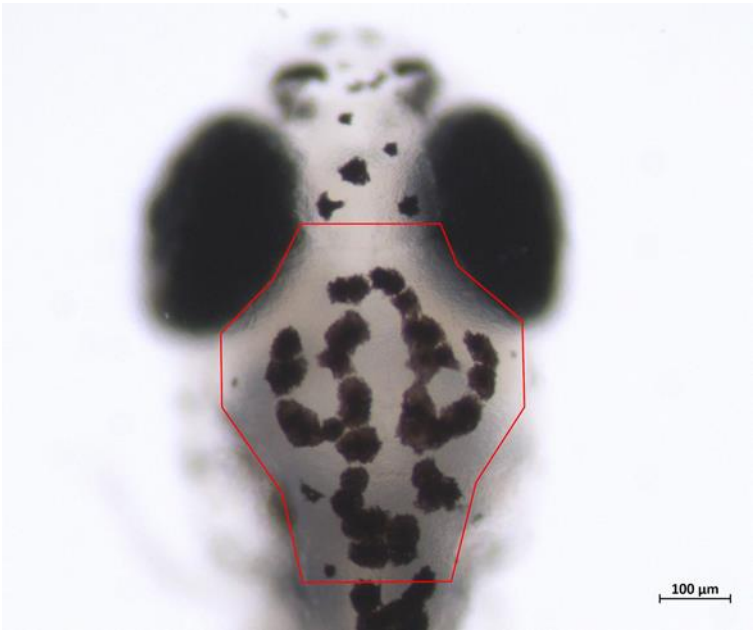

Figure 3. 1 Region of Interest (ROI) where the melanocyte density was compared at each stage of the control and chemical treated zebrafish embryos. (Red color outline indicates the ROI). ROI is defined as the area between midline of the orbs and base of the head, located most anterior part of the dorsal stripe.

3.4 Measuring the melanocyte morphometry

The surface area of melanocytes within the area of ROI was measured in the embryonic stage (2 dpf) and early larval stage (6 dpf) along the periphery of melanocytes with the aid of ZEN 2011 software tools. Here, mounting and imaging were conducted as same as mentioned early and ten embryos (N = 10) were used in each control and chemical treated samples for analyzing the morphometry.

3.5 Analyzing the melanocyte migration

Migrated and non-migrated melanocytes were determined by counting melanocytes at 48 hpf. Ten embryos (N = 10) were used in each control and treatment groups for analyzing the migration, along six distinct regions of the embryo: the anterior head, yolk sac region, yolk sac extension, near the ear, the region between the dorsal stripe and horizontal myoseptum, and the region between the ventral stripe and horizontal myoseptum. Melanocytes which were located on the anterior head (A), yolk sac region (B) and yolk sac extension (C) were classified as a migrated subpopulation of melanocytes and are colored in yellow in Fig. 3.2. Melanocytes which were remained near the ear (D), the region between the dorsal stripe and horizontal myoseptum (E) and the region between the ventral stripe and horizontal myoseptum (F), marked as red in Fig. 3.2 and were referred to as a non-migratory subpopulation of melanocytes. Statistical analysis was conducted to check whether each drug had a significant effect on the number of migrated and non-migrated melanocyte cells. Here, the ratio of migrated to non-migrated melanocyte subpopulations in each group of chemical-treated fish embryos was compared to that of the control.

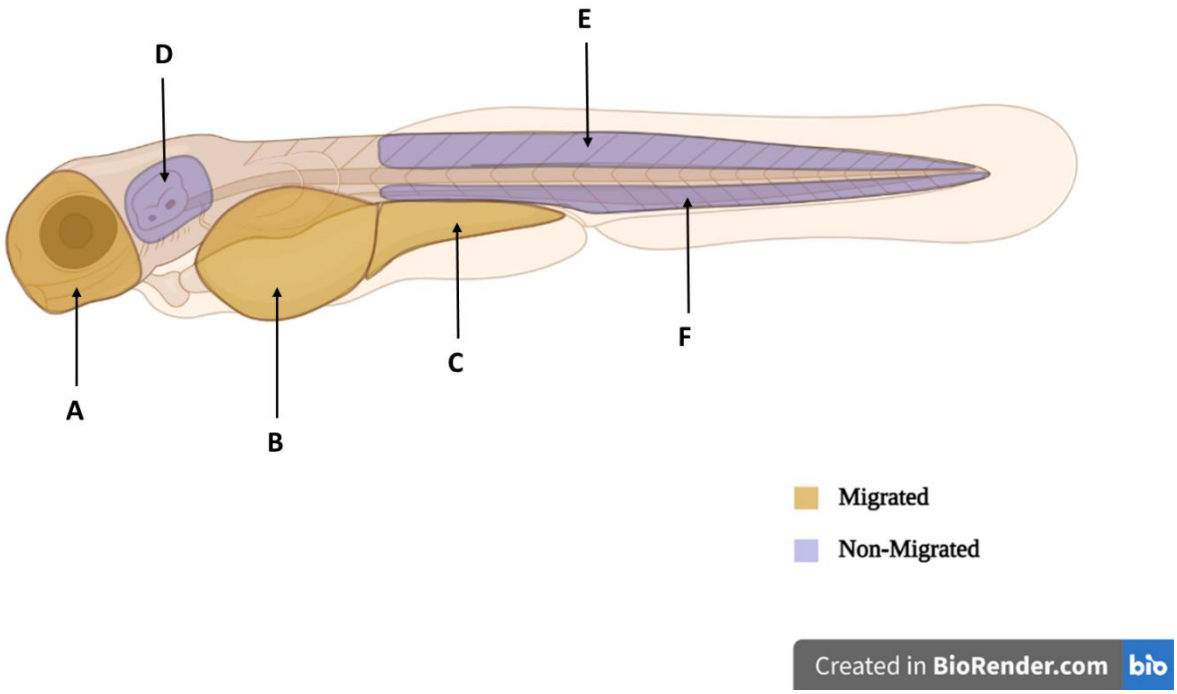

Figure 3.2 Regions in embryo that were used to define migrated and non-migrated melanocytes for quantitative analysis of melanocyte migration. Yellow areas indicate migrated melanocytes on the anterior head, yolk sac region and yolk sac extension. Red areas define non-migrated melanocytes near the ear, in the region between the dorsal stripe and horizontal myoseptum and the region between the ventral stripe and horizontal myoseptum.

3.6 Analyzing the melanocyte arrangement

Melanocyte arrangement and quantification of melanocytes in each stripe were carried out in 6 dpf early developmental larval stage when the four striped melanocyte pattern is established, based on the microscopic examinations. At this stage, melanocyte pattern consists of four stripes of melanocytes (lateral view): the dorsal stripe, the lateral stripe, the ventral stripe and the yolk sac stripe, parallel to the anteroposterior axis along the horizontal myoseptum. Ten embryos (N = 10) in each treatment were used for analyzing the differential effect of drug exposure on the later development of four-stripe melanocyte arrangement at the larval stage and compared with the control. Any deviations of melanocyte arrangement as melanocyte pattern and count differences in each stripe due to chemical exposure were captured using the

Zeiss discovery V8 stereomicroscope. In counting the melanocyte numbers of the dorsal stripe, it was considered the stripe region between the end of the head and tail tip, while the melanocyte count between the stripe region of the end of the yolk-sac and the tip of the tail was accounted by counting the melanocytes in ventral stripe.

3.6.1 Analysis of biased migration of melanocytes along the L-R axis

Biased migration of melanocytes is determined along the L-R axis of lateral melanocyte stripe at 6 dpf, PFA fixed larval fish. The melanocyte cells on both left and the right side of each larval fish were counted. Either, leftward bias or rightward bias was quantified by examining ten larvae (N = 10) of each control and drug-exposed fish.

3.7 Melanin intensity measurement

3.7.1 Melanin intensity measurement of the melanocytes located on the head region

Melanin dispersion was investigated by measuring the mean color intensity values in the larval fish development stages from 4 dpf to 10 dpf age period after fishes were exposed to different chemical treatments. Larvae were mounted in 0.2 % agar in embryo medium without a coverslip. Region of interest (ROI) was imaged in fixed fish in bright field mode with Zeiss discovery V8 stereomicroscope keeping the imaging parameters (light intensity, brightness, exposure time. etc) constant. Melanocytes within the area of 101557.661 μm^2 (r= 359.593 µm) of the ROI which were lying on the rostral portion of the dorsal stripe were considered for measuring the mean intensity. Measurements were taken using the ZEN 2011 software tools from a dorsal view, and wild-type control samples were compared with the mean intensity values of the chemical-treated samples (N = 10). Differences in melanin dispersion in the control sample and chemical-treated samples were analyzed by the differences in mean intensity values. ZEN 2011 software is included intensity value ranges from 0 to 4096 respectively for black and white.

3.7.2 Melanin intensity measurement of the RPE layer of eyes

The integrated density of the melanin pigment in the RPE layer was analyzed in order to check the differential chemical effect on melanin formation in the zebrafish eyes at the embryonic stage 2 dpf. This was examined in the live embryos (N = 10) after anaesthetizing with 0.01 % MS222 and mounting in 0.2 % agar made in embryo medium, without a coverslip. These data

were produced by utilizing the melanocytes within the area of 25950.938 μm^2 (r – 181.774 µm) of zebrafish eye (covering the maximum area of the eyes). ZEN 2011 software is included intensity value ranges from 0 to 4096 respectively for black and white.

3.7.3 Histological and electron microscopic analysis of melanin formation in RPE layer

Melanin formation and melanosome biogenesis in the RPE layer of control and chemical exposed zebrafish eyes were investigated by using toluidine blue staining and TEM sections. Here, control and chemical-exposed zebrafish embryos at 2 dpf and larvae at 6 dpf were euthanized using the 0.1 % MS222 solution made with system water. Fixed fishes were placed in the fixative of 3 % Glutaralde in 0.1M Sorensen's buffer contained in 1.5 ml Eppendorf tubes separately for 3 hrs and made sure that the fixative volume was 10 times greater than the tissue volume and tissues are free floating. After the fixation, the fixative was removed using the Pasteur pipette as much as possible and replaced it with 5 % Sucrose in 0.1M Sorensen's buffer for 1 hr. The previous solution was replaced with the fresh portion of the same 5 % Sucrose in 0.1M Sorensen's buffer solution. Fish samples were kept at 4˚C until delivering samples for the histology lab, in order to process for the toluidine blue and TEM sections. All the steps of the tissue fixation protocol were carried out under the fume hood.

3.8 Spectrophotometric determination of melanin synthesis

Melanin content was analyzed at 48 hpf old embryos as triplicates of nine embryos in each control and chemical-treated fish group. Altogether twenty-seven embryos were used for determining the end product of melanin in the melanogenesis pathway for each condition. All the embryos were dechorionated and euthanized on the day of performing the experiment and transferred into the corresponding autoclaved Eppendorf tube. Euthanizing solution in each tube was removed and filled with 40 µL of RIPA lysis buffer until covering all embryos (Cat. No. CAPI 89900; Fisher Chemicals) added (5 mL 1 M Tris HCL pH 7.5, 0.88 g NaCl, 1 mL 1% Nonidet P40, 0.5 g sodium deoxycholate, 1 mL 10% SDS, and 93 mL H2O). [if it is needed to be stored the samples for future usage, additionally protease inhibitor (Cat. No. 539131; Sigma-Aldrich) should be added to the RIPA lysis buffer according to the ratio of volumes 1000: 10]. Embryos were ground using an autoclaved pipette tip and incubated on ice for 5 min. All the samples were centrifuged at 13,000 RPM, 4℃ for 10 min. Pellets were re-dissolved in 200 µl of 1 M NaOH at 80℃, and vortexed to solubilize the pellet. Optical density was measured at 490 nm using the Nanodrop™ spectrophotometer (Thermo Fisher Scientific Inc.).

Relative melanin content was determined with a modification of the method of previous research work [89]. Spectrophotometric values and statistical significance were compared in each chemical-treated group against the control untreated sample.

3.9 Protein probe preparation

3.9.1 *dct and Wnt3a* probe preparation

Probes were synthesized by following the manufactures instructions of the DIG RNA Labeling kit, SP6/T7), (Cat. No. 11175025910; Roche). Briefly, 4 µl of zebrafish template DNA was mixed with 2 µl of 10X NTP labeling mixture, 2 µl of 10x Transcription buffer, 1 µl of protector RNAase inhibitor, and 2 µl of RNA polymerase. The mixture was mixed gently and centrifuged at 12,000 x g for 1 min. Samples were incubated for 2 hrs in a 37˚C water bath. Next, 2 µl of DNAase 1 was added to the same sample and incubation was continued for another 15 min. In the end, the reaction was stopped by adding 2µl of 0.2M EDTA (pH 8.0).

3.9.2 Detecting *dct* and *Wnt3a* probes

The strength of the probes was detected by using the dot blot analysis technique according to the standard procedure (Appendix 2). Briefly, the hybridization oven was heated to 100 ˚C before starting the probe-detecting protocol. Next, 1 µl spots of diluted *dct* and *Wnt3a* labelled probes were added to the positively charged nylon membrane on separate lanes (Cat. No.11209299001; Roche). Then, the paper was placed in a sterile glass petri dish and incubated for 30 min in the hybridization oven at 100˚C for fixing the nucleic acids. Thereafter, the nitrocellulose paper was soaked in 20 ml of Maleic acid buffer (approximately half of the depth of the dish) and incubated at room temperature for 2 min with shaking (40 RPM). Maleic acid buffer was made using 1.1607 g of 1 M Maleic acid, 0.8766 g of 0.15 M Sodium chloride, and the solution was topped up to 100 ml using Diethyl pyrocarbonate (DepC water). Paper was incubated in the blocking buffer for 20 min with shaking. The 100 ml of blocking buffer was made by adding 2 ml of 2 % Sheep serum (Cat. No. BP2425; MP Biomedicals), 3 g of milk powder (Skimmed milk powder, commercially available) and topped up to 100 ml using the solution with 10 x TBST in DepC. TBST buffer was made by adding 6.05 g of Tris (Cat. No. BP152-500; Fisher Chemicals) and 8.76 g of Sodium chloride in 800 ml of DepC water. The pH was adjusted to 7.5 with 1 M Hydrochloric acid (Cat. No. SA48-1; Fisher Chemicals) and

volume was made up to 1 L with DepC water. Finally, 10 ml of Tween-20 (Cat. No. BP337-100; Fisher Scientific) was added to 1L of TBS buffer. The antibody solution was prepared at this stage and stored in the fridge until required. Nitrocellulose paper was washed with TBST for 5 min with shaking. Paper was incubated in 10 ml of the antibody solution for 30 min. The antibody solution was made by adding 2 µl of antibody (Cat. No. 11093274910; Roche) into 10 ml of TBST buffer. Then, the paper was washed with washing buffer in two washes for 15 min for each with shaking. Each wash was carried out with a fresh washing buffer. The washing buffer was made by adding 1.1607 g of 0.1M Maleic acid, 0.8766 g of 0.15M NaCl and 0.3 ml 0.3 % Tween-20. The final solution was made by adding DepC water to 100 ml. Paper was incubated in the detection buffer for 5 min with shaking.

The detection buffer was made by adding 10 ml of 0.1 M Tris-HCl, 0.5844 g of 0.1 M NaCl, and the final volume was topped up to 100 ml with DepC water. The 1 ml of BCIP/NBT Liquid substrate solution (Cat. No. ICN980771; MP Biomedicals) was added on top of the paper, kept in dark covering the glass petri dish with foil paper, and checked for a color reaction every five min. The first dot was detected at the highest concentration within 5 - 10 min. The reaction was stopped by adding TE buffer. TE buffer was made by adding 1 ml of 10 mM Tris-HCl, 0.2 ml of 1 mM EDTA (Cat. No. 37560; VWR) and the solution was topped up with DepC water to 100 ml.

3.10 Whole-Mount in situ Hybridization (WMISH)

3.10.1 Embryo Fixation

WMISH was performed using the 48 hpf WT zebrafish embryos. All the chemical solutions for this protocol were prepared in DepC water. The 48 hpf zebrafish were euthanized using 0.1% MS222 solution and fixed in 4% PFA for 2 hrs. Next, samples were subjected to dehydration series gradually through methanol (Cat. No. BP1105SS28; Fisher chemicals) series in PBS (25%, 50%, 75%), and samples were stored in 100 % methanol until the day of starting the WMISH experiment.

3.10.2 Whole-mount in situ Hybridization (WMISH)

WMISH was conducted according to the established protocol in the lab (Appendix 3). Here, samples were rehydrated to PBS gradually through the methanol series (75%, 50%, 25%). Next, the samples were washed with PBST solution (1ml PBS in DepC water/1 µl of Tween-10). Samples were bleached for 30 min using 0.5 % Potassium Hydroxide and H_2O_2 solutions made in DepC water. Then, the samples were washed with PBS and PBST solutions at room

temperature. Thereafter, the samples were processed for permeabilization for 23 min using the Proteinase K (1 µl proteinase K / 1000 µl of DepC, (Cat. No. BP1700-100; Fisher Chemicals). Samples were again washed with PBST several times and fixed with 4% PFA under the fume hood. Next, the samples were treated with a freshly made acetic anhydride recipe. Then, the samples were prehybridized in the Hyb (-) solution at 70 ˚C. This Hyb (-) solution was prepared by adding 50 ml of Deionized Formamide 100 % (Cat. No.327235000; Acros), 25 ml of saline sodium citrate 20X (SSC) (Cat. No. BP1325-1; Fisher Chemicals), 0.1 ml Tween-20 final solution was top-up to 100 ml by adding 24.9 ml of DepC water. After that, samples were incubated with *dct* and *wnt3a* probes separately in Hyb (+) solution at 70˚C overnight. Hyb (+) solution was prepared by adding 3.56 ml of Hyb (-), 0.4 ml of Yeast tRNA (5mg/ml) (Cat. No. 10109509001; Roche), 0.04 ml of Heparin (50 µg/ml, Cat. No. BP2425; Fisher Chemicals) and final volume was adjusted to 4 ml adding 0.0368 ml Citric Acid to pH (6.0). After that, high stringency washes were performed to remove the non-specific binding of the probe. Next, samples in each tube with a definite probe type were incubated in the blocking buffer. Blocking buffer was made by adding 3.920 ml of 1x PBST solution and the final volume was adjusted to 4 ml by adding 0.080 ml of 2 % Heat inactivated sheep serum (Cat. No. BP2425; MPBiomedicals) and 0.008 g Bovine serum albumin (2 mg/ml) (Cat. No. SH30574.01; GE Life Sciences, HyClone Labs). 1 µl of Anti-Dig Antibody solution (Cat. No.11093274910; Roche) was added to 9 µl of Blocking Buffer solution. From the Antibody Recipe, 1 µl was added to each tube which already contained Blocking Buffer, and incubated overnight at 4 ˚C while shaking. Next, samples were incubated in TRIS Staining Buffer by adding 1 ml for each tube. After the incubation, the staining buffer was replaced with a Color substrate solution of NBT/BCIP staining for the colorimetric detection of RNA. The reaction was conducted in dark until detecting the proper color expression. The color reaction was examined up to the maximum extent of 40 min. The samples were fixed in 4 % PFA and dehydrated through methanol series. Whole-mount images were captured at the stage of samples were 25 % or 50 % Methanol in PBS using a stereomicroscope (Zeiss discovery V8). In the end, samples were stored in 100 % Methanol in PBS at 4 ˚C for the long term.

3.10 Statistical analysis

Statistical analyses were performed using Excel (2016, Microsoft, USA). Graphical representations were also designed with the same software. One-way ANOVA test was carried out to determine the significant difference in means between the independent groups of the associated variable.

Significant main effects were further decomposed using pairwise comparisons with a post hoc Simple Bonferroni correction with Student's t-test, for multiple comparisons. Data were expressed as Mean ± SEM, and a probability level of 5 % was used as the minimal criterion of significance. $P > 0.05$ was considered non-significant while the P values of ≤ 0.001 (***), ≤ 0.01 (**) and ≤ 0.05 (*) were taken as statistically significant. * depicts the magnitude of the significance. All the significant differences represent in the bar charts of the results chapter were corresponding to the pairwise comparisons with control groups. All the phenotypic analyses of melanocyte numbers (for evaluating the factors of density, morphometry, migration, arrangement and biased migration) and, melanin intensities of the different regions of the zebrafish embryos and in the larval stages were analyzed by utilizing the microscopic tools of the ZEN 2011 software (blue edition, Zeiss, Germany 2011).

CHAPTER 4: RESULTS

4.1 Comparison of the variation in melanocyte density against different chemical treatments

4.1.1 Comparison of the melanocyte density of the control and EtOH treated zebrafish larvae

Figure 4.1.1. 1 Comparison of the melanocyte density of the control and EtOH treated zebrafish larvae from 3 dpf to 10 dpf developmental stages. This figure illustrates the differences in melanocyte density in ethanol treated samples compared to the control group of each life stage. Scale bar: 100 µm

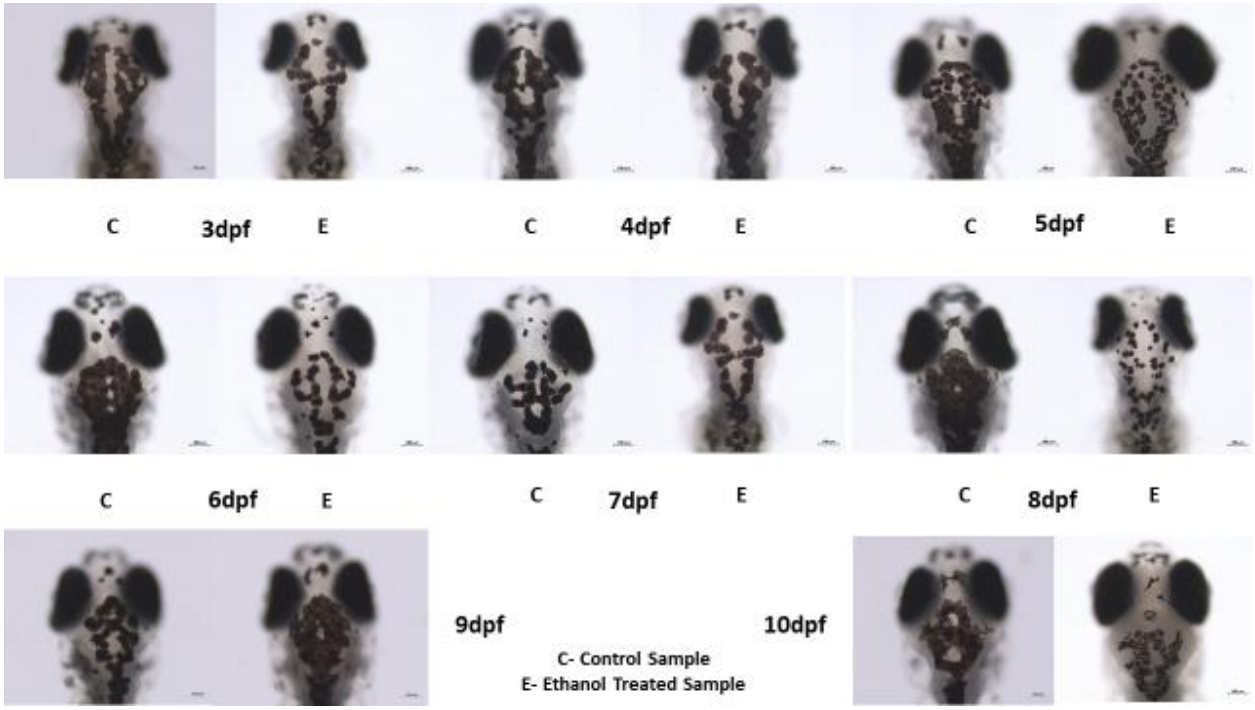

Figure 4.1.1. 2 Comparison of the fluctuation in melanocyte density of the control and EtOH treated zebrafish larvae from 4 dpf to 10 dpf developmental stages.

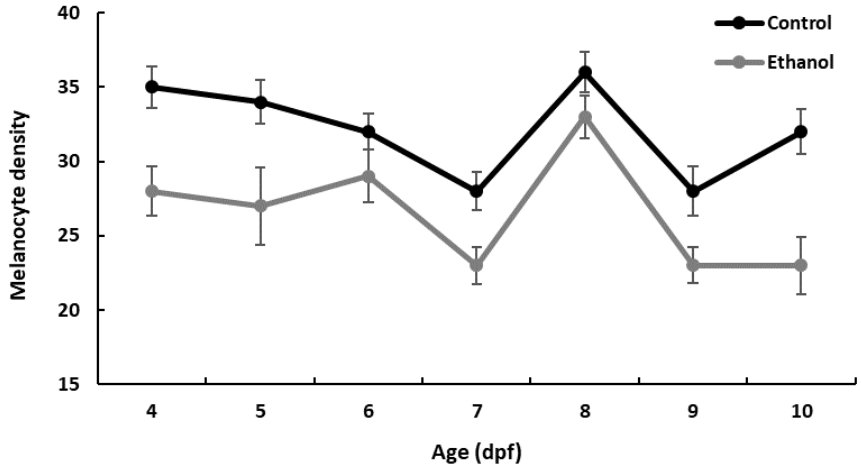

The effect of chemical exposure on melanocyte development in zebrafish was studied using the stereo microscopic examinations. Upon the ethanol treatment from 10 hpf to 22 hpf, changes of melanocyte development were observed from 4 dpf to 10 dpf life stages (Fig. 4.1.1). According to the analysis of these phenotypic data, low values for the melanocyte density were observed at each developmental age of the ethanol treated zebrafish embryos compared to the control sample (Fig. 4.1.1.2). Specifically, reduced melanocyte densities were observed in the zebrafish melanocyte development lineage at 7 dpf and 9 dpf life stages, whereas increased melanocyte density was observed in 8 dpf of the control sample over the considered age groups. However, all the melanocyte counts which are compatible to the above highlighted stages were low in the ethanol treated embryos. These variations of melanocyte densities of the analysis (Fig. 4.1.1.2) were clearly reflected when examining the microscopic images (Fig. 4.1.1.1). It showed the increased or decreased melanocyte counts on the dorsal region of the control and ethanol treated zebrafish embryos. Interestingly, almost similar fluctuation of melanocyte densities was observed in the ethanol exposed fish compared with control sample (Fig. 4.1.1.2). Altogether, exposure to 1% EtOH chemical treatment had a noticeable negative effect on melanocyte development according to the examinations under light microscopy.

4.1.2 Comparison of the melanocyte density of the control and LiCl treated zebrafish larvae

Figure 4.1.2. 1 Comparison of the melanocyte density in the control and LiCl treated zebrafish larvae from 3 dpf to 10 dpf developmental stages. This figure demonstrates the difference in melanocyte development in LiCl treated samples compared to the control group of each life stage. Scale bar: 100 µm.

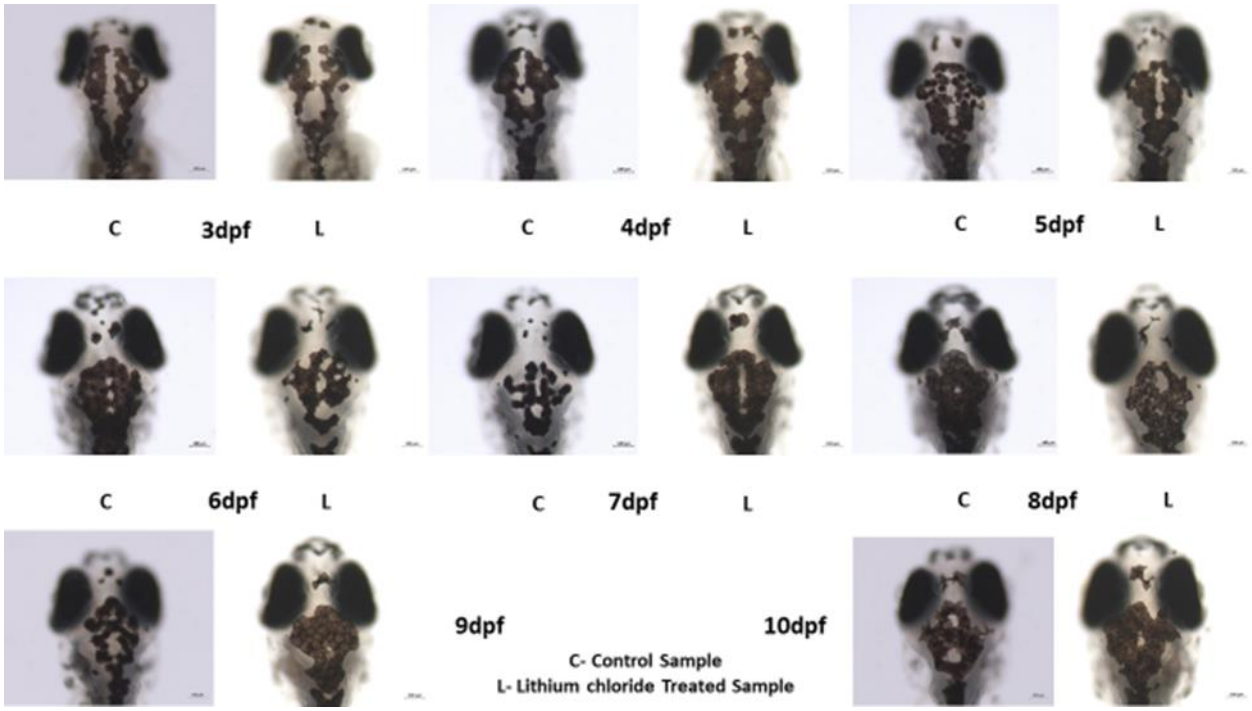

Figure 4.1.2. 2 Comparison of the fluctuation of melanocyte density of the control and LiCl treated zebrafish larvae from 4 dpf to 10 dpf developmental stages.

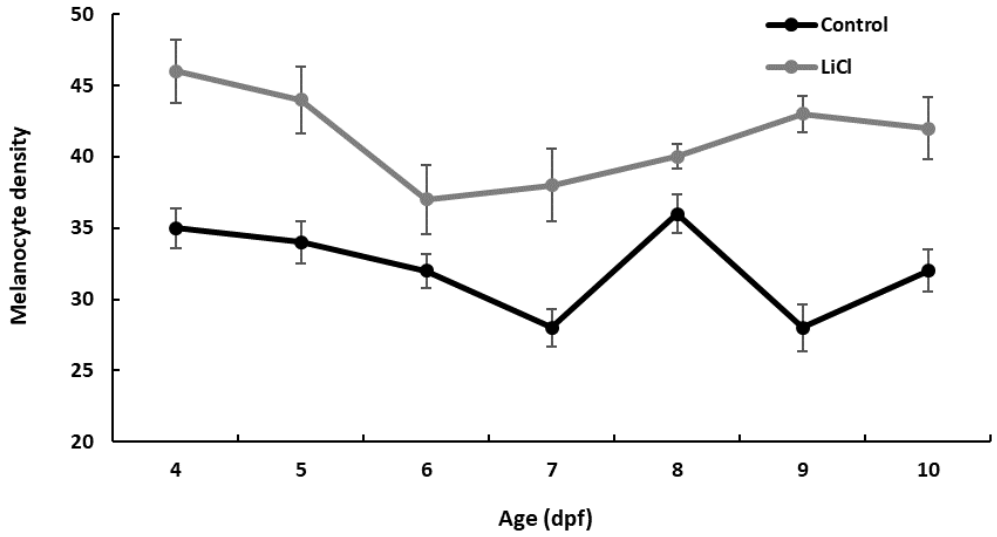

High values for the melanocyte densities were observed at each developmental age of the embryos which were exposed to the LiCl, compared to the control samples (Fig. 4.1.2.2). This phenomenon could be detected in the same manner when examining the control and LiCl treated samples under the microscope (Fig. 4.1.2.1). According to the external gross examination of these microscopic figures, it could be observed that area of the ROI is covered with more melanocytes in the LiCl treated zebrafish embryos compared to untreated control samples (Fig. 4.1.2.1). It indicates the presence of increased melanocyte density at each life stage of the LiCl treated larval fish. The fluctuation of the melanocyte density of the LiCl treated fishes don't follow the same gradient shown in the control. Meanwhile, melanocyte densities observed in the zebrafish melanocyte development lineage at 7 dpf, 8 dpf and 9 dpf life stages, were comparatively higher than the usual melanocyte counts in the control sample (Fig. 4.1.2.2). When the overall melanocyte development of the LiCl treated embryos were considered, it indicated that embryonic exposure to LiCl chemical treatment had a noticeable stimulatory effect on melanocyte development.

4.1.3 Comparison of the melanocyte density of the control and EtOH + LiCl treated zebrafish larvae

Figure 4.1.3. 1 Comparison of the melanocyte density in the control and EtOH + LiCl combine treated zebrafish larvae from 3 dpf to 10 dpf developmental stages. This figure shows the difference in melanocyte development in EtOH + LiCl treated samples compared to the control group of each life stage. Scale bar: 100 µm.

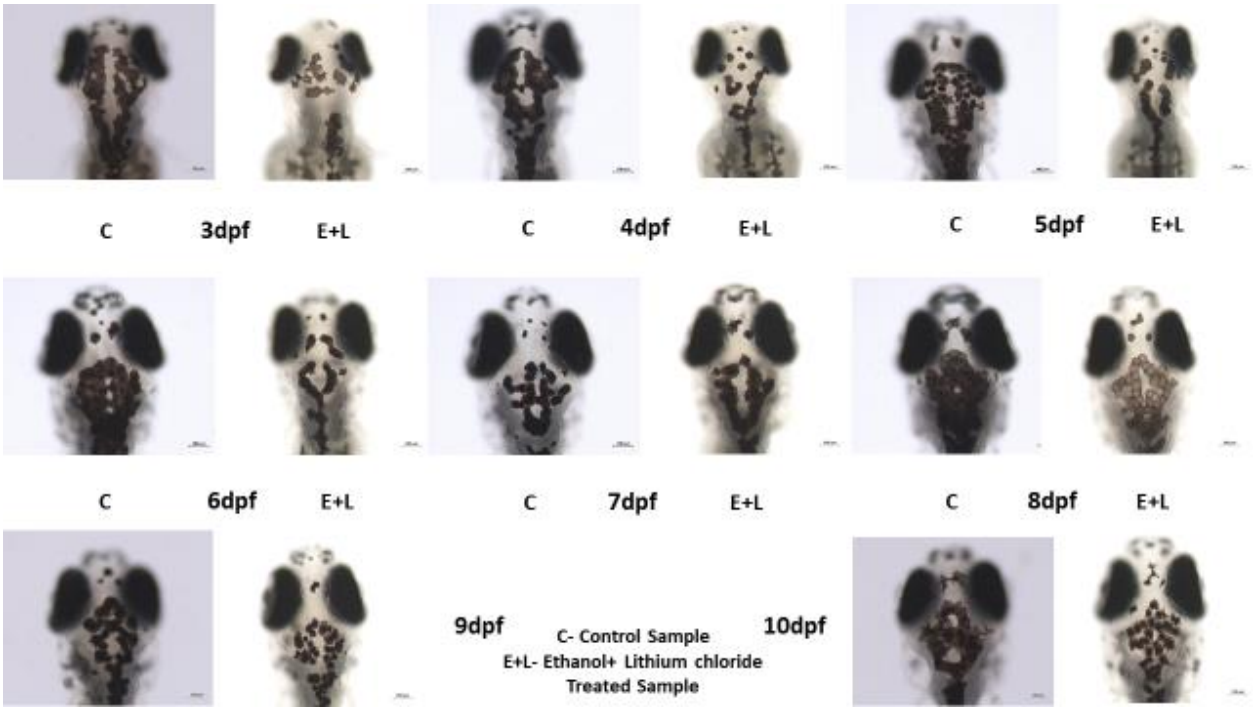

Figure 4.1.3. 2 Comparison of the fluctuation of melanocyte density of the control and EtOH + LiCl treated zebrafish larvae from 4 dpf to 10 dpf developmental stages.

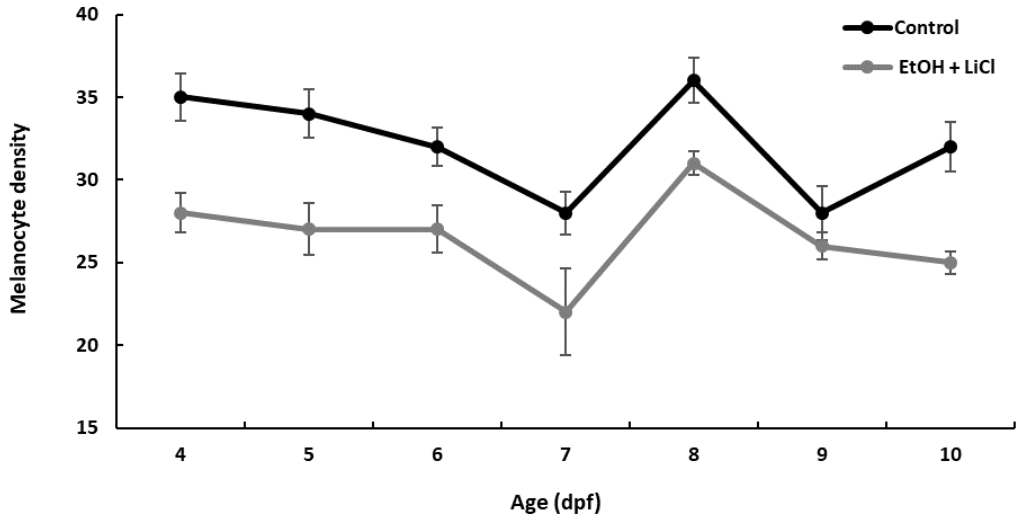

Combined chemical treatment of both EtOH and LiCl resulted low melanocyte counts in the ROI at each developmental age of the zebrafish embryos compared to the untreated control group (Fig. 4.1.3.2). Remarkably, this fluctuation of the melanocyte densities in the combined chemical treatment follows the same fluctuation in the control fish sample as examined in the EtOH treated zebrafish embryos. It could be observed that combined treatment has a drastic effect on melanocyte development than the EtOH single treatment showed previously. The melanocyte densities of each age group in the EtOH + LiCl treatment, was less than the control sample as showing in the figure of melanocyte density fluctuation (Fig. 4.1.3.2). These results reflect similarly from the images captured under the stereo microscope as covering less area within the ROI while showing loose arrangements (Fig. 4.1.3.1). Altogether, embryonic exposure for EtOH + LiCl treatment produced a negative effect on melanocyte development compared to the control sample which was reared in the embryo medium.

4.1.4 Comparison of the melanocyte density in the control and W-C59 treated zebrafish larvae

Figure 4.1.4. 1 Comparison of the melanocyte density in the control and W-C59 treated zebrafish larvae from 3 dpf to 10 dpf developmental stages. This figure elaborates the difference in melanocyte development in W-C59 treated samples compared with control group of each life stage. Scale bar: 100 µm.

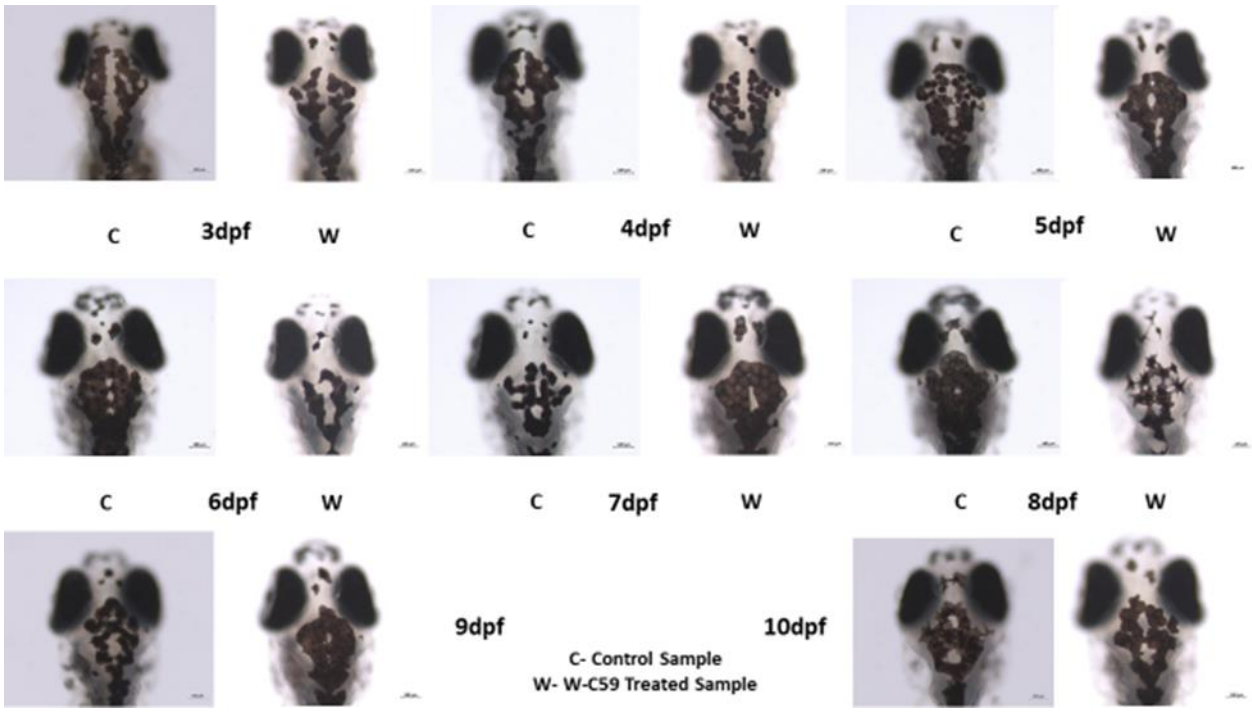

Figure 4.1.4. 2 Comparison of the fluctuation of melanocyte density of the control and W-C59 treated zebrafish larvae from 4 dpf to 10 dpf development stages.

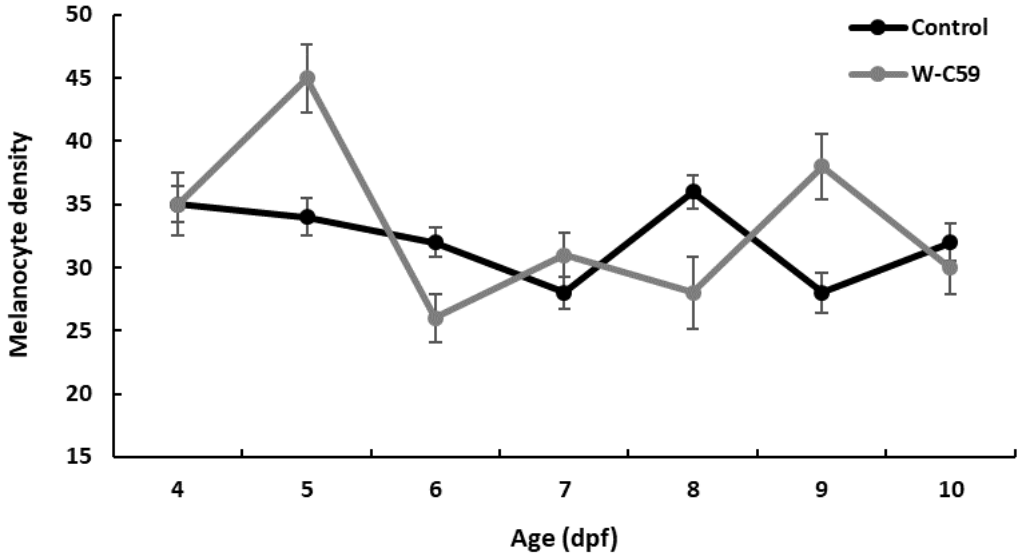

Chemical effect of Wnt signaling inhibitor on melanocyte development did not exhibit a uniform variation as other chemical treatments showed previously, whereas W-C59 exposure effect, consists of sudden fluctuations with ups and downs of the melanocyte numbers relative to the control fish (Fig. 4.1.4.2). However, less melanocyte densities could be observed at some life stages (6 dpf, 8 dpf and 10 dpf), in contrast increased counts were also observed phenotypically by microscopic examinations at some ages of zebrafish development (5 dpf, 7 dpf and 9 dpf) (Fig. 4.1.4.1). Hence, it could not be predicted exactly the role of W-C59 on melanocyte development by looking at first illustration (Fig. 4.1.4.1) but analyzing the phenotypic results, showed that which plays a significant role and conspicuous impact on melanocyte development.

4.1.5 Comparison of the melanocyte density in the control and W-C59 + EtOH treated zebrafish larvae

Figure 4.1.5. 1 Comparison of the melanocyte density of the control and W-C59 + EtOH treated zebrafish larvae from 3 dpf to 10 dpf developmental stages. The figure illustrates the difference in melanocyte development in W-C59 + EtOH treated samples compared with control group of each life stage. Scale bar: 100 µm.

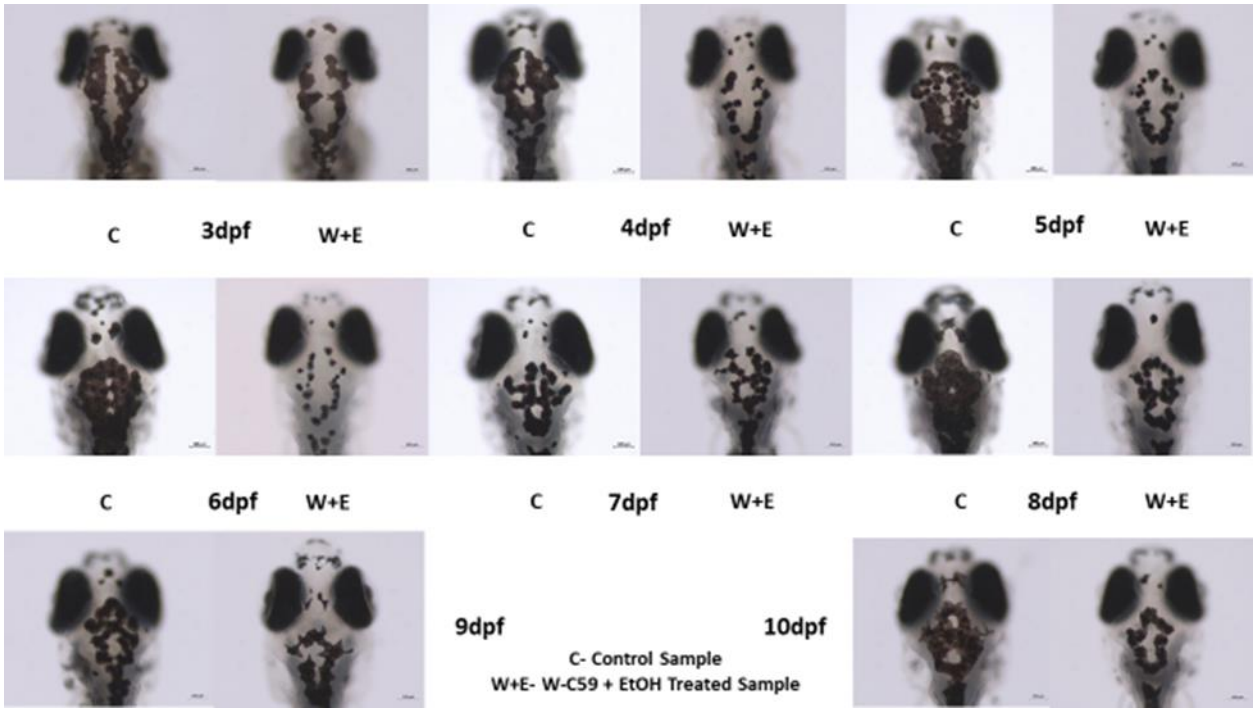

Figure 4.1.5. 2 Comparison of the fluctuation of melanocyte density of the control and W-C59 + EtOH treated zebrafish larvae from 4 dpf to 10 dpf development stages.

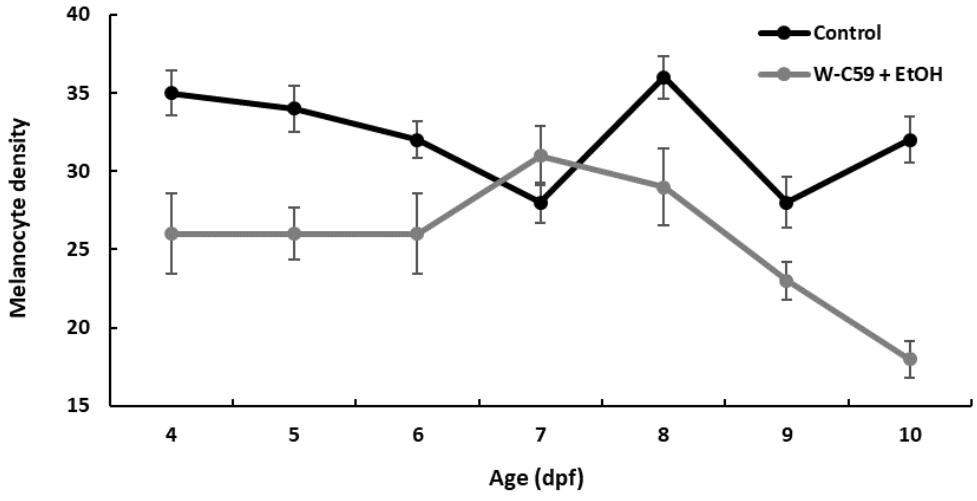

It was evident that embryonic exposure to combined chemical treatment of W-C59 + EtOH has an inhibitory effect on melanocyte development at later larval stages. In the microscopic examinations, observed that the severe decrease of melanocyte number in almost every life stage except the 7 dpf fish. Especially, 4 dpf, 5 dpf and 6 dpf, 8 dpf, 9 dpf and 10 dpf of chemical treated embryos (Fig. 4.1.5.1). Examining the fluctuation of melanocyte density, comparatively a huge gap could be observed between the variations of control and W-C59 + EtOH exposed larval fish in each stage as reflecting from the microscopic images (Fig. 4.1.5.2). In addition, variation of the melanocyte density of the combined treated larval fish was not resemble to the fluctuation of control fish samples. Taken together, these results implied that the combined chemical exposure of W-C59 and EtOH has a major influence on manipulating the melanocyte development.

4.1.6 Comparison of the variation of melanocyte density at 8 dpf against different chemical treatments

Figure 4.1.6.1 Comparison of the melanocyte density of zebrafish larvae at 8 dpf developmental stage treated with each chemical. This bar chart expands the difference in melanocyte development in each chemical treated samples compared with control group at the development stage of 8 dpf.

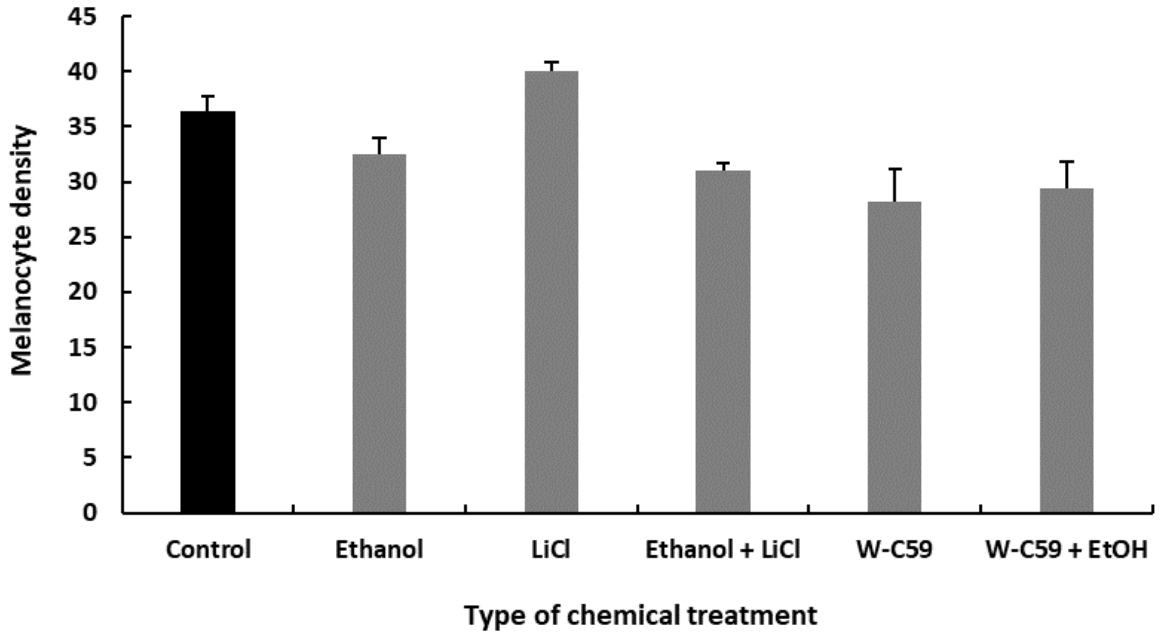

Melanocyte density was investigated at 8 dpf stage of zebrafish separately in terms as it's a crucial stage of the melanocyte development lineage of the fish between the 4 dpf and 10 dpf growth period. As above bar chart illustrates, low melanocyte densities were observed in the W-C59 (28.2 ± 2.88) and combined treatment of W-C59 and EtOH exposed fish, compared to the control fish. Zebrafish larvae which were exposed to EtOH (32.6 ± 1.20) at the embryonic stage, had a less melanocyte density relative to the control fish. Interestingly, the highest melanocyte count was recorded in the LiCl (40 ± 0.86) treated zebrafish larvae. However, no significant difference [$F(5,24) = 1.36$, $P = 0.272$] was found out among the control and other chemical treated larvae with respect to the mean melanocyte densities.

4.1.7 Comparison of the variation of melanocyte density at mid-larval stage against different chemical treatments

Figure 4.1.7.1 Comparison of the melanocyte densities of zebrafish larvae at mid-larval developmental stage treated with each chemical. This bar chart demonstrates the difference in melanocyte development in each chemical treated samples compared with control samples at the mid larval developmental stage of 15 dpf.

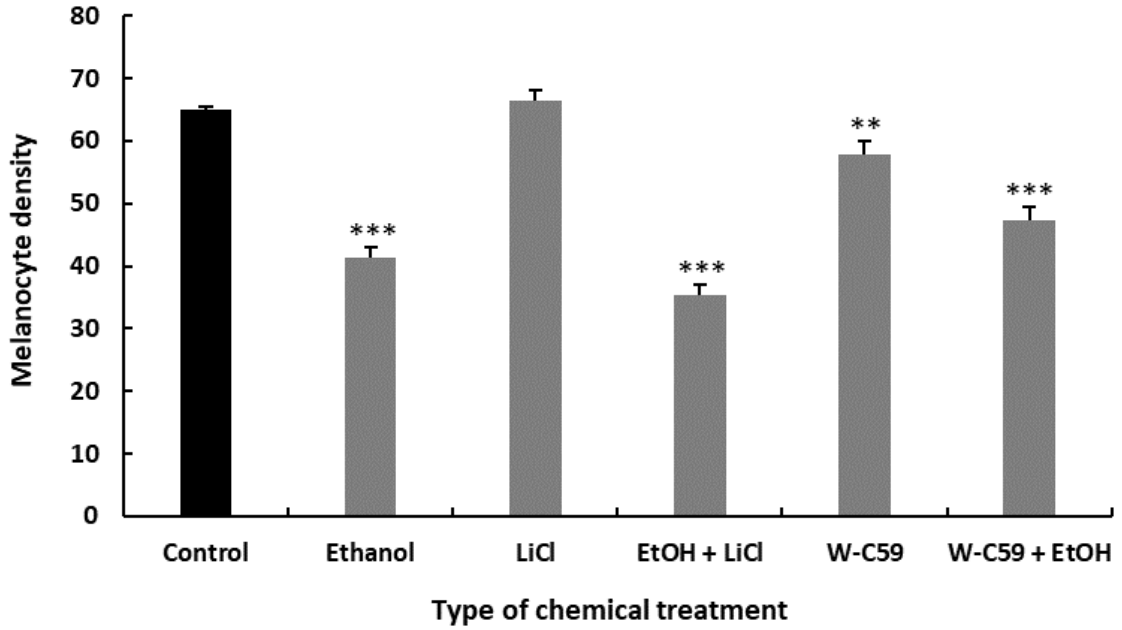

Effect of differential chemical exposures on melanocyte development at mid-larval stage was observed at 15 dpf. There were significant differences in the mean melanocyte densities of chemical exposed fish compared to the control group [$F(4,45) = 75.55$, $P < 0.001$]. Here, conspicuously low melanocyte densities were noticed in the EtOH + LiCl (35.4 ± 1.55), EtOH (41.30 ± 1.78) alone and combined W-C59 + EtOH (47.3 ± 2.25) treatments and all were significantly different with the control group whereas LiCl (66.5 ± 1.64, $P > 0.05$) exposure has directed to increase the melanocyte density of zebrafish, but it was not significantly different with the untreated control sample. Significant decrease in melanocyte density was recorded in W-C59 (57.9 ± 2.12, $P < 0.01$) chemical treated embryos but it was less significant compared to the other above mentioned treated samples. (Refer the Appendix 4)

4.2 Comparison of the differences in melanocyte morphology and morphometry against different chemical treatments

Figure 4.2. 1 Comparison of the melanocyte phenotypic differences at 2 dpf embryonic stage of zebrafish against various chemical treatments.

This figure illustrates the morphological and morphometric differences in melanocytes of untreated Control (A) and which were exposed to different chemicals, denoting from B-F; consecutively, B- EtOH, C- LiCl, D- EtOH + LiCl, E- W-C59 and F- W-C59 + EtOH.

Scale bar: (A, D & F) - 50 µm, (B, C & E) - 100 µm

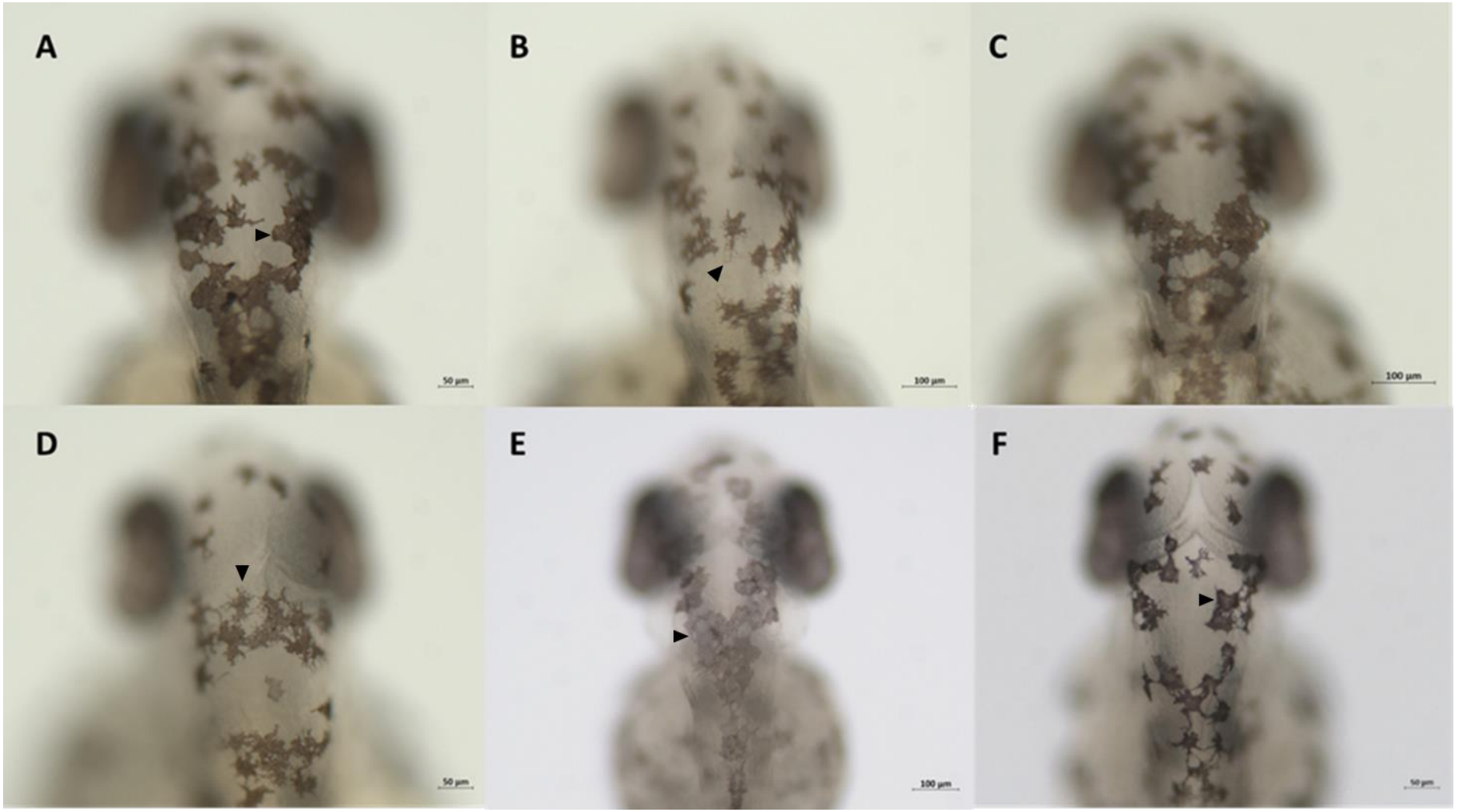
A
B
C
D
E
F

Various defects of melanocyte morphology were detected in the zebrafish embryos which were exposed to chemical treatments compared to the control sample. In the control sample matured melanocytes were thin plaque in shaped with defined margins whereas most of the melanocytes of the chemical treated embryos showed a dendritic / stellate morphology, spreading out of the cell margins. This feature was mostly noticed in the EtOH and combined treatment of EtOH + LiCl fish (black arrow heads of Fig. 4.2.1 B & D). Considering the formation of melanin pigmentation within the cells, more paleness could be noted in the W-C59 treated embryos (black arrow heads of Fig. 4.2.1 E) (Appendix 5) as well as combined treatment of EtOH + LiCl (Fig. 4.2.1 D) and EtOH (Fig. 4.2.1 B) were also lack of melanin pigmentation. However, the pigment intensity and morphology of the melanocytes in the LiCl treated fish were similar with the melanocytes which occupy in the head region of the control sample (Fig. 4.2.1 C). Uneven distribution of melanin pigment within the melanocyte cells were noticed in W-C59 + EtOH (black arrow head of Fig. 4.2.1 F) treated embryos as dark colored pigment accumulation at the margins of the cells while less pigment distribution at the center of the cells.

Figure 4.2.2 Variations of the size of melanocytes at 2 dpf embryonic stage of zebrafish against various chemical treatments. This figure demonstrates the morphometric differences in melanocytes which were exposed to different chemicals.

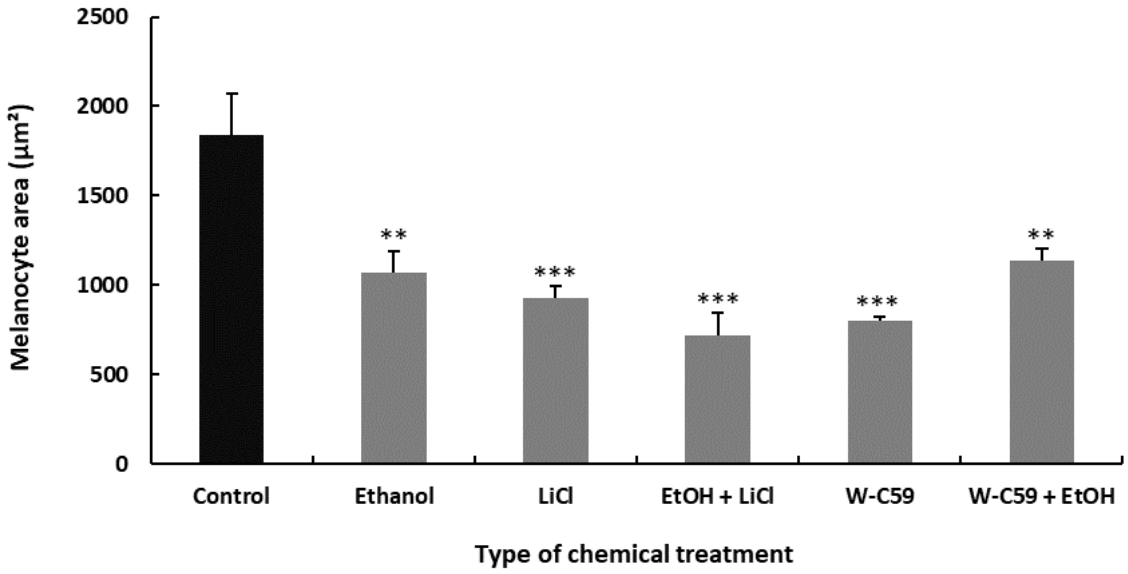

Differences in melanocyte morphometry were found in the chemical exposed embryos, as illustrating in the above bar chart. Melanocyte area was measured using the microscopic software analysis as an indicator to determine the melanosome dispersion. Marked significant difference was recorded in the values of mean melanocyte areas against different chemical exposures of fish [$F(5,54) = 10.63$, $P < 0.001$]. According to the data analysis, the least melanocyte area was found in the EtOH + LiCl treated fish (715.88 ± 128.04) along with lower values were recorded in W-C59 (796.84 ± 28.43) and EtOH (1070.43 ± 114.83) single treatments respectively. Interestingly, all the chemical treated fish at the embryonic stage found with reduced melanocyte area compared with normal rearing control zebrafish. (Refer the Appendix 4)

Figure 4.2.3 Comparison of the melanocyte phenotypic differences at 6 dpf larval stage of zebrafish against various chemical treatments. This figure illustrates the morphological and morphometric differences in melanocytes of untreated Control (A) and which were exposed to different chemicals denoting from B-F; consecutively, B- EtOH, C- LiCl, D- EtOH +LiCl, E- W-C59 and F- W-C59 + EtOH. Scale bar: 100 µm

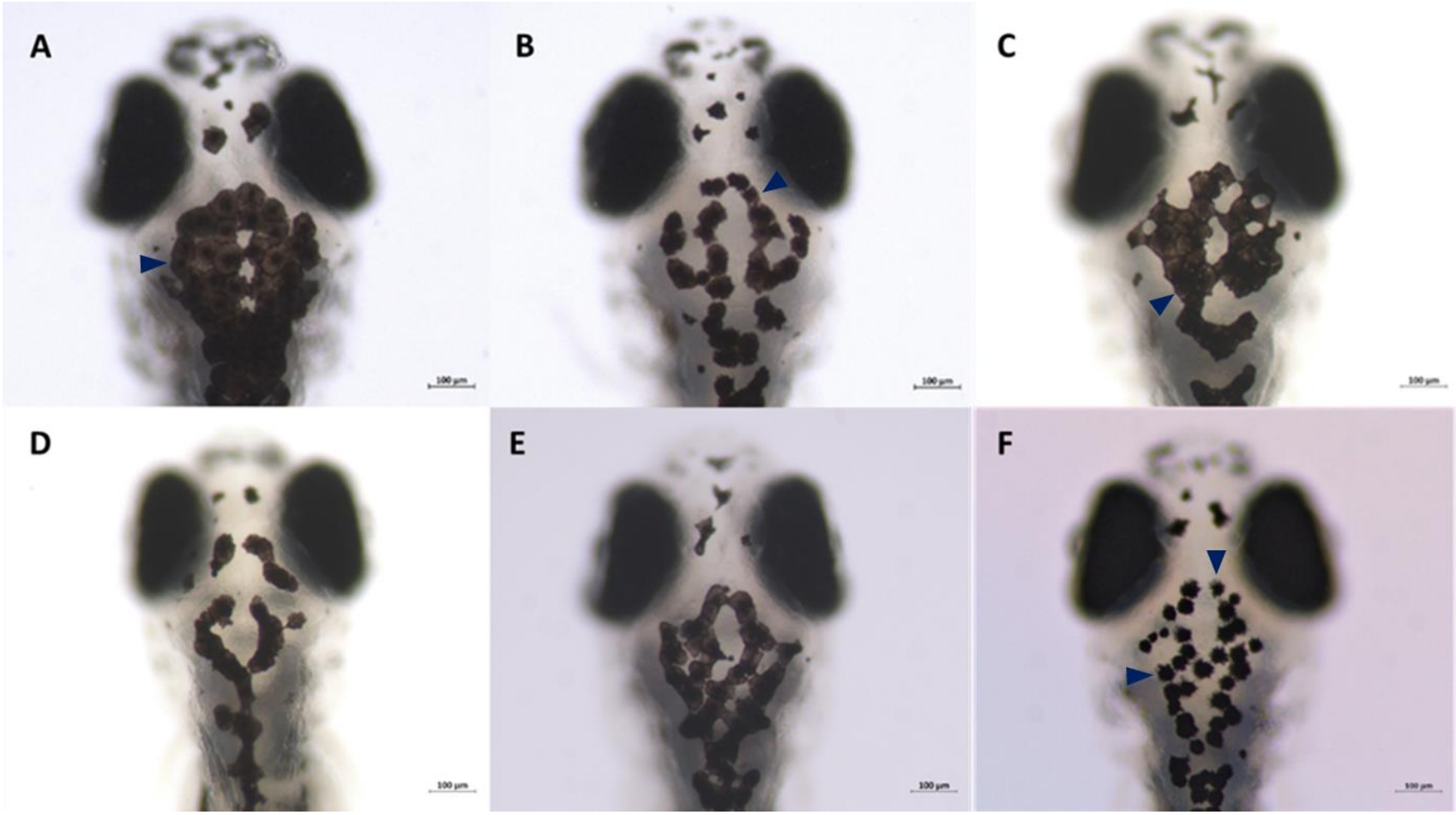

Microscopic examinations of the chemical treated larval stage zebrafish showed numerous deficits in melanocyte morphology. Deviations from the characteristic melanocyte shape could be clearly noticed in the chemical exposed fish groups (Fig. 4.2.3 B-F). Melanocytes in the control fish had a uniform oval / round shape (dark blue arrow head of Fig. 4.2.3 A) whereas different polygonal shapes of melanocytes were examined in other treated larval fish, especially in the EtOH (dark blue arrow head of Fig. 4.2.3 B), W-C59 and W-C59 + EtOH (dark blue arrow heads of Fig. 4.2.3 F) treated fish. Further, melanocytes of W-C59 + EtOH treated larval fish exhibited higher intensity for melanin with stellate shape melanocytes compared to other fish (dark blue arrow heads of Fig. 4.2.3 F). No significant paleness of the melanocytes was noted at the 6 dpf stage but minute pores were examined LiCl treated fish but melanin synthesis and its pigment distribution were quite similar compared to the control fish (dark blue arrow head of Fig. 4.2.3 C).

Figure 4.2.4 Variations of the size of melanocytes at 6 dpf embryonic stage of zebrafish against various chemical treatments. This figure demonstrates the morphometric differences in melanocytes which were exposed to different chemicals.

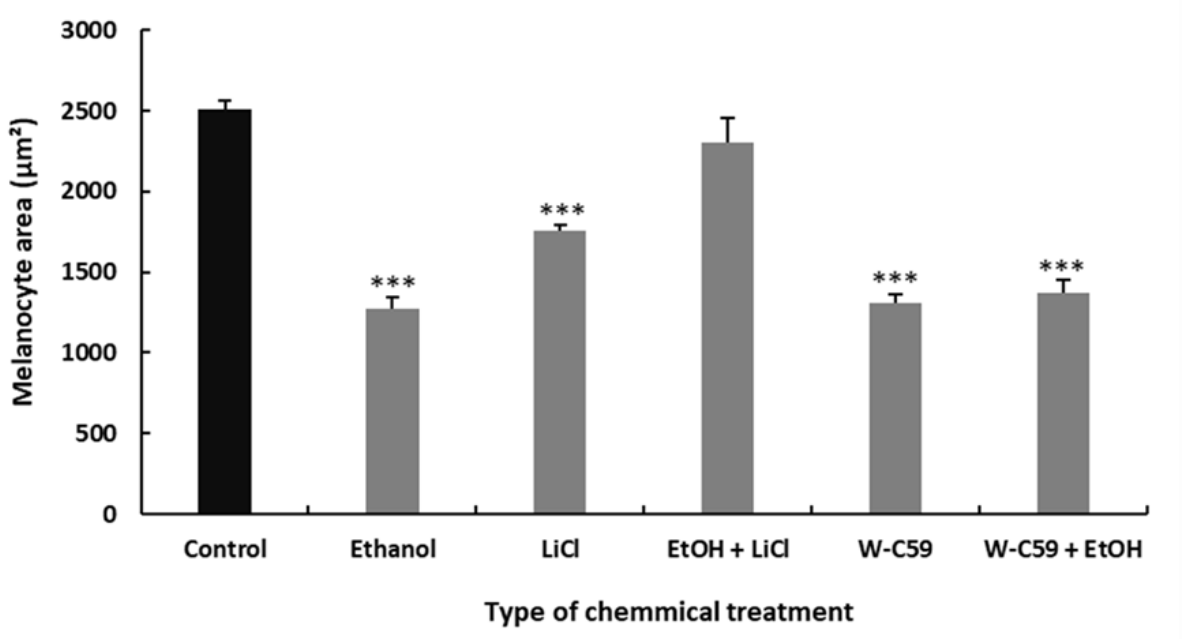

Based on the morphometric data analysis at 6 dpf larval fish, it was revealed that embryonic chemical exposure generates defects in melanocyte morphology even at the early larval stages. Marked significant difference was recorded in the values of mean melanocyte areas against different chemical exposures of fish [$F(5,54) = 42.10$, $P < 0.001$]. The lowest melanocyte area was observed in the EtOH treated larval fish (1274.23 ± 66.74, $P < 0.001$) and additionally W-C59 (1311.04 ± 50.78, $P < 0.001$) and W-C59 + EtOH (1368.22 ± 82.97, $P < 0.001$) fish were found with lower values. The LiCl treated larval fish had comparatively a high surface area except the EtOH + LiCl chemical treated fish and all values were highly significant. Remarkably, combined treated EtOH + LiCl (2303.44 ± 149.75, $P > 0.05$) larval fish had the highest value among other treated fish for the surface area but it was statistically insignificant with the control fish. (Refer the Appendix 4)

4.3 Examination of melanocyte migratory differences against different chemical treatments

Figure 4.3.1 Analysis of migratory defects of melanocytes at 2 dpf embryonic stage of zebrafish against various chemical treatments.

This figure demonstrates the differences in melanocyte migration of untreated Control (A) and which were exposed to different chemicals indicating from B-F; consecutively, B- EtOH, C- LiCl, D- EtOH +LiCl, E- W-C59 and F- W-C59 + EtOH. Scale bar: 200 µm

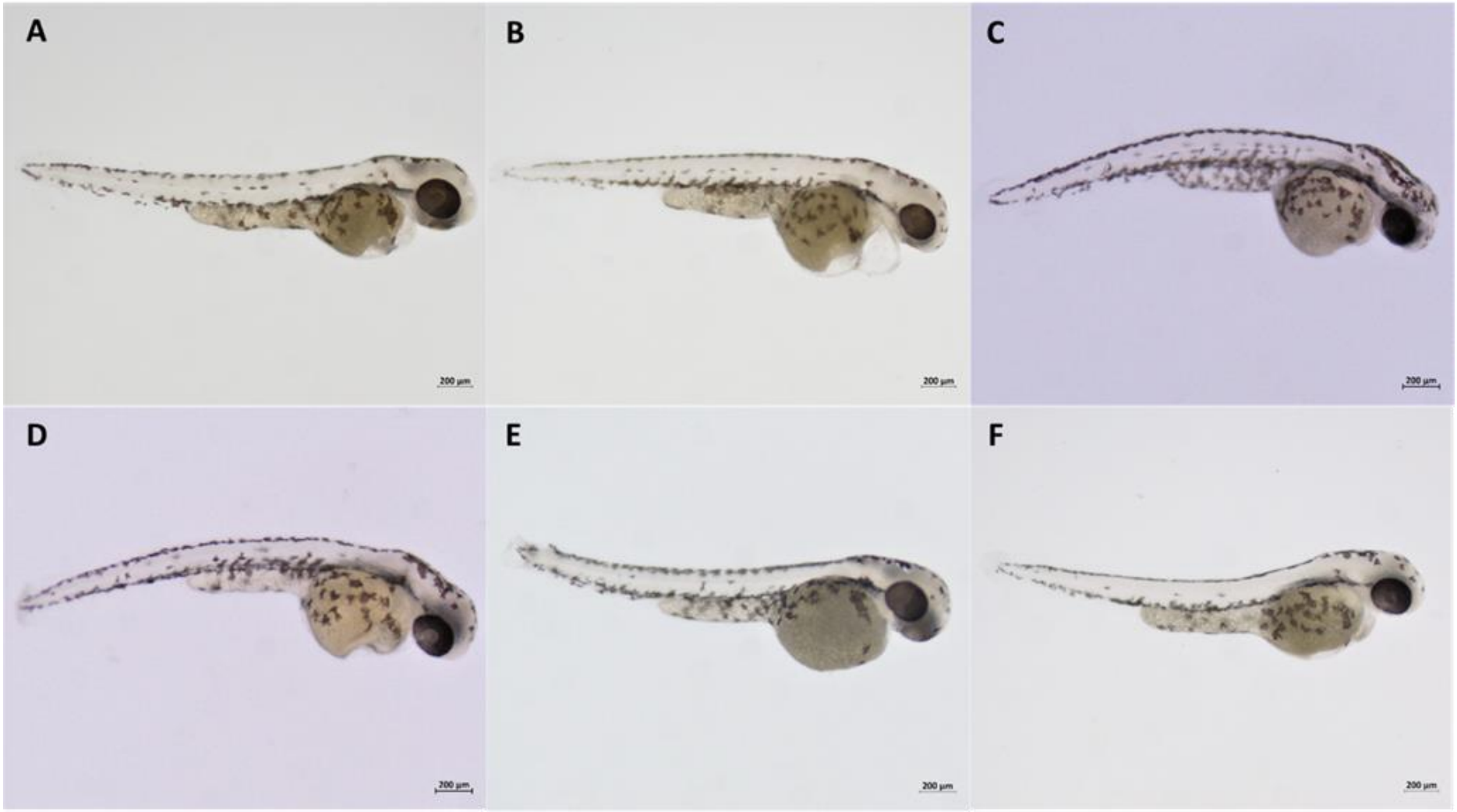
A
200 µm
B
200 µm
C
200 µm
D
200 µm
E
200 µm
F
200 µm

Melanocyte migration was investigated through the microscopic observations as demonstrated in the above figure. According to the captured images, different arrangements in migrated melanocytes in chemical exposed embryos were noticed (Fig. 4.3.1 B-F). Characteristic defects could be examined at each designated migratory and non-migratory sites of the embryos (refer the figure 3.2 in the methodology section) which are unique for each treatment. EtOH treated embryos showed the highest melanocyte density at the anterior head region and comparatively increased melanocyte counts were detected at the yolk sac region (Fig. 4.3.1 B). Further, high melanocyte localization was examined in the non-migratory sites: the regions between the dorsal stripe and horizontal myoseptum and, ventral stripe and horizontal myoseptum. Focusing on the migratory differences of melanocytes in the LiCl treated fish, the highest melanocyte accumulations were recognized in both migrated; yolk sac region and yolk sac extension, and some non-migrated sites, especially the region near the ear of treated fish than other fish (Fig. 4.3.1 C). Presence of high melanocyte count was greatly evident by appearance of the embryos in somewhat darker color due to dispersed melanocyte arrangement throughout the embryos. Interestingly, LiCl + EtOH treated embryos showed relatively high migrated and non-migrated melanocytes in the designated regions compared to control fish (Fig. 4.3.1 D). Considerable elevated melanocyte density was discovered at the anterior head, yolk sac region and non-migrated region lying between the horizontal myoseptum and ventral stripe. As figure shows the least melanocyte counts were marked in the anterior head, yolk sac region and near the ear sites of the fish which were exposed to the combined chemical of W-C59 and EtOH treatment in contrast high melanocyte gathering was viewed between the region of horizontal myoseptum and ventral stripe over the control sample. In addition to that reduced melanocyte count was also examined in the yolk sac extension region (Fig. 4.3.1 F). Wnt inhibitor treatment alone had produced less migrated melanocytes in the regions of anterior head and yolk sac regions at the same time, the least melanocyte count was recorded near the ear (Fig. 4.3.1 E). Embryos which were exposed to the Wnt inhibitor treatment, alone and combining with EtOH had paler in appearance in comparison to other examined fish (Appendix 5). Altogether, examinations of chemical treated embryos showed different aberrations in melanocyte migration and melanocytes were located in both migrated and non-migrated sites of the embryos in various numbers.

4.4. Ectopic pigment cells in the chemical treated embryos are detectable by 48 hpf

Figure 4.4.1 Examination of ectopic melanocytes in the ventral trunk

This figure illustrates the defects in melanocyte migration which were exposed to different chemicals at the embryonic stage. (A) Overview of WT embryo. (B-C) Magnification of lateral views (black box in A) of pigment phenotype at 2 dpf. They show anatomical location of melanocytes in the trunk region of embryos. Cross sections of the magnified trunk regions of control (B) and EtOH treated (C) embryos, shown by respectively in the schematic diagrams of (D) and (E).

Neural tube (NT), notochord (NC) and ventral stripe (VS). Scale bar: 200 μm (A) and 50 μm (B and C).

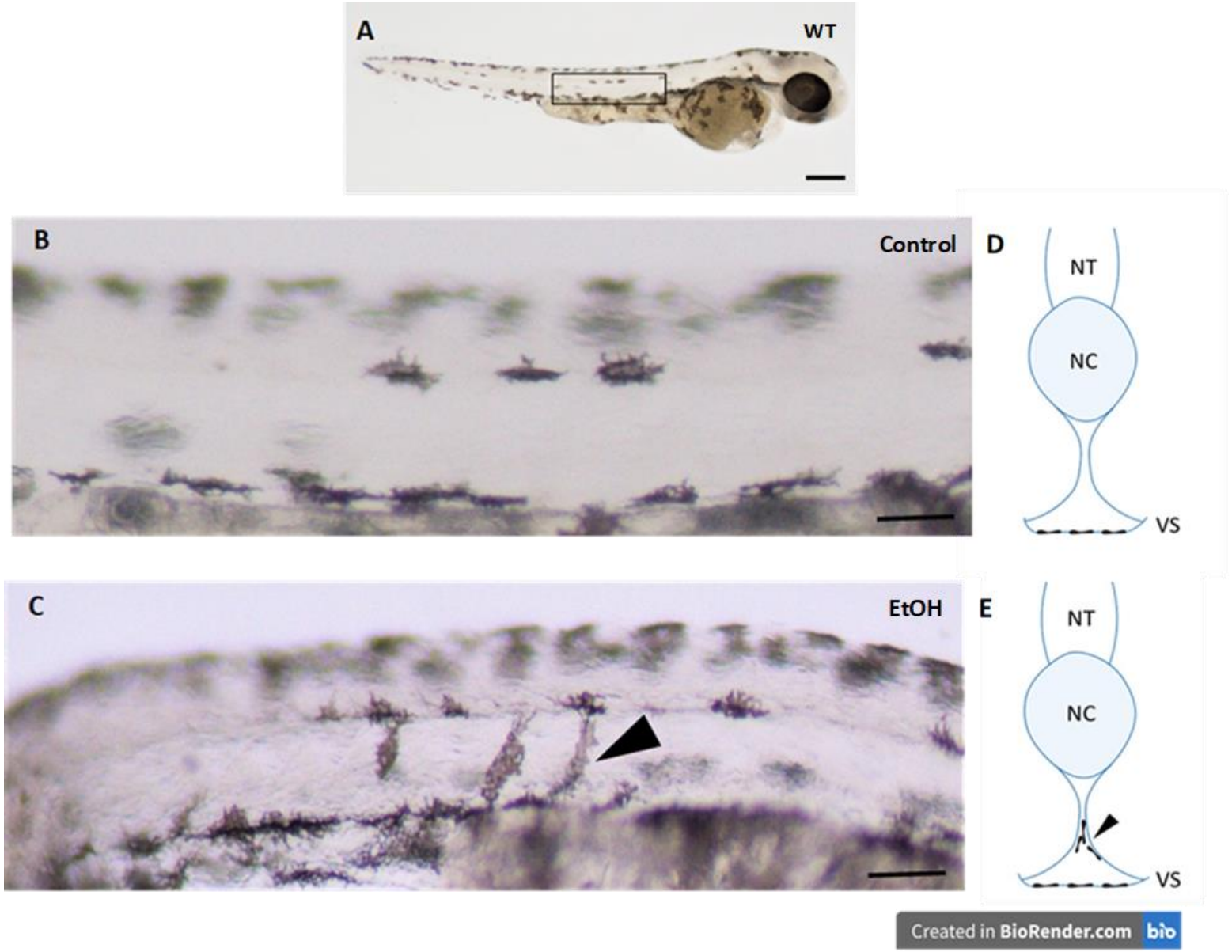
A
WT
B
Control
C
EtOH
D
NT
NC
VS
E
NT
NC
VS
Created in BioRender.com bio

No melanocyte was located in the ventral trunk of the WT control sample as shown in the figure (Fig. 4.4.1 B), further it has been displayed in a schematic cross section, as magnifying the ventral trunk region of control fish (Fig. 4.4.1 D). It clearly shows the absence of melanocytes in the region between the NC and VS. However, ectopic pigment cells were found in high proportions in the ventral trunk regions of the chemical treated embryos. Fig. 4.4.1 C shows the EtOH treated embryos as one of the examples. Black arrowhead, in Fig. 4.4.1 C, points out the localization of ectopic melanocytes between the NC and VS. Further, Fig. 4.4.1 E shows that arrangement of ectopic melanocytes clumping together in separate rows of the migratory pathway.

Figure 4.4.2 Examination of ectopic melanocytes in the Yolk sac extension region.

This figure displays the defects in melanocyte migration, found at the yolk sac extension region of the embryos which were exposed to different chemicals at the embryonic stage. (A) Overview of the control sample of WT embryo. Magnification of lateral views (black box in A) pigment phenotype at 2 dpf. (B, C and D) Migration of melanocytes in yolk sac extension region of embryos. Magnified trunk regions of control (B) and EtOH (C) and LiCl (D) treated embryos. Black arrowheads indicate the melanocyte coverage of the yolk sac extension region and green arrowheads point the changes in melanocyte morphology. Scale bar: 200 μm (A) and 100 μm (B, C and D).

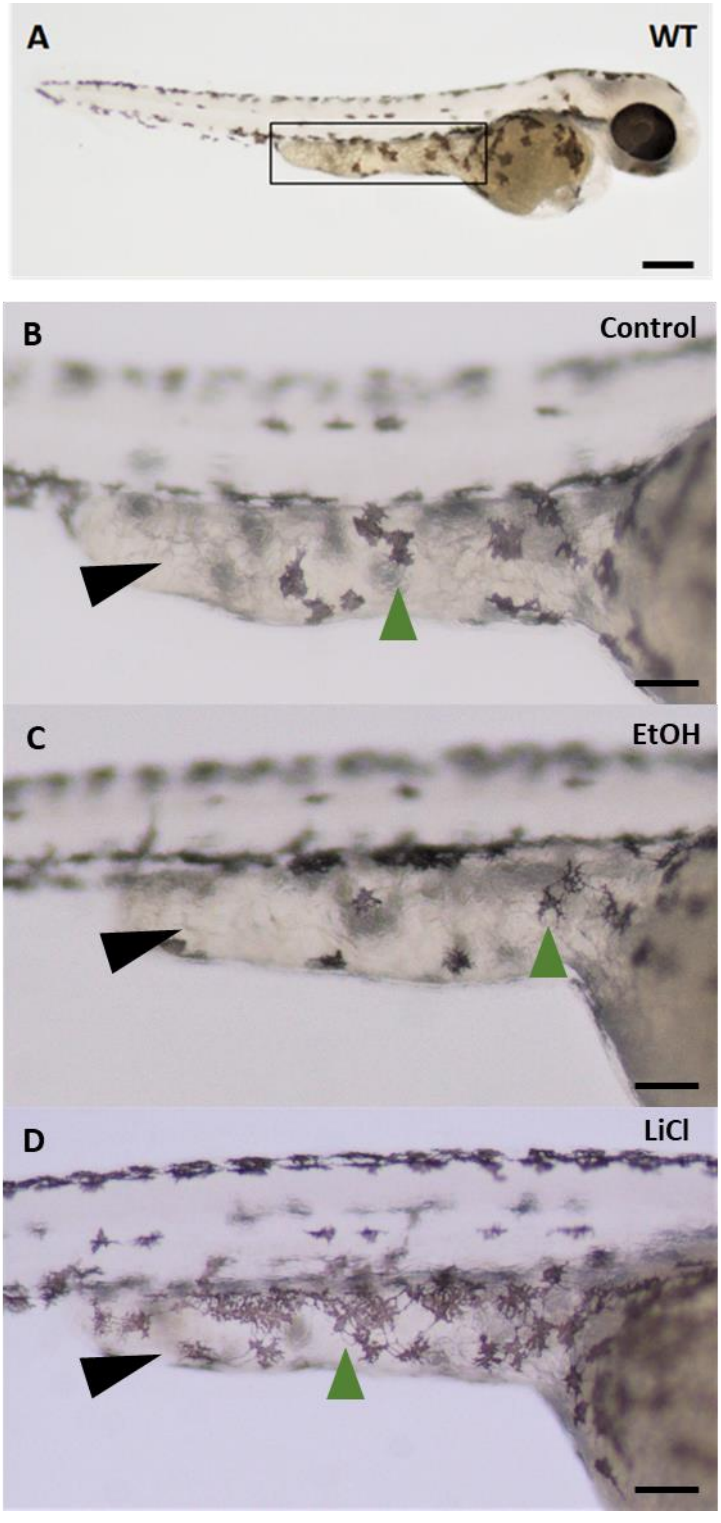
A
WT
B
Control
C
EtOH
D
LiCl

This figure demonstrates the effect of different chemical exposures on the melanocyte migration and arrangement at the yolk sac extension region. It was evident that localization of elevated number of melanocytes in the LiCl treated fish (black arrow head of Fig. 4.4.2 D). In contrast, decreased number of melanocytes had resulted with EtOH exposure (black arrow head of Fig. 4.4.2 C), in comparison of EtOH and LiCl treated embryos with untreated control sample. Significant anomalies of melanocyte phenotype were detected against chemical treatments: EtOH and LiCl had more stellate morphology compared to the control sample (green arrow head of Fig. 4.4.2 C & D respectively). Meanwhile, LiCl treated fish had intensely dispersed melanocytes than the EtOH treated fish. Changes of the melanocyte migration was noticeably presented by its' melanocyte density and arrangement within the site. Collectively, the results disclosed the fact of embryonic chemical exposure has an impact on melanocyte migration.

4.5 Analysis of melanocyte migratory differences against different chemical treatments

Figure 4.5.1 Analysis of migratory defects of melanocytes at 2 dpf embryonic stage of zebrafish against various chemical treatments. This bar chart elaborates the changes in non-migrated and migrated melanocyte numbers in chemical exposed embryos compared with control sample.

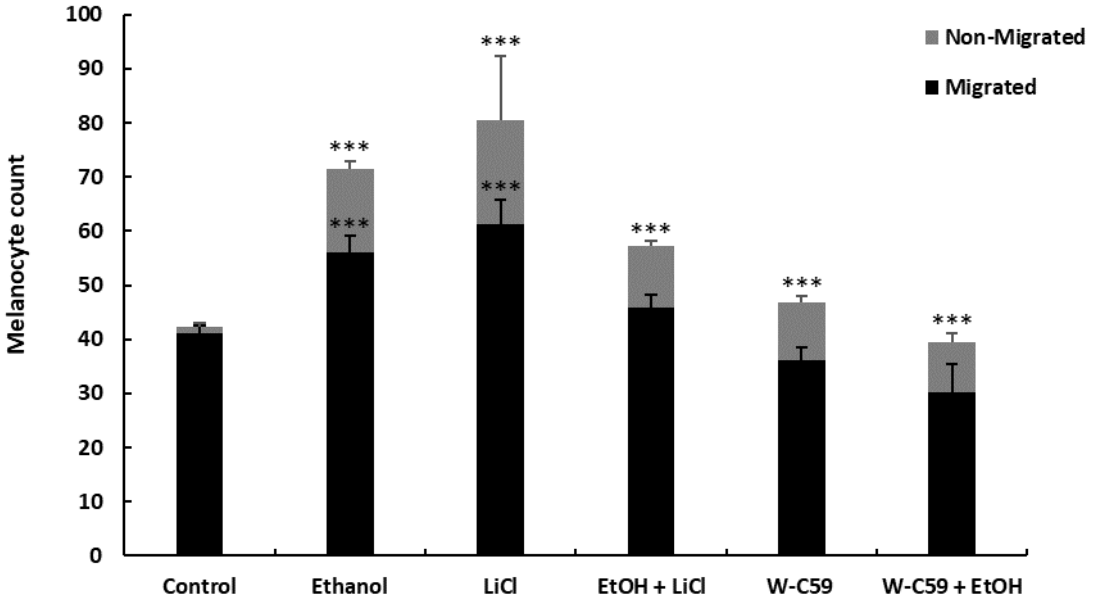

There were high significant differences in both migrated and non-migrated mean melanocyte densities among chemical exposed fish [$F(1,10) = 39.02$, $P < 0.001$]. Highest non-migrated (19.1 ± 12.04, $P < 0.001$) and migrated (61.3 ± 4.54, $P < 0.001$) melanocyte counts were observed in the LiCl treated embryos and the least counts for them were recorded in the W-C59 + EtOH treated fish (30.20 ± 5.22, $P > 0.05$) except for the non-migrated melanocytes, compared to the control sample. EtOH treatment had influenced to enhance the count of both migrated (56.10 ± 2.97, $P < 0.001$) and non-migrated melanocytes (15.3 ± 1.53, $P < 0.001$), irrespective to combining with LiCl. However, EtOH + LiCl combination had less migrated and non-migrated counts relative to the EtOH and LiCl treatments. W-C59 alone treatment displayed less migrated melanocytes and higher non-migrated melanocytes than the control. Interestingly, all the values for the non-migrated melanocyte counts in the chemical treated embryos were significantly different with control sample ($P < 0.001$) whereas EtOH and LiCl treated embryos were only significant for the migrated melanocytes. (Refer the Appendix 4)

4.6 Analysis of melanocyte arrangement differences against different chemical treatments

Figure 4.6.1 Differences in melanocyte arrangement upon various chemical exposures at early larval stage.

This figure evidences the differences in melanocyte arrangement of untreated Control (A) and which were exposed to different chemicals indicating from B-F; consecutively, B- EtOH, C- LiCl, D- EtOH +LiCl, E- W-C59 and F- W-C59 + EtOH. Scale bar: (A, C, D & F) - 500 µm, (B & E) - 200 µm

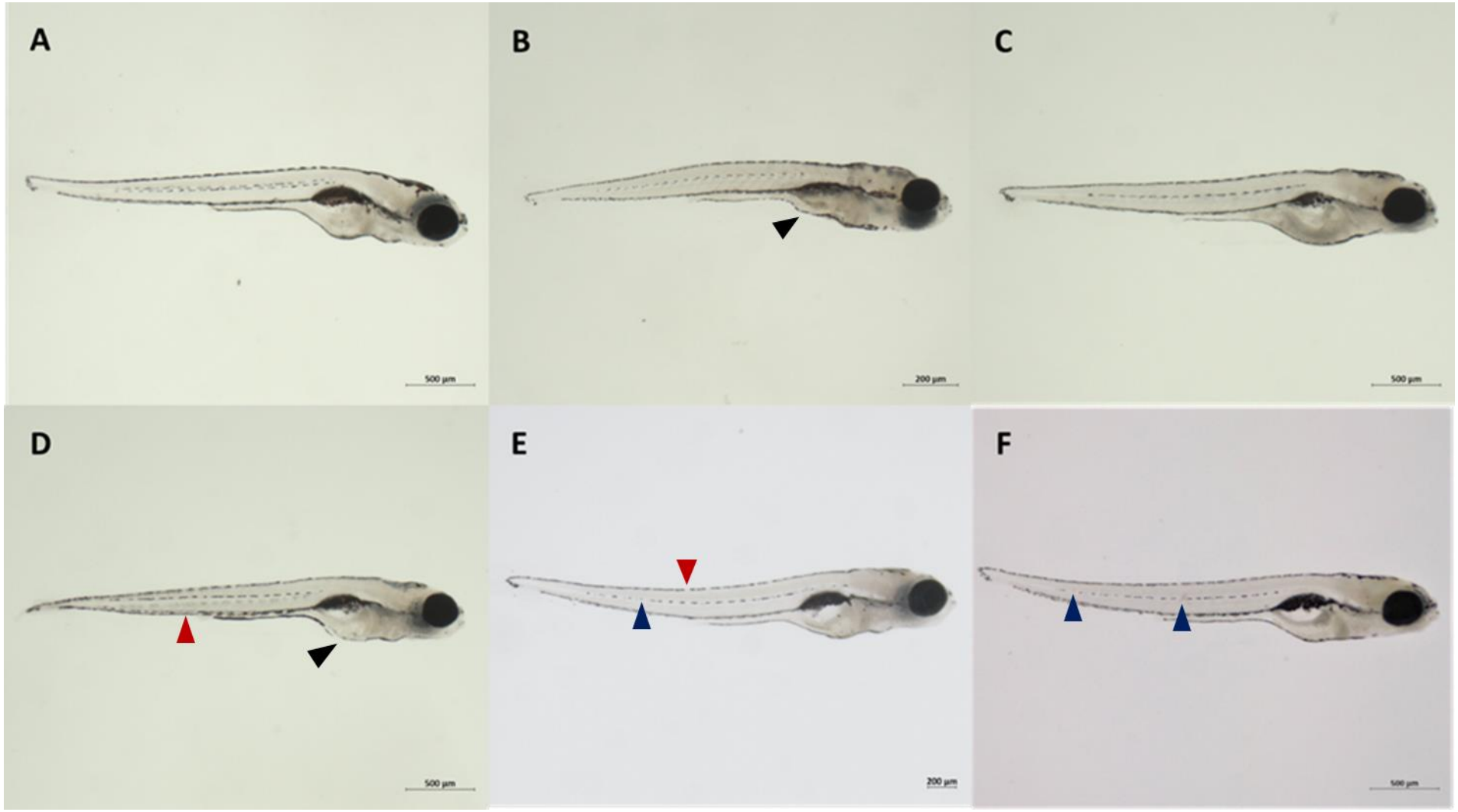
A
500 µm
B
200 µm
C
500 µm
D
500 µm
E
200 µm
F
500 µm

Lateral view of the chemical treated embryos were observed under the microscope and images were captured in order to find the defects in the four stripe melanocyte arrangement as showed in the figure.

As figure shows, no marked dorsal and ventral stripe formation defects were noticed in examining the lateral view of fish (Fig. 4.6.1 B-F). However, it was appeared significant abnormalities in yolk sac stripe formation in the chemical treated embryos which were involved with EtOH (black arrow head of Fig. 4.6.1 B). Significant effect on yolk sac stripe formation was examined in the EtOH treatment combining with LiCl rather than single EtOH treatment (black arrow head of Fig. 4.6.1 D). Similar yolk sac stripe formation was noticed in both control and LiCl exposed in lateral side view (Fig. 4.6.1 A & C). Uniform lateral stripe formation was observed in control sample whereas deficits of stripe formation were recognized with spaces between melanocytes in chemical exposed larval fish. Especially with EtOH exposure, Wnt inhibitor treatment alone and combined treatment of W-C59 + EtOH (dark blue arrow heads of Fig. 4.6.1 E & F). Similar phenomena of lack of melanocytes were prominent in the ventral and dorsal stripe formation in EtOH + LiCl and W-C59 treatments (dark red arrow heads of Fig. 4.6.1 D & E).

4.7. Variations of melanocyte arrangement defects in stripe formation against different chemical treatments

Figure 4.7.1 Variations of melanocyte arrangement in dorsal stripe formation at 6 dpf larval stage of zebrafish against various chemical treatments.

This figure reveals the changes in contribution of melanocyte numbers in dorsal stripe formation of chemical exposed larvae (B-F) compared with control sample (A). Chemical treated fish indicating from B-F; consecutively, B- EtOH, C- LiCl, D- EtOH +LiCl, E- W-C59 and F- W-C59 + EtOH. Scale bar: (A- F)- 200 µm

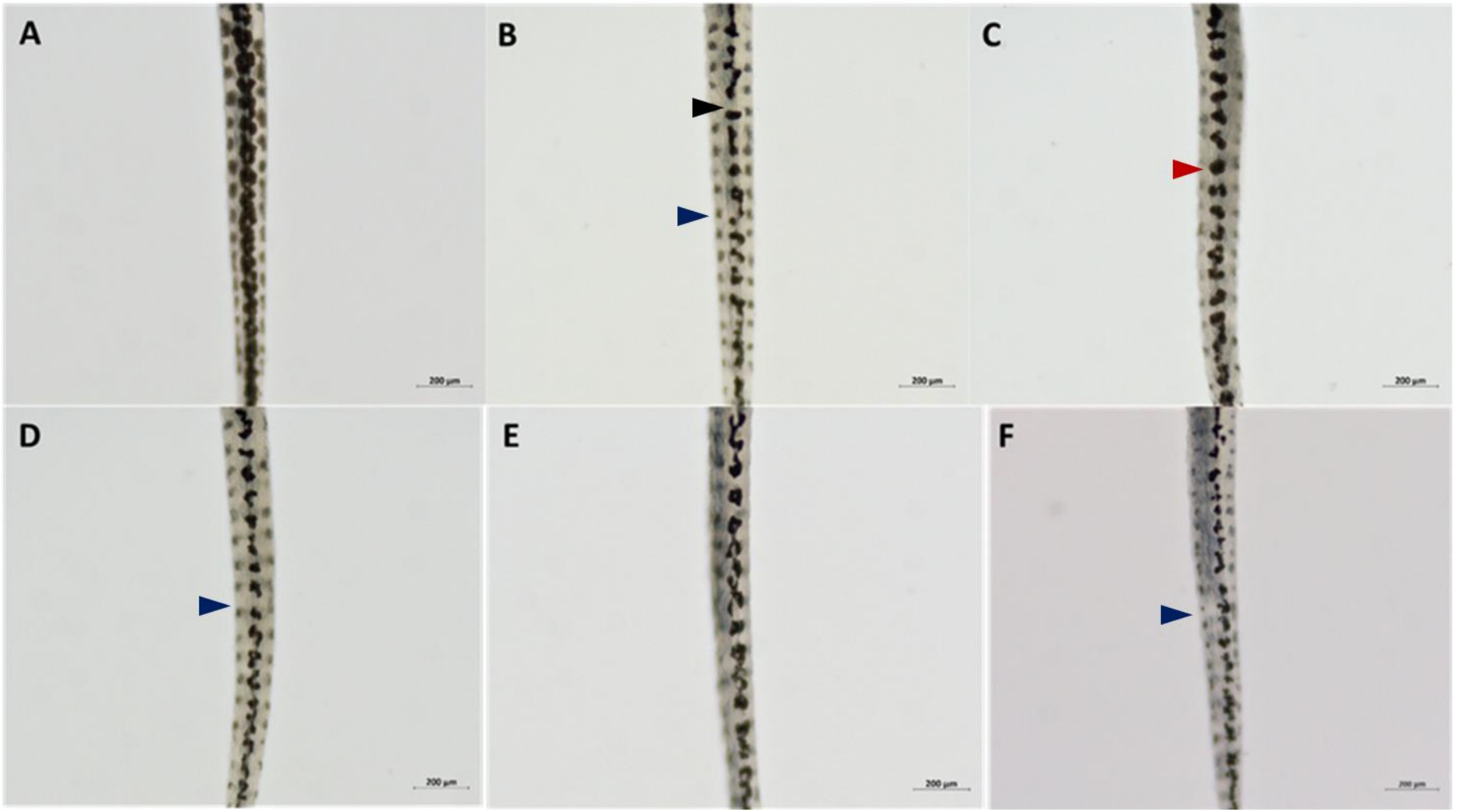
A
B
C
D
E
F

Changes in melanocyte arrangement in dorsal stripe formation were examined on the dorsal view of the fish. Microscopic images show that chemical exposures have altered the dorsal stripe formation (Fig. 4.7.1 B-F). Numerous variations could be observed in the melanocyte arrangement within the stripe and those were mainly comprised with the changes in melanocyte density and shape. It was greatly appeared that all the dorsal stripes of chemical treated larval fish have low melanocyte densities compared to the control fish. It was proved by the presence of more spaces between the melanocytes each other (black arrow head of Fig. 4.7.1 B). Further, it demonstrated the stripe phenotype has been altered with the chemical exposure while having discontinuous and irregular melanocyte arrangement that is dispersed without any definite pattern. EtOH contained chemical treated embryos: EtOH, EtOH +LiCl and W-C59 + EtOH had a considerable effect on stripe formation, resulting with severely damaged melanocytes as illustrated in the figure (dark blue arrow heads of Fig. 4.7.1 B, D & F). Especially, the melanocytes in the dorsal stripe of W-C59 + EtOH treated fish was recorded with highly ablated melanocytes in comparison with other treatments and control sample. Even though, it is appearing less melanocyte counts with the LiCl treatment, melanocyte morphology was somewhat similar to the control fish and it had been less affected (dark red arrow head of Fig. 4.7.1 C).

Figure 4.7. 2 Variations of melanocyte arrangement in yolk sac stripe formation at 6 dpf larval stage of zebrafish against various chemical treatments.

This figure reveals the changes in contribution of melanocyte numbers in yolk sac stripe formation of chemical exposed larvae (B-F) compared with control sample (A). Chemical treated fish indicating from B-F; consecutively, B- EtOH, C- LiCl, D- EtOH +LiCl, E- W-C59 and F- W-C59 + EtOH. Scale bar: (A-C, D & F) 200 µm, (E) -100 µm

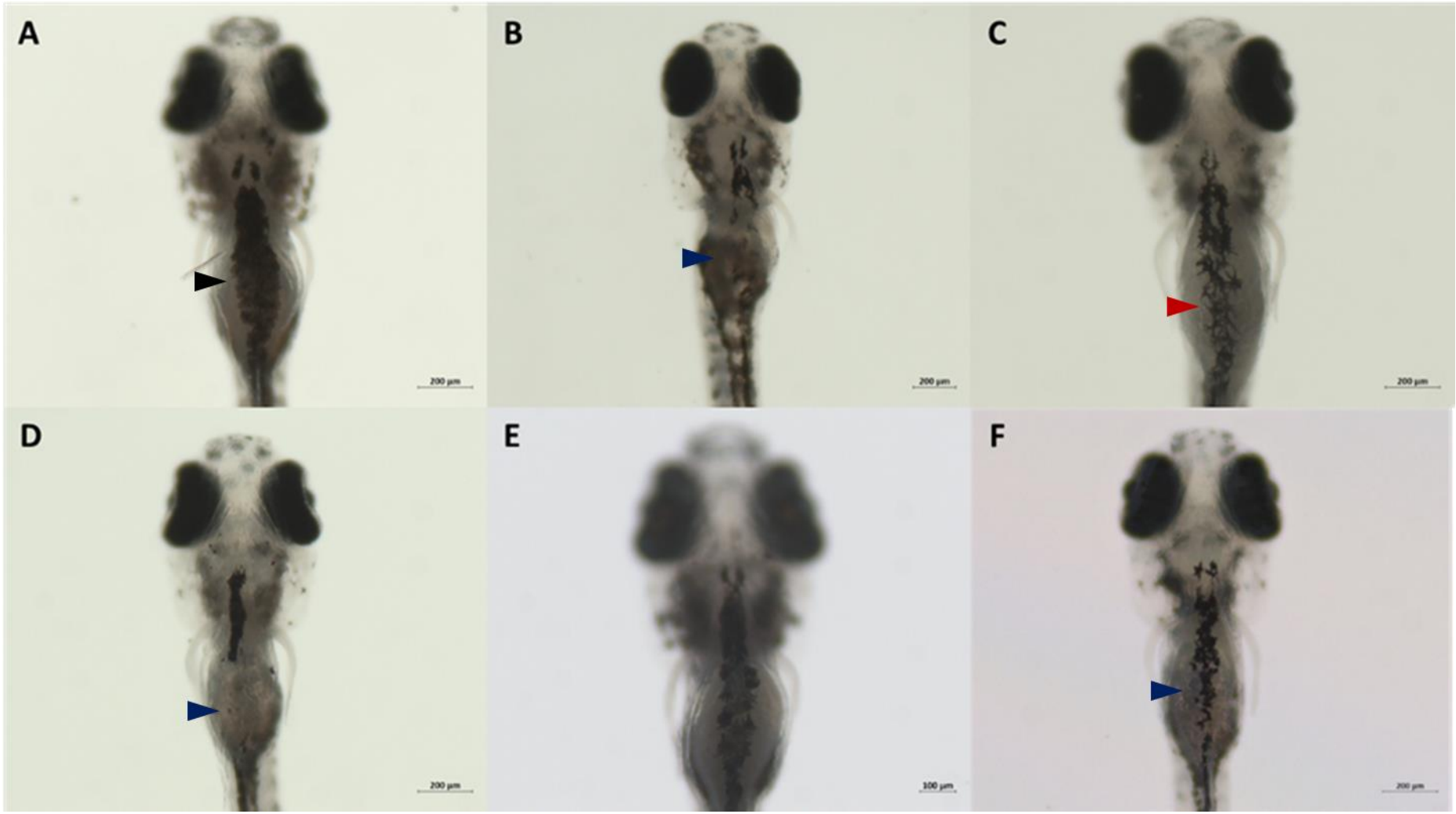
A
B
C
D
E
F

Yolk sac stripe of zebrafish at early larval stage had a characteristic diamond shape arrangement as shown in the control sample in the figure (black arrow head of Fig. 4.7.2 A). But, this arrangement had been malformed in the chemical treated samples. Especially, drastic chemical effect was remarked in the EtOH contained chemical treated embryos; EtOH, EtOH +LiCl and W-C59 + EtOH (dark blue arrow heads of Fig. 4.7.2 B, D & F). Among them, significant loss was examined in the EtOH and EtOH +LiCl treated samples, which had borne with less melanocyte counts compared to the rest of all chemical exposed samples. Typical shape of the yolk sac stripe was also deviated in the treated samples meanwhile stripe phenotypes of the LiCl and Wnt inhibitor treated fish were fairly similar with control stripe formation (Fig. 4.7.2 C & E). Variations in the melanocyte morphology and density in the chemical treated embryos were viewed through the microscopic examinations and all were modified with the chemical effect. Melanocytes in the yolk sac stripe of the LiCl treated fish were more dispersed (dark red arrow head of Fig. 4.7.2 C) and rest of the chemical treated fish had considerably aggregated phenotype compared to the uniform arrangement of the control sample. When all the results considered, it was clearly evident that chemical exposures have effected on the yolk sac stripe formation.

Figure 4.7. 3 Analysis of melanocyte arrangement defects at 6 dpf larval stage of zebrafish against various chemical treatments.

This bar chart illustrates the changes in contribution of melanocyte numbers in four stripe pattern formation of chemical exposed larvae compared with control sample.

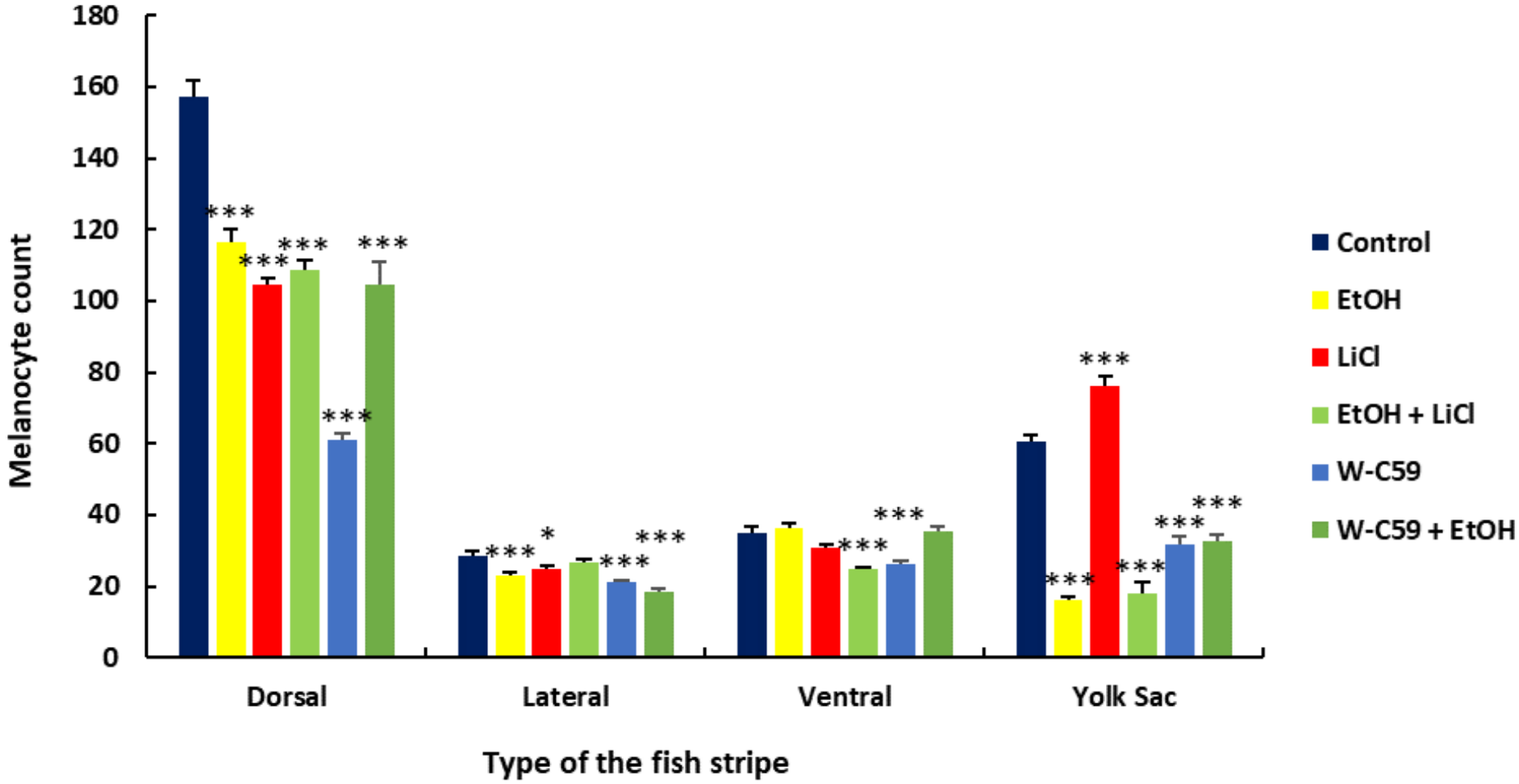
Melanocyte count
180
160
140
120
100
80
60
40
20
0
Dorsal
Lateral
Ventral
Yolk Sac
Type of the fish stripe
Control
EtOH
LiCl
EtOH + LiCl
W-C59
W-C59 + EtOH

Contribution of melanocytes for each dorsal, lateral, ventral and yolk sac stripe formation was quantified by counting as showed in the above bar chart. All the melanocytes of the treated fish had comparatively reduced values for the dorsal stripe formation but the least melanocyte count was recorded in W-C59 treated larval fish (61.1 ± 1.61, $P < 0.001$). Higher melanocyte count was recorded in the dorsal stripe of EtOH treated fish (116.3 ± 03.80, $P < 0.001$) within the chemical treated groups. However, slight variations in melanocyte counts were observed in the chemical exposed fish, but all values were highly significant with the control sample. Lower melanocyte counts had contributed to the lateral stripe formation in the Wnt inhibitor treated larval fish: including W-C59 alone treatment and combine treatment with EtOH, but the least count was recorded in the W-C59 + EtOH exposed fish (18.6 ± 0.49, $P < 0.001$). Here, all the chemical treatments were significant for the melanocyte density in lateral stripe formation against control sample, except the EtOH + LiCl treated fish ($P > 0.05$). Quite interesting results were noted in analyzing the melanocyte counts in ventral stripe formation of each chemical treated larval fish. Here, increased melanocyte number was recorded in the EtOH (36.4.1 ± 1.16, $P > 0.05$) and W-C59 + EtOH treatments (35.3 ± 1.63, $P > 0.05$) relative to the melanocyte count in the control sample. LiCl also had a non-significant melanocyte count compared to the control sample and melanocyte density was little bit lower than the control sample. Unlike the dorsal and lateral stripe formation, EtOH + LiCl (25.0 ± 0.39, $P < 0.001$) treatment had significantly affected to the ventral stripe formation of larval fish with representing the least melanocyte count. Further, a reduced melanocyte count with highly significant value was marked for the W-C59 treated fish as well. In consideration of the analysis of yolk sac stripe formation, substantial enhanced melanocyte count was present in the LiCl (76.0 ± 2.68, $P < 0.001$) treated fish, meanwhile this notable result was not recorded in the previous stripe formations. Yolk sac stripes of EtOH and EtOH + LiCl treated fish had less melanocyte counts while the least was recorded in the EtOH exposed fish (16.2 ± 0.67, $P < 0.001$). However, all the values were highly significant compared to the yolk sac stripe formation of the control sample. (Refer the Appendix 4)

4.8 Analysis of biased migration of melanocytes along the L-R axis

Figure 4.8.1 Examination of biased migration of melanocytes along the L-R axis of zebrafish larvae at 6 dpf against various chemical treatments.

This figure panel illustrates the deficits in the L-R symmetry in melanocyte arrangement in chemical exposed larvae compared to the control sample. (A-B) Overview of WT larvae. (A) and (B) L-R axis of WT larvae. Magnification of lateral views (black boxes in A and B) pigment phenotype at 6 dpf. (C-D) Melanocyte arrangements in the lateral stripe of larvae. Magnified L-R trunk regions of the EtOH treated larvae, black arrow heads point out the defects in melanocyte arrangement.

Left axis (L) and Right axis (R) Scale bar: 200 μm (A-B) and 50 μm (C-D).

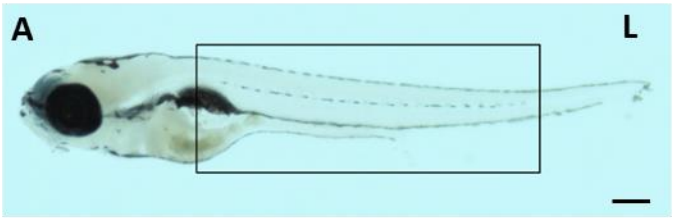
A
L

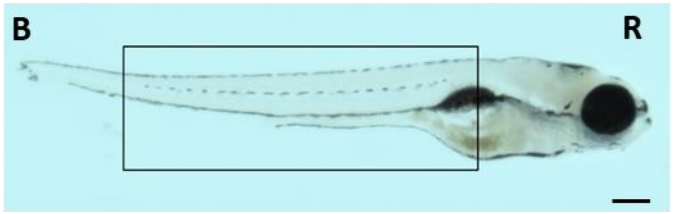
B
R

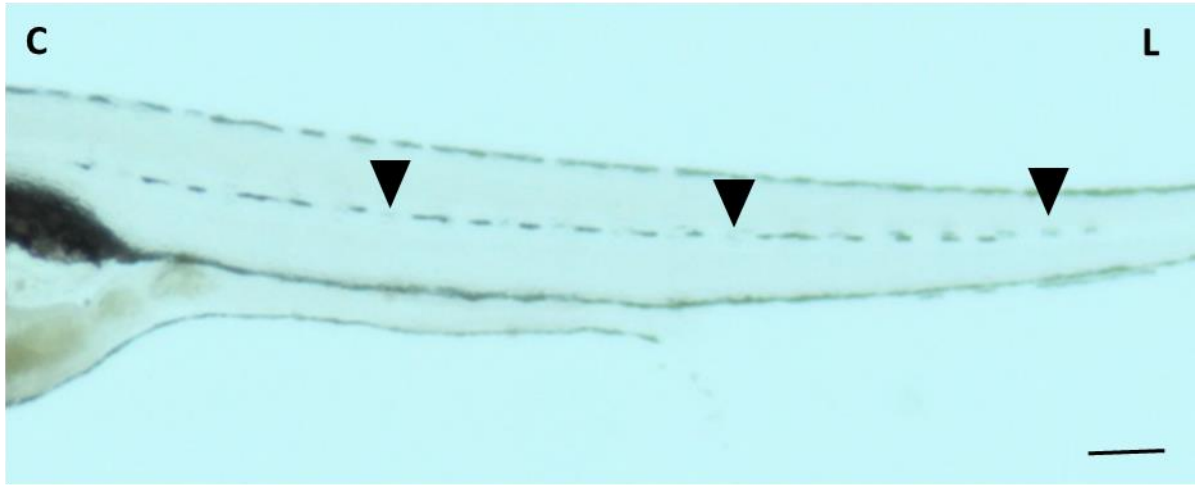
C
L

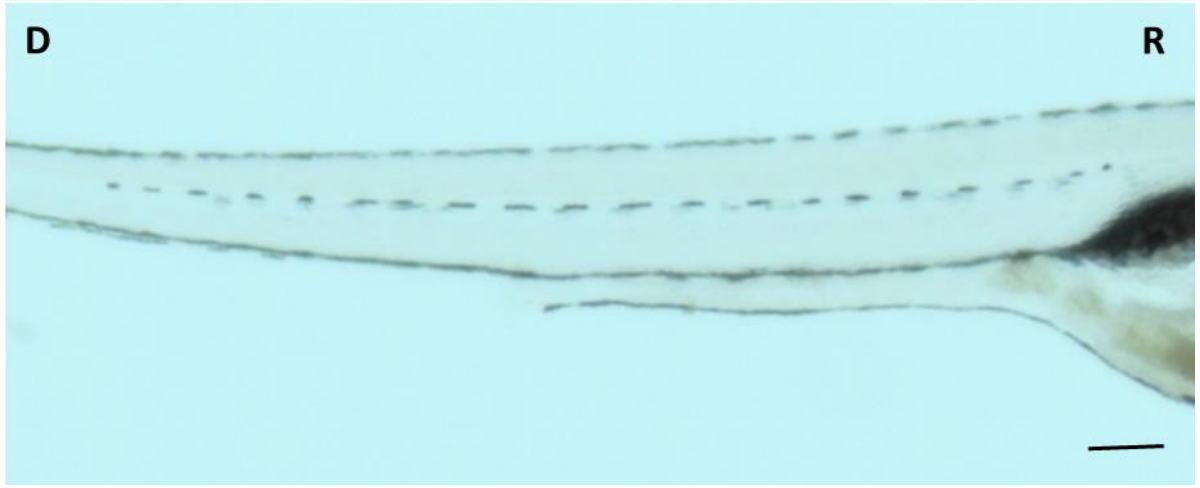
D
R

Defects in the melanocyte arrangement along the L-R axis of the fish were observed in the lateral stripe of 6 dpf larvae. As figure demonstrates, lack of melanocytes were observed in the left axis of the EtOH treated larvae compared to the right side of the same fish. Comparatively huge spaces between the lateral melanocytes along the horizontal axis were examined in the left axis of the fish (black arrow heads Fig. 4.8.1 C) whereas the right axis of the same fish had not exhibited this phenomenon but increased melanocyte count could be inspected (Fig. 4.8.1 D) with uniform melanocyte arrangement along the lateral line.

Figure 4.8.2 Analysis of biased migration of melanocytes along the L-R axis of zebrafish larvae at 6 dpf against various chemical treatments. This bar chart expresses the changes in the L-R symmetry in melanocyte arrangement in chemical exposed embryos compared to the control sample.

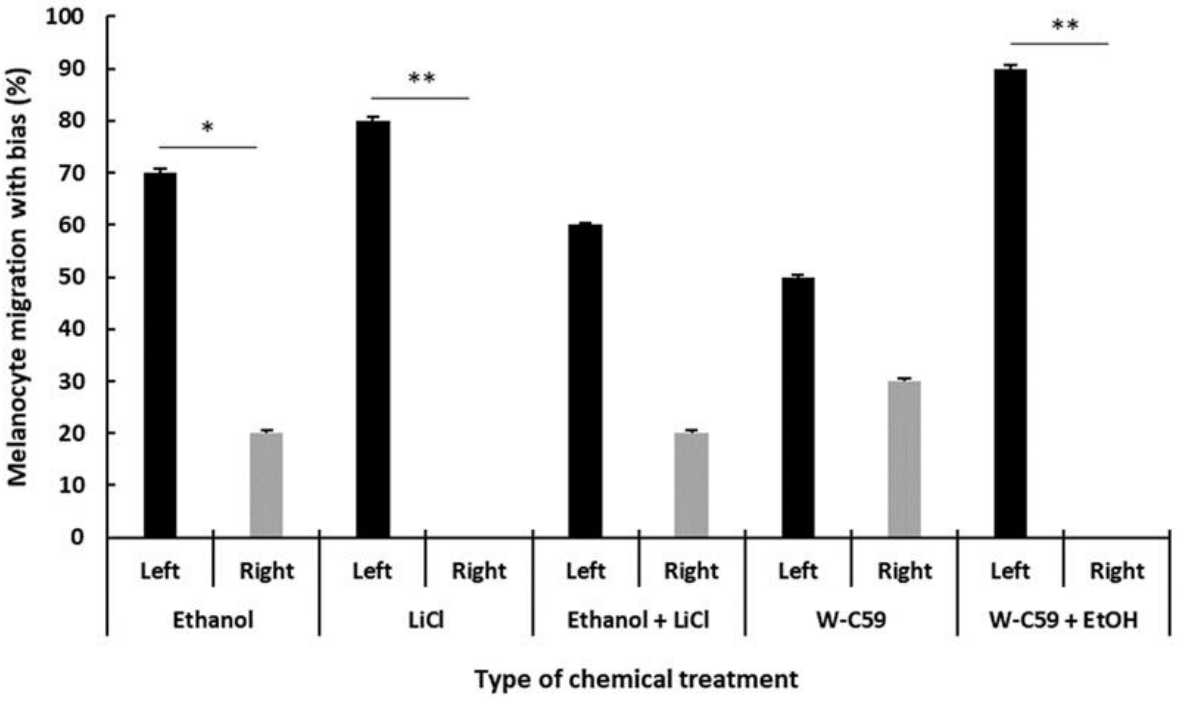

Biased melanocyte migrations along the L-R axis were analyzed by focusing on the melanocyte counts along the lateral stripe of fish in each treatment groups. No changes in the L-R symmetry in the melanocyte arrangements in the untreated control larvae were recorded. However, examining the captured images of the L-R axes of the chemical treated larvae as shown in the Fig: 4.8.2, increased melanocyte counts were displayed prominently on the left side axis than the right-axis of the fish body. Interestingly, all the fish examined in the LiCl and W-C59 + EtOH treatments had trended toward the left-sided melanocyte migration but rest of the chemical treated fish showed biased melanocyte migration on both L-R axes. Significant difference in biased melanocyte counts was not observed in the EtOH + LiCl and W-C59 treated fish but high significant results were shown in LiCl and W-C59 + EtOH exposed larval fish. Embryonic EtOH exposed fish showed a significant mixed biased melanocyte arrangement along the L-R axis but comparatively less right-sided migration was detected against the left-sided migration relative to the data of other chemical treated fish.

4.9 Measuring the melanin intensity / dispersion in the dorsal stripe at the head region.

Figure 4.9. 1 Comparison of the fluctuation of melanin intensity of the control and EtOH treated zebrafish larvae from 4 dpf to 10 dpf developmental stages. This figure illustrates the differences in mean intensity values in the EtOH treated samples compared to the control samples of each life stage.

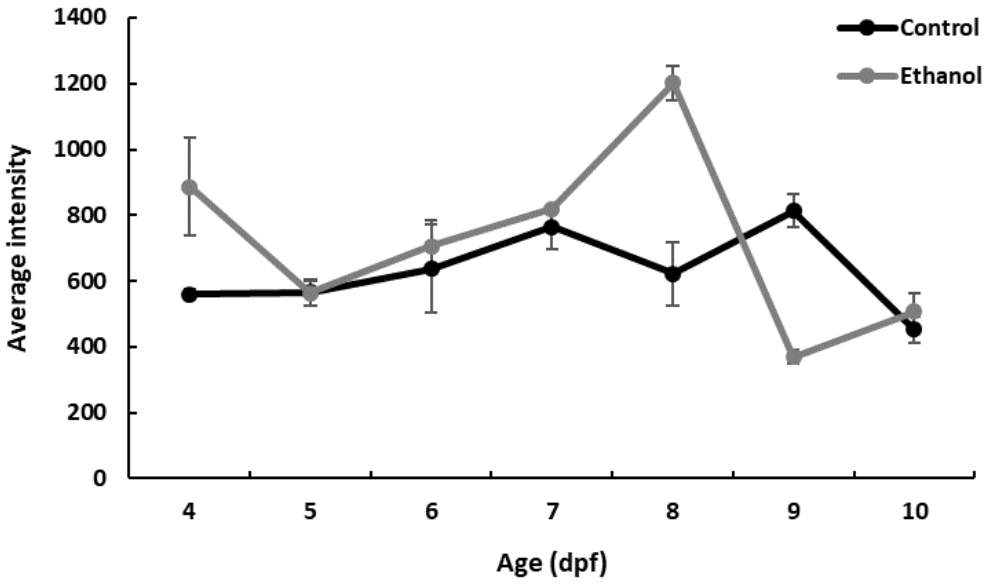

Melanin intensity values were measured at the dorsal stripe on the head region using the microscopic software analysis. Higher intensity values were recorded between the 4-8 dpf life stages in the EtOH treated fish compared to the control sample and the highest value was recorded at 8 dpf. Then it was significantly drop at later stages. Intensity fluctuation of EtOH was similar with control sample but marked differences were encountered at 8 dpf and 9 dpf stages. Considering the overall intensity fluctuation of the control and EtOH treated fish, high average intensity value was marked in the EtOH treated fish.

Figure 4.9.2 Comparison of the fluctuation of melanin intensity of the control and LiCl treated zebrafish larvae from 4 dpf to 10 dpf developmental stages. This figure illustrates the differences in mean intensity values in the LiCl treated samples compared to the control samples of each life stage.

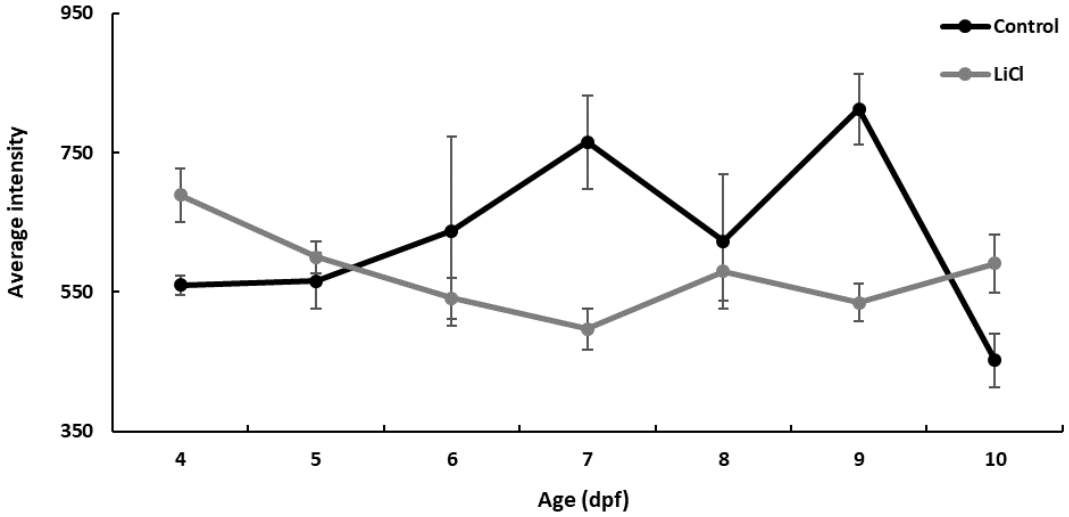

High intensity values were detected at the initial stages of the fish development but low values were observed in later mature stages compared to the control sample and considering the LiCl itself. Huge gaps in the intensity values between the control and LiCl treated fish were observed at 7 dpf and 9 dpf life stages. As a whole, LiCl treatment had a considerable low intensity value in compared to the untreated control fish group.

Figure 4.9. 3 Comparison of the fluctuation of melanin intensity of the control and EtOH + LiCl treated zebrafish larvae from 4 dpf to 10 dpf developmental stages. This figure illustrates the differences in average intensity values in the EtOH + LiCl treated samples compared to the control samples of each life stage.

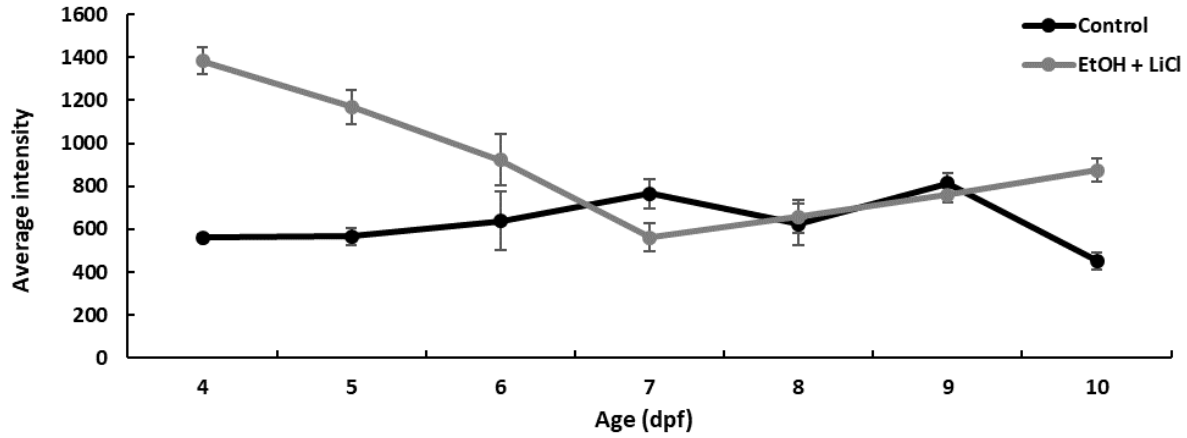

Contrast differences in the intensity values of the control and chemical treatment groups were spotted at the initial stages of the fish development; 4- 5 dpf but the difference was gradually reduced at later stages. After considering all the results during the period of 4-10 dpf, EtOH + LiCl treated fish showed a high average intensity value compared to the control sample.

Figure 4.9. 4. Comparison of the fluctuation of melanin intensity of the control and W-C59 treated zebrafish larvae from 4 dpf to 10 dpf developmental stages. This figure illustrates the differences in average intensity values in W-C59 treated samples compared to the control samples of each life stage.

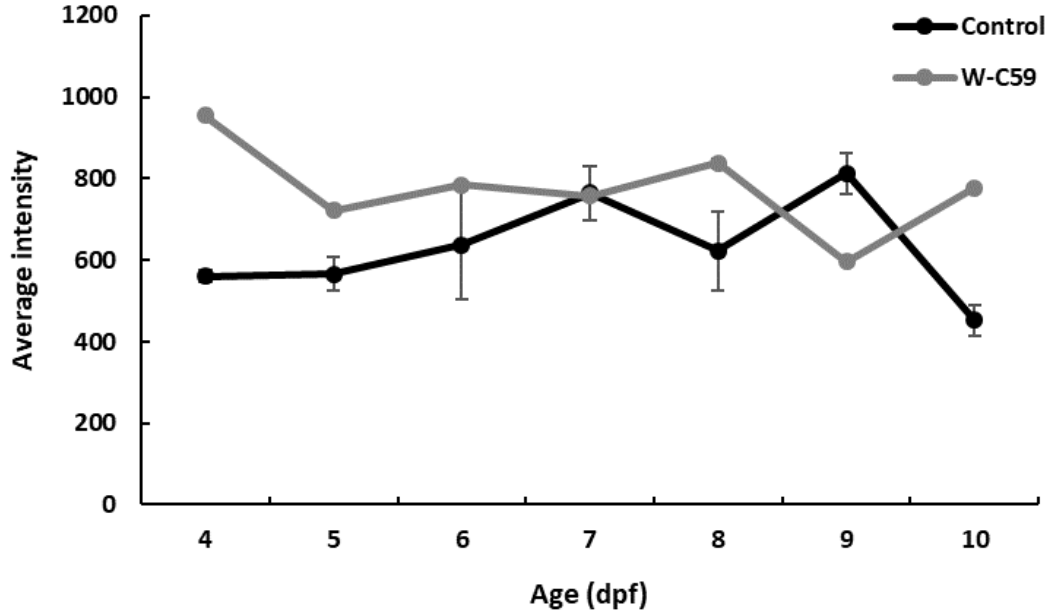

Sudden fluctuations in average intensity values were recorded in the W-C59 chemical treated fish. Higher intensity values were obtained during the 4 dpf to 6 dpf and contrast differences in intensity values were distinguished at later stages of the fish development. Comparatively, a high average intensity value was recognized in the fish which were exposed to the Wnt inhibitor treatment over the control fish.

Figure 4.9.5 Comparison of the fluctuation of melanin intensity of the control and W-C59 + EtOH treated zebrafish larvae from 4 dpf to 10 dpf developmental stages. This figure illustrates the differences in average intensity values in W-C59 + EtOH treated samples compared to the control samples of each life stage.

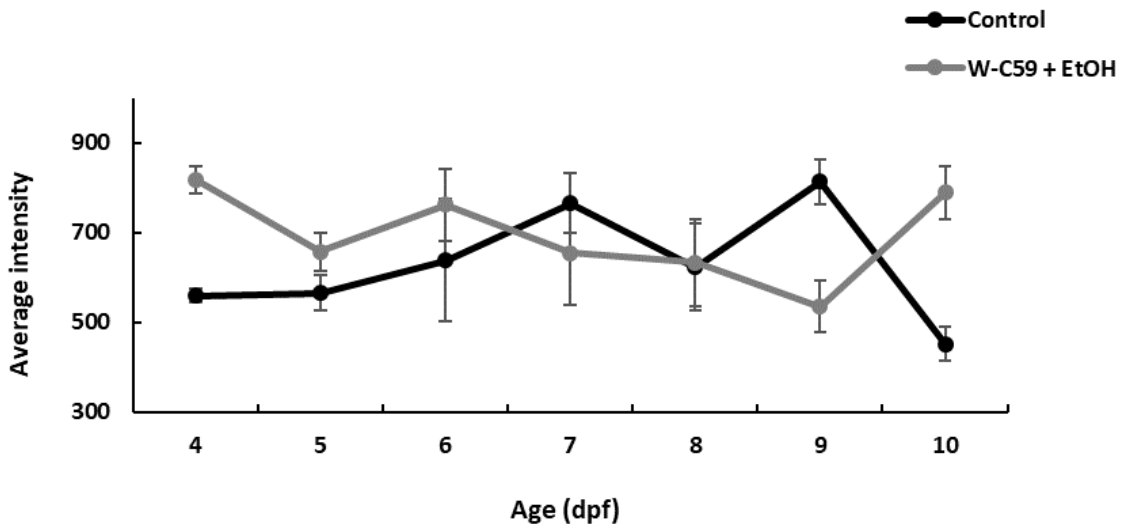

High intensity values were examined during the 4 dpf – 6 dpf growth period of fish relative to the control group but intensity value was distinctly decreased until 9 dpf and enhanced again at 10 dpf. Overall, a high average intensity value was disclosed in the treated fish over the fish development in compared to the control group.

4.10 Investigation of melanin formation in the zebrafish optic vesicles

Figure 4.10.1 Examination of melanogenesis in live zebrafish eyes at 2 dpf embryonic stage against various chemical treatments.

This figure shows the differences in melanin formation in the optic vesicles of untreated Control (A) and which were exposed to the different chemicals indicating from B-F; consecutively, B-EtOH, C- LiCl, D- EtOH +LiCl, E- W-C59 and F- W-C59 + EtOH Scale bar: (A-F) 50 µm

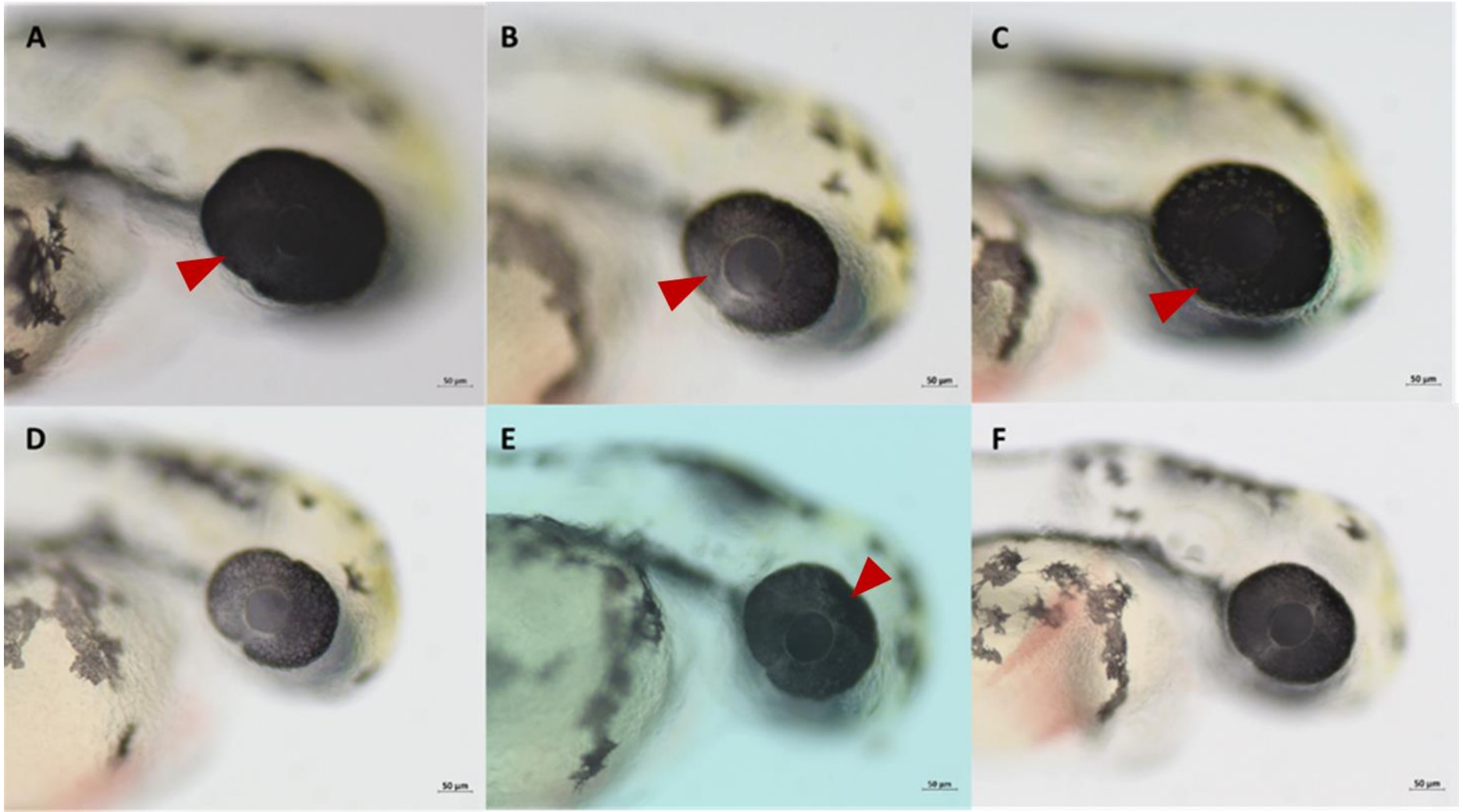
A
B
C
D
E
F

Changes in the melanin formation of the eyes could be observed against different chemical treatments. Lack of melanin pigmentation in the RPE layer of the zebrafish eyes were detected in all the chemical treated embryonic fish except in the LiCl treated samples. Severe defects in the melanin formation were appeared in the fish samples which were contained with EtOH; EtOH, EtOH +LiCl and W-C59 + EtOH (Fig. 4.10.1 B, D and F). It was observed that melanin was highly reduced within the regions where close to the eye lens of the chemical treated samples (dark red arrow head of Fig. 4.10.1 B) and un affected areas were displayed with the high melanin intensity (dark red arrow head of Fig. 4.10.1 E). However, the melanin reduction was mostly uniformed throughout retinal layer of the eyes which were exposed to EtOH +LiCl (Fig. 4.10.1 D). Melanin synthesis of the RPE in the LiCl treated embryos was similar to the eye pigmentation of control fish (dark red arrow heads of Fig. 4.10.1 A & C**)**, expressed with high black coloration under the microscopic observations. Wnt inhibitor treatment alone had negatively impacted on melanin formation in the RPE but it showed a moderate effect relatively to the consequences generated from EtOH treatments (Fig. 4.10.1 E). However, fewer number of W-C59 exposed zebrafish embryos showed albino phenotype of eyes (Fig. 4.13.2- Appendix 5). Microscopic examinations, clearly demonstrated that embryonic chemical exposure manipulates the melanin formation in eyes.

Figure 4.10.2 Estimation of ocular melanin formation at 2 dpf embryonic stage of zebrafish against various chemical treatments. This bar chart illustrates the changes in melanin formation in eyes of the chemical exposed embryos compared with control sample.

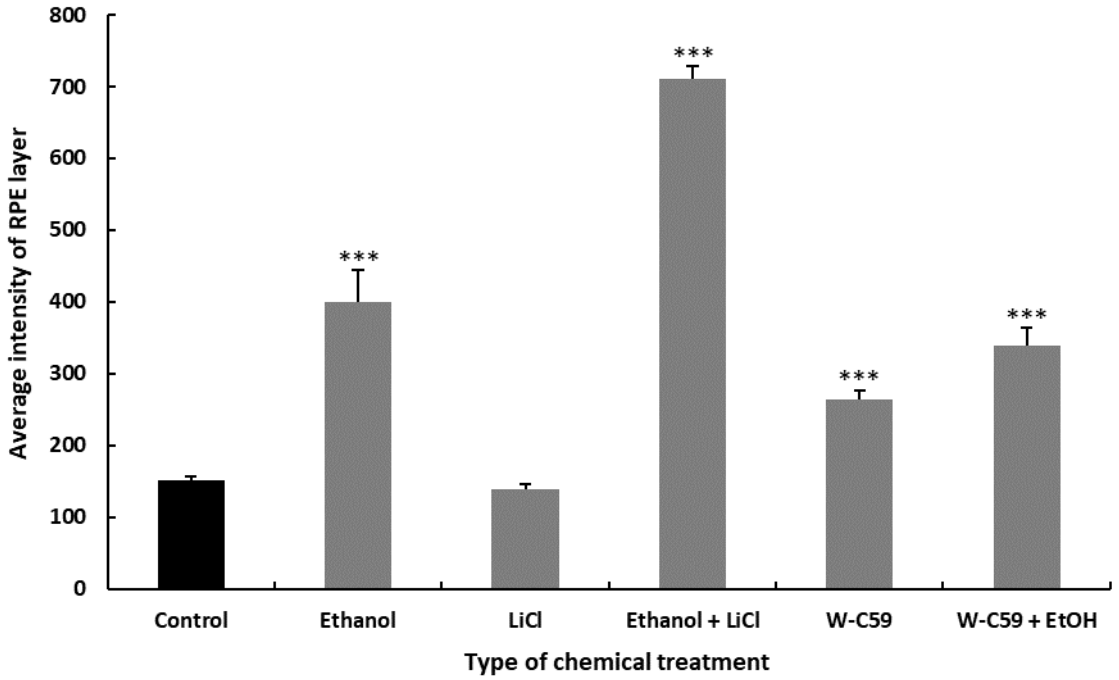

Intensity for melanin pigmentation was analyzed in the eyes of the control and chemical treated embryos using the ZEN 2011 software. According to the analysis, high intensity values were generated in the EtOH involved chemical treatments. EtOH +LiCl had the highest average intensity value meanwhile single treatment of EtOH and combine treatment of W-C59 + EtOH were recorded lesser than it. LiCl treatment had almost a similar intensity value in compared with control while the W-C59 treated embryos showed a moderate intensity value relative to the control and EtOH + LiCl treatment. Further, all the melanin intensity values of the chemical treated embryos were highly significant [$F(5,54) = 86.21$, $P < 0.001$] except the fish in the LiCl treated group. Overall, data analysis provides the evidence on the capability of chemical exposures to regulating the melanin synthesis in the retinal layer of eyes. (Refer the Appendix 4)

Figure 4.10.3 Examination of melanogenesis in toluidine blue-stained sections of zebrafish eyes at 2 dpf embryonic stage against various chemical treatments.

This figure shows the differences in melanin formation in the RPE layer of optic vesicles at 2 dpf of untreated Control (A) and which were exposed to different chemicals (B-F).

A′ and A-F Toluidine blue-stained transversal semi-thin plastic sections (thickness – 300 nm) through the central part of the eyes at 2 dpf. A′- Cross-section of entire head, (A-F) higher magnifications of individual eyes. A- Control, B- EtOH, C- LiCl, D- EtOH +LiCl, E- W-C59 and F- W-C59 + EtOH. Scale bar: (A′, A-F) 1000 nm

Abbreviations*:* L- Lens; NR- Neural retina and RPE- Retinal pigmented epithelium

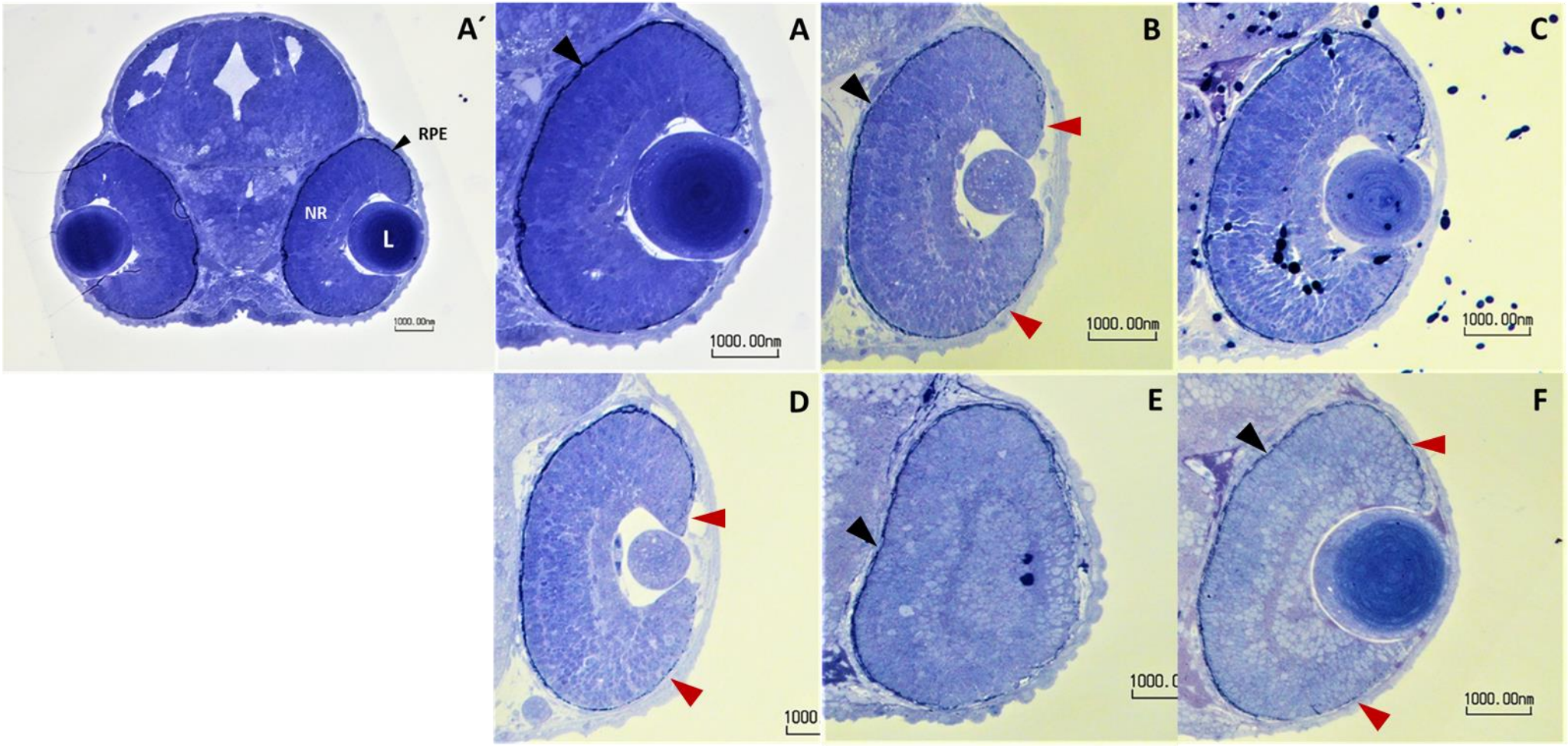
A´
RPE
NR
L
1000.00nm
A
1000.00nm
B
1000.00nm
C
1000.00nm
D
1000
E
1000.0
F
1000.00nm

Changes in RPE development were appeared in examining the histological embryonic eye sections which were exposed to different chemical treatments. RPE layer of untreated control zebrafish appeared darker (black arrow head of Fig. 4.10.3 A) than the RPE coloration of eyes in the rest of chemical incubated embryos. It was clearly noticeable that the RPE layers of all chemical treated embryos has a discontinuous melanin band compared to the WT control fish (black arrow heads of Fig. 4.10.3 B, E & F). Closer inspection of chemical exposed eye phenotypes in toluidine blue cross sections at the light microscopic level, revealed that reduced density of melanin pigment inside of the RPE layer. EtOH and its' combined treatments of EtOH +LiCl and W-C59 + EtOH had a drastic damage in RPE formation (black arrow heads of Fig. 4.10.3 B & F). It was reflected by illustrating the lighter pigmented RPE bands of chemical exposed eyes. The thickness of the dark colored melanin bands of RPE was less in the eyes of chemical treated fish compared to the untreated control (Fig. 4.10.3 B-F). Chemical effects were explicit in the outermost layers of eyes including the RPE and the retinal layers in the center of the eyes. Especially, the strongest effects were more noticeable in the RPE cells which are covering the tips of the neural retina (near the lens) of the chemical exposed eyes (dark red arrow heads of Fig. 4.10.3 B, D & F) than the RPE cells located at the central region of the retina. It was clearly displayed that the RPE cells of the LiCl treated eyes have covered a significantly larger area of the eyes (Fig. 4.10.3 C) compared to the rest of chemical exposed eyes and this result was quite similar to the control fish.

(Appearance of a fuzzy coat over the LiCl eye cross section is not related with the effect of chemical action but an issue with toluidine blue staining procedure)

Figure 4.10.4 Examination of melanosome biogenesis in RPE of zebrafish eyes at 2 dpf embryonic stage against various chemical treatments.

This TEM images of the cytoplasm of RPE melanocytes show the differences in biogenesis of mature melanosomes in the optic vesicles at 2 dpf of untreated Control (A) and which were exposed to the different chemicals (B-F).

A-F High-magnification of TEM images of the mature melanocytes in the RPE of control and chemical treated embryos. A- Control, B- EtOH, C- LiCl, D- EtOH +LiCl, E- W-C59 and F- W-C59 + EtOH. Scale bar: (A-F) 2µ

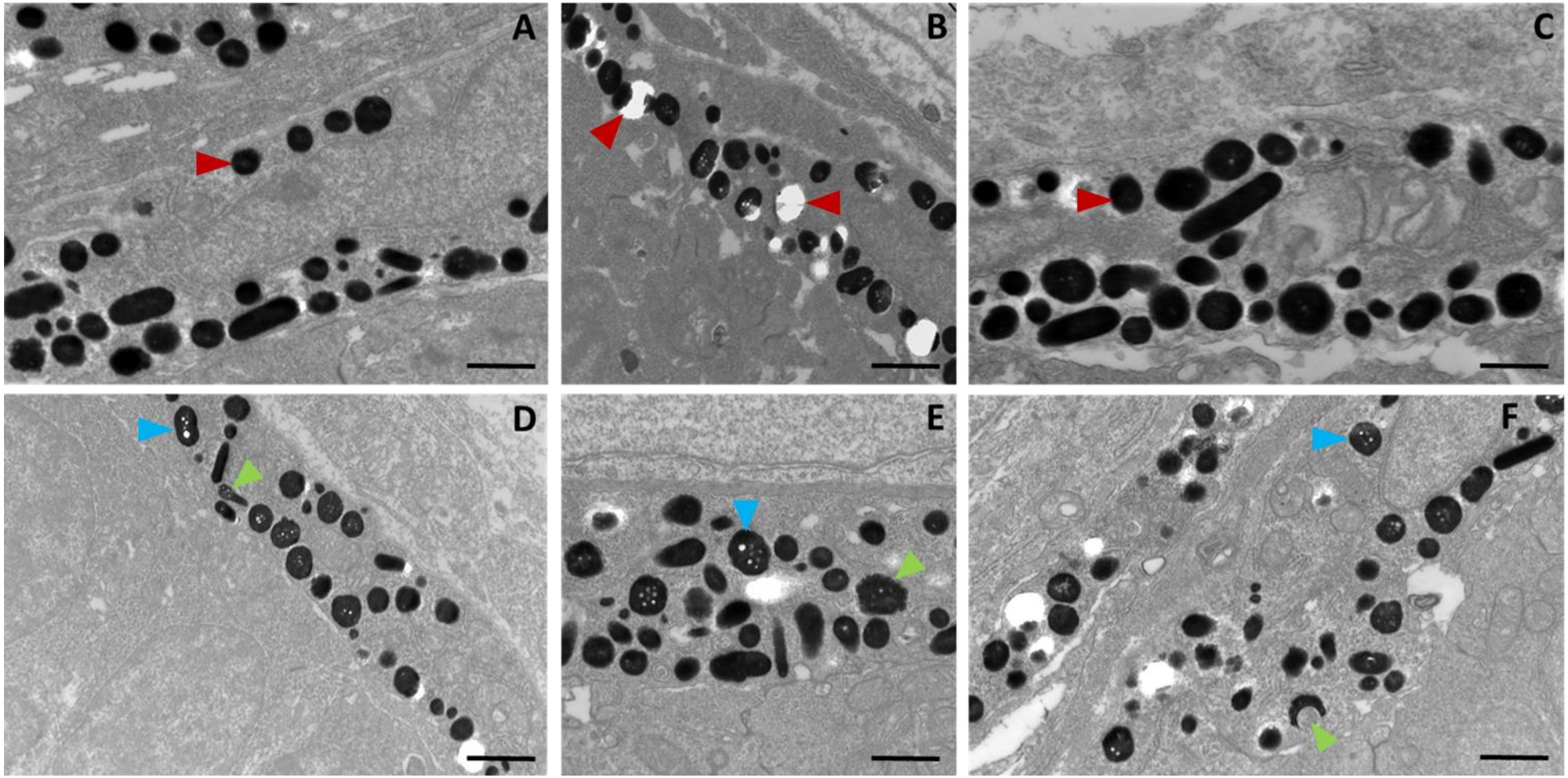
A
B
C
D
E
F

Changes in melanosome biogenesis / phenotype were detected in comparing the ultrathin TEM sections of the chemical treated RPE cells. Intensity of black coloration of melanin pigment contained melanosome vesicles was high in the control and LiCl treated eyes (red arrow heads of Fig. 4.10.4 A & C). Meanwhile lighter pigmented, partially filled and empty melanosome vesicles were recorded in the rest of chemical treated eyes (red arrow heads of Fig. 4.10.4 B). In contrast to oval/spherical and cylindrical melanosomes in the control fish, most of melanin-containing pigment granules in the EtOH +LiCl, W-C59 and W-C59 + EtOH were observed to be uneven, aberrantly shaped and destructed with chemical exposure (light green arrow heads of Fig. 4.10.4 D, E & F). Numerous aberrations in melanosome biogenesis were present in the RPE cells which were exposed to EtOH and its' combined treatments of EtOH +LiCl and W-C59 + EtOH. In contrast, W-C59 + EtOH chemical treatment was appeared to be responsible for generating most of these defects. Lumen of some mature melanosomes had an appearance of 'holes' and this phenotype was prominent in majority of melanosomes in the chemical treated eyes except in the LiCl group (light blue arrow heads of Fig. 4.10.4 D, E & F).

Figure 4.10.5 Examination of melanogenesis in toluidine blue-stained sections of zebrafish eyes at 6 dpf larval stage against various chemical treatments.

This figure shows the differences in melanin formation in the RPE layer of optic vesicles at 6 dpf of untreated Control (A) and which were exposed to different chemicals (B-F).

A′ and A-F Toluidine blue-stained transversal semi-thin plastic sections (thickness – 300 nm) through the central part of the eyes of 6 dpf. A′- Cross-section of entire head, (A-F) higher magnifications of individual eyes. A- Control, B- EtOH, C- LiCl, D- EtOH +LiCl, E- W-C59 and F- W-C59 + EtOH. Scale bar: (A′, A-F) 1000 nm

Abbreviations*:* L- Lens, NR- Neural retina and RPE- Retinal Pigmented epithelium

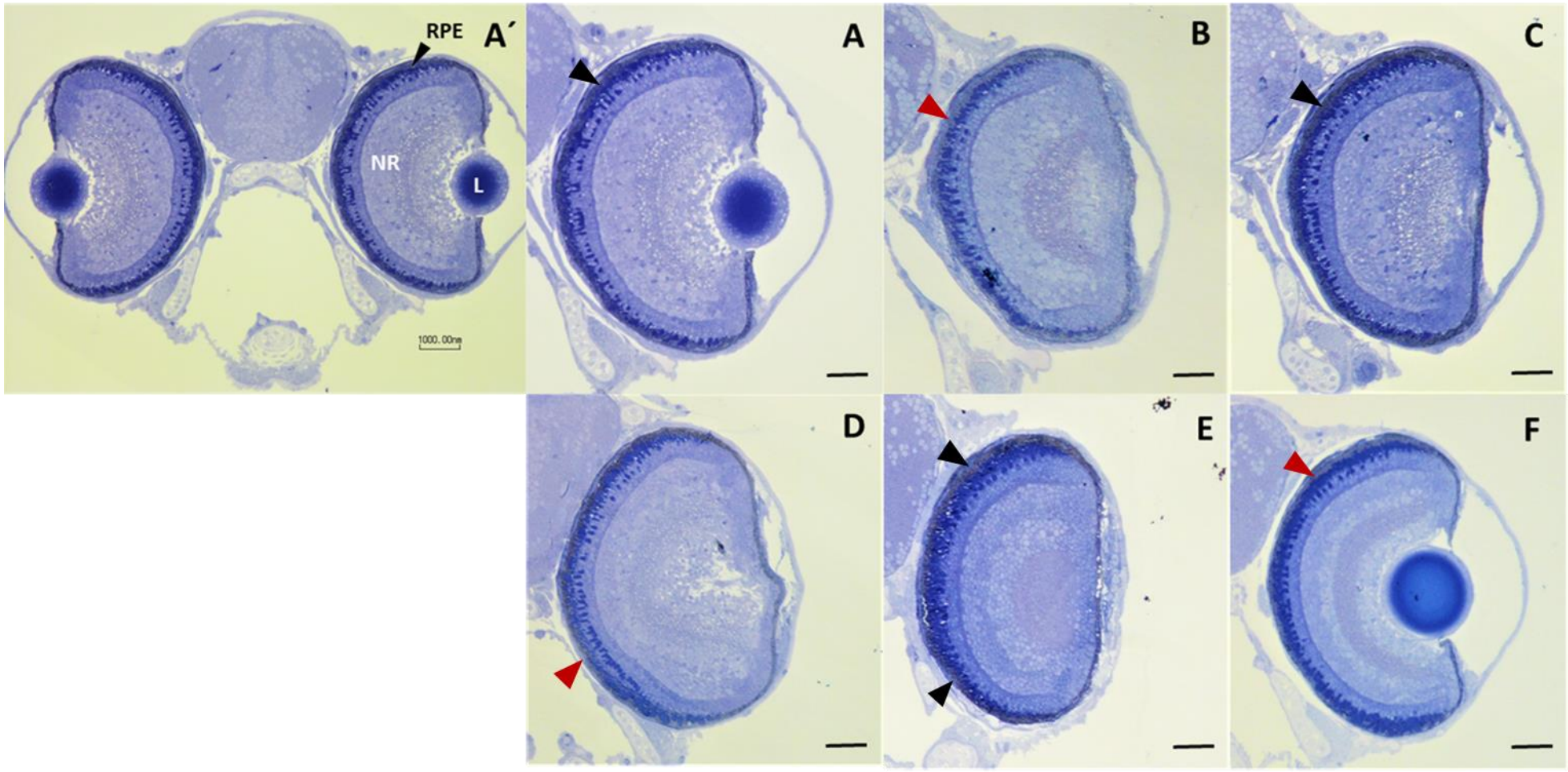
RPE
A´
NR
L
1000.00nm
A
B
C
D
E
F

Slight changes in RPE cell layer formation were express in close light microscopic examinations of the plastic sections of larval eyes which were exposed to different chemical treatments. Comparatively, the darkest RPE layer was observed in the LiCl treated eyes (black arrow head of Fig. 4.10.5 C), meanwhile the darkness of the RPE layer of the control sample was low compared with LiCl eyes (black arrow head of Fig. 4.10.5 A). In addition to them, RPE layer of the W-C59 treatment displayed a dark band but melanin density was appeared to be discontinuous throughout of the layer (black arrow heads of Fig. 4.10.5 E). RPE cell layers which were incubated in EtOH, EtOH +LiCl and W-C59 + EtOH showed paler pigmented RPE bands (dark red arrow heads of Fig. 4.10.5 B, D & F) compared to the untreated control zebrafish and other rest of chemical incubated larval fish. It was clearly noticeable that the RPE layers of all chemical treated embryos has a discontinuous melanin band compared to the WT control fish (Fig. 4.10.5 B, D & F). The thickness of dark colored melanin bands of the RPE was less in the eyes of chemical treated fish except the LiCl treated and untreated control zebrafish.

Figure 4.10.6 Examination of melanosome biogenesis in the RPE of zebrafish eyes at 6 dpf larval stage against various chemical treatments.

This TEM images of the cytoplasm of RPE melanocytes show the differences in biogenesis of mature melanosomes in the optic vesicles at 6 dpf of untreated Control (A) and which were exposed to different chemicals (B-F).

A-F High-magnification TEM images of mature melanocytes in RPE of control and chemical treated embryos. A- Control, B- EtOH, C- LiCl, D- EtOH +LiCl, E- W-C59 and F- W-C59 + EtOH. Scale bar: (A-F) 2 µ

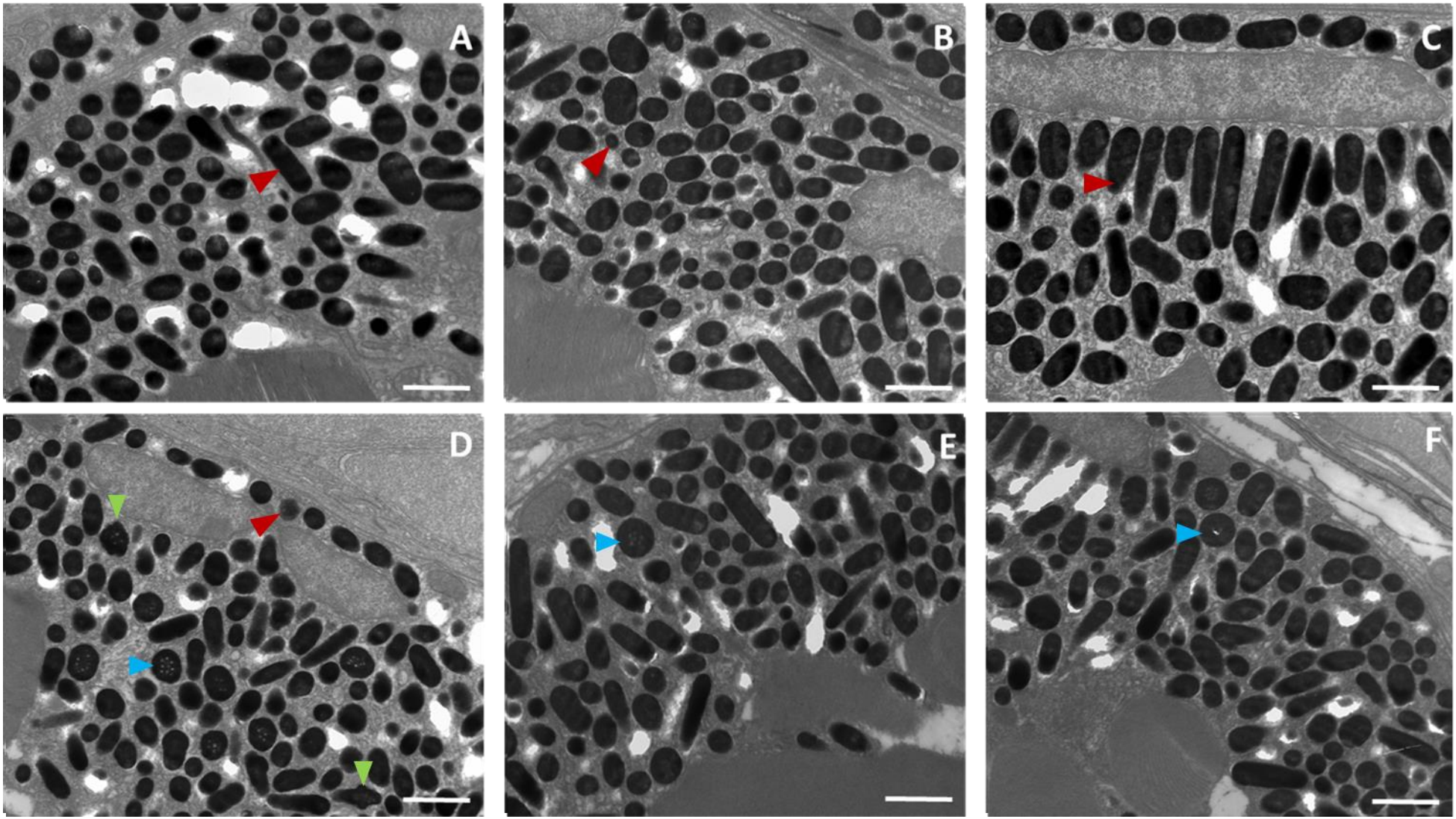
A
B
C
D
E
F

Few defects of melanosome biogenesis and phenotype were apparent in comparing the TEM ultrathin sections of the chemical treated RPE cells. It was clearly appeared that the intensity of black coloration of melanosome vesicles was high in the control and LiCl treated eyes (red arrow heads of Fig. 4.10.6 A & C) while relatively pale melanosome vesicles were recorded in the rest of chemical treated eyes (red arrow head of Fig. 4.10.6 D). Most of the melanosome vesicles in EtOH included and W-C59 chemical treated RPE cells were comparatively small in size (red arrow heads of Fig. 4.10.6 B) and lightly pigmented (red arrow heads of Fig. 4.10.6 D). Uneven and aberrantly shaped melanosomes were recorded in the EtOH and EtOH contained other chemical treatments but high density was recorded in the EtOH +LiCl exposed RPE cells (light green arrow heads of Fig. 4.10.6 D). In addition to that perforated melanosomes dominantly developed in the EtOH +LiCl treated eyes and low numbers were exhibited in the W-C59 and W-C59 + EtOH exposed fish (light blue arrow heads of Fig. 4.10.6 D, E & F).

4.11 Determination of melanin content of zebrafish with chemical exposure

Figure 4.11. 1 Analysis of melanin content at 2 dpf embryonic stage of zebrafish against various chemical treatments.

This figure proves the defects in melanin formation of the chemical exposed zebrafish embryos (B-F) compared with control sample (A). Chemicals which were used for exposing embryos are indicating from B-F; consecutively, B- EtOH, C- LiCl, D- EtOH +LiCl, E- W-C59 and F- W-C59 + EtOH.

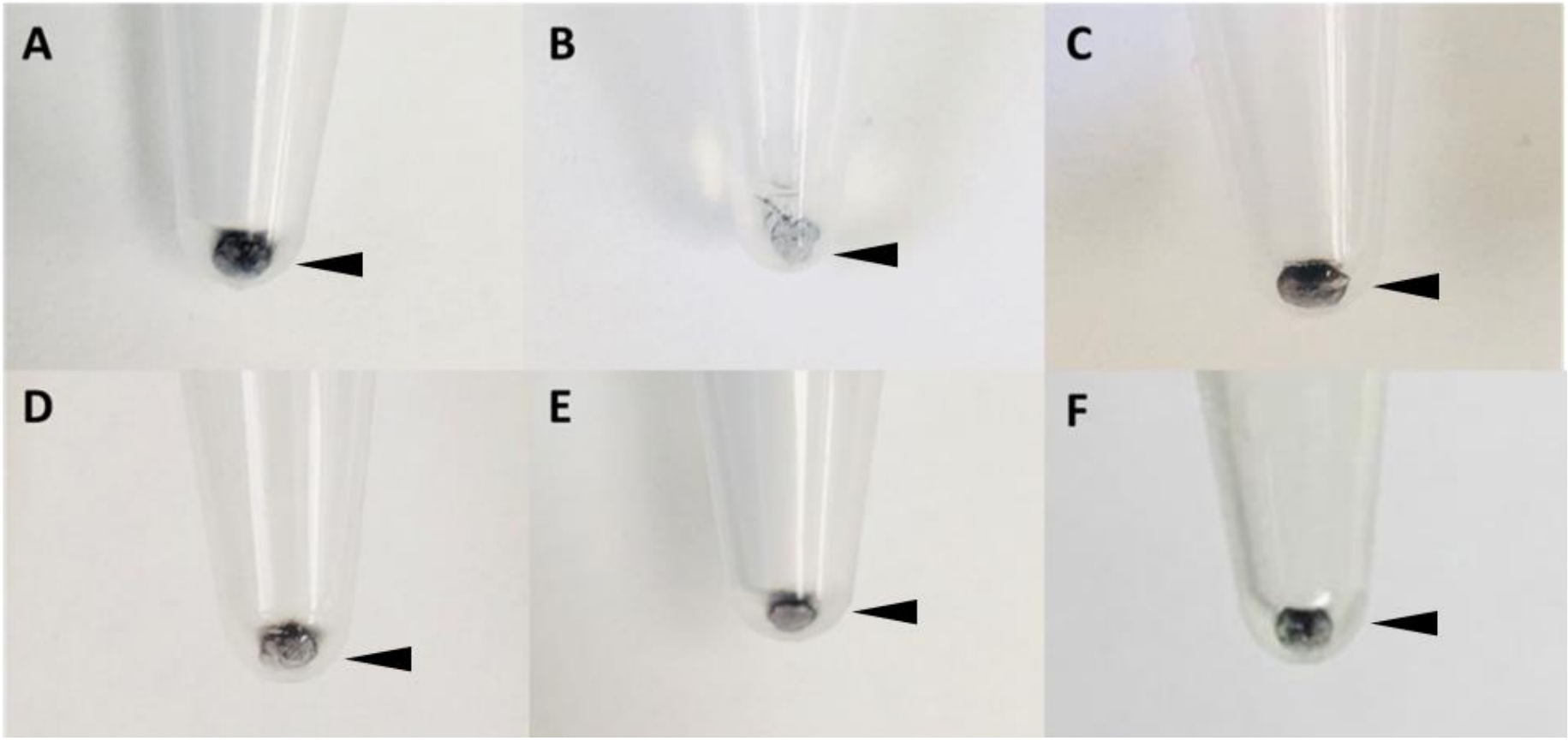
A
B
C
D
E
F

Extracted melanin contents were photographed after the melanin extraction procedure and inspected the chemical effect on melanin synthesis. When compared the color of the pigment pellets, enhanced intensities for black coloration were appeared in the control and LiCl treated fish embryos (black arrow heads of Fig. 4.11.6 A & C). Low darkness levels were observed in the rest of the melanin pellets compared to the control sample. Among them, high levels of paleness showed in the EtOH, EtOH +LiCl and W-C59 treated samples (black arrow heads of Fig. 4.11.6 B, D & E) while the cell pellet of W-C59 + EtOH exposed sample was slightly darker (black arrow heads of Fig. 4.11.6 F). than them.

Figure 4.11.2 Variation in melanin concentration at 2 dpf embryonic stage of zebrafish against various chemical treatments. This bar chart demonstrates the defects in melanin formation of the chemical exposed zebrafish embryos compared to the control sample.

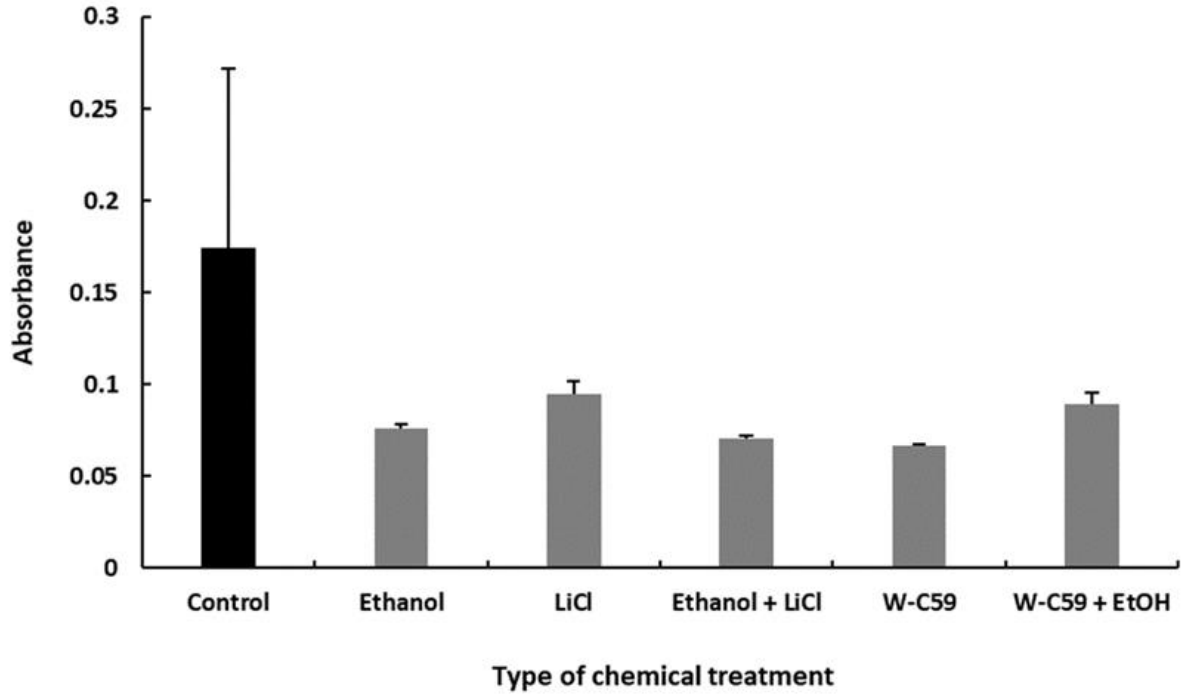

Based on the quantification of melanin pellets resulted from the chemical extractions, the highest absorbance value was recorded in the control sample (0.174 ± 0.097). Considering the results of the chemical exposed samples, Wnt inhibitor treated fish had the least absorbance value (0.067 ± 0.00) and the lower values were also recorded in the pellets of EtOH +LiCl (0.070 ± 0.001) and EtOH (0.076 ± 0.002) treated fish. However, W-C59 + EtOH had the moderate value (0.0893± 0.006) which is less than the LiCl and higher than the EtOH absorbance values. No significant difference [$F(5,12) = 1.02$, $P = 0.447$] was recorded in the absorbance measurements between the control and chemical exposed embryonic fish.

4.12 Whole-mount in situ hybridization (WMISH)

Figure 4.12.1 Whole-Mount in situ Hybridization of 48 hpf zebrafish for *dct* probe.

This Whole mount in situ hybridization showed the changes in melanoblast marker gene of *dct* expression levels in the chemical exposed zebrafish embryos at 48 hpf compared with the control sample. A′: negative control for the experiment, A- control and gene expressions of the chemical treated embryos indicate from B-E; consecutively, B- EtOH, C- LiCl, D- W-C59 and E- W-C59 + EtOH. Scale bar: 50 μm

Figure 4.12.1.1. *dct* expression in the RPE layer of the untreated (control group) zebrafish at 48 hpf. Scale bar: 50 μm

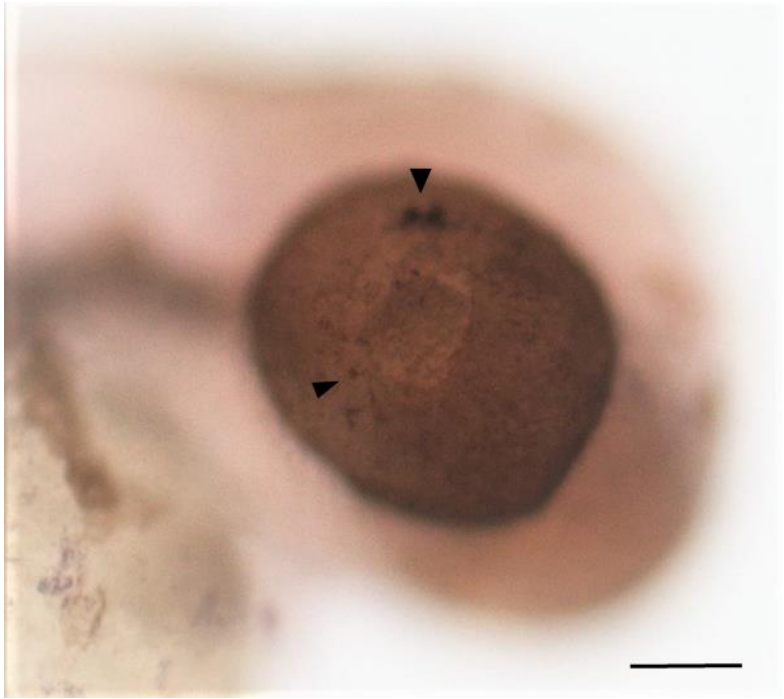

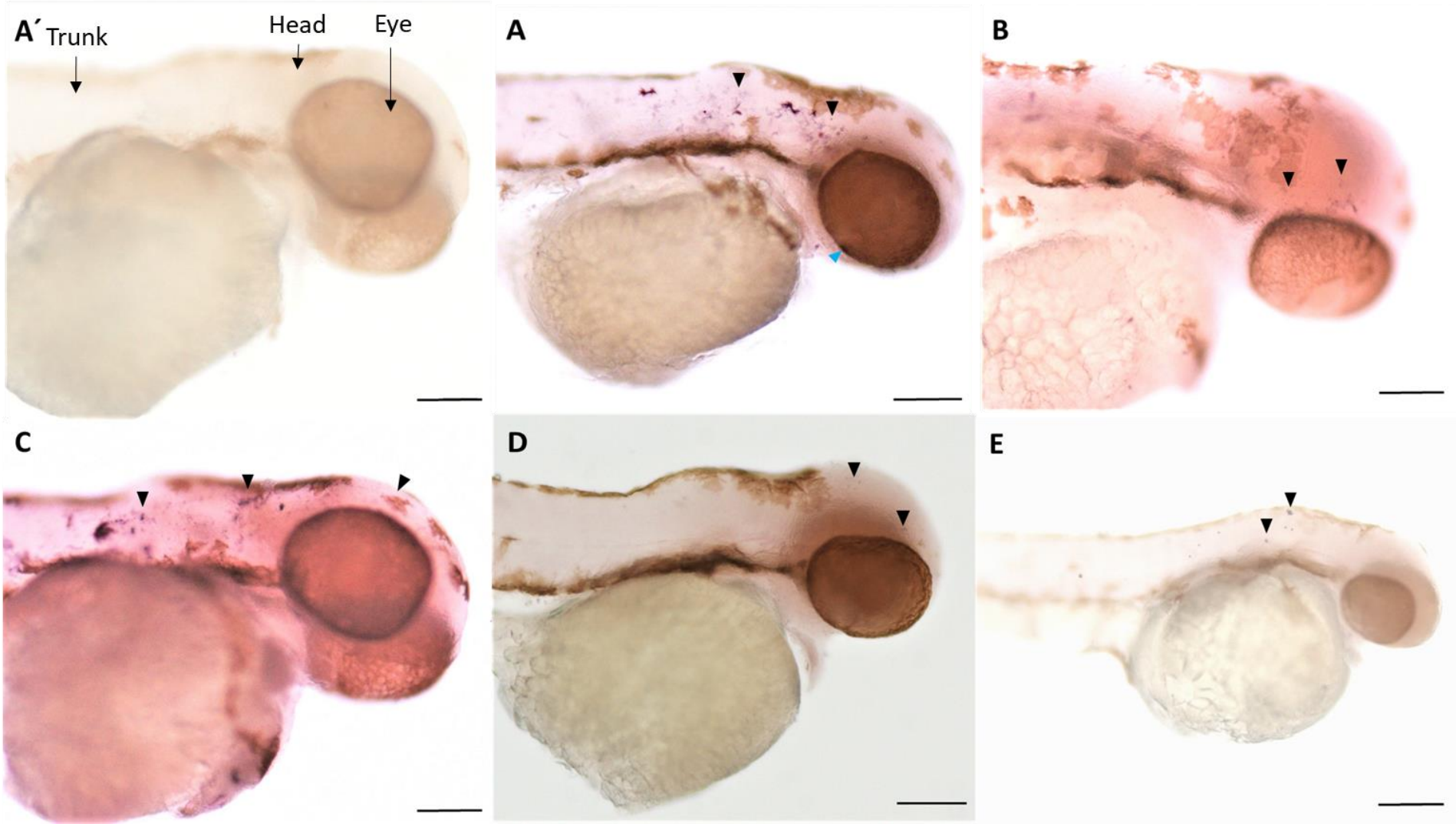
A´ Trunk
Head
Eye
A
B
C
D
E

WMISH was performed for the 48 hpf zebrafish using the *dct* probe, in order to identify the *dct* gene expression in melanocyte stem cells. The expressions of the *dct* upon the chemical treatments were detected using the colorimetric method. The positive cells for the *dct* expression was observed in purple color. The negative control was not treated with the *dct* probe (Fig. 4.12.1 A′). Most of *dct* + melanoblasts were detected prominently in the cranial region, especially at the head region around the eye of the control sample at 48 hpf (black arrowheads of Fig. 4.12.1 A). Meanwhile, *dct* expression was appeared in the melanocytes of the RPE layer as well (black arrowheads of Fig. 4.12.1.1 & light blue arrowhead of Fig. 4.12.1 A).

Dct gene expression in the differentiated melanoblasts of the control sample was express with high purple color intensity (Fig: 4.12.1 A). In contrast, the *dct* expression level of the EtOH treated sample, was reduced compared to the control sample (Fig: 4.12.1 B). Additionally, low density of differentiated melanoblasts (*dct*+) were recorded in the EtOH treated zebrafish embryos at 48 hpf. LiCl exposed fish showed approximately similar *dct* gene expression level and differentiated melanocyte stem cell density compared with control (Fig. 4.12.1 C). W-C59 and W-C59 + EtOH treated samples showed a marked reduction in *dct* expression with reduced densities of *dct*+ cell numbers (Fig. 4.12.1 D & E). Unlike the gene expression levels displayed in the other treatments, the lesser purple color intensity was recorded in the melanoblasts of W-C59 and W-C59 + EtOH exposed zebrafish embryos.

Altogether, the *dct* expression in the chemical treated embryos was reduced compared to the control group except the LiCl exposed fish.

Figure 4.12.2 Whole-Mount in situ Hybridization of 48 hpf zebrafish for *Wnt3a* probe.

This Whole mount in situ hybridization showed the changes in melanoblast marker gene of *Wnt3a* expression levels in chemical exposed zebrafish embryos at 48 hpf compared with the control sample. A′: Negative control for the experiment, A- Control and gene expressions of the chemical treated embryos indicate from B-E; consecutively, B- EtOH, C- LiCl, D- W-C59 and E- W-C59 + EtOH. Scale bar = 50 μm

Figure 4.12.2.1. *Wnt3a* expression in the RPE of the untreated (control group) zebrafish at 48 hpf.

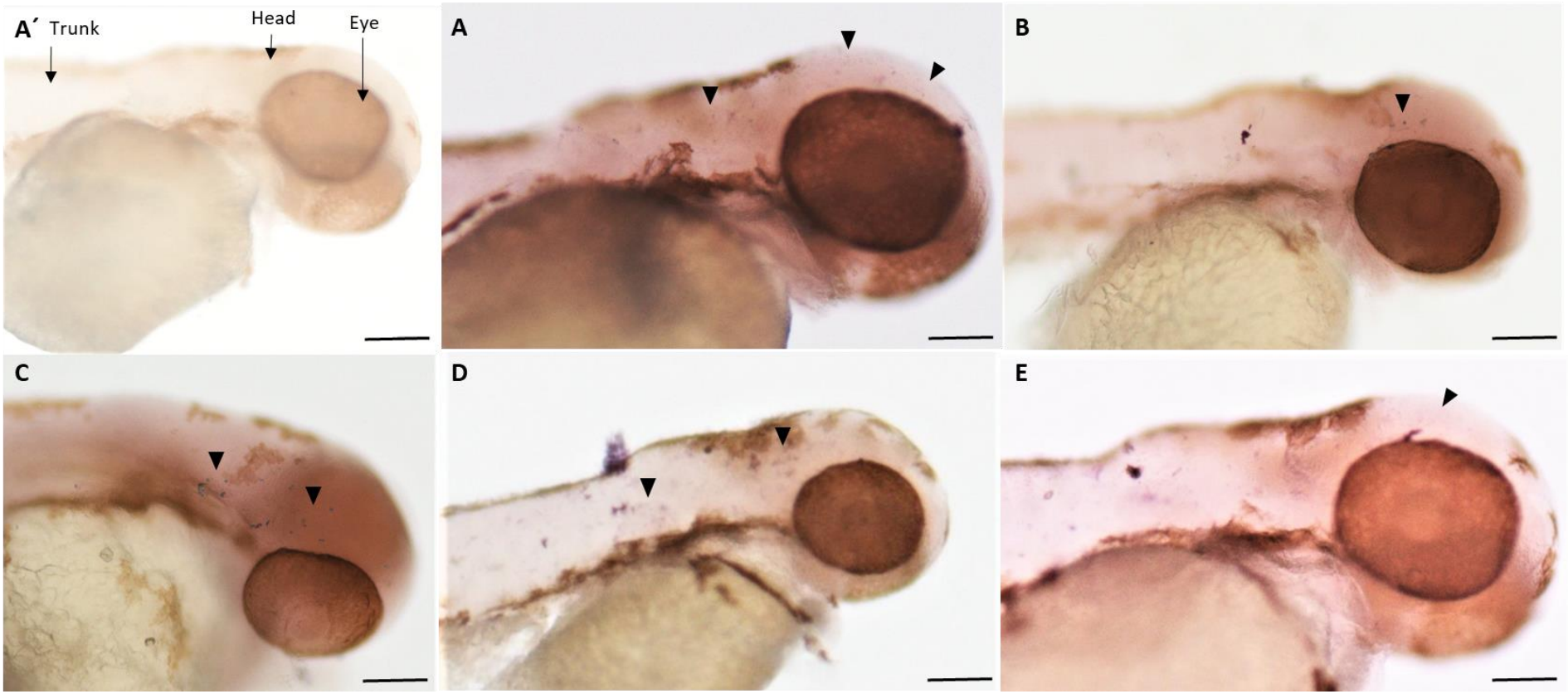
A´ Trunk
Head
Eye
A
B
C
D
E

Wnt3a gene expression in the differentiated melanoblasts of the control sample was appeared in purple color (Fig. 4.12.2 A). High *Wnt3a* + density was recorded anterior to posterior direction of the head region of the control fish. Meanwhile, the *Wnt3a* expression was appeared in the melanocytes of the RPE layer of the control (black arrowheads of Fig. 4.12.2.1), EtOH and LiCl exposed fish. In contrast, the *Wnt3a* expression level and the density of differentiated melanoblast (*wnt3a*+) of the chemical-treated samples, were significantly low compared to the control sample (Fig. 4.12.2 B, D & E) except the LiCl treated fish. However, the LiCl incubated fish showed comparatively a higher intensity level of *Wnt3a* gene expression compared to the control and rest of chemical exposed embryos (Fig. 4.12.2 C). Melanoblasts of the W-C59 and W-C59 + EtOH treated samples showed low *Wnt3a* expression levels with reduced densities of *Wnt3a*+ cell numbers compared to the control and LiCl exposed embryos (Fig. 4.12.2 D & E).

Overall, the *Wnt3a* expression in the chemical treated samples was reduced compared to the control sample, except the LiCl treated group.

CHAPTER 5: DISCUSSION

Embryonic development is associated with the complex coordination of molecular, cellular, and tissue-level processes that must occur according to strict schedules of time and location. This delicate process is influenced by genetic, physiological and many other extrinsic factors.

FASD causes interruptions in normal developmental events as a result of early embryonic alcohol exposure and which leads to generating malformations later, associated with numerous body systems. Craniofacial anomalies, growth retardation in prenatal and postnatal stages, and CNS manifestations are the primary diagnostic criteria and consequences which have been identified in clinical studies.

The present study was focused on the putative functions of EtOH and Wnt cell signaling during the development of embryonic and post-embryonic stages of melanocytes. Therefore, pharmacological treatments during the early development of zebrafish were performed, to examine the effect of prenatal ethanol exposure and altered Wnt signaling level on normal melanocyte development. Following the treatments of embryos, differences in melanocyte density, phenotype, migration, four-strip arrangement, L-R bias migration, melanin dispersion, melanin formation in the eyes, melanosome biogenesis, total melanin content and gene expression patterns of the melanogenic pathway were examined in each chemical exposed groups separately. In the present study, it could be identified that early embryonic EtOH exposure and Wnt inhibition negatively affect melanocyte development, patterning and gene expressions of the melanocyte lineage of zebrafish. Conversely, stimulation of the Wnt pathway promotes the key phenotypic and molecular aspects of melanocyte development focused in the current study.

In summary, the results of this work provide deeper insights into the physiological roles of EtOH and Wnt chemicals in regulating the melanocyte biology of zebrafish. Further, the current study alarms that prenatal exposure to the environmental teratogen of alcohol and Wnt signaling modulators has a major impact on melanocyte development in vertebrates.

5.1 Fluctuation of melanocyte density in zebrafish (*Danio rerio*) from 4-10 dpf

After the establishment of the embryonic melanocyte pattern during the initial development of the zebrafish, it is gradually transferred into the new larval pigment pattern with several changes. Here, the melanocyte counts during the initial larval stage to mid-larval stage are mainly maintained by some of the remaining early embryonic melanocytes and the newly generating melanocytes (2^{nd} wave of melanocytes) derived from melanoblast cells at the embryonic stage [59]. In this transition

old embryonic melanocytes lose from the fish body while differentiating new pigment cells [90]. This phenomenon reflects by the reduction of melanocyte densities between 4 dpf to 7 dpf in the wild-type untreated zebrafish (Fig. 4.1.1.2). As zebrafish acquires new features during the postembryonic development, a marked increase in melanocyte count was observed at the peak of 8 dpf stage (Fig. 4.1.1.2). This finding is compatible with the previous research studies on the dynamics of melanocyte pattern formation in zebrafish [102]. However, the differences in melanocyte formation could be disclosed between the zebrafish species. Continuous increase in melanocyte number has been observed between the 4-8 dpf fish development in the *Brachydanio rerio* while *Danio rerio* in the current study exhibited a different fluctuation in melanocyte generation with the arrival of the second wave of melanoblasts. However, their result can be contrast with the results of the present study as they have only focused on the melanocyte counts in the lateral stripe.

There were still changes in the melanocyte densities at the head region, detected due to degenerating of old cells and the arrival of new melanocytes between the 8-10 dpf. Changes in the melanocyte counts displayed to be little over the 4-10 dpf fish development period of *Danio rerio*, though a small number of melanocytes are added to the melanocyte pattern formation. This result also resembles the previous research findings on melanocyte pattern formation in zebrafish [55, 103].

5.1.1 Variations in melanocyte density of zebrafish after differential chemical exposures

Zebrafish melanocyte development and chromatophore pattern formation take place mainly through a separate and interconnected series of developmental stages: embryonic, larval and larva-to-adult metamorphosis. Further, NCCs, neural crest derived embryonic and post-embryonic progenitor cells, melanocyte stem cell populations and, intrinsic and extrinsic factors govern the entire melanocyte lineage. Early embryonic chemical exposure of zebrafish embryos demonstrated marked differences in melanocyte densities compared to the normal melanocyte development of zebrafish (*Danio rerio*). Many deviations of the melanocyte development appeared considering the fluctuation of melanocyte densities between the 4 -10 dpf of fish growth.

The observations in the present study of deviations in melanocyte densities in larval fish disclose that embryonic exposure to chemicals has an adverse effect on the developing CNS, since abnormal melanocyte cell number is considered indicative of an adverse effect on this system in

developing zebrafish [254]. Focusing on the results, comparatively less melanocyte densities were recorded in the fish which were exposed to the EtOH, EtOH +LiCl and W-C59 + EtOH treatments (Fig. 4.1.1.2, 4.1.3.2 & 4.1.5.2) whereas W-C59 fish group had sudden changes in melanocyte counts (Fig. 4.1.4.2). Interestingly, fish which were incubated in the LiCl, recorded with high melanocyte density throughout the examined life stages (Fig. 4.1.2.2).

Results of the current study prove that EtOH has a major inhibitory effect on melanocyte development relative to the rest of the chemical exposures. Demonstrating the similar fluctuations of melanocyte densities in the EtOH contained other fish groups, compared to the LiCl and W-C59 single chemical treatments, imply that EtOH predominantly regulates melanocyte development more than the impacts of LiCl and W-C59.

The effect of prenatal ethanol and Wnt regulatory chemical exposures on melanocyte development (melanocyte density) has not been observed in any studies using any animal model including zebrafish [255]. Exclusively, this is the first study to investigate the effect of melanocyte density in FASD. Reductions in melanocyte density with some chemical exposures, could be mainly caused by chemical toxicity on early key developmental processes in neurulation: including alterations in the neural crest development, specification of pigment cells from NCCs, defects in the development and proliferation of neural crest cell embryonic progenitors and melanoblasts [256, 257]. Researchers have identified several candidate genes for melanocyte development. Mutations of the *white tail (wit)* and *colourless (cls)* genes in zebrafish, generate a phenotype of melanocytes with normal morphology and pigmentation but a reduced cell number or no cells [258].

Numerous experiments have shown that the zebrafish CNS is more vulnerable to embryonic alcohol exposure compared with other organs. Moreover, Buske and Gerlai [259] has stated that low levels of serotonin in zebrafish after embryonic alcohol exposure, lead to altered neurotransmitter systems and neural dysfunction. In wild-type zebrafish, alcohol exhibits dose-dependent lethality in neuronal cell populations, with higher concentrations causing more damage. In line with other FASD animal models, in zebrafish, the neuronal populations of the CNS are sensitive to alcohol teratogenesis [260] and it has been found that alcohol exposure causes substantial cell degeneration of neural crest progenitors [256, 257]. Studies on analyzing the NCC densities following ethanol exposure reveals that ethanol significantly reduces the cranial and trunk NCC population numbers [261, 262]. Especially, researches have highlighted that the development of cranial NCC populations is most severely affected by ethanol, resulting in

reductions and aberrations in their derived tissues and structures. Meanwhile, trunk neural crest populations are also directed to undergo apoptosis in response to ethanol [263, 264].

Mechanisms underlying this EtOH's neurotoxicity on the apoptosis of premigratory neural crest progenitors in vertebrates are now well-defined [265]. EtOH exposure in embryonic cells initiates a significant increase in intracellular calcium ions which generates from G-protein-coupled signaling via phospholipase C and inositol phosphate [266, 267]. Then the intracellular protein kinase CaMKII is activated by this calcium transient, converting the calcium transient into a lasting effector of neural crest fate. CaMKII involves in destabilizing the transcriptional effector nuclear β-catenin to ablate canonical Wnt signaling and initiate apoptosis [261, 268].

Resulting in low melanocyte densities at each age (4-10 dpf) of the EtOH contained chemical treated fish groups, demonstrate how EtOH single and combined exposures with other Wnt regulatory chemicals negatively affect the early neural crest specification and melanocyte stem cell development along with ultimate melanocyte development.

Remarkably, embryonic exposure of zebrafish embryos for LiCl had a significant increase in melanocyte development (Fig. 4.1.2.2) compared to the rest of chemical-treated fish groups. LiCl is widely used in research as an agonist of the canonical Wnt signalling pathway. The main mechanism of LiCl is stabilizing free β-catenin in the cytosol by inhibiting the GSK-3β activity and ultimately it causes for stimulating the canonical Wnt/β catenin signalling pathway. However, LiCl has not been applied in melanocyte research of zebrafish (*Danio rerio*) as a Wnt signalling pathway enhancer so far.

Research in both mouse and zebrafish have revealed that expression of *MITF* (*MITFa* in zebrafish) in NCCs is vital for melanocyte specification [269, 270]. As mentioned early, *MITF/MITFa* regulates all the key aspects of melanocyte cell biology including specification, proliferation and differentiation of melanoblasts as well as development, morphology and melanogenesis and survival of melanocytes themselves [271, 272]. However, *MITF* transcription is mainly controlled by the Wnt signaling, through the LEF and β-catenin-mediated regulation [273, 274].

Studies which involved mammalian melanocytes have shown that inhibition of GSK-3β activity results upregulation of *MITF* expression and differentiation in normal human melanocytes [275]. Bromoindirubin-3′-oxime (subsequently referred to as BIO) is a well-characterized GSK-3β inhibitor and has been used to investigate the effects of increased Wnt signaling in many model systems [276, 277]. Melanocyte development of zebrafish has been examined using the same Wnt

activator by exposing it to zebrafish embryos and revealed that it increases the melanocyte counts in the head and trunk regions of the 3 dpf fish [278].

In the present study, LiCl exposure resulted in high melanocyte counts in the dorsal head region of the treated fish in contrast to the melanocyte development in the control group. It reflects the effect of LiCl on stimulating the developmental processes of early zebrafish neurulation as the specification of NCCs in melanoblast development and differentiation of melanoblast in melanocyte development via inhibiting the GSK3-β activity. Further, early experiments demonstrated that the overexpression of β-catenin in NCCs has raised the melanocyte cell generation instead of other neuronal cells [77]. Indicating, this present study adds further support to the previous research findings mentioned above.

Past studies, revealed that no change in melanocyte cell number in the dorsal head of zebrafish after the BIO exposure between the development period of 24–72 hpf suggesting that melanocyte specification from NCCs does not extend much beyond 24 hpf [278]. In contrast, a comparatively high melanocyte count has been experienced at 3 dpf after exposure between 15 to 30 hpf [278]. In another study, embryos of *Brachydanio rerio* have been treated with 50 mM LiCl, from 24 hpf until 6 dpf and produced less melanocyte count compared to the control group [279].

Furthermore, the time window used in our study showed that the LiCl treatment from 10 to 22 hpf was also capable to generate elevated numbers of melanocytes at the head region and that persist until the 10 dpf, whereas the data collection of the previous study with BIO treatment was confined only to one age at the very early larval stage. Those results seemingly not enough for postulating and making a conclusion on the stimulating effect of the Wnt signaling pathway on melanocyte development. Nonetheless, the present study revealed that early embryonic exposure to the Wnt signaling up-regulators (LiCl) has a long-lasting effect on fish melanocyte development.

Remarkably, LiCl combined with EtOH produced lower melanocyte counts in the head region compared to the control and LiCl groups as shown in (Fig. 4.1.3.2). Excitingly, this fluctuation of melanocyte densities follows the same variation of control fish and mean melanocyte counts are approximately same to the EtOH exposed fish. This indicates that EtOH has a significant effect on embryonic development, key stages of early neurulation and subsequent melanocyte development over the other chemicals.

Wnt-C59 is considered one of the powerful Wnt signaling pathway inhibitors (antagonist) and has been applied for a variety of model systems: particularly attenuating the signaling cascades of fibrotic disorders and reducing the effects of kidney fibrosis [245]. This drug prevents the Wnt

target genes which are involved in diseases via interrupting β-catenin signaling. Further, this chemical has been used in mouse models to suppress the growth of nasopharyngeal tumors and arrest cancer stem cells [280].Evidence has been found that increased Wnt/β-catenin signaling is associated with tumorigenic pathways in breast cancer cells, and tumor progression can be suppressed with the application of Wnt- antagonist, W-C59 as a therapeutic approach to the patients [281].

In the current study, this pharmacological agent was applied for the first time in zebrafish research to disclose the effect of Wnt signaling inhibition on melanocyte development. Here, the embryonic early exposure of W-C59 displayed sudden ups and downs of melanocyte counts in the head region over 4-10 dpf fish development (Fig. 4.1.4.2). However, any past research evidence is unavailable that explains this chemical action or any other Wnt inhibitory pharmacology agents on melanocyte formation. W-C59 seems likely delay the melanocyte generation, compared with the overall behavior of the rest of the chemical actions EtOH, LiCl and EtOH + LiCl on melanocyte development. When closely examining the melanocyte counts in the head region gradually, every next day it displayed either an increase or a decrease with respect to the previous count and the larval fish reared under normal conditions. This phenomenon could be resulted due to the direct effect of W-C59 on melanocyte specification, differentiation and issues with Wnt-related genes activation. Past studies highlight the importance of Wnt proteins in regulating melanoblast development from the NCCs [282]. Mainly this kind of variation is produced by the delay of the developmental processes in early neurulation: especially as a resulted effect of premigratory neural crest progenitors.

Our observations are further strengthened by past research findings. In zebrafish and mice *Wnt1* and *Wnt3a* genes have been found to express in the neuroectoderm of the neural tube during the stages of NC induction [283, 284]. Moreover, NCCs which receive a high level of Wnt/β-catenin signaling over a longer period are prone to pigment cell fates. In contrast, NCCs that receive low levels of Wnt, form neuronal cell derivatives. These findings clearly declare the requirement of Wnt/β-catenin signaling in the specification process of neural crest pigment cell derivatives over other neuronal derivatives [284, 285].

Melanocyte counts in most stages of treated fish were higher than that of corresponding age groups of EtOH-exposed fish. In addition, EtOH showed a constant inhibition of melanocyte generation compared to the control group. It further confirms the fact that the impact and the inhibitory action of EtOH on melanocyte development is higher than that of PORCN- Wnt inhibitor.

Next, the combined chemical effect of W-C59 and EtOH on melanocyte development was assessed. It was observed that Wnt inhibitor combined with EtOH create a drastic effect on melanocyte generation over the 4 -10 dpf time period (Fig. 4.1.5.2). With respect to the results of other chemical-exposed fish, the least melanocyte counts were recorded in the W-C59 + EtOH incubated fish, except in the 7 and 8 dpf ages where appearing the increased development of the second wave of melanocytes. Interestingly, these melanocyte numbers are lower than the melanocyte densities of the EtOH and W-C59 incubated fish groups. This signifies EtOH and W-C59 both act as very effective inhibitors of melanocyte development.

Collectively, the data in the present study emphasize, for the first time to our knowledge, that early embryonic exposure of zebrafish (*Danio rerio*) for EtOH and Wnt modulators of LiCl and W-C59 during the early neurulation period has a marked effect on the melanocyte generation.

5.1.2 Variation in melanocyte density at 8 dpf zebrafish after embryonic exposure to differential chemicals

The eighth day of zebrafish development is considered to be a crucial stage in postembryonic growth and this is marked by several changes in the pigment pattern [55, 102]. At this stage, zebrafish display new features in pigment pattern development, remodeling and loss of some chromatophores that arose at earlier stages to generate stripes and interstripes [90]. New melanocytes and iridophores also enter in to the pattern formation while existing the early larval melanocytes [90].

Differences in the melanocyte formation were shown on the 8^{th} day of fish development in the current study against different chemical exposures (Fig. 4.1.6.1). As displayed in analyzed melanocyte densities from 4-8 dpf previously, here the highest melanocyte count was recorded in the LiCl fish group and rest of the chemical incubated fish showed approximately similar counts, especially the fish which were in the EtOH included chemical treated groups (Fig. 4.1.6.1). These results indirectly demonstrate the effect of embryonic chemical exposures on the development and patterning of the second wave of melanocytes in fish. Results of this study evidence the stimulatory effect of LiCl on the development and survival of melanocyte stem cells, and the differentiation of melanocytes rather than other chemical agents. Further, this result represents the overall picture of the pharmacological effect on melanocyte development from 4 -10 dpf of fish growth.

5.2 Variation in melanocyte density at mid-larval stages of zebrafish after differential chemical exposures

New melanocytes emerge around the 14 dpf of fish development which occurs at the onset of metamorphosis. Here, with this developmental change, fish melanocyte number is gradually increasing and melanocytes disperse the entire body uniformly [46]. This fact was proved in the present study recording with high melanocyte number in the head region of the control fish compared to the melanocyte number observed on the 8th day (Fig. 4.1.7.1). Next, the impact of the embryonic chemical exposure on the melanocyte development in the mid larval stages was investigated focusing on this metamorphic stage of fish. However, similar melanocyte development could be observed in the 15 dpf stage as well, relative to the 8 dpf melanocyte generation. Especially, EtOH exposed fish: EtOH, EtOH + LiCl and W-C59 + EtOH showed a similar pattern in melanocyte formation relative to the rest of the chemical treated groups: LiCl and W-C59 (Fig. 4.1.7.1).

Melanocytes do not divide, and they only arise from the stem cells (or directly from NCCs), which later differentiate into melanin contained cells. Several studies highlight the possibility of some of the melanocyte precursors which remain quiescent during embryonic and early larval developmental stages and re-enter at their mid-larval stages (as the 3rd wave of new melanocytes), being responsible for the formation and maintenance of the adult pigment pattern [286].

Here, showing significantly fewer melanocyte counts in the EtOH, W-C59 and combined chemical treatments, evidence the persistence of the inhibitory effect on melanoblast generation or /and melanocyte differentiation even in the mid-larval stages. LiCl-treated fish group also displayed a high melanocyte count compared to the control group which means the possibility of standing the stimulatory effect on melanocyte development until the post-embryonic stages.

Alternatively, investigating the overall results of this study indicate that embryonic chemical exposure at the early neurulation stage of zebrafish embryos, doesn’t make an impact only for a shorter period of time but has a prolonged effect on pigment cell (melanocyte) development.

5.3 Melanocyte phenotypic differences at 2 dpf embryonic stage of zebrafish against various chemical treatments.

Cell morphology of immature melanocytes appears highly dendritic at the early embryonic stage of zebrafish as it lies in the early stages of melanin production (~30 hpf post fertilization) [14]. Mature melanocytes appear at 2 dpf which is developed by mainly high cellular melanin production inside of melanosome vesicles and have taken on a flattened (thin plaque-like) morphology (Fig. 4.2.1 A) [14]. Alterations of this melanocyte phenotype are caused by as a response to various environmental factors [8, 287].

In the current study, melanocytes of EtOH, EtOH + LiCl and W-C59 + EtOH exposed fish at 2 dpf showed more dendritic morphology (Fig. 4.2.1 B, D & F) and less melanin pigmentation displayed in the melanocytes of W-C59 (Fig. 4.2.1 E) and EtOH + LiCl fish groups. Defects in melanocyte phenotype could be resulted due to improper differentiation of melanocytes: including the inhibition of Wnt signaling and melanogenic gene expression (*TYR*, *TYRP1* and *Dct*) [14]. It has been reported that MSH promotes melanocyte dendricity [288]. Further, past researches highlight that these modulations of melanosome dispersion and pigmentation are governed by the cAMP pathway and aberrations in gene expressions of *MITF*, *SOX9* and *SOX10* [14]. However, displaying a similar phenotype of LiCl incubated fish with the control group (Fig. 4.2.1 C), indicates that LiCl supports or has a less negative impact on melanocyte differentiation.

However, unlike the present study, in past studies *Xenopus* developing embryos have been exposed to ethanol in different time periods: 24 hrs and 96 hrs, and examined the melanocytes with abnormal pigmentation and morphology [289]. The observations in the present study of abnormal phenotypes of melanocytes in the head region suggest that exposure to ethanol has an adverse effect on the developing melanocyte lineage (gene expressions in melanoblasts). Further, in the developing *Danio rerio*, abnormal melanocytes are considered as indicative of an adverse effect on the gene regulatory system of melanocytes [98].

Our present results support the previous studies on the nature of the effects of ethanol in zebrafish embryos [290, 291]. A concentration of 1.0 % ethanol-induced weak pigmentation with defects in melanocyte morphology.

Considering the melanocyte area, all the chemical exposed fish showed a reduced melanosome dispersion compared to the untreated fish (Fig. 4.2.2). Unlike the melanin formation, melanocyte surface area is determined by the aggregations and dispersions of melanosomes along the melanosome motor activity. According to the analysis of melanocyte area at the embryonic stage,

it clearly implies that chemical exposure resulted in aggregating melanosomes toward center of the cells rather than dispersing toward the periphery. Wnt inhibitor, LiCl + EtOH and Wnt activator made a significant reduction in melanocyte area of the respective fish groups than the fish embryos exposed to single EtOH and W-C59 + EtOH chemicals (Fig. 4.2.2). Melanin distribution of some melanocytes in the W-C59 + EtOH exposed fish was appeared to be different (Fig. 4.2.1 F) than the melanocytes demonstrated in the head region of other chemical treated fish. Here, in some melanocytes, melanosomes are concentrated at the distal edges of the cell margin which is termed as hyper dispersion of melanosomes (black arrowhead of Fig. 4.2.1 F). It brought some paleness at center of the melanocytes while the margins of the cell are hyper pigmented with melanin.

5.4 Melanocyte phenotypic differences at 6 dpf early-larval stage of zebrafish against various chemical treatments.

Next, the effect of embryonic chemical exposure on the melanocyte morphology at the early larval stage was examined at 6 dpf. Phenotypic examination showed a contrast difference in melanocyte morphology of untreated zebrafish (*Danio rerio*) larvae compared to the 2 dpf. Here, the melanocytes in the head region were round in shape with distinct perinuclear areas at center of the cell where the melanosomes are more accumulated (Fig. 4.2.3 A). Melanosomes move from the perinuclear area of melanocytes toward the plasma membrane with equal dispersion.
However, the defects in melanocyte morphology and arrangement in the head region appeared in the chemical-treated fish (Fig. 4.2.3), indicating that the chemical effect is still accompanied with melanocytes. Changes in the melanocyte phenotype were spotted in all the chemical-exposed fish groups except the LiCl-treated fish whose melanocytes were similar to the control group (Fig. 4.2.3 C). However, the melanocyte area was reduced compared to the control group.

This result implies the ability of small molecules like EtOH and Wnt regulatory chemicals to control the regulatory mechanism of intracellular melanosome dispersion and then alter the outer body coloration of fish. Phenotypic differences of melanocytes showed that all the melanosomes of chemical exposed fish are contracted rather than having an equal dispersion throughout the melanocytes (Fig. 4.2.3). These changes made more spaces between the melanocytes each other and further brought a paler appearance to the fish.

According to the analysis of melanocyte area at 6 dpf larval fish, higher melanosome contractions were recorded in the EtOH, W-C59 and W-C59 + EtOH exposed fish (Fig. 4.2.4). Interestingly, change in the melanocyte area transferring from 2 dpf to 6 dpf was lower in the same fish groups mentioned early compared to the melanocyte development of untreated fish (change of the melanocyte area in the control- 670 μm^2). Meanwhile, EtOH + LiCl exposed fish melanocytes had the highest dispersion of melanosomes (change of the melanocyte area- 1588 μm^2). These results disclose the possibility of embryonic EtOH exposure to regulate the melanosome motor activity at the embryonic and post-embryonic stages of zebrafish.

In a previous study, researchers modeled a pharmacological experiment to investigate the effect of cAMP signaling modulators on melanosome motor activity where the wild-type zebrafish (5 dpf) showed aggregations and dispersions of melanosomes in response to inhibitors and activators of the cAMP signaling pathway respectively [84]. The present study focused on the melanosome motor activity against EtOH and Wnt signaling pathway modulators. Findings of the current study for the first time disclosed that early embryonic exposure to the EtOH and Wnt regulatory chemicals, effect melanosome motor activity not only at the embryonic stage but lasts until the early larval stage. Many previous studies have attempted to investigate pigment cell behavior qualitatively and quantitatively, controlled by various environmental and chemical cues. However, the mechanism of melanosome movements within the melanocytes against stimuli is still unknown in terms of cell signaling pathways, hormonal action and gene regulation.

In another study, zebrafish 7 dpf old larvae were exposed to a range of EtOH concentrations (1.5 % to 3 %) and they observed no discernible changes in low exposure time periods, in contrast a noticeable dispersion of melanosomes with changes in the characteristic shape of melanocytes appeared, with increasing exposure period for EtOH [292]. However, the defects in melanocyte morphology generated by EtOH exposure at post-embryonic stages are possibly be mediated through the CNS or are due to the direct action of ethanol on melanocytes [292]. Whereas in the present study, changes in embryonic and larval melanocytes could be led by the direct effect of EtOH on the CNS and melanocyte stem cells.

Alterations in the melanosome movements can lead to aberrations in melanocyte size and shape. These abnormalities are clearly influenced by the mutants which are involved in melanocyte differentiation, in terms of the expression of pigment or cell morphology. It could be greatly affected by the dominance of chemical-induced mutations of the *obscure (obs)* and *union jack (uni)* genes [293]. As shown in (Fig. 4.2.1 & 4.2.3), melanocytes of the chemical-treated samples were morphologically abnormal and deviated from the control samples. Defects in the expression

of the *choker (cho)* and *no tail (ntl)* genes were also found to be mainly responsible for this phenomenon [294, 295].

5.5 Melanocyte migratory differences at 2 dpf embryonic zebrafish against different chemical treatments

The embryonic pigment pattern is formed by the cells derived from NC that migrate along the specific pathways to their final position in the embryo. In zebrafish embryos, melanocytes migrate dorso-laterally and along nerves ventro-medially to form the embryonic pigment pattern. These melanocytes traverse the dorsolateral migration pathway between the somites and epidermis whereas, in the ventromedial pathway, melanocytes traverse along the nerves between the neural tube and somites (Fig. 1.1) [11]. Embryonic melanocytes which migrate along the dorsolateral pathway give rise to the melanocytes in the head, embryonic lateral stripe, yolk sac and yolk sac extension regions. Melanocytes which are located in the head, yolk sac and yolk sac extension regions except the lateral stripe are generated from the ventromedial pathway [57, 296]. Studies have revealed that the entire neural crest along the anterior-posterior axis is responsible for forming melanocytes: including the cranial neural crest, vagal neural crest and trunk neural crest [297]. However, any defect in melanocyte migration has led to stuck the melanocytes along the migratory path without reaching their final destination point. This incident was investigated in the present study and revealed that embryonic chemical exposure caused migratory defects in the embryonic stage (Fig. 4.3.1). Lack of migrated melanocytes as well as ectopic melanocytes have resulted at the designated migrated and non-migrated regions of the zebrafish embryos due to the defects of improper melanocyte migration (Fig. 4.4.1 & 4.4.2). The data analysis showed that a significant increase in migrated and non-migrated melanocyte counts with EtOH and LiCl exposure (Fig. 4.5.1). This was mainly evidenced in the LiCl exposed embryos, by recording supernumerary melanocytes at the head, yolk sac (Fig. 4.3.1 C) and yolk sac extension regions of the fish (Fig. 4.4.2). Meanwhile the most of migrated melanocytes were recorded in the yolk sac area than the yolk sac extension and head regions of the EtOH exposed embryos (Fig. 4.3.1 B & 4.4.2). Results indicated that LiCl has played a drastic effect on melanocyte migration at the embryonic stage, not only as a stimulator but effect by blocking the melanocyte migration.

Many studies have investigated the role of canonical Wnt signaling in melanocyte migration. Researchers have recognized the importance of maintaining Wnt expression from the onset of neural crest emigration until the completion, for a proper melanocyte migration in avian embryos

[247]. Thus, Wnt signaling expression at the right time in accurate levels, effect to proper melanocyte migration of animals [298]. Past studies carried out with the murine models showed that the lack of both *Wnt1* and *Wnt3a* gene expressions is correlated with significant reductions or even the absence of migrating melanocyte cell populations [299, 300]. Another study conducted with *Xenopus* embryos identified that the down-regulation of Wnt signaling pathway by the inhibition of endogenous β-catenin levels of cells leads to complete suppression of cranial NCCs migration and promotes neuronal cell fate [301]. Further, past studies have strongly emphasized the significance of Wnt/β-catenin signaling for the emigration of melanocyte precursors from the dorsal midline of the neural crest and regulating the melanocyte migration by proper directing of migrating melanocytes for melanocyte patterning [247]. Moreover, past studies highlight that a balanced level of Wnt signaling activity is significant for proper cell migration and movements while reduced or increased activity leads to defects [302, 303].

These previous findings on Wnt signaling and NCCs / melanocyte migration are consistent with the present study. High migrated and non-migrated melanocyte counts after the LiCl exposure might be resulted from the elevated levels of Wnt signaling during the early neurulation period (Fig. 4.5.1). Remarkably, the same result was displayed in the fish embryos which were incubated with EtOH. This result could be generated as a result of improper melanocyte migration and disruption of Wnt signaling cascade. Inhibition of Wnt signaling at the embryonic stage showed a reduction in migrated melanocyte count and a significant increase in the non-migrated melanocyte number (Fig. 4.5.1). It proves that the low level of wnt signaling doesn't support melanocyte migration. Further, it is strengthened by producing less migrated melanocyte counts in W-C59 + EtOH exposed fish as well. However, in addition to Wnt signaling, kita signaling has been found to be important in regulating the zebrafish melanocyte migration at the embryonic stage [27].

5.6 Melanocyte arrangement differences at 6 dpf larval zebrafish against different chemical treatments

Zebrafish embryonic melanocyte pattern established at 2 dpf mainly directs for the development of early larval pigment pattern at 6 dpf and additional new melanocytes support for generating the stripe pattern [57]. It was difficult to get a clearer and more direct evidence on the impact of chemical exposure on larval melanocyte pattern development completely, under the whole mount microscopic examinations (Fig. 4.6.1). But close examinations of each stripe of larval fish, displayed a lack of melanocytes at the dorsal, lateral and ventral regions of the body. Dorsal and

yolk sac strip patterns were severely disrupted with a lack of melanocytes, defects in melanocyte phenotype and irregular melanocyte arrangements (Fig. 4.7.1 & 4.7.2). This condition is mainly developed by the defects resulted in embryonic melanocyte migration. Melanoblasts which migrate along the dorsolateral pathway contribute to the formation of all four larval stripes: dorsal, lateral, ventral and yolk sac melanocyte bands while the melanoblasts of the ventromedial route migrate through the horizontal myoseptum and form all the above-mentioned larval stripes except the lateral stripe [57, 296]. Thus, the melanocyte pattern differences in dorsal and yolk sac stripe formation resulted due to the errors in migratory pathways of melanocytes (Fig. 4.7.1 & 4.7.2). Lack of melanocyte migration to the ventral trunk region of the fish body is the main reason for recording fewer melanocyte counts in the ventral stripe and yolk sac stripe formations [304]. This was displayed in the EtOH + LiCl exposed fish as well as appeared in the yolk sac stripe formation of EtOH treated fish (Fig. 4.7.2 B & D). Further, Wnt inhibition also significantly affected the ventral migration of melanoblasts. Lateral stripe formation is only taken place via dorsolateral migratory route, but it was also significantly affected by the EtOH, Wnt inhibition and combining with EtOH (Fig. 4.6.1 B, E & F).

Melanocyte development at the dorsal trunk is regulated by both dorsolateral and ventromedial pathways. The least melanocyte development in the W-C59 treated fish group (Figure 4.7.3) indicated that the Wnt inhibition severely affects the melanocyte migration along both migratory pathways and further these findings express the importance of Wnt signaling pathway on melanocyte migration. High migrated melanocyte counts were recorded previously at the yolk sac and yolk sac extension regions of the LiCl exposed fish (Fig. 4.3.1 & 4.4.2) which could direct the yolk sac stripe formation of the 6 dpf larval fish with high melanocyte numbers (Fig. 4.7.3). For the second, the highest non-migrated melanocyte count was recorded in the EtOH exposed fish (Fig. 4.5 1), and showed the ectopic chromatophores located in a medial position of the ventral trunk (Fig. 4.4.1 C). Besides, the localization of these melanocytes corresponds to the ventral neural crest migration pathway. This might be one of the factors for reducing the melanocyte count and deformation of the yolk sac stripe of the EtOH-treated fish despite the migrated melanocyte counts (Fig. 4.7.2 B & 4.7.3). According to the data analysis, EtOH alone made an increase in migrated and non- migrated melanocyte counts in contrast EtOH combined with LiCl and W-C59 caused to decrease the melanocyte counts than the LiCl and W-C59 alone exposures (Fig. 4.5.1 & 4.7.3) This implies the need of further experiments related to the EtOH effect on melanocyte migration.

Overall, the present study opens an exciting opportunity for future studies to investigate how early embryonic exposure to the EtOH and Wnt signaling pathway modulators affect on melanocyte pattern formation of zebrafish.

5.7 Effect of chemical exposure on melanocyte migration along the L-R axis of zebrafish larvae at 6 dpf

Embryonic chemical exposure of zebrafish embryos demonstrated the biased melanocyte localization along the L-R axis of the larval fish body (Fig. 4.8.1 & 4.8.2). Most the previous studies on L-R asymmetry have been focused on the mechanisms underlying that determine the laterality of major body organs: including cardiac, visceral and other mesodermal derivatives using zebrafish and other numerous vertebrate models [305-307].

According to past studies, most symmetries and asymmetries in organ morphogenesis are examined in the changes of *Nodal-Pitx2* pathway [308], while fewer studies revealed the importance of RA, BMP, inositol polyphosphates, SHH and Lefty1/Lefty2 signaling cascades in determining the organ lateralization [309-312]. Further, Nodal, FGF, Wnt, SHH and Notch signaling pathways involved in key steps of organogenesis of L-R patterning organizers of teleosts [313]. Kupffer's vesicle (KV) is the organizer region that establishes L-R asymmetric patterning in zebrafish. However, no study has been focused to examine the L-R patterning of neural crest derived organs, except the one study which investigated the sidedness of neurally derived tissues in *Xenopus laevis* embryos against differential voltage levels [119].

According to the literature, the development of different melanocyte numbers at lateral L-R trunks of the larval fish observed in our study could be a result of L-R biased differentiation of NCCs into melanocytes or due to biased migration of differentiated melanocytes with embryonic chemical exposure [119]. It could be possible to take place biased melanocyte migration as recorded different melanocyte numbers on lateral stripe with differential chemical exposures. Results of the present study declare the information that L-R asymmetry is not unique to the visceral and neurally-derived tissues but also extends to the behavior of migratory neural crest derivatives.

A similar asymmetry was observed in the neural crest-derived melanocytes of *Xenopus* embryos [119].The lateral organization of melanocytes occurs by following the dorso-lateral migration paths along the sides of the zebrafish embryos while differentiating from NCCs. Inasmuch, the

bias melanocyte migration can be arisen from the defects in L-R lateral migratory routes. Interestingly, the same phenomenon has been examined in the previous study, which revealed that there is no apparent asymmetry in the extent of melanocyte differentiation from the NCCs, prior to the onset of migration, by contrast, L-R asymmetry in the number of melanocytes was found after the migration [119]. This further suggests that the observed asymmetry is due to the asymmetric migration patterns.

All the chemical exposures caused to generate left-sided bias melanocyte migration and significant leftward lateralization was observed in the EtOH (70%), LiCl and W-C59 + EtOH exposed fish (Fig. 4.8.2). Remarkably, 80 % and 90 % of left-sided bias migrations were recorded in the LiCl and W-C59 + EtOH incubated fish respectively (Fig. 4.8.2). These data indicate the significant influence of EtOH and Wnt signaling regulatory chemicals on symmetric migration of neural crest derivatives. The mechanisms that govern the L-R asymmetrically biased response of cells upon the effect of embryonic chemical exposures are needed to be experimented in future studies. Moreover, it would be important for understanding the evolutionary or developmental role of such asymmetric melanocyte distributions of the animal body.

5.8 Effect of chemical exposure on the melanin intensity / dispersion in the head region

Animal body color is expressed by melanocyte number, melanin formation as well as melanosome dispersion within the melanocytes. Melanosome movements and arrangement in the pigment cells are major determinant factors of melanocyte pattern formation, arrangement, and body color formation.

Considering the fluctuation of average intensity values in the head region of the EtOH-exposed embryos, higher intensity values were observed between 4-8 dpf developmental stages but marked reduction was noticed in 9 dpf (Fig. 4.9.1). This result is well-defined when examining the melanocyte phenotype of the EtOH-exposed embryos. Most of the melanocytes in the EtOH exposed fish showed melanosome aggregation, especially 6 dpf to 8 dpf stages compared to the melanocytes of the control group (Fig. 4.1.1.1). Melanosome aggregation within the melanocytes causes to decrease the coverage area of melanocytes, which makes more spaces among the melanocytes and the particular region of the body (ROI), and creates paler appearance to fish [287]. This caused the high average intensity values (low intensity for melanin) for EtOH-exposed

fish during 4-8 dpf. Whereas a huge drop of the average intensity (high intensity for melanin) was marked in 9 dpf due to the dispersion of melanosomes within the ROI.

Considerably, low average intensity values (high intensity values for melanin) were recorded in the LiCl-exposed fish compared to the control sample (Fig. 4.9.2). This could be generated by high melanocyte count, increased melanin content of melanosomes and high expansion of melanosomes (Fig. 4.1.2.1, 7 dpf) resulted with LiCl exposure. These changes made fish darker in appearance at most larval stages of fish development. Interestingly, low intensity values for melanin showed in 4 and 10 dpf life stages of fish, despite recording high melanocyte counts at the same head region (Fig. 4.1.2.2). This implies indirectly, not only the melanocyte counts but the melanin formation within melanosome vesicles and its dispersion within the melanocyte are also critical factors in determining the fish or vertebrate body color.

Early embryonic exposure for EtOH + LiCl promoted melanosome aggregation mostly than melanosome dispersion. It was mostly witnessed at the 4 dpf to 6 dpf and 10 dpf life stages (Fig. 4.1.3.1). This was reflected by showing high average intensity values (low intensity values for melanin) in the same age groups (Fig. 4.9.3). The least average intensity value was recorded at 7 dpf as showing noticeably high dispersion of melanosomes than the rest of other fish ages regardless of low melanocyte count (Fig. 4.1.3.2). Then the average intensity value was gradually increased due to high melanosome aggregation (Fig. 4.1.3.1, 9 dpf and 10 dpf). Overall, most of the fish displayed a paling appearance as a result of EtOH + LiCl exposure.

Most of the fish exposed to Wnt inhibitor (W-C59), had high average intensity values (low intensity values for melanin) (Fig 4.9.4). Especially, the age groups of 4,6 and 8 dpf exhibited melanosome aggregations making more spaces in the head region (Fig. 4.1.4.1). This resulted paler appearance for fish. Interestingly, 5 dpf and 7 dpf fish stages showed less values for melanin even though demonstrated high melanocyte counts at the same ages compared to the untreated fish (Fig. 4.1.4.2).

Lower average values for melanin formation were recorded during the 4-6dpf ages of W-C59 + EtOH fish (Fig. 4.9.4). It was mainly evident by exhibiting melanosome aggregations and paler appearances of head region (Fig. 4.1.5.1). However, intensity values for melanin were increased gradually, even decreasing the melanocyte counts from 7-9 dpf (Fig. 4.1.5.2). It might have resulted with high melanin content in melanosomes and high dispersion of melanosomes with the melanocytes in the head region (Fig. 4.1.5.1).

It is apparent that early embryonic chemical exposures can regulate the melanosome aggregation and dispersion within the melanocytes and, change skin pigment patterns and overall body color. However, these mechanisms are mainly regulated by hormonal influence as well. Past studies have detected that α-MSH involves in promoting melanocyte expansion while MCH promotes aggregation of melanocytes [84, 88, 89]. These hormones are largely responsible for melanocyte behavior [314].

This study reveals that the process of melanosome dispersal in the melanocytes of larval zebrafish could be altered by exposing the embryos to the EtOH and small molecules that regulate the Wnt signaling pathway. However, further studies should be conducted to find out the underlying mechanisms of EtOH and Wnt regulatory action on melanosome movements and body color formation.

5.9 Effect of chemical exposure on melanin formation in the RPE of zebrafish eyes

Differential chemical exposures displayed numerous changes in RPE formation (Fig. 4.10.1). Especially, all the chemical-exposed fish showed the defects in the later development of the RPE layer except the LiCl-exposed fish (Fig. 4.10.1, 4.10.3 & 4.10.5). These chemical-induced defects were possible to be developed by several factors, including the direct effect on the development of RPE precursor cells, defects in differentiation of RPE cells, aberrations of melanocyte development and melanin formation [315, 316]. The presence of melanin is considered an excellent marker of healthy state of the differentiated RPE [317]. The measurements of the average intensity of the RPE layer taken by microscopic software can be used to determine the melanin intensity/content [318]. This technique has been used for many applications in melanocyte research, such as measuring the ocular melanin intensity of zebrafish embryos and determining the melanin intensity of human melanocyte cell cultures [318, 319]. Most of the RPE layers of fish which were incubated in the EtOH, W-C59 and combined chemical treatments displayed amelanotic phenotype (Fig. 4.10.1, 4.10.3 & 4.10.5). This is mainly result of the early aberration of the RPE precursor layer and disruption of the melanogenic pathway.

In early embryonic development, the optic vesicle invaginates to form a bi-layered tissue of neuroepithelial precursor cells. It is called the optic cup. Here, the cells which are located in the inner layer give rise to the neural retina (NR), and the cells in the surrounding tissue develop into the RPE [320]. Zebrafish eye development first becomes morphologically obvious at the 6 somite

stage and the morphological distinction between the retina and RPE is apparent by the 18–19 somite stage [321, 322]. In the present study, these crucial steps of the eye developmental process in zebrafish lies within the chemical exposure time period. Therefore, these resulted defects are mostly associated with the chemical-mediated regulations of embryonic eye development.

Past studies on vertebrate model organisms reveal that cell fate decisions, differentiation of RPE precursor cells, RPE formation, pigment synthesis and physiological functions are governed by the influence of many intercellular signaling pathways, transcription factors, and genes [323-325]. Further extracellular signals, therapeutic drug exposures like ITH12674 (is a melatonin and sulforaphane hybrid drug) and oxidizing agents affect RPE development and cell injury [326, 327].

Previous studies disclosed that zebrafish retinal development is very sensitive to teratogen exposure [328]. Further, early EtOH exposure for the zebrafish embryos from 2–24 hpf with 0.6 % and 0.9 % has led to develop severe retinal cell differentiation defects [329]. Additionally, EtOH exposure has reduced the *Wnt* and *Notch* gene expression levels in the stem cell populations in the CMZ, and the severity of the defects has increased with increasing the EtOH concentration [329].

EtOH is one of the major oxidizing agents and intracellular catabolism causes to generate oxidative stress by producing many ROS. Later, which generates EtOH-mediated neurotoxicity and directs for deleterious effects [330]. The adequate level of oxygen supply is sufficient for maintaining the retinal function [331]. However, generating a high-oxygen microenvironment in the retina makes constant exposure of RPE cells to oxidative stress. This condition is generated from accumulating ROS with EtOH exposure. It was found that high levels of ROS damage the RPE cells, which have associated with the pathogenesis of clinical visual diseases [332]. Here, the increase of intracellular ROS within the RPE cells induced by EtOH leads to damage to the mitochondrial membrane and its DNA and destructs the proteins involved in electron transport chain [333]. Then, it activates the mitochondrial apoptotic pathway due to mitochondrial deficiency in the RPE cells and which drives RPE cell death [334]. Additionally, melanocytes consist of many specific membranous organelles: the melanosomes which hold melanin. Further, melanin plays a crucial role in absorption of free radicals generated within the cytoplasm [335]. However, over-accumulation of free radicals can easily destruct the delicate melanosomes and melanin that reside in the RPE cell layer. Moreover, past studies disclosed that EtOH involves in downregulating the melanin synthesis pathway of vertebrates by reducing the gene expressions of *TYR* and transcription factor *MITF* [336-338]. A past study, found that methanolic crude extracts of plants have an anti-melanogenic activity on zebrafish embryos and lead to decrease the body

melanin pigmentation and ocular melanin content in RPE [339]. This is compatible with our data of the present study, which showed the EtOH-mediated toxicity for RPE cell development and melanin formation at 2 dpf embryonic stage (Fig. 4.10.1 B & 4.10.2). Further, histological examinations and TEM sections at 2 dpf zebrafish, proved the adverse nature of EtOH on melanosome biogenesis by showing the reduced thickness of RPE bands (Fig. 4.10.3 B), and displaying ruptured, partially filled, empty and porous melanosome vesicles in the melanocytes of RPE cells (Fig. 4.10.4 B). However, no study has been conducted so far about the EtOH effect on RPE development in vertebrates.

The relationship of the Wnt signaling pathway on RPE layer development should be studied, to investigate the resulted differential chemical effects in the RPE layers of LiCl and W-C59 treated fish. Previous research has identified the necessity of activated canonical WNT/β-catenin signaling for the differentiation of RPE cells [323, 340] via the activation of Fzd receptors [341]. *MITF* is expressed in the neuroepithelium-derived RPE cells at the beginning of eye development [341]. The WNT/β-catenin pathway plays a major role in differentiating mouse RPE cells and regulates the expression of *MITF* and *Otx2* genes. At the same time, low expression levels of *MITF* and *Otx2* in the presumptive RPE have been experienced with depletion of β-catenin levels [342]. Embryonic chick experiments demonstrated the capability of inducing *MITF* expression in the RPE cells along the co-expression of constitutively active cellular β-catenin and *Otx2* [343]. They showed that neuroepithelium releases Wnts to specify the RPE. Especially, it disclosed the importance of *Wnt2b* gene expression at the right time and right place, in guiding dorsal optic vesicle cells towards the RPE cell fate [343]. Further, the same research declares the evidence that Wnt-mediated GSK-3β inhibition supports the RPE development in vivo by β-catenin nuclear transfer [343]. Moreover, the defects in retinal cell differentiation pathways in EtOH-exposed zebrafish, could have been restored by activating Wnt signaling using the GSK-3β inhibitor (LSN 2105786) [329]. Further, an increased number of Wnt-active stem cells in the CMZ and enhanced retinal precursor cell proliferation and differentiation have been examined after incubating with Wnt agonists [329].

Results of the present study illustrated the stimulatory effect of LiCl as other agonists in RPE development at 2 dpf, by displaying increased melanin formation in eyes (Fig. 4.10.1 C & 4.10.2). Further, histological examinations and TEM sections at 2 dpf zebrafish, demonstrated the upregulation of melanosome biogenesis in the RPE layer as covering a significantly larger area of the eyes (Fig: 4.10.3 C) and, displaying well-developed and densely packed melanosome vesicles contained melanin granules (Fig. 4.10.4 C).

This should be resulted by enhancing the activity of Wnt signalling through GSK-3β inhibition of presumptive RPE cells. This strong Wnt expression activates the *MITF* expression and stimulates later differentiation and melanin synthesis of RPE cells.

The W-C59 treated zebrafish embryos showed some destructive effect in RPE cell differentiation (Fig. 4.10.1 E) at 2 dpf while a significant decrease in melanin formation was evident in the microscopic observations and software analysis (Fig. 4.10.2). Examinations of the toluidine blue plastic sections and TEM thin sections of RPE cells at 2 dpf zebrafish, proved the adverse effects of Wnt inhibitor treatment on melanosome biogenesis. It was evident by showing the paler and reduced thickness of RPE bands with damages along the epithelial layer in the toluidine blue stained cross sections (Fig. 4.10.3 E). Further, ruptured, perforated and deformed melanosome vesicles were recorded in the TEM thin sections as well (Fig. 4.10.4 E).

These results indicate the possibility of interfering to the RPE cell differentiation by early embryonic exposure of W-C59 via regulating canonical Wnt/β–catenin pathway. This drives to suppress the activity of *MITF* and melanogenic tyrosinase-related gene expressions, and ultimately leads to decreasing melanin synthesis.

Combining EtOH with the Wnt signaling inhibitor had a significant negative effect on RPE formation than the W-C59 alone treatment at 2 dpf (Fig 4.10.1 F & 4.10.2). It was apparent, examining the destructive nature of the RPE layer in cross sections of eyes (Fig 4.10.3 F) and close investigation of melanosome formation in TEM images (Fig. 4.10.4 F). A high number of numerous melanosome defects were noticed in the melanosomes of W-C59 + EtOH exposed eyes compared to the rest of the chemical treatments.

Nevertheless, EtOH with Wnt activator of LiCl also displayed drastic adverse effects on RPE layer formation (Fig. 4.10.1 D). Meanwhile, the highest demelanization of eyes was observed in this group (Fig. 4.10.2). The RPE cell layer was not well developed and failed to cover most parts of the eyes (Fig. 4.10.3 D). This was clearly visible in the TEM images, existing lighter and aberrant melanosome vesicles with holes (Fig. 4.10.4 D).

These results reveal that EtOH could act as a powerful Wnt signaling inhibitor in terms of obstructing the RPE cell differentiation and cellular melanin formation. Overall the present study declares the necessity of further studies on investigating EtOH's role in the RPE development of zebrafish eyes.

The CMZ niche harbors stem cell populations found at the tips of the retina (Fig. 1.3) [344] which differentiate and give rise to RPE cells. These differentiated stem cells eventually emigrate from the niche to contribute to new RPE cells of the mature RPE [345]. Thus, most of the immature RPE cells exist in the RPE layer which covers the tips of the neural retina and the mature RPE cells are found in the central (peripheral) region of the RPE layer [345]. This was the main reason for recording the majority of RPE cell destructions in the regions of RPE bands which are adjacent to the lens than the peripheral region of the RPE layer in the chemical treated embryos (Fig. 4.10.3).

Investigating the RPE formation in 6 dpf stage, a lack of melanin pigmentation was evident in the toluidine blue sections of the chemical exposed zebrafish eyes except for the LiCl (Fig. 4.10.5). These defects were mainly noticeable in the EtOH and EtOH contained combined treatments (Fig. 4.10.5 B, D & F). Further, depigmented melanin granules, perforated and small-size melanosome vesicles were distinct in close investigations of the TEM sections of RPE cells (Fig. 4.10.6 B, D & F). Interestingly, strong melanin formation and melanosome biogenesis were recorded in the LiCl-exposed eyes as observed in the eyes at the larval stage (Fig. 4.10.6 C). However, no melanosome ruptures and fewer other melanosome defects were recorded in the 6 dpf stage compared to 2 dpf stage. This could be mainly resulted by the regenerating ability of zebrafish RPE cells [346].

Overall, the current study clearly indicated that embryonic exposure to the EtOH and Wnt signaling pathway inhibitors more adversely impacts melanosome biogenesis and RPE formation at the embryonic stage and defects could persist in later developmental stages of zebrafish as well. In contrast, Wnt signaling pathway enhancers have a stimulatory effect on the differentiation and development of RPE cells of eyes in both embryonic and post-embryonic stages. However, the current study disclosed the capability of recovering the chemical-induced defects in melanosome biogenesis to some extent as development proceeds. This is compatible with past studies as teleost including zebrafish is inherently capable of regenerating the functional RPE monolayer after RPE aberration [347]. However, in other vertebrate classes, such as mammals, the CMZ region has been found to be completely diminished in the mature retina [345]. Therefore, mammalian RPE cells have severely reduced or lack of regeneration capability after aberration [345, 348, 349]. Studies of FASD incidences worldwide have revealed that PAE during the pregnancy period leads to malformations of the eyes with serious consequences to the vision of the affected children [215]. This condition mainly could be generated via the defects in the RPE formation according to the

findings of the present study. Further, past studies disclosed that any damage to the RPE layer impairs the functionality of the surrounding tissues and vision is severely diminished [346].

5.10 Effects of embryonic chemical exposures on melanin synthesis in zebrafish embryos.

In the present study, it is verified that the consequences of EtOH and small molecules of Wnt signaling pathway modulators on melanocyte development and melanogenic activity, in a vertebrate model of zebrafish. As early mentioned, many previous studies have shown the effect of Wnt signaling pathway regulation on melanocyte lineage transcription factors, melanogenic genes and enzymes using murine cell culture studies and vertebrate models of avian and mice embryos [246, 247, 278]. However, in the current study, the attempt was to check the influence of EtOH and Wnt regulatory chemicals on melanin synthesis at the early embryonic stage of zebrafish (*Danio rerio*), as no study has been carried out so far.

By analyzing the overall melanin formation of zebrafish embryos, all the chemical exposures caused to reduce the melanin synthesis compared to the untreated control fish (Fig. 4.11.2). The Highest melanin formation was recorded in the LiCl exposed fish (Fig. 4.11.1 C & 4.11.2) and the least was displayed in the Wnt inhibitor-treated group (Fig. 4.11.1 E & 4.11.2). This finding is similar to the previous research works which found that Wnt signaling inhibition and stimulation are associated with the down-regulation and up-regulation of the melanin synthesis mechanism. For the first time in our research, it could be revealed that embryonic ethanol exposure leads to reduce the melanin formation in vertebrates (Fig. 4.11.1 B & 4.11.2). Further, EtOH had negatively affected the Wnt signaling activation mechanism of LiCl and resulted less melanin formation (Fig. 4.11.1 D & 4.11.2). These results of overall melanin formations of the fish body are reflected by examining the chemical actions on the melanin formation of the RPE cell layer of each group (Fig. 4.10.1). Remarkably, EtOH with Wnt inhibitor directed to increase the melanin formation which was higher than the Wnt inhibitor activity alone but less than the melanin formation of LiCl exposed fish (Fig. 4.11.1 F & 4.11.2).

Melanin biosynthesis is controlled by *TYR*, *TYRP-1*, and *TYRP-2* enzymes [350]. Therefore, the resulted reduced or increased melanin formations (Fig. 4.11.1 & 4.11.2), is also associated with the changes in *TYR* and tyrosinase-related other enzyme activity levels [351]. The expressions of *TYR*, *TYRP-1*, and *TYRP-2* genes are known to be regulated by *MITF* [352]. Low melanin contents displayed in the EtOH, EtOH +LiCl, W-C59 and W-C59 + EtOH exposed groups are caused by Wnt-mediated down-regulation of *TYR*, *TYRP-1*, *TYRP-2*, and *MITF* genes. In contrast, the increment of cellular melanin content observed in the LiCl-exposed fish group, compared to the

rest of chemical-exposed fish groups is associated with the sustainable level expression of melanogenic enzymes, including *TYR*, *TYRP-1*, *TYRP-2* and *MITF* gene expression.

Overall, this present study discloses that early embryonic EtOH exposure reduces the melanogenic activity of vertebrates. On the other hand, exposure to the small molecules of Wnt signaling pathway regulators could regulate melanin formation. As illustrated in the current study, stimulation and suppression of the melanogenic pathway could be controlled by exposing the vertebrate embryos to Wnt enhancers and inhibitors respectively at the early embryonic stage.

5.11 Chemical dependent differential expression of *dct*

Investigating the transcription of *TYRP* genes during embryonic development is very important for determining the melanocyte precursor cell differentiation and development in vertebrates including zebrafish. *Dct* gene is expressed predominantly in the neural crest derived melanoblasts and differentiated melanocytes, while migrating to the different regions of the zebrafish body [81]. Further, this gene expression is distinct in the melanocytes of the RPE that originates from the forebrain neuroepithelium [98, 99]. Previous studies have revealed that *dct* expression is a very early event in the development of the melanocyte lineage together with *MITF*, whereas *TYR* or *TYRP-1* are expressed later in the development [353]. This *dct* gene expression is found to be essential for melanoblast proliferation, survival, differentiation and melanin formation in the melanocytes, and any mutation would be critical for early processes in melanocyte development [354]. However, the main role of this DCT enzyme is melanin biogenesis via catalyzing reactions in the melanogenesis pathway located within the melanosomes [355]. This enzymatic activity is vital for rearranging dopachrome into DHI-2-carboxylic acid (DHICA).Then it supports the chemical reactions of *TYR /TYRP-1* enzymes, in order to synthesize the final product of melanin [354].

In the current study, the effects of EtOH and alternated Wnt signaling levels on the *dct* gene expression of melanocyte precursors cells at 48 hpf zebrafish were examined. The results of the current study, indicated that embryonic exposure to the EtOH and small molecules of Wnt modulators influence the *dct* expression in the melanocyte progenitor cells (Fig. 4.12.1 A-E). It was clearly distinct that EtOH and Wnt signaling pathway inhibitors negatively affect *dct* gene expression (Fig. 4.12.1 B, D & E) whereas Wnt signaling enhancers could promote the gene expression levels, similar to the untreated control group (Fig. 4.12.1 C).

Further, close examinations of the melanogenic marker *dct* revealed, an increased *dct* + melanoblast populations in the control (Fig. 4.12.1 A & Fig. 4.12.1.1) and LiCl treated groups over the rest of chemical exposed fish groups (Fig. 4.12.1 C). Most probably. it could be generated by enhanced Wnt activation. In contrast, EtOH exposure and Wnt inhibition were associated with decreased *dct* gene expression in melanoblast cells. The *dct* + melanocyte precursor cell density around the cranial region was also noticeably low in these chemical-exposed fish groups. (Fig. 4.12.1 B, D & E).

Past studies have proved that activated Wnt signaling allows for nuclear β-catenin, binding with *MITF* and activating *dct* expression [356, 357]. Low levels of Wnt/β-catenin signaling cause downregulating of the *dct* transcription and maintain melanocyte stem cells in an undifferentiated state, whereas increased Wnt/β -catenin signaling promotes terminal differentiation to mature melanocytes via upregulating the *dct* transcription [357]. Data of the past studies are consistent with the results of the current study and indicate that LiCl supports for melanoblast differentiation whereas W-C59 and W-C59 + EtOH exposures lead to suppressing of the differentiation of melanocyte precursor cells and increase the undifferentiated cell count. Moreover, EtOH exposure reduces the Wnt-active stem cell count, retinal precursor cell proliferation and differentiation [329]. Incubation of human melanocyte cell cultures in the plant-based EtOH extractions has significantly suppressed the *dct* gene expression level [358]. This could be the reason for the resulting low *dct* expression levels in the melanoblasts of the cranial region and RPE melanocytes of the EtOH-treated embryos in this study.

DCT enzyme catalyzes the reactions in the melanin synthesis pathway by acting downstream of *TYR* and upstream of *TYRP-1* [359, 360]. Hence, DCT enzyme is detected as an obvious candidate for human albinism [355]. However, pathogenic DCT/ *TYRP-2* genotypes have been recorded in patients with ocular albinism and mild hypopigmentation of the skin, hair, and eyes [355]. The current study further declares evidence that defects in *DCT/TYRP-2* gene can lead to oculocutaneous albinism in humans.

5.12 Chemical dependent differential expression of *Wnt3a*

Wnt genes play a crucial role in melanocyte development lineage. Especially, *Wnt3a* has been identified as an important regulator of activating the Wnt/β-catenin pathway and mainly involves in melanoblast specification, differentiation and proliferation of vertebrates [361].

Past research reveals that *dct* is not expressed in the melanoblasts of murine models which are mutants for *Wnt3a* [77, 299]. This indicates the failure of the early expansion of NCCs derived melanocyte formation with the absence of *Wnt3a* gene expression and the importance of *Wnt3a* expression in melanocyte precursor cells in order to up-regulate the genes which are responsible for melanocyte differentiation [77, 299]. Similarly, in vivo and in vitro studies also indicate that *Wnt3a* stimulates the differentiation and expansion of melanocytes in cultured chick and mouse NC cells [31, 247]. In contrast, the suppression of β-catenin activation reduces the *Wnt3a* gene expression and melanoblast development during the embryonic development of mice [362].

In the current study, LiCl exposure showed a similar *Wnt3a* expression to the control sample in melanoblasts with high *Wnt3a* + density (Fig. 4.12.2 A & C). However, lower expression levels were distinct in other chemical-treated fish (Fig. 4.12.2 B, D & E). This finding further indicates the stimulatory activity of LiCl in Wnt signaling activation and promoting melanoblast development by early embryonic exposure. In contrast, Wnt signaling pathway inhibitors had led to producing less *Wnt3a* gene expression of melanoblasts with low *Wnt3a* + melanoblast density at the head region (Fig. 4.12.2 D), indicating that early embryonic Wnt inhibition affects the development of melanocyte precursor cells and Wnt gene expression of them. A similar phenomenon was examined in the EtOH and combined chemical exposure of W-C59 + EtOH (Fig. 4.12.2 B & E).

Overall, the increased melanocyte density, high melanin synthesis in the pigment cells and body organs, and proper melanocyte development observed in the present study were likely to be associated with the elevated levels of *dct* + and *Wnt3a* + gene expressions. It was caused by enhanced Wnt levels in the mealanoblast cells after exogenous LiCl exposure. Downregulation of *dct* and *Wnt* gene expressions in melanocyte precursor cells could be the factor for producing less melanocyte density, low melanin synthesis and phenotypic defects of melanocytes resulted in the W-C59, W-C59 + EtOH and EtOH treated fish groups.

CHAPTER 6: CONCLUSION

In summary, our work defines EtOH and Wnt signaling involvement in zebrafish melanocyte development in vivo. This research identified that prenatal EtOH exposure and altered Wnt signaling activity influence normal melanocyte development and patterning in the vertebrate body. Early embryonic chemical exposure results marked differences in melanocyte densities. Exogenous EtOH exposure and Wnt inhibition of embryos at the early neurulation period lead to the production of reduced melanocyte numbers while Wnt signal stimulation promotes melanocyte formation and produces melanocytes in high numbers at post-embryonic stages of life. Especially, Wnt inhibition delays melanocyte generation. EtOH and Wnt modulators are capable of regulating the melanosome motility, change the phenotypic characteristics of the skin melanocytes and deciding the overall body color eventually. Chemical exposure causes migratory defects in the embryonic stage. Increased and decreased migrated melanocytes as well as localization of ectopic melanocytes in different regions of the animal body occur due to the defects in melanocyte migration along the migratory routes. These aberrations are mainly caused by the altered cellular signaling cues with the EtOH and Wnt exposures. This condition leads to making malformed melanocyte patterns in the animal body at later development stages of animal life. These defects in melanocyte pattern formation are consisted of, a lack of melanocytes along with severely disrupted irregular melanocyte arrangements. Biased L-R melanocyte patterning observed in this study, is possible to be arisen from the chemical-induced defects of early embryogenesis and signaling cascades. As illustrated in the current study, stimulation and suppression of the melanogenic pathway can be controlled by exposing the vertebrate embryos to Wnt enhancers and inhibitors respectively at the early embryonic stage. Additionally, exposure to the EtOH at the prenatal stage tends to reduce melanogenic activity. This phenomenon is same for the melanin-contained body organs. Wnt activators promote melanoblast development, *dct* + and *Wnt3a* + gene expressions in melanocyte precursor cells and melanosome biogenesis whereas EtOH and Wnt inhibitors down-regulate the above-mentioned factors. The results of this study reveal the requirement of a balanced Wnt signaling level for proper melanocyte development. Canonical Wnt activation and inhibition would be applied as a new therapeutic strategy in melanocyte defects in the future. Any exogenous teratogen exposure at early embryogenesis can lead to defects in melanocyte lineage and persist for a long period, intact with animal life. So far, FASD is clinically diagnosed by the characteristic features of craniofacial malformations, microphthalmia and growth retardation. The present study declares that the defects of melanocyte development in the skin and body organs of infants or children can be used as a new criterion for the diagnosis of FASD.

CHAPTER 7: APPENDIX

Appendix 1

Zebrafish Embryo Bleaching Protocol

1. Embryos are transferred from petri dish to a tea strainer (25 embryos at a time) and gently swirled in the bowl filled with bleach solution for 5 min without touching the bottom of the bowl.

2. The tea strainer with eggs is gently swirled for 3 min in the rinse 1st bowl filled with embryo medium.

3. The tea strainer with eggs is gently swirled for 3 min in the rinse 2nd bowl filled with new embryo medium.

4. The tea strainer with eggs is gently swirled for exactly 1 min in the bowl filled with pronase solution.

5. The tea strainer with eggs is gently swirled for exactly 3 min in the rinse 3rd bowl filled with new embryo medium.

5. The bleached embryos are returned from the tea strainer to new properly labelled petri dishes (N = 25) to avoid the contamination from original ones.

Appendix 2

DIG High Prime DNA Labeling and Detection protocol

1. Make sure that hybridization oven is on and preheated to 100 ˚C.

2. Cut out the nitrocellulose membrane big enough to fit in the petri dish. Cut a wedge out of one corner in order to indicate the top left corner.

3. Apply a 1 µl of each of your labeled diluted probe from the prepared dilution series (10^{-2}, 10^{-3}, 10^{-4} and $10^{-5)}$ and labeled control probe to the nitrocellulose membrane.

4. Fix the nucleic acid by baking for 30 min at 100 ˚C in a sterile glass petri dish.

5. Transfer nitrocellulose membrane into the plastic dish (sterile) with 10 ml of Maleic acid buffer (refer the preparation protocol mentioned below).

(approx. ½ the depth of the dish, enough to cover the membrane). Incubate (20 ˚C) with shaking (40 RPM) for 2 min.

6. Incubate (20 ˚C) for 20 min in Blocking solution (refer the preparation protocol mentioned below) with shaking 40 RPM.

7. Prepare Anti-Digoxigenin-AP antibody solution (refer the preparation protocol mentioned below).

8. Wash for 5 min with 10 × TBST in DepC H_2O and incubate (20 ˚C) with shaking (40 RPM).

9. Incubate (20 ˚C) with 10 ml Anti-Digoxigenin-AP antibody solution for 30 min with shaking (40 RPM).

10. Wash with Washing buffer (refer the preparation protocol mentioned below). Incubate (20 ˚C) with shaking (40 RPM). Carry this out twice for 15 min each, the second time with fresh washing buffer, save the antibody solution.

12. Equilibrate for 5 min in the Detection buffer (refer the preparation protocol mentioned below). Incubate (20 ˚C) with shaking (40 RPM).

13. Incubated at room temperature in a dark drawer (due to light sensitivity) in 10 ml of NBT/BCIP color substrate solution. No shaking. Check approximately every 2 min for any color change.

□ Maleic Acid Buffer Recipe

Maleic Acid Buffer Recipe	100 ml Sample
(0.1 M) Maleic Acid	1.1607 g
(0.15 M) NaCl	0.8766 g
pH 7.5 adjust with solid NaOH	
DepC H_2O	To 100 ml

□ Blocking Solution Recipe

Blocking Solution Recipe	100 ml Sample
Sheep serum (2%)	2g
Milk powder (3%)	3g
10 × TBST in DepC H_2O	To 100 ml

- Note- Store in - 4˚C until usage

□ Anti-Digoxigenin-AP Antibody Solution Recipe

Antibody Solution Recipe	10 ml Sample
Anti-Digoxigenin-AP , Fab fragments	1µl
10 × TBST in DepC H_2O	To 10 ml

- Note- Store in -4˚C until usage

□ Washing Buffer Recipe

Washing Buffer Recipe	100 ml Sample
(0.1 M) Maleic Acid	1.1607 g
(0.15 M) NaCl	0.8766 g
pH 7.5 adjust with solid NaOH	
Tween 20 (0.3%)	0.3 ml
DepC H_2O	To 100 ml

□ Detection Buffer Recipe

Detection Buffer Recipe	**100 ml Sample**
(0.1 M) Tris-HCl	10 ml
(0.1 M) NaCl	0.5844g
DepC H_2O	To 100 ml

Appendix 3

Whole-Mount in situ Hybridization Protocol

Important considerations before starting

- ✓ All solutions should be made with DepC H_2O unless otherwise stated in protocol
- ✓ Gloves should be worn at all times to reduce contamination
- ✓ Countertop work surface should be RNAase zapped to reduce contamination before use
- ✓ All plastic containers/tubes should be DNAase/RNAase free
- ✓ Autoclaved pipette tips and Gilson Pipettes are to be used

Prep Day (Collection of embryo's and fish) (Approx. 2 hrs + Overnights)

- Collect Embryos
  - □ Dechorinate 48 hpf embryos and euthanize in 0.1% MS222.
  - □ Fix in 4% PFA (RNAase free) for 2 hrs at room temperature or overnight at 4°C.
- Dehydrate in series

□ 25% MeOH in PBS	30 min at RT	1x
□ 50% MeOH in PBS	30 min at RT	1x
□ 75% MeOH in PBS	30 min at RT	1x
□ 100% MeOH	at least overnight	Store in -20°C

- Note
  - □ MS222 is a powder that should be made into 0.01% and 0.1% solutions fresh for each day.

Day 1: Bleach Day (Approx. 1.5 hrs, longer if older fish)

- Rehydrate embryos

□ 75% MeOH in PBS	5 min at RT	1x
□ 50% MeOH in PBS	5 min at RT	1x
□ 25% MeOH in PBS	5 min at RT	1x

- Wash
  - ☐ PBST 5 min at RT 1x

- Bleach
  - ☐ Bleach according to the time below, or until the embryo is a creamy white. Ensure eyes do not become bulgy.
  - ☐ General timeline for fish

Age	Approx. Bleach Time
48 hpf	30 min

  - ☐ Bleach Recipe – Make Fresh on the day

Total Amount	20 ml
KOH (.5%)	.1000 g
H_2O_2 (3% of 30%)	600 ul
DepC H_2O	To 20 ml

- Wash
  - ☐ PBS 5 min at RT 1x
    - Note: Embryos can be very sticky in PBS/MeOH solutions

- Dehydrate in series
  - ☐ 25% MeOH in PBS 5 min at RT 1x
  - ☐ 50% MeOH in PBS 5 min at RT 1x
  - ☐ 75% MeOH in PBS 5 min at RT 1x

  - ☐ Transfer into new 1.5 ml eppendorff tube
  - ☐ 100% MeOH Store in -20° C Overnight

✓ Embryos can now be stored in 100% MeOH at -20° C for several weeks or at minimum of 2 hrs before continuing on

Day 2: Pro-K and Treatment Day (Approximately 5 hrs, longer if older fish)

- Rehydrate embryos in 1.5 ml eppendorf tubes
  - □ 75% MeOH in PBS 5 min at RT 1x
  - □ 50% MeOH in PBS 5 min at RT 1x
  - □ 25% MeOH in PBS 5 min at RT 1x

- Wash
  - □ PBST 5 min at RT 4x

- Permeabilize: With Proteinase K (10 ug/ml in DepC)
  - □ If using a 10 mg/ml stock, dilute by adding 1 ul of stock solution to 1000 ul of DepC H_2O

Age	Approx. Pro-K Time
48 hpf	23 min

- Wash
  - □ PBST 5 min at RT 2x

- Fix (In fume hood)

□ 4% PFA (DepC Treated) 20 min at RT 1x

- Wash
  - □ PBST 5 min at RT 2x

- Treat (In fume hood) – Make fresh on the day
  - □ Acetic Anhydride 30 min at RT 1x

Acetic Anhydride Recipe	18 ml Batch
DepC Water	13.5 ml
Triethanolamamine (upstairs lab cabinet)	239.7 ul
pH to 7.0	
DepC Water	To 18 ml
Acidic anhydride (under fume hood)	45 ul

- Wash
  - □ PBST 10 min at RT 2x

- Prehybridize
  - □ Hyb (-) 2 hrs at 70°C/35 rpm

    Note: See last page for Hyb (-) recipe.

✓ **<u>Stop Point:</u>** Embryos can be stored in Hyb (-) for several weeks, or you can continue to the next step.

Day (1/3): Hyb (+) – Adding the probe (Approx. 2 hrs)

- Pre Hyb (-)
  - □ Hyb (-) 2 hrs at 70°C/35rpm

  Note: Repeating this step to ensure the embryos are at the same permeability /solubility as previous

- Adding Hyb (+)
  - □ Add 1 ml of Hyb (+) to each sample

Hyb (+) Recipe	Per tube (1 ml)
Hyb (-)	890 ul
Yeast tRNA (5 mg/ml)	100 ul of 50 mg/ml stock
Heparin (50 ug/ml)	10 ul of 5 mg/ml stock
pH to 6.0 with Citric Acid	9.2 ul of 1 M citric acid

- Adding probe
  - □ Add 2-3 ul of probe (depending on strength) to each of the sample tubes.
  - □ Notes
    - Probe should not be left out of the freezer long. Putting them on ice is recommended.

- Ensure probe is mixed – flick with finger and centrifuge liquid back down for 2-3 seconds.

- Incubate overnight at 70ºC/35rpm

Day (2/4): Washes and Antibody (Approx. 7 hrs, with 3-4 hour break in middle)

- Washes
  - □ 75% Hyb (-) + 25% 2xSSC 15 min at 70ºC/35 rpm 1x
  - □ 50% Hyb (-) + 50% 2xSSC 15 min at 70ºC/35 rpm 1x
  - □ 25% Hyb (-) + 75% 2xSSC 15 min at 70ºC/35 rpm 1x

    Note: These solutions should be premade and stored in the -20ºC freezer

  - □ Change to fresh eppendorf tubes – Hyb (-) is very slippery and the tube caps tend not to stay in place at this point. The tubes will also likely have white precipitate throughout.

  - □ 2xSSC 10 min at 70ºC/35rpm 2x
  - □ 0.2xSSC 30 min at 70ºC/35rpm 3x

  - □ Start sheep serum inactivation 30 min at 60ºC
    (amount based on Blocking Buffer Recipe)

  - □ 75% 0.2xSSC + 25% PBST 10 min at Room temp/60 rpm 1x
  - □ 50% 0.2xSSC + 50% PBST 10 min at Room temp/60 rpm 1x
  - □ 25% 0.2xSSC + 75% PBST 10 min at Room temp/60 rpm 1x
  - □ 100% PBST 10 min at Room temp/60 rpm 1x

- Incubate in blocking buffer for 3-4 hrs
    - □ Add 1 ml of Blocking buffer to each tube

      Make Fresh on the day

Blocking Buffer recipe	1 ml/Sample
1 x PBST	980 ul
2% Heat inactivated Sheep serum	20 ul
Bovine serum albumin (2 mg/ml)	0.002 g

      Note: Save at least 10 ul of blocking buffer. It is required in making the antibody recipe.

- Adding antibody

Antibody Recipe	
Blocking Buffer (saved from before)	9 ul
Anti-Dig Antibody	1 ul
Optional – Fish powder	A few pieces

    - □ Allow antibody to sit in blocking buffer for at least 10 min before adding the antibody solution to the samples. This allows pre absorption to occur, and reduces background.
    - □ Add 1 ul of above antibody recipe to each sample tube already containing the 1 ml of blocking buffer from 4-5 hrs prior.

- Incubate overnight at 4 ^{o}C while shaking (keep the samples in the cold room after fixing the samples on the shaker)

Day (3/5): Antibody and Color Reaction (Approx. 4 hrs then overnight)

- Remove samples from incubator and discard antibody solution

- Washes
  - □ PBST 5 min at RT

  - □ PBST 15 min at RT on same shaker 12x

- Place embryo's in glass pettridishes – Ensure proper labeling

- Incubate TRIS Staining Buffer
  - □ Add 1 ml of TRIS Staining Buffer to each sample 5 min at room temp 3x

  - □ Make Fresh on the day

Reagent	Stock	Final	20 ml Batch
TRIS pH 9.0	1 M	100 mM	2 ml
$MgCl_2$	1 M	50 mM	1 ml
NaCl	5 M	100 mM	400 ul
Tween	10%	0.1%	20 ul
Levamisole		2 mM	0.019 g
DepC H_2O			To 20 ml

Note: When determining batch size, allow for three change-over's per tube as well as enough for mixing NBT/BCIP staining solution

- Remove TRIS staining buffer and add NBT/BCIP staining color reaction solution
  - □ Add approximately 1 ml of NBT/BCIP staining solution per sample
  - □ Keep the embryos with staining solution in dark (covering with foil papers) and check the gene expression / color reaction of embryos every 15 min under the microscope

Day (4/6): Stopping Color Reaction (Approx. 2 hrs)

- Wash
  - □ PBST — 5 min at Room Temperature — 6x

- Fix (in fume hood)
  - □ 4% PFA — 20 mins at room temperature — 1x

- Dehydrate
  - □ 25% MeOH in PBS — 10 min at RT — 1x
  - □ 50% MeOH in PBS — 10 min at RT — 1x
  - □ 75% MeOH in PBS — 10 min at RT — 1x
  - ✓ 100% MeOH — Store in 4ºC in sample box

Note: Photo's should be taken while sample is in 25% or 50% MeOH/PBS

Reagent Recipes

Hyb (-)

Reagent	% in final solution	150 ml Batch (ideal)
Deionized Formamide 100%	50	75 ml
SSC 20x	5x	37.5 ml
Tween 10% (stock solution)	0.1	150 ul
DepC Water		Top to 150 ml

Note: Make in fume hood. Ensure contents are well mixed. Aliquot into 50 ml flacon tube and store in -20ºC.

PBS

Reagent for 1 L Batch	
NaCl	8.0 g
KCl	0.2 g
Na_2PO_4	1.386 g
KH_2PO_4	0.2 g
Top to 1 L with DepC H_2O	
pH to 7	

To make PBST add 50 ul of Tween-10 to 50 ml of PBS

DepC H_2O

- ✓ Per 1 L of distilled water add 100 ul of DepC (found in upstairs fridge).
- ✓ Carry out in fume hood.
- ✓ Shake for 30 min vigorously.
- ✓ Autoclave

Appendix 4

3.1 Statistical analysis for the variation of melanocyte density at 15 dpf against different chemical treatments

Table 3.2: Bonferroni pairwise comparison for the average melanocyte density at 15 dpf of control and treated samples

Treatments pair	Bonferroni p-value	Bonferroni inference
Control - EtOH	2.3673E-10	*** p<0.001
Control - LiCl	0.369039805	insignificant
Control – EtOH + LiCl	7.15288E-13	*** p<0.001
Control – WC59	0.005090486	** p<0.01
Control - WC59 + EtOH	5.37263E-07	*** p<0.001
EtOH - LiCl	4.6962e-13	*** p<0.001
EtOH – EtOH + LiCl	0.3030643	insignificant
EtOH – WC59	1.6727e-07	*** p<0.001
EtOH - WC59 + EtOH	0.2741716	insignificant
LiCl – EtOH + LiCl	0.0000e+00	*** p<0.001
LiCl – WC59	0.0146173	*p<0.05
LiCl - WC59 + EtOH	3.2523e-09	*** p<0.001
EtOH + LiCl – WC59	2.3491e-11	*** p<0.001
EtOH + LiCl - WC59 + EtOH	0.0001768	*** p<0.001
WC59 - WC59 + EtOH	0.0010804	** p<0.01

3.2 Statistical analysis for the variation of the size of melanocytes of zebrafish against various chemical treatments

Table 3.3: Bonferroni pairwise comparison for the average size of melanocytes at 2 dpf embryonic stage of control and treated samples

Treatments pair	Bonferroni p-value	Bonferroni inference
Control - EtOH	0.00804	** p<0.01
Control - LiCl	4.4126e-05	*** p<0.001
Control – EtOH + LiCl	5.5792e-07	*** p<0.001
Control – WC59	3.0920e-06	*** p<0.001
Control - WC59 + EtOH	0.0027722	** p<0.01
EtOH - LiCl	6.1434385	insignificant
EtOH – EtOH + LiCl	0.7202313	insignificant
EtOH – WC59	1.8648027	insignificant
EtOH - WC59 + EtOH	10.6661640	insignificant
LiCl – EtOH + LiCl	3.5767142	insignificant
LiCl – WC59	7.0275646	insignificant
LiCl - WC59 + EtOH	3.5105328	insignificant
EtOH + LiCl – WC59	9.6890714	insignificant
EtOH + LiCl - WC59 + EtOH	0.3013688	insignificant
WC59 - WC59 + EtOH	0.8762464	insignificant

Table 3.4: Bonferroni pairwise comparison for the average size of melanocytes at 6 dpf larval stage of control and treated samples

Treatments pair	Bonferroni p-value	Bonferroni inference
Control - EtOH	1.5987e-13	*** p<0.001
Control - LiCl	5.5996e-07	*** p<0.001
Control – EtOH + LiCl	1.2766978	insignificant
Control – WC59	4.7629e-13	*** p<0.001
Control - WC59 + EtOH	2.6812e-12	*** p<0.001
EtOH - LiCl	0.0019536	** p<0.01
EtOH – EtOH + LiCl	8.3989e-11	*** p<0.001
EtOH – WC59	11.3212671	insignificant
EtOH - WC59 + EtOH	6.3941543	insignificant
LiCl – EtOH + LiCl	0.0003210	*** p<0.001
LiCl – WC59	0.0054049	** p<0.01
LiCl - WC59 + EtOH	0.0242561	*p<0.05
EtOH + LiCl – WC59	2.6618e-10	*** p<0.001
EtOH + LiCl - WC59 + EtOH	1.6186e-09	*** p<0.001
WC59 - WC59 + EtOH	9.4164393	insignificant

3.3 Statistical analysis for the variation of melanocyte migratory differences at embryonic stage of zebrafish against various chemical treatments

Table 3.5: Bonferroni pairwise comparison for the average migrated- melanocyte counts at 2 dpf embryonic stage of control and treated samples

Treatments pair	Bonferroni p-value	Bonferroni inference
Control - EtOH	0.000271269	*** p<0.001
Control - LiCl	0.000508833	*** p<0.001
Control – EtOH + LiCl	0.112601085	insignificant
Control – WC59	0.096114357	insignificant
Control - WC59 + EtOH	0.059915621	insignificant
EtOH - LiCl	0.8867163	insignificant
EtOH – EtOH + LiCl	0.2919126	insignificant
EtOH – WC59	0.0017404	** p<0.01
EtOH - WC59 + EtOH	0.0010053	** p<0.01
LiCl – EtOH + LiCl	0.0269862	* p<0.05
LiCl – WC59	0.0010053	** p<0.01
LiCl - WC59 + EtOH	0.0010053	** p<0.01
EtOH + LiCl – WC59	0.3573845	insignificant
EtOH + LiCl - WC59 + EtOH	0.0255358	* p<0.05
WC59 - WC59 + EtOH	0.8055659	insignificant

Table 3.6: Bonferroni pairwise comparison for the average non-migrated melanocyte counts at 2 dpf embryonic stage of control and treated samples

Treatments pair	Bonferroni p-value	Bonferroni inference
Control - EtOH	7.7372e-05	*** p<0.001
Control - LiCl	5.2833e-07	*** p<0.001
Control – EtOH + LiCl	0.00085769	*** p<0.001
Control – WC59	0.000206481	*** p<0.001
Control - WC59 + EtOH	0.000791397	*** p<0.001
EtOH - LiCl	2.6732853	insignificant
EtOH – EtOH + LiCl	2.5088551	insignificant
EtOH – WC59	1.4603552	insignificant
EtOH - WC59 + EtOH	0.5361579	insignificant
LiCl – EtOH + LiCl	0.1169246	insignificant
LiCl – WC59	0.0529670	insignificant
LiCl - WC59 + EtOH	0.0133688	* p<0.05
EtOH + LiCl – WC59	11.6263022	insignificant
EtOH + LiCl - WC59 + EtOH	6.8136371	insignificant
WC59 - WC59 + EtOH	9.6395266	insignificant

3.4 Statistical analysis for the variation of melanocyte arrangement defects at larval stage of zebrafish against various chemical treatments

Table 3.7: Bonferroni pairwise comparison for the average dorsal stripe melanocyte counts at 6 dpf larval stage of control and treated samples

Treatments pair	Bonferroni p-value	Bonferroni inference
Control - EtOH	1.4343e-08	*** p<0.001
Control - LiCl	4.9394e-12	*** p<0.001
Control – EtOH + LiCl	8.8259e-11	*** p<0.001
Control – WC59	0.0000e+00	*** p<0.001
Control - WC59 + EtOH	4.9394e-12	*** p<0.001
EtOH - LiCl	0.5182897	insignificant
EtOH – EtOH + LiCl	2.6299273	insignificant
EtOH – WC59	1.1224e-12	*** p<0.001
EtOH - WC59 + EtOH	0.5182897	insignificant
LiCl – EtOH + LiCl	6.4507199	insignificant
LiCl – WC59	3.0420e-09	*** p<0.001
LiCl - WC59 + EtOH	15.0000000	insignificant
EtOH + LiCl – WC59	1.6029e-10	*** p<0.001
EtOH + LiCl - WC59 + EtOH	6.4507199	insignificant
WC59 - WC59 + EtOH	3.0420e-09	*** p<0.001

Table 3.8: Bonferroni pairwise comparison for the average lateral stripe melanocyte counts at 6 dpf larval stage of control and treated samples

Treatments pair	Bonferroni p-value	Bonferroni inference
Control - EtOH	0.0004745	*** p<0.001
Control - LiCl	0.0348962	* p<0.05
Control – EtOH + LiCl	2.0375389	insignificant
Control – WC59	1.5217e-06	*** p<0.001
Control - WC59 + EtOH	4.3976e-10	*** p<0.001
EtOH - LiCl	2.7596008	insignificant
EtOH – EtOH + LiCl	0.0565170	insignificant
EtOH – WC59	1.7375100	insignificant
EtOH - WC59 + EtOH	0.0058074	** p<0.01
LiCl – EtOH + LiCl	1.4742307	insignificant
LiCl – WC59	0.0715285	insignificant
LiCl - WC59 + EtOH	6.0339e-05	*** p<0.001
EtOH + LiCl – WC59	0.0003553	*** p<0.001
EtOH + LiCl - WC59 + EtOH	1.2416e-07	*** p<0.001
WC59 - WC59 + EtOH	0.4963872	insignificant

Table 3.9: Bonferroni pairwise comparison for the average ventral stripe melanocyte counts at 6 dpf larval stage of control and treated samples

Treatments pair	Bonferroni p-value	Bonferroni inference
Control - EtOH	5.0597843	insignificant
Control - LiCl	0.4585956	insignificant
Control – EtOH + LiCl	1.4658e-05	*** p<0.001
Control – WC59	0.0002511	*** p<0.001
Control - WC59 + EtOH	11.0088086	insignificant
EtOH - LiCl	0.0356573	* p<0.05
EtOH – EtOH + LiCl	4.1228e-07	*** p<0.001
EtOH – WC59	7.8610e-06	*** p<0.001
EtOH - WC59 + EtOH	8.0053113	insignificant
LiCl – EtOH + LiCl	0.0255312	* p<0.05
LiCl – WC59	0.2290553	insignificant
LiCl - WC59 + EtOH	0.1981676	insignificant
EtOH + LiCl – WC59	6.4320079	insignificant
EtOH + LiCl - WC59 + EtOH	4.2003e-06	*** p<0.001
WC59 - WC59 + EtOH	7.5482e-05	*** p<0.001

Table 3.10: Bonferroni pairwise comparison for the average yolk sac stripe melanocyte counts at 6 dpf larval stage of control and treated samples

Treatments pair	Bonferroni p-value	Bonferroni inference
Control - EtOH	0.0000e+00	*** p<0.001
Control - LiCl	0.0002131	*** p<0.001
Control – EtOH + LiCl	0.0000e+00	*** p<0.001
Control – WC59	8.2551e-11	*** p<0.001
Control - WC59 + EtOH	2.0275e-10	*** p<0.001
EtOH - LiCl	0.0000e+00	*** p<0.001
EtOH – EtOH + LiCl	9.0757509	insignificant
EtOH – WC59	0.0002371	*** p<0.001
EtOH - WC59 + EtOH	0.0001004	*** p<0.001
LiCl – EtOH + LiCl	0.0000e+00	*** p<0.001
LiCl – WC59	0.0000e+00	*** p<0.001
LiCl - WC59 + EtOH	0.0000e+00	*** p<0.001
EtOH + LiCl – WC59	0.0013977	** p<0.01
EtOH + LiCl - WC59 + EtOH	0.0006125	*** p<0.001
WC59 - WC59 + EtOH	12.1130843	insignificant

3.5 Statistical analysis for the ocular melanin formation at 2 dpf embryonic stage of zebrafish against various chemical treatments

Table 3.11: Bonferroni pairwise comparison for the average intensity of RPE layer at 2 dpf embryonic stage of control and treated samples

Treatments pair	Bonferroni p-value	Bonferroni inference
Control - EtOH	3.7930e-09	*** p<0.001
Control - LiCl	10.8986934	insignificant
Control – EtOH + LiCl	0.0000e+00	*** p<0.001
Control – WC59	0.000134967	*** p<0.001
Control - WC59 + EtOH	4.2693e-06	*** p<0.001
EtOH - LiCl	1.0265e-09	*** p<0.001
EtOH – EtOH + LiCl	3.2441e-12	*** p<0.001
EtOH – WC59	0.0013538	** p<0.01
EtOH - WC59 + EtOH	0.9701811	insignificant
LiCl – EtOH + LiCl	0.0000e+00	*** p<0.001
LiCl – WC59	0.0044866	** p<0.01
LiCl - WC59 + EtOH	1.1650e-06	*** p<0.001
EtOH + LiCl – WC59	0.0000e+00	*** p<0.001
EtOH + LiCl - WC59 + EtOH	6.6613e-15	*** p<0.001
WC59 - WC59 + EtOH	0.3398450	insignificant

Appendix 5

Key observations of W-C59 exposed zebrafish embryos

Figure 4.13.1 Key observation of producing albino like zebrafish embryos at 2 dpf with the defects of melanocyte development, patterning and melanogenesis

Figure 4.13.2 Significant observation of producing albino like zebrafish embryos with the least melanin formation in eyes (labelled with dark red arrow head), at 2 dpf embryonic stage

CHAPTER 8: REFERENCES

1. Kleisner, K., *Re-semblance and re-evolution: Paramorphism and semiotic co-option may explain the re-evolution of similar phenotypes.* Sign Systems Studies, 2010. **38**(1/4): p. 378-390.
2. Gould, S.J. and E.S. Vrba, *Exaptation—a missing term in the science of form.* Paleobiology, 1982. **8**(1): p. 4-15.
3. Kang, C., Y.E. Kim, and Y. Jang, *Colour and pattern change against visually heterogeneous backgrounds in the tree frog Hyla japonica.* Scientific reports, 2016. **6**(1): p. 1-12.
4. Caro, T. *The colours of extant mammals*. in *Seminars in Cell & Developmental Biology*. 2013. Elsevier.
5. Jablonski, D., et al., *Axanthism in amphibians: A review and the first record in the widespread toad of the Bufotes viridis complex (Anura: Bufonidae).* Belgian Journal of Zoology, 2014. **144**(2).
6. Haffter, P., et al., *Mutations affecting pigmentation and shape of the adult zebrafish.* Development genes and evolution, 1996. **206**(4): p. 260-276.
7. Kelsh, R.N., et al., *Zebrafish pigmentation mutations and the processes of neural crest development.* Development, 1996. **123**(1): p. 369-389.
8. FUJII*, R., *The regulation of motile activity in fish chromatophores.* Pigment Cell Research, 2000. **13**(5): p. 300-319.
9. Fujii, R., *Cytophysiology of fish chromatophores*, in *International review of cytology*. 1993, Elsevier. p. 191-255.
10. Baxter, L.L., et al., *A curated gene list for expanding the horizons of pigmentation biology.* Pigment cell & melanoma research, 2019. **32**(3): p. 348-358.
11. Le Douarin, N., N.M. LeDouarin, and C. Kalcheim, *The neural crest*. 1999: Cambridge university press.
12. Nguyen, V.H., et al., *Dorsal and intermediate neuronal cell types of the spinal cord are established by a BMP signaling pathway.* Development, 2000. **127**(6): p. 1209-1220.
13. Painter, K., *Models for pigment pattern formation in the skin of fishes*, in *Mathematical models for biological pattern formation*. 2001, Springer. p. 59-81.
14. Cooper, C.D. and D.W. Raible. *Mechanisms for reaching the differentiated state: Insights from neural crest-derived melanocytes*. in *Seminars in cell & developmental biology*. 2009. Elsevier.
15. Lin, J.Y. and D.E. Fisher, *Melanocyte biology and skin pigmentation.* Nature, 2007. **445**(7130): p. 843-850.
16. Pavan, W.J. and D.W. Raible, *Specification of neural crest into sensory neuron and melanocyte lineages.* Developmental biology, 2012. **366**(1): p. 55-63.
17. Hawkes, J.W., *The structure of fish skin.* Cell and Tissue Research, 1974. **149**(2): p. 147-158.
18. Michiels, N.K., et al., *Red fluorescence in reef fish: a novel signalling mechanism?* BMC ecology, 2008. **8**(1): p. 1-14.
19. Sparks, J.S., et al., *The covert world of fish biofluorescence: a phylogenetically widespread and phenotypically variable phenomenon.* PLoS One, 2014. **9**(1): p. e83259.
20. Olsson, M., D. Stuart-Fox, and C. Ballen. *Genetics and evolution of colour patterns in reptiles*. in *Seminars in cell & developmental biology*. 2013. Elsevier.
21. Grether, G.F., G.R. Kolluru, and K. Nersissian, *Individual colour patches as multicomponent signals.* Biological Reviews, 2004. **79**(3): p. 583-610.
22. Schartl, M., et al., *What is a vertebrate pigment cell?* Pigment cell & melanoma research, 2016. **29**(1): p. 8-14.
23. Cichorek, M., et al., *Skin melanocytes: biology and development.* Advances in Dermatology and Allergology/Postępy Dermatologii i Alergologii, 2013. **30**(1): p. 30-41.
24. Thody, A. and S. Shuster, *Melanophores, melanocytes and melanin: Endocrinology and pharmacology*, in *Pharmacology of the Skin I*. 1989, Springer. p. 257-269.
25. Mills, M.G. and L.B. Patterson. *Not just black and white: pigment pattern development and evolution in vertebrates*. in *Seminars in cell & developmental biology*. 2009. Elsevier.

26. Miller, C.T., et al., *cis-Regulatory changes in Kit ligand expression and parallel evolution of pigmentation in sticklebacks and humans.* Cell, 2007. **131**(6): p. 1179-1189.
27. Hultman, K.A., et al., *Gene duplication of the zebrafish kit ligand and partitioning of melanocyte development functions to kit ligand a.* PLoS genetics, 2007. **3**(1): p. e17.
28. Henion, P.D. and J.A. Weston, *Timing and pattern of cell fate restrictions in the neural crest lineage.* Development, 1997. **124**(21): p. 4351-4359.
29. Reedy, M.V., C.D. Faraco, and C.A. Erickson, *The delayed entry of thoracic neural crest cells into the dorsolateral path is a consequence of the late emigration of melanogenic neural crest cells from the neural tube.* Developmental biology, 1998. **200**(2): p. 234-246.
30. Erickson, C.A. and T.L. Goins, *Avian neural crest cells can migrate in the dorsolateral path only if they are specified as melanocytes.* Development, 1995. **121**(3): p. 915-924.
31. Dunn, K.J., et al., *WNT1 and WNT3a promote expansion of melanocytes through distinct modes of action.* Pigment cell research, 2005. **18**(3): p. 167-180.
32. Aoki, Y., et al., *Sox10 regulates the development of neural crest-derived melanocytes in Xenopus.* Developmental biology, 2003. **259**(1): p. 19-33.
33. Casane, D. and S. Rétaux, *Evolutionary genetics of the cavefish Astyanax mexicanus.* Advances in genetics, 2016. **95**: p. 117-159.
34. Detrich III, H.W., M. Westerfield, and L.I. Zon, *Overview of the zebrafish system.* Methods in cell biology, 1998. **59**: p. 3-10.
35. Driever, W. and M.C. Fishman, *The zebrafish: heritable disorders in transparent embryos.* The Journal of clinical investigation, 1996. **97**(8): p. 1788-1794.
36. Zhang, C., C. Willett, and T. Fremgen, *Zebrafish: an animal model for toxicological studies.* Current Protocols in Toxicology, 2003. **17**(1): p. 1.7. 1-1.7. 18.
37. Adatto, I., et al., *A new system for the rapid collection of large numbers of developmentally staged zebrafish embryos.* PloS one, 2011. **6**(6): p. e21715.
38. Kari, G., U. Rodeck, and A.P. Dicker, *Zebrafish: an emerging model system for human disease and drug discovery.* Clinical Pharmacology & Therapeutics, 2007. **82**(1): p. 70-80.
39. Bootorabi, F., et al., *Zebrafish as a model organism for the development of drugs for skin cancer.* International journal of molecular sciences, 2017. **18**(7): p. 1550.
40. Kimmel, C.B., *Genetics and early development of zebrafish.* Trends in Genetics, 1989. **5**: p. 283-288.
41. Howe, K., et al., *The zebrafish reference genome sequence and its relationship to the human genome.* Nature, 2013. **496**(7446): p. 498-503.
42. Van Otterloo, E., et al., *Differentiation of zebrafish melanophores depends on transcription factors AP2 alpha and AP2 epsilon.* PLoS genetics, 2010. **6**(9): p. e1001122.
43. Cooper, C.D., *Insights from zebrafish on human pigment cell disease and treatment.* Developmental dynamics, 2017. **246**(11): p. 889-896.
44. Kimmel, C.B., et al., *Stages of embryonic development of the zebrafish.* Developmental dynamics, 1995. **203**(3): p. 253-310.
45. Kelsh, R.N., et al. *Stripes and belly-spots—a review of pigment cell morphogenesis in vertebrates*. in *Seminars in cell & developmental biology*. 2009. Elsevier.
46. Johnson, S.L., et al., *Genetic control of adult pigment stripe development in zebrafish.* Developmental biology, 1995. **167**(1): p. 27-33.
47. Thomas, A.J. and C.A. Erickson, *The making of a melanocyte: the specification of melanoblasts from the neural crest.* Pigment cell & melanoma research, 2008. **21**(6): p. 598-610.
48. Erickson, C.A. and M.V. Reedy, *5 Neural Crest Development: The Interplay between Morphogenesis and Cell Differentiation.* Current topics in developmental biology, 1998. **40**: p. 177-209.
49. Mayor, R. and E. Theveneau, *The neural crest.* Development, 2013. **140**(11): p. 2247-2251.
50. Meulemans, D. and M. Bronner-Fraser, *Gene-regulatory interactions in neural crest evolution and development.* Developmental cell, 2004. **7**(3): p. 291-299.

51. Cornell, R.A. and J.S. Eisen, *Delta/Notch signaling promotes formation of zebrafish neural crest by repressing Neurogenin 1 function.* 2002.
52. Martik, M.L. and M.E. Bronner, *Regulatory logic underlying diversification of the neural crest.* Trends in Genetics, 2017. **33**(10): p. 715-727.
53. Rocha, M., et al., *Zebrafish Cdx4 regulates neural crest cell specification and migratory behaviors in the posterior body.* Developmental Biology, 2021. **480**: p. 25-38.
54. Rocha, M., et al., *Neural crest development: insights from the zebrafish.* Developmental Dynamics, 2020. **249**(1): p. 88-111.
55. Hultman, K.A. and S.L. Johnson, *Differential contribution of direct-developing and stem cell-derived melanocytes to the zebrafish larval pigment pattern.* Developmental biology, 2010. **337**(2): p. 425-431.
56. Budi, E.H., L.B. Patterson, and D.M. Parichy, *Embryonic requirements for ErbB signaling in neural crest development and adult pigment pattern formation.* 2008.
57. Dooley, C.M., et al., *On the embryonic origin of adult melanophores: the role of ErbB and Kit signalling in establishing melanophore stem cells in zebrafish.* Development, 2013. **140**(5): p. 1003-1013.
58. Budi, E.H., L.B. Patterson, and D.M. Parichy, *Post-embryonic nerve-associated precursors to adult pigment cells: genetic requirements and dynamics of morphogenesis and differentiation.* PLoS genetics, 2011. **7**(5): p. e1002044.
59. Patterson, L.B. and D.M. Parichy, *Zebrafish pigment pattern formation: insights into the development and evolution of adult form.* Annual review of genetics, 2019. **53**: p. 505-530.
60. Kimmel, C.B., et al., *Stages of embryonic development of the zebrafish.* Dev Dyn, 1995. **203**(3): p. 253-310.
61. D'Mello, S.A., et al., *Signaling pathways in melanogenesis.* International journal of molecular sciences, 2016. **17**(7): p. 1144.
62. Serre, C., V. Busuttil, and J.M. Botto, *Intrinsic and extrinsic regulation of human skin melanogenesis and pigmentation.* International journal of cosmetic science, 2018. **40**(4): p. 328-347.
63. Lee, C.S., et al., *Liver X receptor activation inhibits melanogenesis through the acceleration of ERK-mediated MITF degradation.* Journal of Investigative Dermatology, 2013. **133**(4): p. 1063-1071.
64. Yamaguchi, Y. and V.J. Hearing, *Physiological factors that regulate skin pigmentation.* Biofactors, 2009. **35**(2): p. 193-199.
65. Béjar, J., Y. Hong, and M. Schartl, *Mitf expression is sufficient to direct differentiation of medaka blastula derived stem cells to melanocytes.* 2003.
66. Pillaiyar, T., M. Manickam, and S.-H. Jung, *Recent development of signaling pathways inhibitors of melanogenesis.* Cellular signalling, 2017. **40**: p. 99-115.
67. Yamaguchi, Y. and V.J. Hearing, *Melanocyte distribution and function in human skin*, in *From Melanocytes to Melanoma*. 2006, Springer. p. 101-115.
68. Hodgkinson, C.A., et al., *Mutations at the mouse microphthalmia locus are associated with defects in a gene encoding a novel basic-helix-loop-helix-zipper protein.* Cell, 1993. **74**(2): p. 395-404.
69. Weintraub, H., et al., *The myoD gene family: nodal point during specification of the muscle cell lineage.* Science, 1991. **251**(4995): p. 761-766.
70. Price, E.R. and D.E. Fisher, *Sensorineural deafness and pigmentation genes: melanocytes and the Mitf transcriptional network.* Neuron, 2001. **30**(1): p. 15-18.
71. Opdecamp, K., et al., *The rat microphthalmia-associated transcription factor gene (Mitf) maps at 4q34-q41 and is mutated in the mib rats.* Mammalian genome, 1998. **9**(8): p. 617-621.
72. Hodgkinson, C.A., et al., *Mutation at the Anophthalmia White Locus in Syrian Hamsters: Hploinsufficiency in the Mitf Gene Mimics Human Waardenburg Syndrome Type 2.* Human molecular genetics, 1998. **7**(4): p. 703-708.

73. Mochii, M., et al., *Spontaneous transdifferentiation of quail pigmented epithelial cell is accompanied by a mutation in theMitfGene.* Developmental biology, 1998. **196**(2): p. 145-159.
74. Mansouri, A., et al., *Dysgenesis of cephalic neural crest derivatives in Pax7−/− mutant mice.* Development, 1996. **122**(3): p. 831-838.
75. Minchin, J.E. and S.M. Hughes, *Sequential actions of Pax3 and Pax7 drive xanthophore development in zebrafish neural crest.* Developmental biology, 2008. **317**(2): p. 508-522.
76. Elworthy, S., et al., *Transcriptional regulation of mitfa accounts for the sox10 requirement in zebrafish melanophore development.* 2003.
77. Dorsky, R.I., R.T. Moon, and D.W. Raible, *Control of neural crest cell fate by the Wnt signalling pathway.* Nature, 1998. **396**(6709): p. 370-373.
78. Del Marmol, V. and F. Beermann, *Tyrosinase and related proteins in mammalian pigmentation.* FEBS letters, 1996. **381**(3): p. 165-168.
79. Kameyama, K., et al., *Pigment production in murine melanoma cells is regulated by tyrosinase, tyrosinase-related protein 1 (TRP1), DOPAchrome tautomerase (TRP2), and a melanogenic inhibitor.* Journal of Investigative Dermatology, 1993. **100**(2): p. 126-131.
80. Kobayashi, T. and V.J. Hearing, *Direct interaction of tyrosinase with Tyrp1 to form heterodimeric complexes in vivo.* Journal of Cell Science, 2007. **120**(24): p. 4261-4268.
81. Kelsh, R.N. and J.S. Eisen, *The zebrafish colourless gene regulates development of non-ectomesenchymal neural crest derivatives.* Development, 2000. **127**(3): p. 515-525.
82. Camp-Dotlic, E. and M. Lardelli, *Tyrosinase gene expression in zebrafish embryos.* 2001.
83. Hammer, J.A. and X.S. Wu, *Organelle motility: running on unleadened.* Current Biology, 2007. **17**(23): p. R1017-R1019.
84. Sheets, L., et al., *Zebrafish melanophilin facilitates melanosome dispersion by regulating dynein.* Current Biology, 2007. **17**(20): p. 1721-1734.
85. García-Borrón, J.C., B.L. Sánchez-Laorden, and C. Jiménez-Cervantes, *Melanocortin-1 receptor structure and functional regulation.* Pigment cell research, 2005. **18**(6): p. 393-410.
86. Logan, D.W., et al., *The structure and evolution of the melanocortin and MCH receptors in fish and mammals.* Genomics, 2003. **81**(2): p. 184-191.
87. Chhajlani, V. and J.E. Wikberg, *Molecular cloning and expression of the human melanocyte stimulating hormone receptor cDNA.* FEBS letters, 1992. **309**(3): p. 417-420.
88. Logan, D.W., S.F. Burn, and I.J. Jackson, *Regulation of pigmentation in zebrafish melanophores.* Pigment cell research, 2006. **19**(3): p. 206-213.
89. Choi, T.Y., et al., *Zebrafish as a new model for phenotype-based screening of melanogenic regulatory compounds.* Pigment Cell Research, 2007. **20**(2): p. 120-127.
90. McMenamin, S.K., et al., *Thyroid hormone–dependent adult pigment cell lineage and pattern in zebrafish.* Science, 2014. **345**(6202): p. 1358-1361.
91. Shah, M., I.F. Orengo, and T. Rosen, *High prevalence of hypothyroidism in male patients with cutaneous melanoma.* Dermatology Online Journal, 2006. **12**(2).
92. Yamaguchi, Y., M. Brenner, and V.J. Hearing, *The regulation of skin pigmentation.* Journal of biological chemistry, 2007. **282**(38): p. 27557-27561.
93. Aspengren, S., D. Hedberg, and M. Wallin, *Studies of pigment transfer between Xenopus laevis melanophores and fibroblasts in vitro and in vivo 1.* Pigment cell research, 2006. **19**(2): p. 136-145.
94. Le Guellec, D., G. Morvan-Dubois, and J.-Y. Sire, *Skin development in bony fish with particular emphasis on collagen deposition in the dermis of the zebrafish (Danio rerio).* International Journal of Developmental Biology, 2003. **48**(2-3): p. 217-231.
95. Rouzaud, F., et al., *MC1R and the response of melanocytes to ultraviolet radiation.* Mutation Research/Fundamental and Molecular Mechanisms of Mutagenesis, 2005. **571**(1-2): p. 133-152.
96. Jackson, I.J., et al., *Characterization of TRP-1 mRNA levels in dominant and recessive mutations at the mouse brown (b) locus.* Genetics, 1990. **126**(2): p. 451-459.

97. Tsukamoto, K., et al., *A second tyrosinase-related protein, TRP-2, is a melanogenic enzyme termed DOPAchrome tautomerase.* The EMBO journal, 1992. **11**(2): p. 519-526.
98. Kelsh, R.N., B. Schmid, and J.S. Eisen, *Genetic analysis of melanophore development in zebrafish embryos.* Developmental biology, 2000. **225**(2): p. 277-293.
99. Camp, E. and M. Lardelli, *Tyrosinase gene expression in zebrafish embryos.* Development Genes & Evolution, 2001. **211**(3).
100. Steel, K.P., D.R. Davidson, and I. Jackson, *TRP-2/DT, a new early melanoblast marker, shows that steel growth factor (c-kit ligand) is a survival factor.* Development, 1992. **115**(4): p. 1111-1119.
101. Yang, C.-T. and S.L. Johnson, *Small molecule-induced ablation and subsequent regeneration of larval zebrafish melanocytes.* 2006.
102. Milos, N. and A.D. Dingle, *Dynamics of pigment pattern formation in the zebrafish, Brachydanio rerio. I. Establishment and regulation of the lateral line melanophore stripe during the first eight days of development.* Journal of Experimental Zoology, 1978. **205**(2): p. 205-216.
103. Milos, N. and A.D. Dingle, *Dynamics of pigment pattern formation in the zebrafish, Brachydanio rerio. II. Lability of lateral line stripe formation and regulation of pattern defects.* Journal of Experimental Zoology, 1978. **205**(2): p. 217-224.
104. Quigley, I.K. and D.M. Parichy, *Pigment pattern formation in zebrafish: a model for developmental genetics and the evolution of form.* Microscopy research and technique, 2002. **58**(6): p. 442-455.
105. Hisaoka, K.K. and H.I. Battle, *The normal developmental stages of the zebrafish, Brachydanio rerio (Hamilton-Buchanan).* Journal of Morphology, 1958. **102**(2): p. 311-327.
106. Brown, D.D., *The role of thyroid hormone in zebrafish and axolotl development.* Proceedings of the National Academy of Sciences, 1997. **94**(24): p. 13011-13016.
107. Parichy, D.M., et al., *An orthologue of the kit-related gene fms is required for development of neural crest-derived xanthophores and a subpopulation of adult melanocytes in the zebrafish, Danio rerio.* Development, 2000. **127**(14): p. 3031-3044.
108. Parichy, D.M. and J.M. Turner, *Zebrafish puma mutant decouples pigment pattern and somatic metamorphosis.* Developmental biology, 2003. **256**(2): p. 242-257.
109. Patterson, L.B. and D.M. Parichy, *Interactions with iridophores and the tissue environment required for patterning melanophores and xanthophores during zebrafish adult pigment stripe formation.* PLoS genetics, 2013. **9**(5): p. e1003561.
110. Takahashi, G. and S. Kondo, *Melanophores in the stripes of adult zebrafish do not have the nature to gather, but disperse when they have the space to move.* Pigment cell & melanoma research, 2008. **21**(6): p. 677-686.
111. Blum, M. and T. Ott, *Animal left–right asymmetry.* Current Biology, 2018. **28**(7): p. R301-R304.
112. Levin, M., *Left–right asymmetry in embryonic development: a comprehensive review.* Mechanisms of development, 2005. **122**(1): p. 3-25.
113. Hyatt, B.A., J.L. Lohr, and H.J. Yost, *Initiation of vertebrate left–right axis formation by maternal Vg1.* Nature, 1996. **384**(6604): p. 62-65.
114. Sturtevant, A.H., *Inheritance of direction of coiling in Limnaea.* Science, 1923. **58**(1501): p. 269-270.
115. Hachisuga, M., et al., *Hyperglycemia impairs left–right axis formation and thereby disturbs heart morphogenesis in mouse embryos.* Proceedings of the National Academy of Sciences, 2015. **112**(38): p. E5300-E5307.
116. Ma, L., et al., *Maternal control of visceral asymmetry evolution in Astyanax cavefish.* Scientific reports, 2021. **11**(1): p. 1-14.
117. Chen, J.N., et al., *Genetic steps to organ laterality in zebrafish.* Comparative and functional genomics, 2001. **2**(2): p. 60-68.

118. Tan, S.Y., et al., *Heterotaxy and complex structural heart defects in a mutant mouse model of primary ciliary dyskinesia.* The Journal of clinical investigation, 2007. **117**(12): p. 3742-3752.
119. Pai, V.P., et al., *Neurally derived tissues in Xenopus laevis embryos exhibit a consistent bioelectrical left-right asymmetry.* Stem cells international, 2012. **2012**.
120. Laddha, U., H. Mahajan, and R. Patel, *An insight to ocular in situ gelling systems.* Int J Adv Pharm, 2017. **6**(02): p. 31-40.
121. Babich, R. and R.J. Van Beneden, *Effect of arsenic exposure on early eye development in zebrafish (Danio rerio).* Journal of Applied Toxicology, 2019. **39**(6): p. 824-831.
122. Gestri, G., B.A. Link, and S.C. Neuhauss, *The visual system of zebrafish and its use to model human ocular diseases.* Developmental neurobiology, 2012. **72**(3): p. 302-327.
123. Loosli, F., S. Winkler, and J. Wittbrodt, *Six3 overexpression initiates the formation of ectopic retina.* Genes & development, 1999. **13**(6): p. 649-654.
124. Nornes, S., et al., *Zebrafish contains two pax6 genes involved in eye development.* Mechanisms of development, 1998. **77**(2): p. 185-196.
125. Malicki, J., et al., *Mutations affecting development of the zebrafish retina.* Development, 1996. **123**(1): p. 263-273.
126. Neuhauss, S.C., *Zebrafish vision: structure and function of the zebrafish visual system*, in *Fish Physiology*. 2010, Elsevier. p. 81-122.
127. Richardson, R., et al., *The zebrafish eye—a paradigm for investigating human ocular genetics.* Eye, 2017. **31**(1): p. 68-86.
128. Chhetri, J., G. Jacobson, and N. Gueven, *Zebrafish—on the move towards ophthalmological research.* Eye, 2014. **28**(4): p. 367-380.
129. Levin, L.A. and D.M. Albert, *Ocular Disease: Mechanisms and Management E-Book*. 2010: Elsevier Health Sciences.
130. Strauss, O., *The retinal pigment epithelium in visual function.* Physiological reviews, 2005. **85**(3): p. 845-881.
131. Różanowska, M., et al., *Free radical scavenging properties of melanin: interaction of eu-and pheo-melanin models with reducing and oxidising radicals.* Free Radical Biology and Medicine, 1999. **26**(5-6): p. 518-525.
132. Pane, A.R. and L.W. Hirst, *Ultraviolet light exposure as a risk factor for ocular melanoma in Queensland, Australia.* Ophthalmic epidemiology, 2000. **7**(3): p. 159-167.
133. Sarna, T., *New trends in photobiology: properties and function of the ocular melanin—a photobiophysical view.* Journal of Photochemistry and Photobiology B: Biology, 1992. **12**(3): p. 215-258.
134. Nadler, Z., et al., *Clinical application of ocular imaging.* Optometry and Vision Science, 2012. **89**(5): p. E543.
135. Ilginis, T., J. Clarke, and P.J. Patel, *Ophthalmic imaging.* British medical bulletin, 2014. **111**(1).
136. Ernfors, P., *Cellular origin and developmental mechanisms during the formation of skin melanocytes.* Experimental cell research, 2010. **316**(8): p. 1397-1407.
137. O'Rahilly, R. and F. Müller, *The development of the neural crest in the human.* Journal of anatomy, 2007. **211**(3): p. 335-351.
138. Miot, L.D.B., et al., *Physiopathology of melasma.* Anais brasileiros de dermatologia, 2009. **84**: p. 623-635.
139. Roberts, D.S. and F.H. Linthicum Jr, *Distribution of melanocytes in the human cochlea.* Otology & neurotology: official publication of the American Otological Society, American Neurotology Society [and] European Academy of Otology and Neurotology, 2015. **36**(3): p. e99.
140. Haschek, W.M., et al., *Haschek and Rousseaux's handbook of toxicologic pathology*. 2013: Academic Press.
141. FITZPATRICK, T.B., *The epidermal melanin unit system.* Dermatol. Wochenschr., 1963. **147**: p. 481-489.

142. Plonka, P.M., et al., *What are melanocytes really doing all day long…?* Experimental dermatology, 2009. **18**(9): p. 799-819.
143. Haass, N.K. and M. Herlyn. *Normal human melanocyte homeostasis as a paradigm for understanding melanoma*. in *Journal of Investigative Dermatology Symposium Proceedings*. 2005. Elsevier.
144. Lee, A.-Y., *Role of keratinocytes in the development of vitiligo.* Annals of dermatology, 2012. **24**(2): p. 115-125.
145. Sulaimon, S.S. and B.E. Kitchell, *The biology of melanocytes.* Veterinary dermatology, 2003. **14**(2): p. 57-65.
146. Costin, G.-E. and V.J. Hearing, *Human skin pigmentation: melanocytes modulate skin color in response to stress.* The FASEB journal, 2007. **21**(4): p. 976-994.
147. Choi, W., L. Kolbe, and V.J. Hearing, *Characterization of the bioactive motif of neuregulin-1, a fibroblast-derived paracrine factor that regulates the constitutive color and the function of melanocytes in human skin.* Pigment cell & melanoma research, 2012. **25**(4): p. 477-481.
148. Slominski, A., et al., *Melanin pigmentation in mammalian skin and its hormonal regulation.* Physiological reviews, 2004. **84**(4): p. 1155-1228.
149. Ito, S. and K. Wakamatsu, *Diversity of human hair pigmentation as studied by chemical analysis of eumelanin and pheomelanin.* Journal of the European Academy of Dermatology and Venereology, 2011. **25**(12): p. 1369-1380.
150. Abdel-Malek, Z.A., A.L. Kadekaro, and V.B. Swope, *Stepping up melanocytes to the challenge of UV exposure.* Pigment cell & melanoma research, 2010. **23**(2): p. 171-186.
151. Hearing, V.J., *Determination of melanin synthetic pathways.* The Journal of investigative dermatology, 2011. **131**(E1): p. E8.
152. Schiaffino, M.V., *Signaling pathways in melanosome biogenesis and pathology.* The international journal of biochemistry & cell biology, 2010. **42**(7): p. 1094-1104.
153. Le Douarin, N.M., et al., *Neural crest cell plasticity and its limits.* 2004.
154. Cramer, S., *The histogenesis of acquired melanocytic nevi. Based on a new concept of melanocytic differentiation.* The American Journal of dermatopathology, 1984. **6**: p. 289-298.
155. Cramer, S.F. and A. Fesyuk, *On the development of neurocutaneous units—implications for the histogenesis of congenital, acquired, and dysplastic nevi.* The American Journal of dermatopathology, 2012. **34**(1): p. 60-81.
156. Aoki, H., et al., *Two distinct types of mouse melanocyte: differential signaling requirement for the maintenance of non-cutaneous and dermal versus epidermal melanocytes.* 2009.
157. Gleason, B.C., C.P. Crum, and G.F. Murphy, *Expression patterns of MITF during human cutaneous embryogenesis: evidence for bulge epithelial expression and persistence of dermal melanoblasts.* Journal of cutaneous pathology, 2008. **35**(7): p. 615-622.
158. Nishimura, E.K., *Melanocyte stem cells: a melanocyte reservoir in hair follicles for hair and skin pigmentation.* Pigment cell & melanoma research, 2011. **24**(3): p. 401-410.
159. Betters, E., et al., *Analysis of early human neural crest development.* Developmental biology, 2010. **344**(2): p. 578-592.
160. Vance, K.W. and C.R. Goding, *The transcription network regulating melanocyte development and melanoma.* Pigment cell research, 2004. **17**(4): p. 318-325.
161. Hirobe, T., *How are proliferation and differentiation of melanocytes regulated?* Pigment cell & melanoma research, 2011. **24**(3): p. 462-478.
162. Dupin, E. and L. Sommer, *Neural crest progenitors and stem cells: from early development to adulthood.* Developmental biology, 2012. **366**(1): p. 83-95.
163. McCullough, J.L. and K.M. Kelly, *Prevention and treatment of skin aging.* Annals of the New York Academy of Sciences, 2006. **1067**(1): p. 323-331.
164. Baxter, L.L. and W.J. Pavan, *The etiology and molecular genetics of human pigmentation disorders.* Wiley Interdisciplinary Reviews: Developmental Biology, 2013. **2**(3): p. 379-392.

165. Duval, C., et al., *Key regulatory role of dermal fibroblasts in pigmentation as demonstrated using a reconstructed skin model: impact of photo-aging.* PLoS One, 2014. **9**(12): p. e114182.
166. Sturm, R.A., *Molecular genetics of human pigmentation diversity.* Human molecular genetics, 2009. **18**(R1): p. R9-R17.
167. Spritz, R.A., *Molecular basis of human piebaldism.* Journal of investigative dermatology, 1994. **103**.
168. Sánchez-Martín, M., et al., *SLUG (SNAI2) deletions in patients with Waardenburg disease.* Human molecular genetics, 2002. **11**(25): p. 3231-3236.
169. Hennekam, R.C. and R.J. Gorlin, *Confirmation of the Yemenite (Warburg) deaf-blind hypopigmentation syndrome.* American journal of medical genetics, 1996. **65**(2): p. 146-148.
170. Bondurand, N., et al., *A molecular analysis of the yemenite deaf-blind hypopigmentation syndrome: SOX10 dysfunction causes different neurocristopathies.* Human Molecular Genetics, 1999. **8**(9): p. 1785-1789.
171. Ko, H. and M.-M. Kim, *H2O2 promotes the aging process of melanogenesis through modulation of MITF and Nrf2.* Molecular biology reports, 2019. **46**(2): p. 2461-2471.
172. Selvaraj, V., et al., *Computational analysis of deleterious SNPs of SLC45A2 involved in oculocutaneous albinism type 4.* Gene Reports, 2018. **12**: p. 248-254.
173. Oetting, W.S., *The tyrosinase gene and oculocutaneous albinism type 1 (OCA1): a model for understanding the molecular biology of melanin formation.* Pigment cell research, 2000. **13**(5): p. 320-325.
174. Montoliu, L., et al., *Increasing the complexity: new genes and new types of albinism.* Pigment cell & melanoma research, 2014. **27**(1): p. 11-18.
175. Dell'Angelica, E.C., *The building BLOC (k) s of lysosomes and related organelles.* Current opinion in cell biology, 2004. **16**(4): p. 458-464.
176. Li, W., et al., *Murine Hermansky–Pudlak syndrome genes: regulators of lysosome-related organelles.* Bioessays, 2004. **26**(6): p. 616-628.
177. Amyere, M., et al., *KITLG mutations cause familial progressive hyper-and hypopigmentation.* Journal of investigative dermatology, 2011. **131**(6): p. 1234-1239.
178. Malaquias, A.C. and A.A. Jorge, *Developmental Syndromes of Ras/MAPK Pathway Dysregulation.* eLS.
179. Pérez, B., et al., *Germline mutations of the CBL gene define a new genetic syndrome with predisposition to juvenile myelomonocytic leukaemia.* Journal of medical genetics, 2010. **47**(10): p. 686-691.
180. De Jager, T., A. Cockrell, and S. Du Plessis, *Ultraviolet light induced generation of reactive oxygen species.* Ultraviolet Light in Human Health, Diseases and Environment, 2017: p. 15-23.
181. Zhang, X., et al., *Identification of possible reactive oxygen species involved in ultraviolet radiation-induced oxidative DNA damage.* Free Radical Biology and Medicine, 1997. **23**(7): p. 980-985.
182. Trouba, K.J., et al., *Oxidative stress and its role in skin disease.* Antioxidants and Redox Signaling, 2002. **4**(4): p. 665-673.
183. Shen, J., et al., *Mitochondrial DNA 4977-base pair common deletion in blood leukocytes and melanoma risk.* Pigment cell & melanoma research, 2016. **29**(3): p. 372-378.
184. Gu, Y., et al., *Biomarkers, oxidative stress and autophagy in skin aging.* Ageing research reviews, 2020. **59**: p. 101036.
185. Rodboon, T., S. Okada, and P. Suwannalert, *Germinated riceberry rice enhanced protocatechuic acid and vanillic acid to suppress melanogenesis through cellular oxidant-related tyrosinase activity in B16 cells.* Antioxidants, 2020. **9**(3): p. 247.
186. Temple, I., et al., *De novo deletion of Xp22. 2-pter in a female with linear skin lesions of the face and neck, microphthalmia, and anterior chamber eye anomalies.* Journal of medical genetics, 1990. **27**(1): p. 56-58.

187. Ashapkin, V.V., et al., *Are there common mechanisms between the Hutchinson–Gilford progeria syndrome and natural aging?* Frontiers in genetics, 2019. **10**: p. 455.
188. Lu, L., W. Jin, and L.L. Wang, *Aging in Rothmund-Thomson syndrome and related RECQL4 genetic disorders.* Ageing research reviews, 2017. **33**: p. 30-35.
189. Che, R., et al., *Multifaceted Fanconi anemia signaling.* Trends in Genetics, 2018. **34**(3): p. 171-183.
190. Mangaonkar, A.A. and M.M. Patnaik. *Short telomere syndromes in clinical practice: bridging bench and bedside*. in *Mayo Clinic Proceedings*. 2018. Elsevier.
191. Opresko, P.L. and J.W. Shay, *Telomere-associated aging disorders.* Ageing research reviews, 2017. **33**: p. 52-66.
192. Ruggiero, J.L., et al., *Cutaneous findings in Fanconi anemia.* Journal of the American Academy of Dermatology, 2021. **85**(5): p. 1253-1258.
193. Paolino, G., P. Bearzi, and S.R. Mercuri, *Onset of vitiligo in a patient with acquired secondary hypogonadism under treatment with testosterone gel 2%: inside the pathogenesis.* Anais brasileiros de dermatologia, 2020. **95**: p. 661-662.
194. Goh, C. and C. Dlova, *A retrospective study on the clinical presentation and treatment outcome of melasma in a tertiary dermatological referral centre in Singapore.* Singapore medical journal, 1999. **40**(7): p. 455-458.
195. Robins, A.H., *Skin melanin concentrations in schizophrenia.* The British Journal of Psychiatry, 1972. **121**(565): p. 613-617.
196. Lapeere, H., et al., *Hypomelanoses and hypermelanoses*, in *Fitzpatrick's dermatology in general medicine*. 2012, Mc Graw Hill Medical. p. 804-826.
197. Lennartsson, J., et al., *Phosphorylation of Shc by Src family kinases is necessary for stem cell factor receptor/c-kit mediated activation of the Ras/MAP kinase pathway and c-fos induction.* Oncogene, 1999. **18**(40): p. 5546-5553.
198. Molokhia, M.M. and B. Portnoy, *Trace elements and skin pigmentation.* British Journal of Dermatology, 1973. **89**(2): p. 207-209.
199. Gilchrest, B.A., et al., *Mechanisms of ultraviolet light-induced pigmentation.* Photochemistry and photobiology, 1996. **63**(1): p. 1-10.
200. Hoyme, H.E., et al., *A practical clinical approach to diagnosis of fetal alcohol spectrum disorders: clarification of the 1996 institute of medicine criteria.* Pediatrics, 2005. **115**(1): p. 39-47.
201. Ouko, L.A., et al., *Effect of alcohol consumption on CpG methylation in the differentially methylated regions of H19 and IG-DMR in male gametes—Implications for fetal alcohol spectrum disorders.* Alcoholism: Clinical and Experimental Research, 2009. **33**(9): p. 1615-1627.
202. Eaton, B., D. Gangluff, and M. Mengel, *Fetal alcohol spectrum disorders: flying under the radar.* The Journal of the Arkansas Medical Society, 2011. **107**(12): p. 260-262.
203. Gupta, K.K., V.K. Gupta, and T. Shirasaka, *An Update on Fetal Alcohol Syndrome-Pathogenesis, Risks, and Treatment.* Alcohol Clin Exp Res, 2016. **40**(8): p. 1594-602.
204. Maier, S.E. and J.R. West, *Drinking patterns and alcohol-related birth defects.* Alcohol research & health : the journal of the National Institute on Alcohol Abuse and Alcoholism, 2001. **25**(3): p. 168-174.
205. Reik, W., W. Dean, and J. Walter, *Epigenetic reprogramming in mammalian development.* Science, 2001. **293**(5532): p. 1089-1093.
206. Pal-Bhadra, M., et al., *Distinct methylation patterns in histone H3 at Lys-4 and Lys-9 correlate with up-& down-regulation of genes by ethanol in hepatocytes.* Life sciences, 2007. **81**(12): p. 979-987.
207. Sathyan, P., H.B. Golden, and R.C. Miranda, *Competing interactions between micro-RNAs determine neural progenitor survival and proliferation after ethanol exposure: evidence from*

an ex vivo model of the fetal cerebral cortical neuroepithelium. Journal of Neuroscience, 2007. **27**(32): p. 8546-8557.
208. de la Monte, S.M. and J.R. Wands, *Role of central nervous system insulin resistance in fetal alcohol spectrum disorders.* Journal of population therapeutics and clinical pharmacology= Journal de la therapeutique des populations et de la pharamcologie clinique, 2010. **17**(3): p. e390.
209. Haron, M.H., et al., *Feasibility of medaka (Oryzias latipes) as an animal model to study fetal alcohol spectrum disorder*, in *Advances in Molecular Toxicology*. 2012, Elsevier. p. 77-128.
210. Ramanathan, R., et al., *Alcohol inhibits cell-cell adhesion mediated by human L1.* Journal of Cell Biology, 1996. **133**(2): p. 381-390.
211. Minana, R., et al., *Alcohol exposure alters the expression pattern of neural cell adhesion molecules during brain development.* Journal of neurochemistry, 2000. **75**(3): p. 954-964.
212. Cohen-Kerem, R. and G. Koren, *Antioxidants and fetal protection against ethanol teratogenicity: I. Review of the experimental data and implications to humans.* Neurotoxicology and teratology, 2003. **25**(1): p. 1-9.
213. Gemma, S., S. Vichi, and E. Testai, *Metabolic and genetic factors contributing to alcohol induced effects and fetal alcohol syndrome.* Neuroscience & Biobehavioral Reviews, 2007. **31**(2): p. 221-229.
214. Strömland, K., *Visual impairment and ocular abnormalities in children with fetal alcohol syndrome.* Addiction biology, 2004. **9**(2): p. 153-157.
215. Strömland, K., *Ocular involvement in the fetal alcohol syndrome.* Survey of ophthalmology, 1987. **31**(4): p. 277-284.
216. Fu, J., et al., *Effects of Embryonic Exposure to Ethanol on Zebrafish Survival, Growth Pattern, Locomotor Activity and Retinal Development.* Alternative Therapies in Health and Medicine, 2021. **27**(5): p. 120-128.
217. Eason, J., et al., *Differences in neural crest sensitivity to ethanol account for the infrequency of anterior segment defects in the eye compared with craniofacial anomalies in a zebrafish model of fetal alcohol syndrome.* Birth defects research, 2017. **109**(15): p. 1212-1227.
218. Muralidharan, P., S. Sarmah, and J.A. Marrs, *Zebrafish retinal defects induced by ethanol exposure are rescued by retinoic acid and folic acid supplement.* Alcohol, 2015. **49**(2): p. 149-163.
219. WALTMAN, R. and E.S. INIQUEZ, *Placental transfer of ethanol and its elimination at term.* Obstetrics & Gynecology, 1972. **40**(2): p. 180-185.
220. Pizon, A.F., C.E. Becker, and D. Bikin, *The clinical significance of variations in ethanol toxicokinetics.* Journal of Medical Toxicology, 2007. **3**(2): p. 63-72.
221. Jelski, W. and M. Szmitkowski, *Alcohol dehydrogenase (ADH) and aldehyde dehydrogenase (ALDH) in the cancer diseases.* Clinica chimica acta, 2008. **395**(1-2): p. 1-5.
222. Lieber, C.S. and L.M. DeCarli, *Hepatic microsomal ethanol-oxidizing system: in vitro characteristics and adaptive properties in vivo.* Journal of Biological Chemistry, 1970. **245**(10): p. 2505-2512.
223. Hakkola, J., et al., *Xenobiotic-metabolizing cytochrome P450 enzymes in the human feto-placental unit: role in intrauterine toxicity.* Critical reviews in toxicology, 1998. **28**(1): p. 35-72.
224. Carpenter, S.P., J.M. Lasker, and J.L. Raucy, *Expression, induction, and catalytic activity of the ethanol-inducible cytochrome P450 (CYP2E1) in human fetal liver and hepatocytes.* Molecular pharmacology, 1996. **49**(2): p. 260-268.
225. Modena, A.B. and S. Fieni, *Amniotic fluid dynamics.* Acta bio-medica: Atenei Parmensis, 2004. **75**: p. 11-13.
226. Brien, J.F., et al., *Disposition of ethanol in human maternal venous blood and amniotic fluid.* American journal of obstetrics and gynecology, 1983. **146**(2): p. 181-186.
227. Clevers, H., *Wnt/β-catenin signaling in development and disease.* Cell, 2006. **127**(3): p. 469-480.

228. van Amerongen, R. and R. Nusse, *Towards an integrated view of Wnt signaling in development.* Development, 2009. **136**(19): p. 3205-3214.
229. Angers, S. and R.T. Moon, *Proximal events in Wnt signal transduction.* Nature reviews Molecular cell biology, 2009. **10**(7): p. 468-477.
230. Ruzicka, L., et al., *The Zebrafish Information Network: new support for non-coding genes, richer Gene Ontology annotations and the Alliance of Genome Resources.* Nucleic acids research, 2019. **47**(D1): p. D867-D873.
231. Bilic, J., et al., *Wnt induces LRP6 signalosomes and promotes dishevelled-dependent LRP6 phosphorylation.* Science, 2007. **316**(5831): p. 1619-1622.
232. Huelsken, J. and J. Behrens, *The Wnt signalling pathway.* Journal of cell science, 2002. **115**(21): p. 3977-3978.
233. Zeng, X., et al., *A dual-kinase mechanism for Wnt co-receptor phosphorylation and activation.* Nature, 2005. **438**(7069): p. 873-877.
234. Zeng, X., et al., *Initiation of Wnt signaling: control of Wnt coreceptor Lrp6 phosphorylation/activation via frizzled, dishevelled and axin functions.* 2008.
235. Li, V.S., et al., *Wnt signaling through inhibition of β-catenin degradation in an intact Axin1 complex.* Cell, 2012. **149**(6): p. 1245-1256.
236. Voronkov, A. and S. Krauss, *Wnt/beta-catenin signaling and small molecule inhibitors.* Current pharmaceutical design, 2013. **19**(4): p. 634-664.
237. MacDonald, B.T., K. Tamai, and X. He, *Wnt/β-catenin signaling: components, mechanisms, and diseases.* Developmental cell, 2009. **17**(1): p. 9-26.
238. Leal, L.F., et al., *Inhibition of the Tcf/beta-catenin complex increases apoptosis and impairs adrenocortical tumor cell proliferation and adrenal steroidogenesis.* Oncotarget, 2015. **6**(40): p. 43016.
239. Henderson Jr, W.R., et al., *Inhibition of Wnt/β-catenin/CREB binding protein (CBP) signaling reverses pulmonary fibrosis.* Proceedings of the National Academy of Sciences, 2010. **107**(32): p. 14309-14314.
240. Shan, J., et al., *Identification of a specific inhibitor of the dishevelled PDZ domain.* Biochemistry, 2005. **44**(47): p. 15495-15503.
241. Zhang, X., et al., *Wnt blockers inhibit the proliferation of lung cancer stem cells.* Drug design, development and therapy, 2015. **9**: p. 2399.
242. Kim, Y.-M. and M. Kahn, *The role of the Wnt signaling pathway in cancer stem cells: prospects for drug development.* Research and reports in biochemistry, 2014. **4**: p. 1.
243. Wang, X., et al., *The development of highly potent inhibitors for porcupine.* Journal of medicinal chemistry, 2013. **56**(6): p. 2700-2704.
244. Galli, C., et al., *GSK 3b-inhibitor lithium chloride enhances activation of Wnt canonical signaling and osteoblast differentiation on hydrophilic titanium surfaces.* Clinical oral implants research, 2013. **24**(8): p. 921-927.
245. Madan, B., et al., *Experimental inhibition of porcupine-mediated Wnt O-acylation attenuates kidney fibrosis.* Kidney international, 2016. **89**(5): p. 1062-1074.
246. Dorsky, R.I., D.W. Raible, and R.T. Moon, *Direct regulation of nacre, a zebrafish MITF homolog required for pigment cell formation, by the Wnt pathway.* Genes & development, 2000. **14**(2): p. 158-162.
247. Jin, E.-J., et al., *Wnt and BMP signaling govern lineage segregation of melanocytes in the avian embryo.* Developmental biology, 2001. **233**(1): p. 22-37.
248. Steingrímsson, E., N.G. Copeland, and N.A. Jenkins, *Melanocytes and the microphthalmia transcription factor network.* Annu. Rev. Genet., 2004. **38**: p. 365-411.
249. Takeda, K., et al., *Induction of melanocyte-specific microphthalmia-associated transcription factor by Wnt-3a.* Journal of Biological Chemistry, 2000. **275**(19): p. 14013-14016.

250. Widlund, H.R., et al., *β-Catenin–induced melanoma growth requires the downstream target Microphthalmia-associated transcription factor.* The Journal of cell biology, 2002. **158**(6): p. 1079-1087.
251. Yamaguchi, Y., et al., *The effects of dickkopf 1 on gene expression and Wnt signaling by melanocytes: mechanisms underlying its suppression of melanocyte function and proliferation.* Journal of Investigative Dermatology, 2007. **127**(5): p. 1217-1225.
252. Li, Y., et al., *Dkk1 stabilizes Wnt co-receptor LRP6: implication for Wnt ligand-induced LRP6 down-regulation.* PLoS One, 2010. **5**(6): p. e11014.
253. Guillot, R., et al., *Thyroid hormones regulate zebrafish melanogenesis in a gender-specific manner.* PloS one, 2016. **11**(11): p. e0166152.
254. Eum, J., et al., *3D visualization of developmental toxicity of 2, 4, 6-trinitrotoluene in zebrafish embryogenesis using light-sheet microscopy.* International journal of molecular sciences, 2016. **17**(11): p. 1925.
255. Smith, S.M., et al., *Neural crest development in fetal alcohol syndrome.* Birth Defects Research Part C: Embryo Today: Reviews, 2014. **102**(3): p. 210-220.
256. Sulik, K.K. *Critical periods for alcohol teratogenesis in mice, with special reference to the gastrulation stage of embryogenesis*. in *Ciba Foundation Symposium*. 1984.
257. Kotch, L.E. and K.K. Sulik, *Experimental fetal alcohol syndrome: proposed pathogenic basis for a variety of associated facial and brain anomalies.* American journal of medical genetics, 1992. **44**(2): p. 168-176.
258. Jiang, Y.-J., et al., *Mutations affecting neurogenesis and brain morphology in the zebrafish, Danio rerio.* Development, 1996. **123**(1): p. 205-216.
259. Buske, C. and R. Gerlai, *Early embryonic ethanol exposure impairs shoaling and the dopaminergic and serotoninergic systems in adult zebrafish.* Neurotoxicology and teratology, 2011. **33**(6): p. 698-707.
260. Buckley, D.M., et al., *Differentially sensitive neuronal subpopulations in the central nervous system and the formation of hindbrain heterotopias in ethanol-exposed zebrafish.* Birth defects research, 2019. **111**(12): p. 700-713.
261. Flentke, G.R., et al., *Calcium-mediated repression of β-catenin and its transcriptional signaling mediates neural crest cell death in an avian model of fetal alcohol syndrome.* Birth Defects Research Part A: Clinical and Molecular Teratology, 2011. **91**(7): p. 591-602.
262. Flentke, G.R., et al., *An evolutionarily conserved mechanism of calcium-dependent neurotoxicity in a zebrafish model of fetal alcohol spectrum disorders.* Alcoholism: Clinical and Experimental Research, 2014. **38**(5): p. 1255-1265.
263. Czarnobaj, J., et al., *The different effects on cranial and trunk neural crest cell behaviour following exposure to a low concentration of alcohol in vitro.* Archives of oral biology, 2014. **59**(5): p. 500-512.
264. Rovasio, R.A. and N.L. Battiato, *Ethanol induces morphological and dynamic changes on in vivo and in vitro neural crest cells.* Alcoholism: Clinical and Experimental Research, 2002. **26**(8): p. 1286-1298.
265. Dunty Jr, W.C., et al., *Selective vulnerability of embryonic cell populations to ethanol-induced apoptosis: implications for alcohol-related birth defects and neurodevelopmental disorder.* Alcoholism: Clinical and Experimental Research, 2001. **25**(10): p. 1523-1535.
266. Debelak-Kragtorp, K.A., D. Randall Armant, and S.M. Smith, *Ethanol-induced cephalic apoptosis requires phospholipase C-dependent intracellular calcium signaling.* Alcoholism: Clinical and Experimental Research, 2003. **27**(3): p. 515-523.
267. Garic-Stankovic, A., et al., *Ethanol Triggers Neural Crest Apoptosis through the Selective Activation of a Pertussis Toxin–Sensitive G Protein and a Phospholipase Cβ–Dependent Ca2+ Transient.* Alcoholism: Clinical and Experimental Research, 2005. **29**(7): p. 1237-1246.

268. Flentke, G.R., et al., *CaMKII represses transcriptionally active β-catenin to mediate acute ethanol neurodegeneration and can phosphorylate β-catenin.* Journal of neurochemistry, 2014. **128**(4): p. 523-535.
269. Lister, J.A., et al., *Nacre encodes a zebrafish microphthalmia-related protein that regulates neural-crest-derived pigment cell fate.* Development, 1999. **126**(17): p. 3757-3767.
270. Watanabe, K.i., et al., *Identification of a distal enhancer for the melanocyte-specific promoter of the MITF gene.* Pigment cell research, 2002. **15**(3): p. 201-211.
271. Cheli, Y., et al., *Fifteen-year quest for microphthalmia-associated transcription factor target genes.* Pigment cell & melanoma research, 2010. **23**(1): p. 27-40.
272. Levy, C., M. Khaled, and D.E. Fisher, *MITF: master regulator of melanocyte development and melanoma oncogene.* Trends in molecular medicine, 2006. **12**(9): p. 406-414.
273. Hari, L., et al., *Temporal control of neural crest lineage generation by Wnt/β-catenin signaling.* Development, 2012. **139**(12): p. 2107-2117.
274. Lee, H.-Y., et al., *Instructive role of Wnt/ß-catenin in sensory fate specification in neural crest stem cells.* Science, 2004. **303**(5660): p. 1020-1023.
275. Bellei, B., et al., *GSK3β inhibition promotes melanogenesis in mouse B16 melanoma cells and normal human melanocytes.* Cellular signalling, 2008. **20**(10): p. 1750-1761.
276. Alexander, C., et al., *Wnt signaling interacts with bmp and edn1 to regulate dorsal-ventral patterning and growth of the craniofacial skeleton.* PLoS Genetics, 2014. **10**(7): p. e1004479.
277. Moro, E., et al., *In vivo Wnt signaling tracing through a transgenic biosensor fish reveals novel activity domains.* Developmental biology, 2012. **366**(2): p. 327-340.
278. Vibert, L., et al., *An ongoing role for Wnt signaling in differentiating melanocytes in vivo.* Pigment cell & melanoma research, 2017. **30**(2): p. 219-232.
279. Jin, E.-J. and G. Thibaudeau, *Effects of lithium on pigmentation in the embryonic zebrafish (Brachydanio rerio).* Biochimica et Biophysica Acta (BBA)-Molecular Cell Research, 1999. **1449**(1): p. 93-99.
280. Cheng, Y., et al., *Wnt-C59 arrests stemness and suppresses growth of nasopharyngeal carcinoma in mice by inhibiting the Wnt pathway in the tumor microenvironment.* Oncotarget, 2015. **6**(16): p. 14428.
281. Dey, N., et al., *Wnt signaling in triple negative breast cancer is associated with metastasis.* BMC cancer, 2013. **13**(1): p. 1-15.
282. Cichorek, M., M. Wachulska, and A. Stasiewicz, *Heterogeneity of neural crest-derived melanocytes.* Open Life Sciences, 2013. **8**(4): p. 315-330.
283. Parr, B.A., et al., *Mouse Wnt genes exhibit discrete domains of expression in the early embryonic CNS and limb buds.* Development, 1993. **119**(1): p. 247-261.
284. DorskyRI, M., *RaibleDW (1998).* Control of neural crest cell fate by the Wnt signalling pathway. Nature. **396**: p. 370-373.
285. Nitzan, E., et al., *A dynamic code of dorsal neural tube genes regulates the segregation between neurogenic and melanogenic neural crest cells.* Development, 2013. **140**(11): p. 2269-2279.
286. Rawls, J.F. and S.L. Johnson, *Zebrafish kit mutation reveals primary and secondary regulation of melanocyte development during fin stripe regeneration.* Development, 2000. **127**(17): p. 3715-3724.
287. Richardson, J., et al., *mc1r Pathway regulation of zebrafish melanosome dispersion.* Zebrafish, 2008. **5**(4): p. 289-295.
288. Sugimoto, M., *Morphological color changes in fish: regulation of pigment cell density and morphology.* Microscopy research and technique, 2002. **58**(6): p. 496-503.
289. Nakatsuji, N., *Craniofacial malformation in Xenopus laevis tadpoles caused by the exposure of early embryos to ethanol.* Teratology, 1983. **28**(2): p. 299-305.
290. Baumann, M. and K. Sander, *Bipartite axiation follows incomplete epiboly in zebrafish embryos treated with chemical teratogens.* Journal of Experimental Zoology, 1984. **230**(3): p. 363-376.

291. Hallare, A., et al., *Comparative embryotoxicity and proteotoxicity of three carrier solvents to zebrafish (Danio rerio) embryos.* Ecotoxicology and environmental safety, 2006. **63**(3): p. 378-388.
292. Lockwood, B., et al., *Acute effects of alcohol on larval zebrafish: a genetic system for large-scale screening.* Pharmacology Biochemistry and Behavior, 2004. **77**(3): p. 647-654.
293. Schilling, T.F., et al., *Jaw and branchial arch mutants in zebrafish I: branchial arches.* Development, 1996. **123**(1): p. 329-344.
294. Halpern, M.E., et al., *Induction of muscle pioneers and floor plate is distinguished by the zebrafish no tail mutation.* Cell, 1993. **75**(1): p. 99-111.
295. Odenthal, J., et al., *Mutations affecting the formation of the notochord in the zebrafish, Danio rerio.* Development, 1996. **123**(1): p. 103-115.
296. Theveneau, E. and R. Mayor, *Neural crest delamination and migration: from epithelium-to-mesenchyme transition to collective cell migration.* Developmental biology, 2012. **366**(1): p. 34-54.
297. Sutton, G., R.N. Kelsh, and S. Scholpp, *The Role of Wnt/β-Catenin Signalling in Neural Crest Development in Zebrafish.* Frontiers in Cell and Developmental Biology, 2021: p. 3450.
298. Dickinson, M.E., et al., *Dorsalization of the neural tube by the non-neural ectoderm.* Development, 1995. **121**(7): p. 2099-2106.
299. Ikeya, M., et al., *Wnt signalling required for expansion of neural crest and CNS progenitors.* Nature, 1997. **389**(6654): p. 966-970.
300. Serbedzija, G.N. and A.P. McMahon, *Analysis of neural crest cell migration in Splotch mice using a neural crest-specific LacZ reporter.* Developmental biology, 1997. **185**(2): p. 139-147.
301. Borchers, A., R. David, and D. Wedlich, *Xenopus cadherin-11 restrains cranial neural crest migration and influences neural crest specification.* 2001.
302. Tada, M. and J. Smith, *Xwnt11 is a target of Xenopus Brachyury: regulation of gastrulation movements via Dishevelled, but not through the canonical Wnt pathway.* Development, 2000. **127**(10): p. 2227-2238.
303. Schambony, A. and D. Wedlich, *Wnt signaling and cell migration*, in *Madame Curie Bioscience Database [Internet]*. 2013, Landes Bioscience.
304. Camargo-Sosa, K., et al., *Endothelin receptor Aa regulates proliferation and differentiation of Erb-dependent pigment progenitors in zebrafish.* PLoS genetics, 2019. **15**(2): p. e1007941.
305. Roussigne, M., P. Blader, and S.W. Wilson, *Breaking symmetry: the zebrafish as a model for understanding left-right asymmetry in the developing brain.* Developmental neurobiology, 2012. **72**(3): p. 269-281.
306. Smith, K.A. and V. Uribe, *Getting to the Heart of Left–Right Asymmetry: Contributions from the Zebrafish Model.* Journal of Cardiovascular Development and Disease, 2021. **8**(6): p. 64.
307. Grimes, D.T., et al., *Left-right asymmetric heart jogging increases the robustness of dextral heart looping in zebrafish.* Developmental biology, 2020. **459**(2): p. 79-86.
308. Grimes, D.T. and R.D. Burdine, *Left–right patterning: breaking symmetry to asymmetric morphogenesis.* Trends in Genetics, 2017. **33**(9): p. 616-628.
309. Franco, P.G., et al., *Functional association of retinoic acid and hedgehog signaling in Xenopus primary neurogenesis.* Development, 1999. **126**(19): p. 4257-4265.
310. Sarmah, B., et al., *Inositol polyphosphates regulate zebrafish left-right asymmetry.* Developmental cell, 2005. **9**(1): p. 133-145.
311. Chocron, S., et al., *Zebrafish Bmp4 regulates left–right asymmetry at two distinct developmental time points.* Developmental biology, 2007. **305**(2): p. 577-588.
312. Schilling, T.F., J.-P. Concordet, and P.W. Ingham, *Regulation of left–right asymmetries in the zebrafish by Shh and BMP4.* Developmental biology, 1999. **210**(2): p. 277-287.
313. Matsui, T. and Y. Bessho, *Left–right asymmetry in zebrafish.* Cellular and Molecular Life Sciences, 2012. **69**(18): p. 3069-3077.

314. Baker, B.I., *The role of melanin-concentrating hormone in color change.* Annals of the New York Academy of Sciences, 1993. **680**(1): p. 279-289.
315. Ma, X., et al., *The transcription factor MITF in RPE function and dysfunction.* Progress in retinal and eye research, 2019. **73**: p. 100766.
316. Istrate, M., et al., *Photoprotection role of melanin in the human retinal pigment epithelium. Imaging techniques for retinal melanin.* Romanian Journal of Ophthalmology, 2020. **64**(2): p. 100.
317. Raymond, S.M. and I.J. Jackson, *The retinal pigmented epithelium is required for development and maintenance of the mouse neural retina.* Current Biology, 1995. **5**(11): p. 1286-1295.
318. Dong, W., et al., *The PBDE metabolite 6-OH-BDE 47 affects melanin pigmentation and THRβ MRNA expression in the eye of zebrafish embryos.* Endocrine Disruptors, 2014. **2**(1): p. e969072.
319. Chow, S.Y.A., et al., *Human sensory neurons modulate melanocytes through secretion of RGMB.* Cell Reports, 2022. **40**(12): p. 111366.
320. Miesfeld, J.B. and N.L. Brown, *Eye organogenesis: A hierarchical view of ocular development.* Current topics in developmental biology, 2019. **132**: p. 351-393.
321. Schmitt, E.A. and J.E. Dowling, *Early retinal development in the zebrafish, Danio rerio: light and electron microscopic analyses.* Journal of Comparative Neurology, 1999. **404**(4): p. 515-536.
322. Gross, J.M., et al., *Identification of zebrafish insertional mutants with defects in visual system development and function.* Genetics, 2005. **170**(1): p. 245-261.
323. Steinfeld, J., et al., *RPE specification in the chick is mediated by surface ectoderm-derived BMP and Wnt signalling.* Development, 2013. **140**(24): p. 4959-4969.
324. Kokkinaki, M., et al., *Klotho regulates retinal pigment epithelial functions and protects against oxidative stress.* Journal of Neuroscience, 2013. **33**(41): p. 16346-16359.
325. Rowan, S., et al., *Transdifferentiation of the retina into pigmented cells in ocular retardation mice defines a new function of the homeodomain gene Chx10.* 2004.
326. Chong, C.-M. and W. Zheng, *Artemisinin protects human retinal pigment epithelial cells from hydrogen peroxide-induced oxidative damage through activation of ERK/CREB signaling.* Redox biology, 2016. **9**: p. 50-56.
327. Campello, L., et al., *New Nrf2-inducer compound ITH12674 slows the progression of retinitis pigmentosa in the mouse model rd10.* Cellular Physiology & Biochemistry, 2020.
328. Tandon, A. and A. Mulvihill, *Ocular teratogens: old acquaintances and new dangers.* Eye, 2009. **23**(6): p. 1269-1274.
329. Muralidharan, P., S. Sarmah, and J.A. Marrs, *Retinal Wnt signaling defect in a zebrafish fetal alcohol spectrum disorder model.* PLoS One, 2018. **13**(8): p. e0201659.
330. Müller, T.E., et al., *Repeated ethanol exposure alters social behavior and oxidative stress parameters of zebrafish.* Progress in Neuro-Psychopharmacology and Biological Psychiatry, 2017. **79**: p. 105-111.
331. Yu, D.-Y. and S.J. Cringle, *Oxygen distribution and consumption within the retina in vascularised and avascular retinas and in animal models of retinal disease.* Progress in retinal and eye research, 2001. **20**(2): p. 175-208.
332. Organisciak, D.T. and D.K. Vaughan, *Retinal light damage: mechanisms and protection.* Progress in retinal and eye research, 2010. **29**(2): p. 113-134.
333. Lin, H., et al., *Mitochondrial DNA damage and repair in RPE associated with aging and age-related macular degeneration.* Investigative ophthalmology & visual science, 2011. **52**(6): p. 3521-3529.
334. Lin, M.T. and M.F. Beal, *Mitochondrial dysfunction and oxidative stress in neurodegenerative diseases.* Nature, 2006. **443**(7113): p. 787-795.
335. Velioglu, Y., et al., *Antioxidant activity and total phenolics in selected fruits, vegetables, and grain products.* Journal of agricultural and food chemistry, 1998. **46**(10): p. 4113-4117.

336. Lee, S.-C., et al., *Inhibitory effect of Cinnamomum osmophloeum Kanehira ethanol extracts on melanin synthesis via repression of tyrosinase expression.* Journal of bioscience and bioengineering, 2016. **122**(3): p. 263-269.
337. Kim, J.-Y., et al., *Anti-oxidant property and inhibition of melanin synthesis of eight plant extracts.* Microbiology and Biotechnology Letters, 2010. **38**(4): p. 414-419.
338. Lee, J.Y., et al., *Anti-melanogenic and anti-oxidant activities of ethanol extract of Kummerowia striata: Kummerowia striata regulate anti-melanogenic activity through down-regulation of TRP-1, TRP-2 and MITF expression.* Toxicology reports, 2019. **6**: p. 10-17.
339. Grisola, M.A.C. and R.G. Fuentes, *Phenotype-based screening of selected mangrove methanolic crude extracts with anti-melanogenic activity using zebrafish (Danio rerio) as a model.* ScienceAsia, 2017. **43**: p. 163-168.
340. Steinfeld, J., et al., *BMP-induced reprogramming of the neural retina into retinal pigment epithelium requires Wnt signalling.* Biology Open, 2017. **6**(7): p. 979-992.
341. Hou, L. and W.J. Pavan, *Transcriptional and signaling regulation in neural crest stem cell-derived melanocyte development: do all roads lead to Mitf?* Cell research, 2008. **18**(12): p. 1163-1176.
342. Westenskow, P., S. Piccolo, and S. Fuhrmann, *β-catenin controls differentiation of the retinal pigment epithelium in the mouse optic cup by regulating Mitf and Otx2 expression.* 2009.
343. Westenskow, P.D., et al., *Ectopic Mitf in the embryonic chick retina by co-transfection of β-catenin and Otx2.* Investigative ophthalmology & visual science, 2010. **51**(10): p. 5328-5335.
344. Tang, X., et al., *Bipotent progenitors as embryonic origin of retinal stem cells.* Journal of Cell Biology, 2017. **216**(6): p. 1833-1847.
345. Miles, A. and V. Tropepe, *Retinal stem cell 'retirement plans': Growth, regulation and species adaptations in the retinal ciliary marginal zone.* International Journal of Molecular Sciences, 2021. **22**(12): p. 6528.
346. Leach, L.L., et al., *The immune response is a critical regulator of zebrafish retinal pigment epithelium regeneration.* Proceedings of the National Academy of Sciences, 2021. **118**(21): p. e2017198118.
347. Hanovice, N.J., et al., *Regeneration of the zebrafish retinal pigment epithelium after widespread genetic ablation.* PLoS genetics, 2019. **15**(1): p. e1007939.
348. Dvoriantchikova, G., R.J. Seemungal, and D. Ivanov, *The epigenetic basis for the impaired ability of adult murine retinal pigment epithelium cells to regenerate retinal tissue.* Scientific reports, 2019. **9**(1): p. 1-13.
349. Tropepe, V., et al., *Retinal stem cells in the adult mammalian eye.* Science, 2000. **287**(5460): p. 2032-2036.
350. Kippenberger, S., et al., *Quantification of tyrosinase, TRP-1, and Trp-2 transcripts in human melanocytes by reverse transcriptase-competitive multiplex PCR–regulation by steroid hormones.* Journal of investigative dermatology, 1998. **110**(4): p. 364-367.
351. Park, Y.-D., et al., *TXM13 human melanoma cells: a novel source for the inhibition kinetics of human tyrosinase and for screening whitening agents.* Biochemistry and cell biology, 2006. **84**(1): p. 112-116.
352. Tuerxuntayi, A., et al., *Kaliziri extract upregulates tyrosinase, TRP-1, TRP-2 and MITF expression in murine B16 melanoma cells.* BMC complementary and Alternative Medicine, 2014. **14**(1): p. 1-9.
353. Mort, R.L., I.J. Jackson, and E.E. Patton, *The melanocyte lineage in development and disease.* Development, 2015. **142**(4): p. 620-632.
354. Milac, A.L. and G. Negroiu, *The multiple roles of tyrosinase-related protein-2/L-dopachrome tautomerase in melanoma: Biomarker, therapeutic target, and molecular driver in tumor progression.* Human Skin Cancers: Pathways, Mechanisms, Targets and Treatments, 2018: p. 45.

355. Pennamen, P., et al., *Dopachrome tautomerase variants in patients with oculocutaneous albinism.* Genetics in Medicine, 2021. **23**(3): p. 479-487.
356. Lang, D., et al., *Pax3 functions at a nodal point in melanocyte stem cell differentiation.* Nature, 2005. **433**(7028): p. 884-887.
357. Lim, X. and R. Nusse, *Wnt signaling in skin development, homeostasis, and disease.* Cold Spring Harbor perspectives in biology, 2013. **5**(2): p. a008029.
358. Netcharoensirisuk, P., et al., *Cajanin suppresses melanin synthesis through modulating MITF in human melanin-producing cells.* Molecules, 2021. **26**(19): p. 6040.
359. Murisier, F. and F. Beermann, *Genetics of pigment cells, lessons from the tyrosinase gene family.* Histology and histopathology, 2006.
360. Budd, P.S. and I.J. Jackson, *Structure of the mouse tyrosinase-related protein-2/dopachrome tautomerase (Tyrp2/Dct) gene and sequence of two novel slaty alleles.* Genomics, 1995. **29**(1): p. 35-43.
361. Giles, R.H., J.H. Van Es, and H. Clevers, *Caught up in a Wnt storm: Wnt signaling in cancer.* Biochimica et Biophysica Acta (BBA)-Reviews on Cancer, 2003. **1653**(1): p. 1-24.
362. Hari, L., et al., *Lineage-specific requirements of β-catenin in neural crest development.* The Journal of cell biology, 2002. **159**(5): p. 867-880.